




2020

Pneumovirus Infections: Understanding RSV and HMPV Entry, Replication, and Spread

Jonathan T. Kinder

University of Kentucky, jtkinder0376@gmail.com

Author ORCID Identifier:

 <https://orcid.org/0000-0001-7207-0639>

Digital Object Identifier: <https://doi.org/10.13023/etd.2020.414>

[Right click to open a feedback form in a new tab to let us know how this document benefits you.](#)

Recommended Citation

Kinder, Jonathan T., "Pneumovirus Infections: Understanding RSV and HMPV Entry, Replication, and Spread" (2020). *Theses and Dissertations--Molecular and Cellular Biochemistry*. 48.
https://uknowledge.uky.edu/biochem_etds/48

This Doctoral Dissertation is brought to you for free and open access by the Molecular and Cellular Biochemistry at UKnowledge. It has been accepted for inclusion in Theses and Dissertations--Molecular and Cellular Biochemistry by an authorized administrator of UKnowledge. For more information, please contact UKnowledge@lsv.uky.edu.

STUDENT AGREEMENT:

I represent that my thesis or dissertation and abstract are my original work. Proper attribution has been given to all outside sources. I understand that I am solely responsible for obtaining any needed copyright permissions. I have obtained needed written permission statement(s) from the owner(s) of each third-party copyrighted matter to be included in my work, allowing electronic distribution (if such use is not permitted by the fair use doctrine) which will be submitted to UKnowledge as Additional File.

I hereby grant to The University of Kentucky and its agents the irrevocable, non-exclusive, and royalty-free license to archive and make accessible my work in whole or in part in all forms of media, now or hereafter known. I agree that the document mentioned above may be made available immediately for worldwide access unless an embargo applies.

I retain all other ownership rights to the copyright of my work. I also retain the right to use in future works (such as articles or books) all or part of my work. I understand that I am free to register the copyright to my work.

REVIEW, APPROVAL AND ACCEPTANCE

The document mentioned above has been reviewed and accepted by the student's advisor, on behalf of the advisory committee, and by the Director of Graduate Studies (DGS), on behalf of the program; we verify that this is the final, approved version of the student's thesis including all changes required by the advisory committee. The undersigned agree to abide by the statements above.

Jonathan T. Kinder, Student

Dr. Rebecca Dutch, Major Professor

Dr. Trevor Creamer, Director of Graduate Studies

PNEUMOVIRUS INFECTIONS: UNDERSTANDING
RSV AND HMPV ENTRY, REPLICATION, AND SPREAD

Dissertation

A dissertation submitted in partial fulfillment of the
requirements for the degree of Doctor of Philosophy in the
College of Medicine
at the University of Kentucky

By

Jonathan Tyler Kinder

Director: Dr. Rebecca E. Dutch, Professor and Chair

Molecular and Cellular Biochemistry

Lexington, Kentucky

2020

Copyright © Jonathan Tyler Kinder 2020
<https://orcid.org/0000-0001-7207-0639>

ABSTRACT OF DISSERTATION

PNEUMOVIRUS INFECTIONS: UNDERSTANDING RSV AND HMPV ENTRY, REPLICATION, AND SPREAD

Pneumoviruses including human metapneumovirus (HMPV) and respiratory syncytial virus (RSV) are significant causes of respiratory tract infections globally. Children, elderly, and immunocompromised patients are at the greatest risk for developing severe infections, which can have devastating outcomes. Although these viruses are ubiquitous with significant impacts on human health, there are no antivirals or vaccines available. The only FDA approved therapy is a monoclonal antibody for RSV, given prophylactically during the infectious season, and this treatment is only available for high risk infants. The work presented in this thesis aims to increase our understanding of how these viruses enter, replicate, and spread to better characterize the basic molecular mechanisms used, opening avenues for potential antiviral therapies. We first analyzed the fusion protein of HMPV and how low pH is important for entry of some viral strains. We analyzed previously uncharacterized strains and found that residues initially hypothesized to be critical for low pH fusion are not always required, suggesting a more complex regulation of fusion. We then explored the role of the proteolytic cleavage event which is required for HMPV F as well as many other important respiratory pathogens, including influenza. We found that many proteases involved in activating influenza HA are also important for activating HMPV F, which has not previously been reported. We then used our understanding of cleavage to employ a treatment strategy targeting host proteases involved in this activation to prevent entry and spread. We next conducted a side-by-side comparison of infection, spread, and inhibition using a physiologically relevant 3-D human airway epithelial model system. We found that RSV and HMPV demonstrate significantly different infection and spread kinetics as well as phenotypes during infection, highlighting an interesting dichotomy between two closely related viruses. We further analyzed therapeutic potential for several monoclonal antibodies, finding that prophylactic

interventions prevent entry and spread, but treatment after entry suggests that both HMPV and RSV can be inhibited during entry. However, RSV likely spreads through cellular release and re-entry whereas HMPV utilizes a mechanism that is antibody independent after establishing the initial infection. Lastly, we examined the concept of viral co-infections, as co-infections with RSV and HMPV have been reported to cause more severe disease in patients. We provide evidence that RSV and HMPV co-infected cells can occupy the same inclusion bodies, but further investigation suggests that HMPV and RSV replication synergy may be limited. Collectively, the data presented in this dissertation provide new understanding of pneumovirus infections and reveals important information about the molecular mechanisms of pneumovirus entry and spread.

KEYWORDS: Human metapneumovirus, Respiratory syncytial virus, human airway epithelium, inclusion bodies, co-infection, fusion protein.

Jonathan Tyler Kinder

Student's signature

July 20, 2020

Date

PNEUMOVIRUS INFECTIONS: UNDERSTANDING
RSV AND HMPV ENTRY, REPLICATION, AND SPREAD

By

Jonathan Tyler Kinder

Rebecca E. Dutch, Ph.D.

Director of Dissertation

Trevor Creamer, Ph.D.

Director of Graduate Studies

July 20, 2020

Date

ACKNOWLEDGMENTS

The work presented in this dissertation would not have been possible without the encouragement, dedication, support, and guidance of many people. First and foremost, I would like to thank my mentor, Dr. Rebecca Dutch for being an incredible role model, source of inspiration, and pillar of support during my dissertation. Her constant motivation and encouragement helped me to develop as a scientist, pushing me to think independently and critically about my work to help address difficult questions and develop innovative solutions. My scientific accomplishments could not have been achieved if it were not for the amazing support, she has provided for me during my training. Not only is she an accomplished scientist, but a leader and an innovator in all aspects of her life. The impact she has had on me as a mentor and a role model, both personally and professionally, has been invaluable and I cannot thank her enough for everything she has done.

I would also like to thank my dissertation committee: Dr. Tianyan Gao, Dr. Michael Goodin and Dr. Wally Whiteheart. They are remarkable scientists who have provided critical feedback, expertise, and guidance during my training and I would not be where I am without their mentorship. I would also like to thank my outside examiner, Dr. Beth Garvy, for her time and effort to review this dissertation. I would also like to offer a very sincere thank you to Dr. Brett Spear, a fantastic scientist I had the pleasure to meet at a conference during my undergraduate career who helped me to start my graduate education at UK and provided support and encouragement during my time here.

A special thanks to Dr. Carole Moncman, who provided significant expertise in microscopy and willingness to help me during my graduate work and I appreciate the advice and knowledge shared that contributed greatly to my scientific development. I would also like to thank the current DGS, Dr. Trevor Creamer, who created an inclusive environment of support and development for graduate students in Biochemistry, contributing greatly to the growth and development of the next generation of scientists. The administrative staff here has been integral

to the success of our department, and I want to give my sincerest thanks to Rachel Putty, Brenda Wood, Phil Dickson, and Tonya Simon. I would also like to thank my undergraduate mentor, Dr. Tesfaye Belay, who provided a strong scientific foundation and encouragement.

To the current members of the Dutch lab, I want to thank you all so much for an incredible working environment, filled with support, fun, friendship and collaboration, which makes coming to work everyday something I look forward to. Through the good times and the bad, you have been my family and I will miss all of you greatly. Specifically, to Chelsea Barrett, Nicolas Cifuentes, and Stacy Webb, you made the last 5 years wonderful and I cannot thank you enough. You are wonderful and talented scientists that I am honored to have worked with. In addition to being my co-workers, you are very close and life-long friends that I am very lucky to have in my life. I would also like to say a special thanks to Stacy Smith, who not only helped keep the lab running smooth, but also contributed greatly to the development of our community and graduate training. I would also like to thank all the graduate students who help make this department wonderful and progressive from the bottom up. I would like to thank Sveta, who has given me immense support and companionship during my last year.

Finally, I would like to thank my family, who has provided me unconditional love and support. To my parents, Donna and Rick, you have given me encouragement and motivation to accomplish anything I set my mind to, no matter what it was. I could not have done any of this without your commitment and sacrifices. I hope that my accomplishments make you both as proud to be my parents as I am to be your son.

Table of Contents

ACKNOWLEDGMENTS	iii
List of Figures	viii
List of Tables	x
Chapter 1: Introduction	1
Paramyxo- and pneumovirus classification, epidemiology, and human health impact.....	1
Human metapneumovirus.....	2
Paramyxo- and pneumovirus structure and the role of glycoproteins in infection	5
Fusion protein mediated entry	7
Transcription and Replication	12
Viral Assembly and spread	14
Dissertation overview.....	19
Chapter 2: Material and Methods	27
Cell Lines.....	27
Plasmids, Antibodies and Proteases.....	27
Viruses.....	27
Transfection.....	28
Syncytia Assay.....	29
Luciferase Reporter Gene Fusion Assay.....	29
Gel Electrophoresis and Western Blotting.....	30
Expression, metabolic labelling and immunoprecipitation.....	30
Surface biotinylation protein labeling.....	31
Rescue of mCherry HMPV.....	31
Inhibition of HMPV viral infection in cell culture by SPINT2.....	32
Cleavage and inhibition of HMPV F by SPINT2.....	32
Fluorescence-activated cell sorting (FACS) analysis.....	33
Recombinant antibody production.....	33
Confocal Microscopy.....	34
Stellaris Fluorescent in situ hybridization (FISH) for viral RNA detection.....	34
Fluorescence threshold analysis.....	34
Infection of Human Airway Epithelial (HAE) tissues.....	35

Microneutralization and spread in HAE tissues.....	35
Statistical analysis.....	36
Chapter 3: Human metapneumovirus fusion protein triggering: Increasing complexities by analysis of new strains.....	37
Introduction.....	37
Results.....	39
Discussion.....	43
Chapter 4: SPINT2 inhibits proteases involved in activation of both influenza viruses and metapneumoviruses.....	50
Introduction.....	50
Results.....	54
SPINT2 inhibits recombinant human respiratory tract proteases that cleave HMPV F and HA cleavage site peptide mimics.....	54
Cleavage of distinct full-length HA subtypes and HMPV F is efficiently inhibited by SPINT.....	56
SPINT2 inhibits HA mediated cell-cell fusion.....	58
SPINT2 reduces viral growth in cell culture.....	58
Discussion.....	60
Chapter 5: Respiratory syncytial virus and human metapneumovirus infections in 3-D airway tissues expose an interesting dichotomy in viral replication, spread, and inhibition by neutralizing antibodies.....	75
Introduction.....	75
Results.....	79
HMPV and RSV induce the formation of replicative inclusion bodies.....	80
HMPV and RSV form extensions but no syncytia in HAE tissues.....	81
Nirsevimab, palivizumab and 54G10 block viral entry and spread in HAE tissues.....	83
Discussion.....	85
Chapter 6: RSV and HMPV viral co-infections.....	104
Introduction.....	104
Results and Discussion.....	106
HMPV and RSV coinfections in immortalized cell lines.....	106
HMPV and RSV heterologous protein complementation.....	107
Chapter 7: Discussion and Future Directions.....	118
Low pH mediate triggering of HMPV F: Analysis of new strains reveals complex requirements for fusion.....	118
Identifying and targeting proteases for antiviral treatment of HMPV.....	121
Complex 3-D human airway epithelial tissues as a model system of infection.....	124
Viral co-infections: Potential synergy for HMPV and RSV co-infected cells.....	127

Appendix 1: Designing a clinical testing platform for the merging SARS-CoV-2 (COVID-19) pandemic	130
Introduction	130
Material and Methods	134
Thermocycler and PCR kit:.....	134
RNA isolation:.....	134
Lyra RT-qPCR:.....	134
Limit of detection analysis:.....	135
Results and Discussion:.....	135
Appendix 2: List of Abbreviations	141
References.....	142
Vita	205

List of Figures

Figure 1.1: Schematic representation of the HMPV particle structure and genomic layout.	22
Figure 1.2 HMPV Fusion protein cleavage, structure, and fusion mechanism.....	23
Figure 1.3: Viral lifecycle of HMPV.	24
Figure 1.4: HMPV mechanisms of entry and spread.....	25
Figure 1.5: Human airway epithelial tissue (HAE) culture model system.	26
Figure 3.1. HMPV F proteins from different strains exhibit variable fusion activity promoted by low pH.....	46
Figure 3.2. HMPV F protein expression and cleavage by exogenous trypsin.	47
Figure 3.3: HMPV residues identified thus far involved in low pH mediated fusion.	48
Figure 3.4: Addition of HMPV G to TN96-12 F is unable to mediate fusion at low pH.....	49
Figure 4.1: Cytotoxicity assay to evaluate the cytotoxic effect of SPINT2.....	66
Figure 4.2: SPINT2 inhibits cleavage of HA protein expressed in 293T cells.	68
Figure 4.3: TMPRSS2, HAT, matriptase and KLK5 cleave HMPV F and SPINT2 is able to prevent cleavage by exogenous proteases.	70
Figure 4.4: SPINT2 inhibits HA-mediated cell-cell fusion.....	71
Figure 4.5: SPINT2 reduces IAV growth in cell culture.....	72
Figure 4.6: SPINT2 mitigates the spread of HMPV in cell culture.....	73
Figure 4.7: SPINT2 reduces viral growth when added 24 hours post infection.....	74
Figure 5.1: RSV and HMPV infection, spread and release in HAE tissues.....	92
Figure 5.2: RSV inclusion body formation in HAE.	93
Figure 5.3: HMPV inclusion body formation in HAE.	94
Figure 5.4: HMPV forms intercellular extensions significantly more than RSV.	95
Figure 5.5: Nirsevimab and palivizumab inhibition of RSV entry.	97
Figure 5.6: 54G10 inhibition of HMPV entry.....	99
Figure 5.7: Nirsevimab inhibits spread significantly more potently than palivizumab.....	101

Figure 5.8: 54G10 significantly inhibits spread of HMPV.	103
Figure 6.1: Recombinant mCherry HMPV shows efficient growth.....	112
Figure 6.2: HMPV and RSV growth in infected cells.	113
Figure 6.3: Analysis of HMPV and RSV co-infections.....	114
Figure 6.4: HMPV and RSV in co-infected cells can occupy the same IB	115
Figure 6.5: Recombinant RSV or HMPV N and P expression alter inclusion body formation	116
Figure 6.6: HMPV and RSV mini-replicon complementation, synergy, and dominant negative effects.	117

List of Tables

Table 4.1: Cleavage of HMPV F and SPINT2 inhibition of peptide cleavage of various proteases:.....	65
---	-----------

Chapter 1: Introduction

Paramyxo- and pneumovirus classification, epidemiology, and human health impact

Mononegavirales is an order of viruses containing a negative sense, single-stranded RNA genome. This Order is made of up eight different families: *Bornaviridae*, *Filoviridae*, *Myonnaviridae*, *Namiviridae*, *Paramyxoviridae*, *Pneumoviridae*, *Rhabdoviridae* and *Sunviridae* (1). Paramyxoviruses, in particular, have well known members responsible for significant health and economic burden worldwide. Members of paramyxoviridae cause disease in animals and humans, with potential for zoonotic transmission (2). One of the most highly pathogenic and well-known members is measles virus (MeV), which has become an increasing health concern in recent years due to decreased compliance with current vaccination regimens (3, 4). MeV is typically contracted during childhood and causes respiratory illness that can progress and cause complications such as pneumonia and encephalitis. MeV was responsible for severe morbidity and mortality until a vaccine developed in the 1960's led to significant reduction in the incidence, associated deaths, and hospitalizations (5). Another paramyxovirus, mumps virus (MuV), also causes disease during adolescence but vaccination led to fewer deaths and hospitalizations. Recently, particularly in developed nations, the vaccine that targets MeV and MuV (MMR vaccine) has been scrutinized and therefore, large populations have become non-compliant with the current vaccination regimen. This opposition to vaccination has led to a significant increase in MeV and MuV outbreaks, particularly in the United States and has once again become a major global health concern (3-5).

Other important members include Hendra (HeV) and Nipah (NiV) which cause respiratory disease and encephalitis in horses (HeV) and pigs (NiV). HeV and NiV have had reports of zoonotic transmission to humans with mortality rates ranging between 40-100%, but the amount of cases has been low (6-13). For these viruses, there is no current therapeutic treatment or vaccination in humans.

However, there has been a prophylactic treatments and vaccinations developed for horses against HeV that has demonstrated strong potential in high risk situations (14, 15). Parainfluenza viruses (PIV) cause significant morbidity and mortality in humans and PIV1-3 are responsible for respiratory illness in immunocompromised patients, infants, and children (16, 17).

Two other significant viruses are respiratory syncytial virus (RSV) and human metapneumovirus (HMPV, further described below), both of which cause widespread and severe respiratory tract infections. Both viruses were previously a sub-family of paramyxoviridae, but were recently reclassified to a new family, pneumoviridae (18). Although this places them in their own family, many aspects of viral infection and protein function remain highly conserved between them, allowing us to compare and contrast with information currently known about paramyxoviruses.

RSV was first isolated in 1956 from a chimpanzee presenting with a respiratory tract infection, and eventually determined to be of human origin (19, 20). RSV is now known as one of the leading causes of respiratory tract infections in infants and children, and it is estimated that there are 34 million infections and 3.4 million hospitalizations per year in children under 5 years of age (21, 22). In addition to infecting children, RSV causes severe infections in premature infants, elderly and immunocompromised patients (21-27). Even though this virus was identified more than 60 years ago, there are currently no vaccines or antivirals available other than a prophylactic treatment given during the infectious season to high risk infants that blocks a protein on the surface required for entry (28, 29). Therefore, RSV remains one of the most detrimental pediatric viruses.

Human metapneumovirus

Another significant but less well-known respiratory virus, HMPV, was isolated in 2001 from children exhibiting symptoms similar to those infected with RSV (30). Even though it was only recently identified, it is thought to have been circulating in humans as early as 1958 (30-32). When examining the origin of

HMPV, it is hypothesized that it recently evolved from zoonotic transmission of another member of the pneumoviridae family, avian metapneumovirus C (AMPV), based on high sequence homology (30). In addition, the genetic mapping of HMPV is also closely related to that of RSV, which encodes for the same proteins as well as two additional non-structural proteins (33).

Since its discovery, HMPV has been characterized as a major human pathogen, causing significant respiratory illness worldwide. Nearly everyone has been infected by the age of 5, is seropositive by the age of 10, and reinfection is common throughout life (30, 34-36). It is second to RSV as the cause of lower respiratory tract infections in children (36, 37). Similar to RSV, children, elderly, and immunocompromised patients are more likely to harbor serious infections. Importantly, some infants hospitalized with RSV for severe bronchiolitis showed co-infection with HMPV, which suggests co-infection with both viruses may lead to more severe disease. (38-40). Within the normal, healthy population, HMPV infection appears symptomatically similar to etiologic agents of upper respiratory infections, including cough, sneezing, rhinitis and other symptoms categorized as the “common cold” (41). However, in patients with limited capacity to fight infection, it causes more severe symptoms including wheezing, croup, bronchiolitis, and respiratory distress which can often lead to hospitalization or death (30, 31, 36, 37, 42-49). In long-term care patients over the age of 65, some studies suggest that HMPV can cause illness in up to 72% of patients during outbreaks (50-54). Furthermore, HMPV has been associated with myocarditis and those with congenital heart defects are at significant risk for developing severe infections (36, 48, 55-57). Patients with chronic respiratory illness are also at high risk, including those with cystic fibrosis, asthma, or chronic obstructive pulmonary disease. Severe infection with HMPV during childhood has also been associated with complications in adulthood such as increased incidences of asthma or hyperresponsiveness in the respiratory tract (58-64).

Immunocompromised individuals, including those infected with HIV, transplant recipients, or cancer patients have a significantly diminished immune

system, allowing for opportunistic infections to develop. HMPV infected patients with HIV were 5.4 times as likely to be hospitalized compared with HIV negative children (65). Additionally, pediatric patients with cancer were hospitalized nearly 50% of the time due to weakened immunity (66). While HMPV infection is transmitted through the respiratory tract, there has been HMPV RNA detected in the central nervous system and brain tissues of patients with fatal encephalitis (67-69). HMPV has also demonstrated mechanisms for establishing viral persistence. HMPV infections without respiratory symptoms have been reported in stem cell transplant patients, resulting in serious and sometimes fatal illness (70, 71). In animal models, replicating HMPV could be recovered at 60 days post infection (dpi) and detected more than 180 dpi by PCR (63, 72, 73). HMPV was shown to be present in neuronal processes in the lung suggesting immune privileged sites can keep the virus hidden from the immune system. This eventually leads to the viral reactivation following decreased immune function such as glucocorticoid administration (74). HMPV also demonstrates the ability to prevent apoptosis in cell culture which could offer a potential mechanism used to establish persistence (75).

HMPV infections follow behind annual influenza and respiratory syncytial virus seasons, with yearly epidemics peaking between November and April (76, 77). There are two subgroups of HMPV (A and B) which are further divided into A1, A2, B1 and B2 based on viral glycoprotein sequences (78, 79) (Fig. 1A). Both A and B can co-circulate and lineage dominance varies from year to year (80-84). Most research studies found that between 5 and 15% of respiratory tract infections are due to HMPV, trailing behind RSV and influenza (32, 43, 45, 46, 48, 84-86). While HMPV is ubiquitous and responsible for severe upper and lower respiratory tract infections, there are still no current FDA approved antiviral or vaccinations available. Therefore, a more thorough understanding of the viral lifecycle and molecular mechanisms required for infection is needed to discover novel antiviral targets against this significant human pathogen.

Paramyxo- and pneumovirus structure and the role of glycoproteins in infection

All paramyxo- and pneumoviruses have a negative sense, single-stranded RNA genome between 13-19kb in length which encodes for 6-10 proteins. These proteins perform all the requirements to enter target cells, recruit host factors, replicate, and assemble viral components, and mediate transmission to a naïve host (87). These viruses encapsidate the negative sense RNA genome (vRNA) in the viral nucleoprotein (N). This encapsidated RNA then associates with the large RNA-dependent RNA polymerase (L) and the phosphoprotein (P), a polymerase co-factor. vRNA, N, P and L coalesce to make up the ribonucleoprotein (RNP) complex which associates with the matrix protein (M) just below the lipid bilayer. Within the lipid bilayer are at least two surface glycoproteins: the fusion protein (F) and the attachment protein (HN, H or G). The attachment protein nomenclature is based on the ability to bind (H) or bind and cleave (HN) sialic acid. Attachment proteins that cannot bind or cleave sialic acid are referred to as G (88, 89). These proteins are the minimal components required for infection and family members encode additional proteins that serve various functions specific for that virus (89). HMPV contains a viral genome between 12 and 13kb in length. Within this genome, it encodes for 8 viral proteins that make up the infectious particle and replication machinery. On the outside of the particle, there is a lipid bilayer derived from the infected host cell. Within this membrane are 3 surface glycoproteins: F, G and the small hydrophobic protein (SH). Just below the lipid bilayer lies a layer of M that is associated with the lipid membrane, membrane glycoproteins, and the RNP complex. Two other proteins, M2-1 and M2-2, act as processivity and transcription factors for generating genome and messenger RNA for viral protein production (Fig. 1B). The genomic layout for HMPV is: 3'-N-P-M-F-M2-SH-G-L-5' (Fig. 1C) (30, 90-93).

In order for enveloped viruses to enter cells, it must fuse the viral and cellular membranes. The initial viral interactions are mediated by viral surface glycoproteins. This interaction subsequently promotes the fusion protein to fuse

the two membranes and mediate viral entry. F is essential for paramyxo- and pneumovirus entry due to the requirement of enveloped viruses for membrane fusion to initiate infection (covered in more detail below). Inhibiting F through various methods including mutagenesis, small molecule inhibitors and neutralizing antibodies prevents its function and subsequently, mitigates infection. This mechanism of targeting F is utilized by the immune system in order to neutralize the virus. This approach is also one of the leading targets for antiviral therapeutics of viruses that require fusion for entry (94-104). Simplistically, the attachment protein is thought to bring the virus into close proximity with a target cell, allowing F to then mediate entry. However, some fusion proteins in the absence of their cognate attachment protein are unable to mediate fusion, suggesting that the attachment protein of some viruses is specifically involved in activating F (105-113). Both HMPV and RSV G proteins have also been implicated in mitigating the immune system as well, suggesting other roles in addition to their proposed attachment function (114-120).

Some family members also encode the SH protein, but these demonstrate less conservation compared with the fusion or attachment proteins. In addition, little is known about the specific functions during infection. Some studies have shown recombinant viruses lacking SH have minimal growth defects in cell culture (121-125). In pneumoviruses, including HMPV, RSV and AMPV, recombinant viruses lacking SH showed a decrease in viral fitness and replication in animal models, suggesting the role of SH is important in a more physiologically relevant system (124, 126, 127). Further studies focusing on the role of SH have suggested a role in modulating the immune system or preventing host cell death through inhibition of apoptosis (128-130). Interestingly, both RSV and HMPV SH proteins demonstrate viroporin like activity (131, 132) which allows the movement of small molecules across the membrane, similar to the ion channel, M2, from influenza A virus (IAV) (133). Recombinant RSV and HMPV viruses containing F but lacking G and/or SH, still promote infection and spread, albeit less efficiently than WT viruses (91, 120, 121, 123, 124, 134-136). These findings support that F is the main mediator of entry for pneumoviruses while G and SH are not essential.

In some clinical isolates, there has been a duplication in G for both RSV and HMPV which suggests a boost in pathogenicity or viral fitness (137-142). More recently for RSV, it was suggested that virus grown in cell culture was unaffected by G neutralizing antibodies whereas use in 3-D tissue model systems demonstrated significantly reduced infectivity (143, 144). Furthermore, all current analyses of both RSV and HMPV isolates show G and SH are present, suggesting that keeping these genes increases viral fitness (31).

Fusion protein mediated entry

All paramyxo- and pneumoviruses contain a type I fusion protein (89, 145, 146). Other well studied class I fusion proteins include IAV HA (147), human immunodeficiency virus type 1 (HIV) envelope protein (gp160) (148), coronaviruses (CoV) including severe acute respiratory syndrome (SARS) (149, 150) and middle eastern respiratory syndrome (MERS) (150, 151) spike protein (S), and EboV glycoprotein (GP) (152, 153). Studies examining these viruses has allowed for a significant understanding of how they function and what factors are important for mediating entry. Type I fusion proteins are a single pass transmembrane protein with a predominantly alpha-helical conformation (154). For paramyxo- and pneumoviruses, these proteins contain a similar domain organization and protein structure. The N-terminus of the protein contains a protein cleavage site, followed by a hydrophobic fusion peptide (FP). Just beyond the FP is the heptad repeat A (HRA) region, the HRB region, transmembrane domain (TM) and C-terminal tail (CT) (Fig 1.2A) (87, 89, 155-164). After synthesis, these monomers subsequently trimerize to form a homo-trimeric protein complex. This form of the protein contains of a globular head, composed of the HRA and N-terminus of the protein, and a helical stalk domain, which contains the HRB, TM and CT (Fig 1.2B). These proteins are subsequently trafficked through secretory pathways to viral assembly sites through the endoplasmic reticulum and golgi apparatus where they are post translationally modified by glycosylation (155, 156). Addition of post translational modifications are important for many processes including protein folding, trafficking, molecular association, target cell entry,

immune evasion, and viral tropism for many viruses that utilize type I fusion proteins (165-168).

Type I fusion proteins of paramyxo- and pneumoviruses require proteolytic activation in order to function properly. These cleavage events occur just before a stretch of hydrophobic amino acids, termed the fusion peptide (FP). This cleavage process cuts the full length F0 precursor to yield a disulfide linked heterodimer composed of F1 and F2 subunits (Fig 1.1A). This cleavage activates the protein and generates the meta-stable, pre-fusion form presents on the outside of the virus (154, 155). The proteases required for cleavage differ greatly depending on the virus. For IAV, the pancreatic derived serine protease, trypsin, has been historically used to activate the HA protein, but trypsin is not present in the airway (147). More recent studies have identified several type-II transmembrane and secreted serine proteases which are present in the airway cleave a single basic amino acid residue within HA (169-178). Furthermore, these airway proteases demonstrate further specificity to specific strains of the virus (173, 175, 176). For highly pathogenic pandemic forms of IAV, this cleavage motif has been mutated, allowing intercellular cleavage by proteases recognizing multibasic cleavage sites such as furin and other furin-like pro-protein convertases (179, 180). These mutations completely alter HA cleavage efficiency and subsequently, its pathogenicity. Another example is the closely related pneumovirus, RSV, which utilizes this same family of pro-protein convertases. Unlike other type I fusion proteins, RSV F is cleaved at two separate cleavage motifs, removing a small 27 amino acid peptide and creating a fusogenically active fusion protein (155, 181, 182).

Coronaviruses, including SARS and MERS, have emerged as significant human pathogens in recent history, causing severe morbidity and mortality. Studies have identified key aspects of viral infection to better understand how these viruses emerged, transmitted to humans, and caused severe disease. More recently, a novel coronavirus, SARS-CoV2, emerged in late 2019, leading to a global pandemic (183-185). The SARS fusion protein, S, has been shown to be proteolytically processed at a single basic residue, similar to the IAV HA protein as

well as at an additional aliphatic residue. The novel SARS-CoV2 shares high homology to SARS S, where a single basic amino acid arginine (R) cleavage site is present at the canonical basic residue cleavage motif (186, 187). Sequencing of SARS-CoV2 S revealed an insertion of amino acids n-terminal to the original basic cleavage site, which increases recognition by furin-like proteases, similar to mutations observed for that of highly pathogenic influenza (188). It has been suggested that this small modification to one cleavage site within SARS-CoV2 S has increased its cleavage efficiency which likely lead to increased infectivity.

In HMPV, the fusion protein cleavage has not been extensively characterized. HMPV F is proteolytically processed at a motif, RQSR, with cleavage occurring just after the c-terminal arginine, allowing the FP to be released for fusion (30, 121, 189, 190). This RXXR motif has been previously characterized for furin as a minimal recognition sequence (191). However, furin and other pro-protein convertase family members that recognize this basic motif have not been reported to cleave this site in HMPV F. To date, only two proteases have been identified: trypsin and TMPRSS2 (192), a type II trans-membrane protease that is also involved with processing IAV HA and SARS S (170, 173, 176, 187). The majority of HMPV strains require the addition of exogenous trypsin in order to propagate efficiently. However, there are some identified strains that possess a cleavage site mutation, where RQSR has mutated to RQPR. This single amino acid change generates a trypsin independent cleavage site, allowing viruses to propagate efficiently in the absence of exogenous trypsin (193, 194) although it doesn't appear to affect cleavage (189). In addition, this motif has been suggested as a potential furin cleavage site, similar to that found in pseudomonas endotoxin (195). However, what endogenous proteases can cleave HMPV F has not been previously examined.

After cleavage, these meta-stable fusion proteins must be activated in order to initiate fusion. This activated form is important and must be regulated both temporally and spatially to ensure that fusion results in entry. However, the pre-fusion form is dynamic, where intermolecular and intramolecular interactions

generate a protein “breathing”, allowing for tolerance of the changing environment without prematurely triggering the protein (196, 197). This protein flexibility allows the virus to withstand a variety of conditions while keeping the protein active and stable until fusion can be initiated. For many paramyxoviruses, this initiation is accomplished through the interaction of the attachment protein. When the attachment protein interacts with the appropriate cellular factor, it then transduces a signal to F which begins a dramatic refolding process from the pre-fusion form (87, 89, 94, 95, 106, 145, 155, 156, 163, 164, 198). Crystal structure determination of F proteins has been a key factor in our ability to understand how these proteins function and recent advances in biochemistry and molecular biology has allowed for isolation and modifications of a significant number of proteins. These studies have generated pre-fusion [NiV (199), HeV (200), PIV3 , MeV (201), PIV5 (202, 203), RSV (204), and HMPV (205)] and post-fusion structures [NDV (206), RSV (207), and HMPV (208)] for a variety of paramyxo- and pneumovirus fusion proteins. Understanding the structural characteristics of these proteins has generated tools to better understand the dynamic refolding process and fusion intermediates through biochemical analysis in other type I fusion proteins (161, 209-211).

Upon triggering, the F protein inserts the helical hydrophobic FP into the membrane of the target cell. Once the FP is inserted, F continues to refold, forming a fusion intermediate hairpin structure. This refolding continues, pulling the target and viral membranes together. Full fusion is mediated by the interaction of the helical HRA and FP with the HRB and TM domains of the protein, which come together, forming an energetically stable six-helical bundle (6-HB), indicative of the post-fusion form of the protein (Fig 1.2C) (87, 89, 94, 106, 145, 155-164, 198, 211). Merging two lipid bilayers requires overcoming a significant energy barrier. Membrane fusion mediated by the F protein is an ATP independent process. Therefore, it is hypothesized that the energy required to fulfill complete fusion is stored as potential energy between the pre- and post-fusion forms and appropriate stimulus generates activation energy needed to initiate refolding. This fusion event is comparable to SNARE mediated vesicle fusion, where a target and receptor

SNARE protein pair interact and “zipper” to merge two membranes (212-214). The energetically favorable interaction provides energy to merge two membranes together and release the vesicle cargo. This highly stable SNARE protein complex must then be separated in an ATP dependent manner to be recycled and used again. However, our current knowledge suggests F proteins are unable to revert from the post-fusion to pre-fusion state. In addition to this intermolecular association, viruses also utilize other mechanisms to overcome energy barriers during entry. Enveloped viruses utilize the interface between lipid microdomains and the adjacent plasma membrane, which modify the lipid membrane. More specifically, cholesterol present in these domains bends the lipid membrane similar to that of early hemi-fusion intermediates. This change in membrane architecture is favored by viral fusion due to by lowering the energy threshold required for entry (215-219). In combination with this, viruses likely utilize multiple copies of the fusion protein. For studies looking at HIV gp160, it was suggested that only one fusion protein contains enough energy to mediate viral entry whereas other viruses require more (220-223).

Fusion for most paramxoviruses occurs at neutral pH, which suggests that viral membrane fusion occurs at the plasma membrane (89, 106, 145, 155). For some type I fusion glycoproteins, there is no attachment protein, and entry is mediated by a single surface glycoprotein. Alternatively, some viruses contain an attachment protein that does not mediate the activation of F and therefore, some other stimuli must activate the fusion protein (145). For IAV HA, the virus is taken up through endocytosis after binding sialic acid on the surface of target cells. The virus traffics through the endosomal pathway where a steady decrease in pH occurs. This increase in acidity is used as a timing mechanism, as sufficiently low pH will eventually trigger the HA protein to mediate fusion (147, 224-227). Another example is GP from EboV. EboV enters through cellular micropinocytosis by expressing phosphatidyl-serine on the outside of its viral membrane which is recognized by host proteins on the cell surface, such as TIM-1. Once taken up by the cells, GP protein is processed by host proteases in the endosomal pathway. This cleavage process allows the GP protein to interact with its internal cellular

receptor, Neiman-Pick C1 (NPC1), and this interaction initiates fusion (152, 228-237). In addition to cleavage and receptor interaction, some studies have suggested the use of cations such as calcium and potassium as well as low pH as a potential trigger to enhance fusion, although there is inconclusive evidence (152, 235-238).

Our lab and others have demonstrated some strains of HMPV (subtype A2) utilize a similar mechanism to IAV for fusion activation (239-242). Previous studies found that HMPV interacts with its surface attachment and entry factors, heparan sulfate and $\alpha V\beta 1$ integrin. These interactions allow HMPV to bind and enter through clathrin-mediated endocytosis (123, 243). As HMPV moves through the endosomal pathway, a steady decrease in pH occurs. This subset of HMPV F proteins use an increase in acidity to activate fusion and initiate viral entry (Fig 1.3). However, low pH induced fusion is only predicted to be in strains harboring specific amino acids uniquely found within the A2 subtype (239-242). There are a limited number of strains available for analysis and more information is needed to further our understanding of these residues involved in fusion. Furthermore, other factors that activate F proteins, such as cellular receptors or cofactors that are unaffected by low pH have yet to be elucidated.

Transcription and Replication

Once fusion has occurred and the RNP is released into the cytoplasm, the L protein of HMPV begins viral replication to generate the positive sense antigenomic RNA which acts as a template for replicating the negative sense viral genome (vRNA) (89). In addition, L also functions to generate the viral mRNA from the genomic template. L follows a start-stop model of transcription, resulting in a gradient of mRNA where the 3' genes are more highly transcribed than 5' (244-246). However, the factors that contribute to whether the polymerase chooses to generate vRNA, antigenomic RNA, or mRNA has largely remained unknown but recent studies have generated interesting hypotheses for how this process may occur. For RSV, studies have reconstituted the L and P proteins to study their

ability to replicate RNA *de novo*. In order for transcription or replication to occur, L must be loaded with a nucleotide triphosphate, which allows binding to the template strand to initiate elongation. The beginning of the genome contains the sequence 3' UGC 5' and which nucleotide is loaded in the polymerase determines whether it will initiate transcription or replication (247). Genome replication occurs when an ATP nucleotide is present and binds to the first position and replicates the entire genome. Polymerases loaded with GTP will mediate binding to position 3 and therefore, unable to replicate the entire genome, shifting to transcription of viral genes. This finding suggests RSV utilizes the cellular nucleotide pool concentrations as a timing mechanism to switch between these two functions (248-250). While this process has not been published for HMPV yet, these same principles likely apply and may help explain the function of all polymerases within mononegavirales (250).

As viral protein synthesis occurs, both RSV and HMPV form punctate cytosolic structures which reside close to the nucleus (251, 252). These structures, termed inclusion bodies (IBs), are minimally composed of N, P, L, M2-1 and vRNA (Fig 1.3) (251-255). It is suggested that IBs function to keep the required viral and host factors in close proximity to each other for efficient viral transcription and replication. Another hypothesis is that IBs keep the viral RNA sequestered from the cellular response factors that recognize double stranded RNA, such as RIG-I and MDA5 (253). These structures have been reported for a wide variety of other viruses in mononegavirales including plant and animal RabV (256-260), EboV (261), Marburg virus (262), vesicular stomatitis virus (263), PIV3 (264, 265), and PIV5 (266), suggesting that this type of structure is likely a conserved and important function during the viral lifecycle. The origin of these structures is varied depending on the virus. For example, PIV3 is able to restructure the endoplasmic reticulum membranes, generating viral replication compartments in the cytoplasm (265). This same tactic is utilized by many positive sense single stranded RNA viruses to meet the needs for viral replication (267, 268).

Pneumovirus IBs have been examined more closely and interestingly, they do not demonstrate molecular kinetics similar to those structures surrounded by a membrane. Instead, these organelles demonstrate dynamics of a phenomenon called liquid-liquid phase separation, something that has been also reported for RaV, VSV and MeV(269-271). In this process, pH, salt concentration, molecular density, and electrostatic interactions are thought to mediate association. These molecular aggregates eventually separate out from the surrounding solution primarily based on intramolecular interactions that drive an energetically favorable process to form a liquid-liquid interface (272-275). This process for RSV and HMPV selects for viral specific components, keeping them in close proximity for efficient replication. Viral proteins may also recruit other cellular factors that are required for these processes and exclude host antiviral factors. Due to the lack of lipid membrane, some molecules may diffuse in or out of the organelle much quicker, allowing for import of nutrients and export of viral factors. Further investigation of IBs in RSV infection demonstrated an internal compartmentalization of IBs, termed IB associated granules (IBAGs), serving unique functions for RNA synthesis and viral transcription (255).

While many viral factors have been identified, cellular factors utilized by the virus and sequestered in IBs have not yet been elucidated. Understanding the components of IBs could reveal important information about viral and cellular requirements for efficient transcription and replication. These factors could then be targeted for a wide range of viruses that utilize these during infection, offering potential for broad-spectrum antiviral therapy.

Viral Assembly and spread

Once viral proteins have reached adequate concentrations, they are trafficked to sites of assembly at the plasma membrane (88, 89, 156). The RNP complex is then shuttled from IBs where they interact with proteins present at assembly sites. Once this association has occurred, there are two methods of viral particle formation (Figure 1.3). The first is the classical pathway for enveloped

viruses (276, 277). The viral proteins and RNP complex associate and begin pinching the plasma membrane, releasing an infectious virus. This virus is then able to release from the infected cell and move to a naïve host, bind, and enter to start the infectious process. However, recent studies of many viruses have demonstrated that this is not always the case (278-280). Other mechanisms for these viruses show that while some viral particles are spherical, many tend to be pleomorphic in nature. Some viruses are filamentous, generating tubular extensions from the cellular membrane composed of viral proteins and RNA (84, 279, 281-286) and these often lead to varying particle sizes and morphologies. Some other viruses remain largely cell associated, with minimal released virus detected (279, 287, 288). The current understanding of viral assembly and spread for many enveloped viruses is rapidly changing with increases in the technology we have to study them.

One interesting example is MeV which enters the respiratory tract through aerosol droplets, similar to other respiratory viruses. Once inside a naïve host, MeV particles bind host dendritic cells and alveolar macrophages through the interaction between the measles fusion protein, H, and cellular receptors CD150 (also called signaling lymphocytic activation molecule, SLAM), the complement system protein, CD46 (also called membrane cofactor protein, MCP) and the attachment factor DC-SIGN. CD46 is the receptor for the vaccine strain while circulating MeV utilized SLAM for entry. Interestingly, MeV has been shown to infect some cell lines independently of either MCP or SLAM, suggesting another potential mediator of viral entry (289-291). More thorough analysis determined this receptor was Nectin-4, a protein that is expressed primarily in the adherens junctions during cellular polarization in the airway epithelial. This basolateral restriction prevents MeV from interacting with this factor during entry (292). Upon infection, MeV activates the immune system, causing respiratory tract inflammation, resulting in damage to the epithelial layer. This disruption allows MeV to access the Nectin-4 protein in cell-cell junctions to begin infecting the lung epithelial layer. Nectin-4 is then utilized in a mechanism of direct cell-to-cell spread of MeV from one cell to a neighboring cell, independent of apical release of the

virus (292, 293). However, at later stages of infection, Nectin-4 also plays a role in viral release where mediates direct transfer of virus to lymphocytes and subsequent exit from the host via aerosols.

Studies using 3-D human airway epithelial model systems which more accurately recapitulate the lung environment (covered in more detail below) have further demonstrated the interesting entry and spread dynamics of MeV (292, 294-297). These have confirmed the importance of Nectin-4 in direct cell-to-cell transfer but have also revealed another interesting mechanism of spread. In these environments, MeV utilizes F-actin to transfer the RNP complex directly from one cell to another. This allows the virus to theoretically bypass the first several hours of infection by skipping the need to assemble and release a new viral particle which then re-enters a cell to initiate infection. Additionally, multiple replication competent complexes are also introduced which increases infectivity and replication efficiency before the immune response can inhibit these processes.

The changing paradigms are seen for both RSV and HMPV as well, as recent studies suggest cell-to-cell spread is an important aspect for the pneumovirus lifecycle (251, 280, 288, 298, 299). These methods of spread include the formation of syncytia, intercellular extensions, and polyploid virions (Figure 1.4). It has been widely demonstrated that enveloped viruses ultimately use fusion as a means of viral entry (146, 154). This same mechanism also generates multinucleated bodies when two or more cells fuse together. Fusion of the cytoplasm of a non-infected cell with an infected one subsequently increases nutrients and resources. This process also mediates infection of a naïve cell during the process. Using this mechanism of spread avoids viral release and reentry which greatly benefits infectivity and replication (279, 280, 300). For RSV, syncytia formation has been examined in viruses that possess a hyperfusogenic fusion protein, forming large syncytia in cell culture. Infection of mice with this recombinant virus demonstrated increased pathogenic effects suggesting that this increased fusogenicity and syncytia formation is beneficial for virus replication (301).

Both RSV and HMPV form filamentous structures that extend toward neighboring cells. RSV induced the formation of actin based, actin-related protein (Arp2) dependent filopodia in A549 lung epithelial cells that is important for viral spread (298). HMPV also forms long actin-based extensions that extend from infected cells. These structures are important for direct cell-to-cell spread of the virus in the presence of neutralizing antibody, where spread was only modestly decreased (288). We hypothesize these extensions are likely aiding in direct transfer of RNP complexes, similar to that of MeV or aiding in the surfing of viral particles from one cell to another along the extensions, which has been seen for viruses such as HIV (Fig 1.4) (279, 280, 300).

These same filamentous structures play another role in the transfer of virus released from cells. Viral protein and RNP complexes that coalesce at the plasma membrane are associated with the formation of the filamentous form of viruses. Filamentous forms of the virus generate virions that contain multiple copies of the viral genome within the same particle (Fig 1.4). This creates an infectious particle with an increased chance of initiating successful infection by delivering more viral templates and replication machinery (302-304). While not demonstrated for RSV or HMPV, other paramyxoviruses have shown that polyploid viruses are common, suggesting a viral fitness advantage (279, 280, 300).

Current mechanisms and 3-D model systems for studying respiratory virus infections

The respiratory tract is a complex organ system that promotes movement of air from the nasal passages through the sinuses, down the pharynx, and into the lungs. This canal is primarily lined with pseudostratified columnar epithelial cells. There are other specific cell types that perform unique functions, such as goblet cells that produce mucus, basal cells that differentiate and restore the epithelial layer, and ciliated cells that move mucus up and out of the respiratory tract. This organ system is critical for gas exchange that not only supplies oxygen but also removes carbon dioxide, regulating blood pH, and controlling water

balance. In addition to its physiological role, it is also an important immune barrier against invading pathogens (305, 306). Cells in the respiratory tract secrete a range of proteases that cleave the extracellular matrix and secrete antimicrobial proteins. The innate and adaptive immune systems also play a critical role in protecting the tissues from infection by recognizing and breaking down invading bacteria, viruses or fungi (307-311). Taken together, the complexity of the respiratory tract makes it difficult to study infection and more physiologically relevant models are needed to further our understanding of infection.

The current methodology to study viruses uses immortalized cell lines grown in 2-D monolayers. These cell lines are often selected for specific features that enhance growth, replication and recovery of virus. Infection in cell monolayers allows us to better understand viral-host interactions, how the cell responds to infection, and how the virus subverts cellular mechanisms to evade detection and use cellular components to benefit viral replication. While these studies are invaluable and ground-breaking research has been conducted using these, ultimately, they lack some key characteristics from tissues that must be considered. This pitfall is partially mitigated with the use of animal model systems to study infection. While these model systems consider the complexity of entire organ systems, humans only share partial conservation of key cellular factors that can complicate translation to humans. These limitations make it important to explore and develop other model systems that consider both tissue type and organism specificity.

Human airway epithelial tissues (HAE) have been developed as a model system to overcome the gap in current methods of research. Primary airway cells isolated from the nasal passage or lung, which maintain proliferative ability and pluripotency, are seeded on a trans-well (312, 313). After reaching confluency, the media from the apical surface is removed, generating an air-liquid interface mimicking the environment present in the lung. This then stimulates the differentiation of cells into a multi-layer pseudostratified cellular layer composed of bronchial or nasal epithelial cells and goblet cells. These cultures can recapitulate

the 3-D environment and contain functional cilia as well as mucus production (Fig 1.5). These tissues are a model system to study respiratory pathogen-host interaction and develop anti-viral therapeutics. HAE tissues have been widely utilized to study important pathogens such as IAV, RSV, PIV3 and MeV (107, 144, 291, 294, 296, 297, 314-332). HMPV infection in these tissues has been examined, although few studies have been reported (121, 135, 318, 333). This model system offers significant advantage to understand HMPV infection *in vivo* while maintaining a simplistic *in vitro* approach allowing for validation of important aspects of viral infection as well as discovering other important host-viral interactions.

Dissertation overview

Human metapneumovirus is a recently discovered and important respiratory virus that infects nearly everyone during their life. It's severity ranges from mild "cold-like" symptoms to severe respiratory illness or even death. There are currently no antiviral or vaccine available and understanding more about the viral lifecycle will help to develop novel targets to treat and prevent infection. RSV, another important respiratory pathogen similar to HMPV, also lacks a critical molecular understanding of viral lifecycle needed to develop novel therapeutics to fight infection. The data presented in this dissertation aims to further our understanding of the molecular mechanisms of HMPV and RSV infection through 4-main questions.

First, we examine the function of the HMPV F fusion protein by analyzing molecular interactions at the protein level. It is currently unknown which factors contribute to triggering the F conformational changes required for membrane fusion. However, a subset of HMPV F proteins were shown to use low pH as a biological sensor to initiate this process. Analysis of F proteins currently available in our lab and others suggests there are specific residues that contribute to this phenotype. However, there are few strains examined and more are needed to better understand which amino acids are critical for this function. We analyzed the

F protein from strains of HMPV not previously characterized that contain key residues previously implicated in low pH mediated fusion. We find that there are key electrostatic interactions involved in this phenomenon and identify novel interactions that modulate fusogenic activity and protein dynamics.

Next, we then investigated the proteolytic processing of the HMPV F protein which is required for activation and the proteases that are able to cleave HMPV F have not been previously determined. Exogenous trypsin is able to cleave a basic amino acid residue just n-terminal to the fusion peptide. Addition of trypsin has traditionally been used to propagate HMPV in cell culture. Another group demonstrated that overexpressing a transmembrane serine protease, TMPRSS2, also led to efficiently replication *in vitro*. Here, we demonstrate that HMPV can utilize a variety of serine proteases that are also important for other respiratory viruses including SARS and influenza A virus. We then explore this conserved phenomenon as a means for broad spectrum anti-viral development against several viruses that require serine proteases for activation by using a naturally occurring protease inhibitor.

In addition to understanding the molecular mechanisms of HMPV F, we then focused on comparing the two pneumoviruses, HMPV and RSV, in a 3-D human airway epithelial (HAE) model system. Using HAE tissues, we find that RSV and HMPV infection and spread kinetics are significantly different. To determine why these closely related viruses demonstrate drastically different phenotypes, we probed several different aspects of viral entry, replication and spread. We then explored the use of neutralizing antibodies to examine the therapeutic potential for inhibiting entry and spread for both viruses.

Co-infections for both RSV and HMPV have been reported, resulting in increased disease severity. To better understand this phenomenon, we analyzed co-infected cells to identify how both viruses interact during replication and spread *in vitro*. We find that these RSV and HMPV can occupy the same replication organelles, where vRNA and protein from both viruses coalesce. We examined

several protein interactions involved in replication to understand how coalescence in IBs affects viral replication and spread during infection and how this may lead to increased disease severity.

Altogether, the results presented in this dissertation generate novel information on the molecular mechanisms and processing of the HMPV F protein not previously known. These findings identify key molecular aspects of low pH fusing strains as well as which host factors are involved in proteolytic processing for activation. We then examined two closely related pneumoviruses and conducted a side-by-side comparison of infection, replication, and spread in HAE tissues, which has not been previously examined. We find an interesting dichotomy between two closely related pneumoviruses and generate a better understanding for how these viruses can mediate infection and spread using an *in vitro* 3-D airway epithelial model system. We then test the therapeutic potential of neutralizing antibodies for both RSV and HMPV. Lastly, we examined the synergistic capability of cells co-infected with RSV and HMPV and determined how this affects viral replication and spread. Overall, we identify novel information at the protein level as well as viral infection in a physiologically relevant model system. These findings further our understanding of infection and highlight potential for therapeutic intervention against RSV and HMPV as well as other respiratory viruses that utilize similar molecular mechanisms during infection.

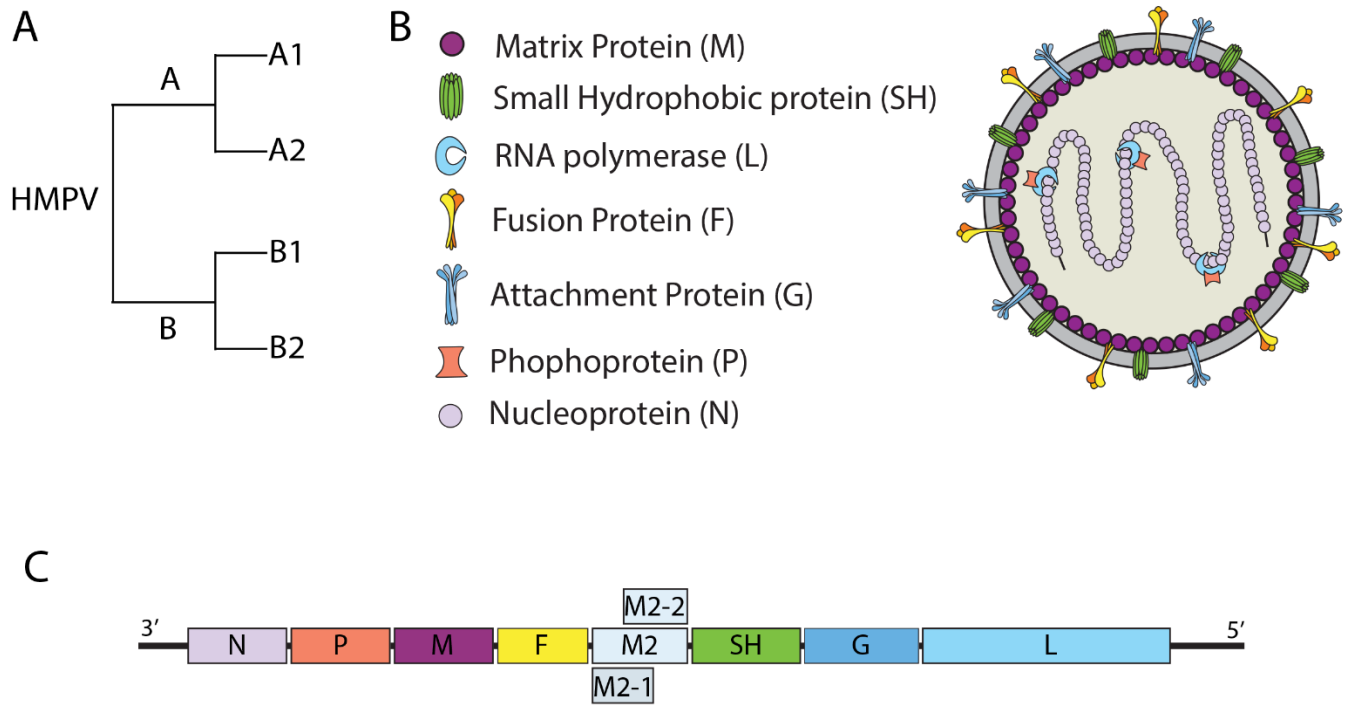


Figure 1.1: Schematic representation of the HMPV particle structure and genomic layout. (A) Phylogenetic classification of HMPV. **(B)** HMPV particle depicting the basic structure and protein localization of an infectious particle. **(C)** Genomic layout of the negative sense genome and protein open reading frame position.

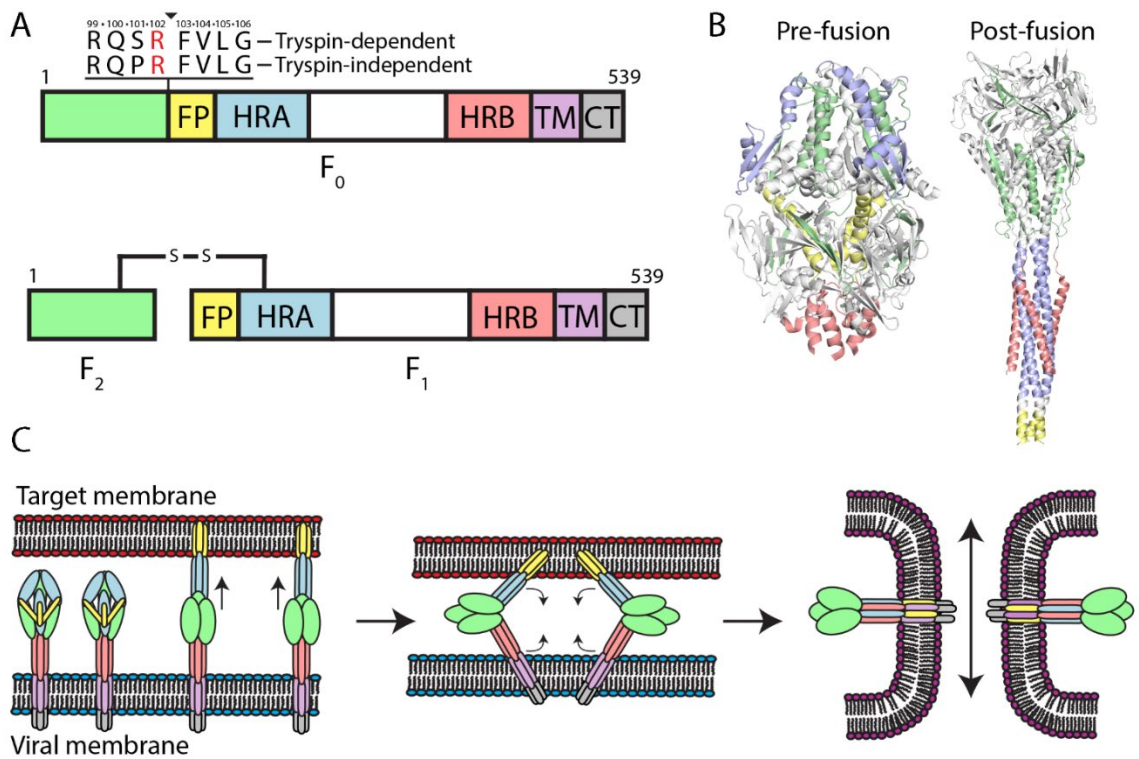


Figure 1.2 HMPV Fusion protein cleavage, structure, and fusion mechanism. (A) HMPV F is synthesized as a monomeric 539 aa polypeptide which is then cleaved at single basic amino acid residue N-terminal to the fusion peptide (FP). The basic layout is shown for protein domains including the heptad repeat A (HRA) and B (HRB) domains, followed by the transmembrane (TM) and C-terminal tail (CT). **(B)** The 3-D protein crystal structure of the pre and post fusion F protein demonstrating the globular head and helical stalk domains. Colors correspond to the protein schematic in A. **(C)** Upon appropriate stimulation, HMPV mediates membrane fusion by inserting the fusion peptide into a target membrane, undergoing a large conformational change from the pre- to post-fusion state (shown in B), mediating fusion of the viral and target membranes.

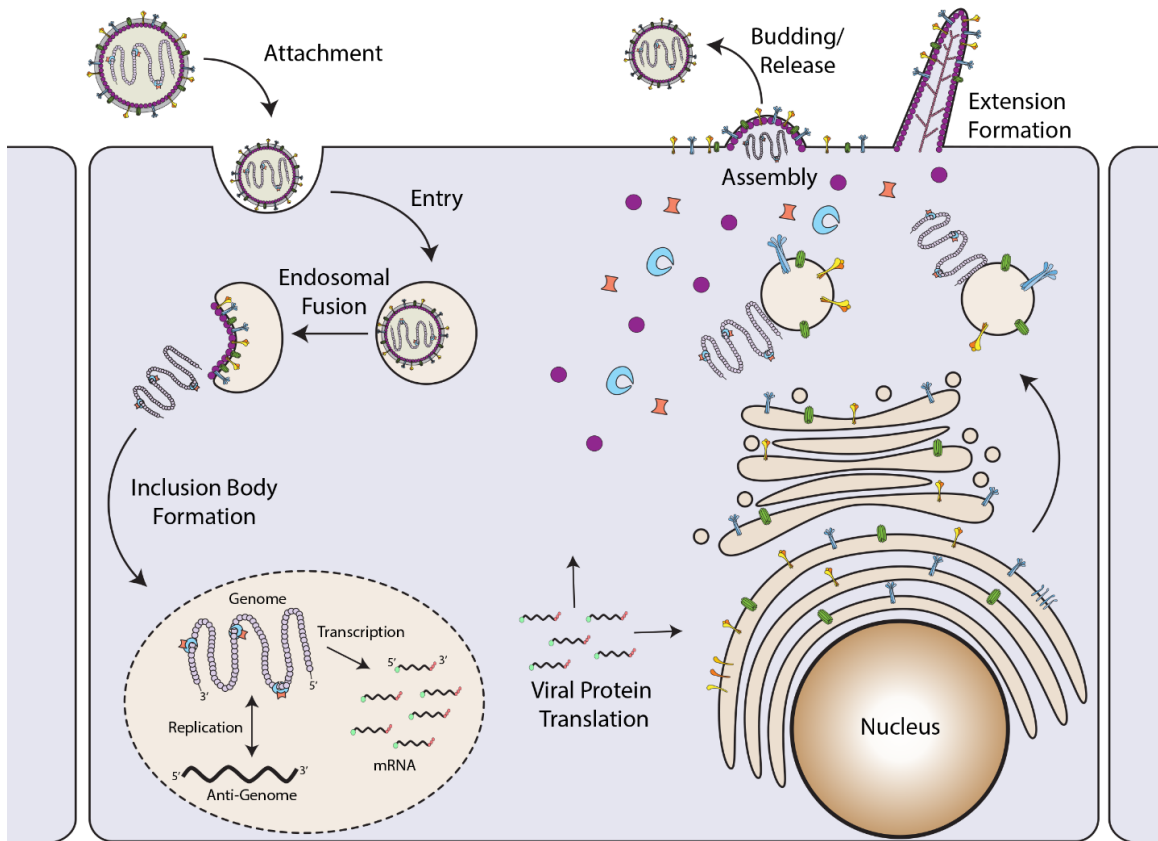


Figure 1.3: Viral lifecycle of HMPV. HMPV attaches to a target cells and enters through clathrin mediated endocytosis where fusion with the endosomal membrane releases the viral ribonucleoprotein complex. Transcription of viral proteins mediates the formation of inclusion bodies for genomic replication and transcription. Newly synthesized viral genome and proteins then accumulate at the plasma membrane at assembly sites where newly synthesized particles will undergo budding or mediate the formation of filamentous extensions for cell-to-cell spread.

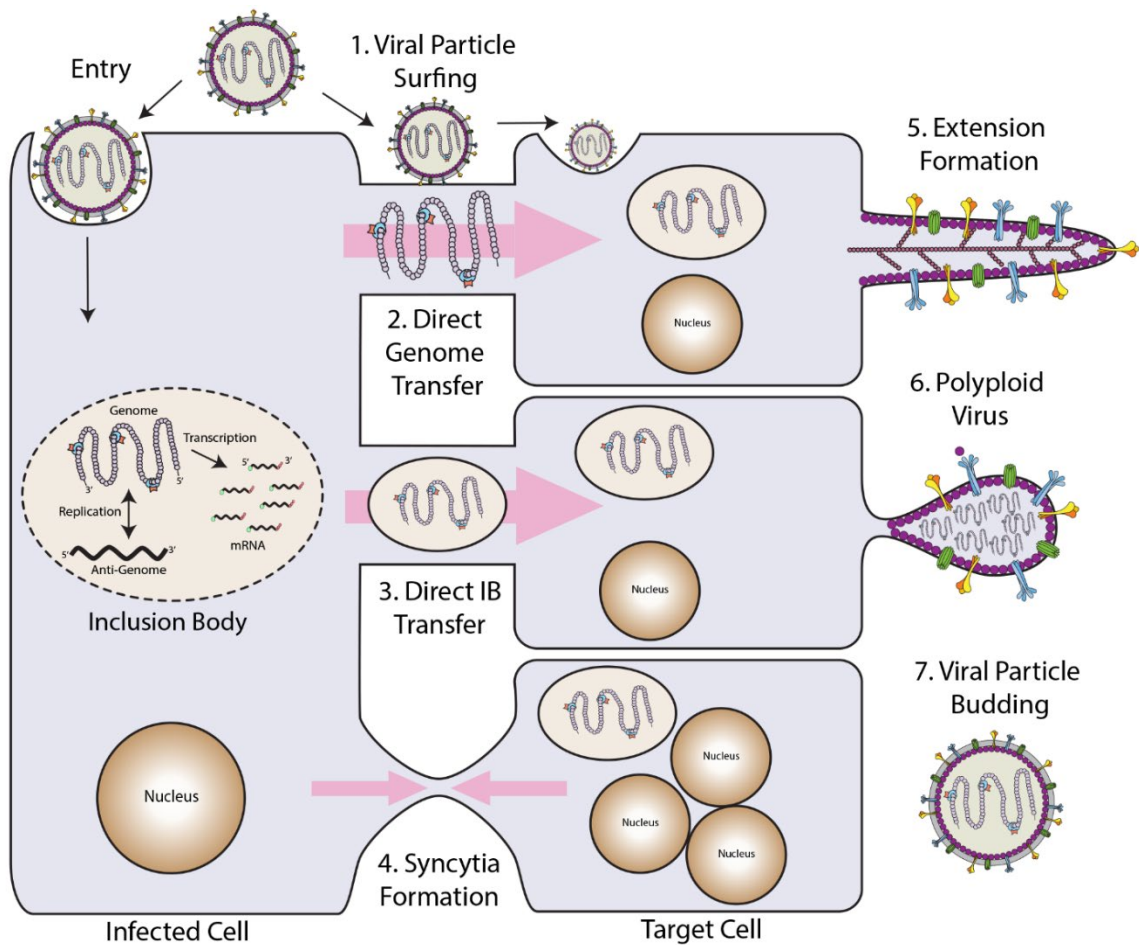


Figure 1.4: HMPV mechanisms of entry and spread. After viral entry and replication, HMPV spreads to uninfected cells. Formation of extensions between infected cells mediates direct cell-to-cell spread. These extensions allow viral particles to **(1)** move along the surface **(2)** directly transfer nucleic acid materials or **(3)** move replication organelles from one cell to another. Alternatively, virus fusion may mediate the formation of syncytia **(4)**, which can also infect cells and mediate genome or replication body transfer. Infected cells then mediate spread of HMPV through **(5)** formation of intercellular extensions **(6)** polyploid viruses containing multiple genome copies or **(7)** particle budding which will spread from infected to non-infected cells.

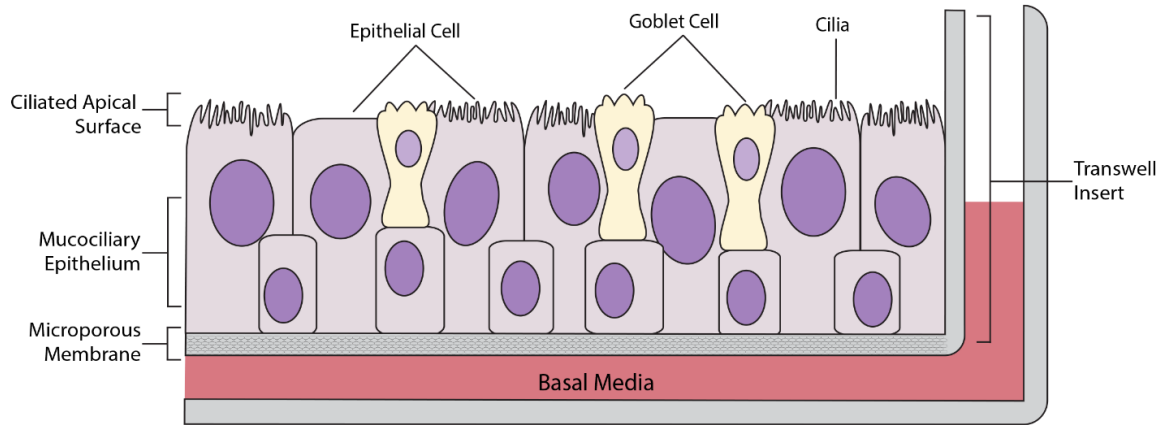


Figure 1.5: Human airway epithelial tissue (HAE) culture model system. 3-D HAE tissues contain both epithelial and goblet cells present in a pseudostratified tissue layer. These tissues are then grown on a trans-well with an air-liquid interface containing an exposed apical surface and a nutrient rich media at the basolateral surface. These tissues also contain functional cilia as well as mucus production, creating an authentic primary cell culture model system.

Chapter 2: Material and Methods

Cell Lines. VERO (ATCC), BSR (provided by Karl-Klaus Conzelmann, Max Pettenkofer Institut) and LLC-MK2 (ATCC) cells were grown in Dulbecco's Modified Eagles Media (DMEM;Hyclone) supplemented with 10% fetal bovine serum (FBS; Sigma). For BSRs, 0.5 mg/mL G418 was added every third passage to keep selection for cells constitutively expressing the T7 polymerase. BEAS-2B (ATCC) and HEp-2 (Medimmune) cells were maintained in Opti-MEM (Invitrogen) supplemented with 2% FBS or BEBM supplemented with BEGM Single Quot Kit and growth factors (Lonza). 293 Freestyle cells (Invitrogen) were maintained in 293 Freestyle expression media on an orbital shaker. All cells were maintained at 37°C and 5% CO₂.

Plasmids, Antibodies and Proteases. HMPV Fusion protein (F) within pGEM-3Zf (+) was kindly provided by Ursula J. Buchholz (NIAID, Bethesda, Maryland). All HMPV F proteins mutants were completed using Quick-Change site-directed mutagenesis and confirmed by sequencing (Stratagene). F genes were then subcloned to pCAGGS by digesting with EcoR1 and Sph1 (New England Biolabs). Plasmids for pcDNA3.1-TMPRSS2-Myc, pcDNA3.1-HAT-Myc and pcDNA3.1-Matriptase were provided by Dr. Marco Strauss and Dr. Gary Whittaker (Cornell University). TMPRSS2 and HAT plasmids were subcloned into pCAGGS by EcoRI and NdeI. Colonies were picked and sequenced to determine proper insertion. 54G10 anti-HMPV F monoclonal antibody plasmid was kindly provided by John Williams (University of Pittsburgh, Children's Hospital; please see recombinant antibody production). pTM1 L, M2-1, N, P and CAT-Luciferase minigenome reporter assay plasmids for HMPV were a kind gift from Dr. Rachel Fearn (Boston University). pcDNA3.1 L, P, M2-1, N and luciferase minigenome were kindly provided by Dr. Richard Plemper (Georgia State University). Both reporter gene systems utilize the T7 promoter.

Viruses. Recombinant green fluorescent protein expressing human metapneumovirus strain CAN 97-83 (rgHMPV) with a codon stabilized SH gene

was kindly provided by Peter L. Collins and Ursula J. Buchholz (NIAID, Bethesda, Maryland). HMPV (MOI 0.01) was propagated in VERO cells and incubated at 37°C in Opti-MEM supplemented with 2 mM L-glutamine and 0.3 µg/mL TPCK-trypsin every other day. After 10 days, 1x SPG (218mM Sucrose, 4.9 mM L-glutamic acid, 3.8 mM KH₂PO₄, 7.2 mM K₂HPO₄) from the 10x stock was added to the media and cells were scraped and kept cold. Cell pellets were spun down at 2500 rpm for 10 min on a Sorvall ST-8R centrifuge (Thermo). Supernatants were added to 20% sucrose in TNE buffer (50 mM Tris-HCL, pH 7.4, 100mM NaCl, 0.1 mM EDTA) cushion. Virus was pelleted at 27,000 rpm in a SW-28 rotor on an Optima XPN-90 ultracentrifuge (Beckman). Supernatant was aspirated and 100 µL of Opti-MEM was added to each tube and incubated rocking overnight. The next day, pellets were fully resuspended and aliquoted and snap frozen. Recombinant green fluorescent protein expressing human respiratory syncytial virus A2 (rgRSV) long was a kind gift from Medimmune/Astrazeneca. rgRSV MOI 0.1 was added to HEp-2 cells in Opti-MEM and after 3 h incubation, Opti-MEM with 2 mM glutamine was added and cells were incubated for 4 to 5 days until CPE developed. Cells were then scraped and freeze-thawed 1 time. Cell debris was spun at 2500rpm and supernatant was mixed with sucrose phosphate from a 10x stock to make 1x (Hyclone, special order from Astrazeneca/Medimmune). Virus was then flash frozen. Viral titers determined by infected Vero cells and counting fluorescent particle formation.

Transfection. All HMPV F and protease constructs were transiently expressed using the mammalian expression vector pCAGGS allowing for high levels of protein expression in mammalian cell culture. Cell lines were transiently transfected with plasmid DNA using either Lipofectamine reagent/ Plus reagent (Invitrogen) according to manufacturer's protocol. Mini-replicon plasmids were transiently expressed by transfection using Lipofectamine 3000 reagent (Invitrogen). Manufacturer's protocols were followed accordingly unless stated otherwise. 293 Freestyle cells were transfected using 293-fectin according to the manufacturers protocol.

Syncytia Assay. Vero cells (80-90%) were split into 6-well plates and transiently transfected with 2 µg pCAGGS-HMPV F or empty pCAGGS using Lipofectamine and Plus Reagent. The next day, cells were washed with PBS and incubated for 1hr in Opti-MEM with 0.3 µg/mL TPCK-trypsin. Cells were then rinsed once with PBS pH 7.2 (GIBCO) before adding PBS buffered with 10 mM HEPES and 5 mM MES at low (pH 5) or normal (pH 7) for 4 min. Cells were then placed back in Opti-MEM with TPCK-trypsin for 2 h. These steps were repeated a total of 4 times. After the final treatment, normal culture media was placed on the cells and syncytia formation was observed at 24 to 48h post transfection. Images were taken using a Nikon Ti2 with a 4x or 10x objective. The fusion index (f) was calculated as $f = [1 - (C/N)]$, where C is the number of cells in a field after fusion and N is the number of nuclei.

Luciferase Reporter Gene Fusion Assay. Vero cells in 60 mm dishes were transfected with 1.5 µg of HMPV F wild type or variant and 1.5 µg of T7 control plasmid containing luciferase cDNA (Promega) under the T7 promoter using lipofectamine reagent and plus reagent according to the manufacturers protocol. The next day, Vero cells were lifted with trypsin-EDTA, resuspended in DMEM supplemented with 10% FBS and overlaid onto two 35 mm dishes or two wells in a 6-well plate of confluent BSR cells, which constitutively express the T7 polymerase. Combined cells were incubated at 37°C for 60 min. Cells were then rinsed once with PBS pH 7.2 before adding PBS buffered with 10 mM HEPES and 5 mM MES low or normal pH. Cells were treated for 4 min and then Opti-MEM supplemented with 0.3 µg/mL TPCK trypsin was added and incubated for 1 h at 37°C. Cells were once again treated as described. After treatment, DMEM supplemented with 10% FBS was added and cells were incubated for 4 h at 37°C. Cells were analyzed for luciferase activity according to the luciferase activity system (Promega) and analyzed on the Spectramax iD3 (Molecular Devices).

Gel Electrophoresis and Western Blotting. Protein samples were analyzed via 15% SDS-PAGE, unless otherwise noted. For recombinant protein expression, protein samples were taken pre- and post-induction to assess expression using in-stain gels (Bio-Rad) or using Coomassie staining. For Western blot analysis, immunoprecipitated protein was transferred to polyvinylidene difluoride (PVDF) membrane (Fisher) at 50 V for 80 min at 4°C. After blocking with 5% milk in Tris-buffered saline with 0.05% Tween-20 (TBS-T), membranes were incubated with corresponding antibody. Membranes were washed with TBS-T and incubated with anti-mouse or anti-rabbit 700/800 infrared secondary antibody at 1:10,000 (Jackson). Membranes were washed again with TBS-T and visualized with the Bio-Rad ChemiDoc system or LiCor imaging systems.

Expression, metabolic labelling and immunoprecipitation. Vero cells (approx. 80-90% confluent) in 6-well plates were transiently transfected using Lipofectamine and Plus reagent (4 µg of total pDNA). 18 to 24 h post-transfection, cells were washed with PBS and starved for 45 min in DMEM deficient in cysteine and methionine and subsequently labeled for 3h with cysteine/methionine deficient DMEM containing Tran³⁵S-label (50 µCi/mL; MP Biomedicals). After labelling, wells were washed 2x with PBS and lysed in 500 µL RIPA lysis buffer [100 mM Tris-HCl, pH 7.4, 150 mM NaCl, 0.1% SDS, 1% Triton X-100, 1% deoxycholic acid, 1 mM phenylmethylsulfonyl fluoride, 25 mM iodoacetamide, and complete mini-EDTA protease inhibitor (Roche)] and frozen. Plates were then thawed and scraped. Lysates were centrifuged at 136,500xg for 15 min at 4°C. Supernatants were moved to 1.5 mL Eppendorf tubes and mixed with 6 µg of 54G10 antibody for HMPV F and incubated rocking for 3 h rocking. Proteins were then immunoprecipitated by incubating with 30 µL of Protein A-Sepharose beads (GE Healthcare) for 30 min. The beads were washed 2X with RIPA + 0.30 M NaCl, 2X with RIPA + 0.15 M NaCl, and 2X with SDS Wash II (150 mM NaCl, 50 mM Tris-HCl, pH 7.4, 2.5 mM EDTA).

Surface biotinylation protein labeling. Vero cells (approx. 80-90% confluent) in 6-well plates were transiently transfected using Lipofectamine and Plus reagent (4 µg of total pDNA). 18 to 24h post-transfection, cells were washed with PBS and starved for 45 min in DMEM deficient in cysteine and methionine and subsequently labeled for 3 h with cysteine/methionine deficient DMEM containing Tran³⁵S-label (100 µCi/mL; MP Biomedicals). Cells were washed 3 times with 3 mL of ice-cold PBS pH 8.0, and surface proteins were biotinylated using 1 mg/mL EZ-Link Sulfo-NSH-Biotin (Pierce) in PBS with rocking for 35 min at 4°C followed by incubation at room temperature for 15 min. Cells were then washed 2 times with ice-cold PBS and lysed with 500 µL of RIPA lysis buffer. Cellular lysates were centrifuged at 136,500xg for 15 min at 4°C. The supernatant was placed into a 1.5 mL microcentrifuge tube, and 6 µg of 54G10 antibody was added and incubated rocking for 3h at 4°C. Proteins were then immunoprecipitated by incubating with 30µL of Protein A-Sepharose beads for 30 min. The beads were washed 2X with RIPA + 0.30 M NaCl, 2X with RIPA + 0.15 M NaCl, and 2X with SDS Wash II (150 mM NaCl, 50 mM Tris-HCl, pH 7.4, 2.5 mM EDTA). Then, 60 µL of 10% SDS was added, and the boiled for 10min, removed to a new tube, and repeated with 40 µL of 10% SDS for a total of 100µL. Ten microliters of the supernatant was removed to analyze the total protein population. To the remaining supernatant, 30 µL of Streptavidin beads (Pierce) and 400µL of biotinylation dilution buffer (20 mM Tris (pH 8), 150 mM NaCl, 5 mM EDTA, 1% Triton X—100, 0.2% bovine serum albumin) were then added for 1 h at 4°C with rocking. HMPV F was analyzed by 15% SDS-PAGE and imaged using the Typhoon imaging system (GE Healthcare). Band densitometry was completed using ImageQuantTL to quantify protein expression (% expression= Sum of F₀ and F₁, normalized to WT).

Rescue of mCherry HMPV. The plasmids for rescue of HMPV strain JPS07E2, p(+)-JPS07E2, pCITE-76N, pCITE-76P, pCITE-76M2-1 and pCITE-76L were a kind gift of Dr. Makoto Takeda (National Institute of Infectious Diseases, Tokyo). We replaced the GFP cassette in p(+)-JPS07E2 with an mCherry cassette, using restriction sites NheI and SacI. For virus rescue, BSR cells were transfected with

2.5 µg of p(+)-JPS07E2, 1 µg of pCITE-76N, 1 µg of pCITE-76P, 0.5 µg of pCITE-76M2-1 and 0.5 µg of pCITE-76L using Lipofectamine3000. 48 h post transfection, BSR cells were scrapped and overlaid on top of Vero cells growing in a 60 mm plate. Co-cultured cells were kept in Optimem supplemented with glutamine 2 mM and TPCK-Trypsin 0.3 µg/mL. Virus was harvested at day 6 post-infection and tittered in Vero cells as previously described (288).

Inhibition of HMPV viral infection in cell culture by SPINT2. VERO (200,000) cells were plated into 24-well plates. The following day, cells were infected with MOI 1 rgHMPV for 3 h. Cells were washed with PBS and 500 µL OPTI-mem with or without 500nM SPINT2 (Provided by Dr. Gary Whittaker) and 0.3 µg/mL of TPCK-trypsin was added and incubated for up to 96 h. The SPINT2 and trypsin was replenished in new OPTI-mem every 24 h. For each time point, media was aspirated and 100 µL of OPTI-mem was added to cells followed by scraping and flash freezing. These samples were then titered on confluent VERO cells up to a dilution of 10^{-6} to calculate viral titer. Graph shows 4 independent replicates with internal duplicates plotted as individual points. Some data points not shown are due to sample loss during preparation, with a minimum of 6 points per group and 3 independent replicates.

Cleavage and inhibition of HMPV F by SPINT2. VERO cells were plated into 6-well plates. The following day, 2µg HMPV F or 1:1 with a plasmid containing TMPRSS2, HAT or Matriptase was transfected in using Lipofectamine and plus reagent. The following day, cells were radiolabeled with 50 µC of S^{35} for 4 h and exogenous proteases KLK5 (150 µM), KLK12 (150 µM) and Matriptase (200 µM) were added during the label. 3 µg/mL of TPCK trypsin was used as a control for both transfected and exogenous proteases. For cleavage inhibition, KLK5, KLK12 and Matriptase were pre-incubated with 0 nm, 10 nm or 500 nm of SPINT2 for 10 min and then added to cells for 4 h. Cells were washed and lysed in RIPA lysis buffer and processed for gel electrophoresis and imaging.

Fluorescence-activated cell sorting (FACS) analysis. 50,000 VERO cells were plated into 24 well plates and subsequently infected with rgHMPV or rgRSV with or without prior treatment in Opti-MEM for 3 h and then washed and placed in normal culture media. Cells were then incubated overnight at 37°C. The following day, cells were washed with PBS and lifted with 100 µL of Trypsin-EDTA. Lifted wells were placed into 5 mL snap-cap tubes and mixed 1:1 with 2x fixation buffer [4% paraformaldehyde (PFA), 100 mM EDTA pH 8] for a final concentration of 2% PFA and 50 mM EDTA. Samples were mixed by vortexing and then analyzed by FACS analysis.

Recombinant antibody production. 54G10 recombinant protein expression system was kindly provided by Dr. John Williams (University of Pittsburg, Children's Hospital). Suspension 293F cells were split 1.5×10^7 cells per T-75 flask in 28 mL of expression media. The next day, 60 µL of 293-fectin was mixed with 60 µg of heavy chain plasmid and 60 µg of light chain plasmid in a total of 2mL Opti-MEM (per flask). Cells were then incubated for an additional 4 days and then spun down at 300xg for 5 min and the supernatant was collected and stored at 4°C and the pellet was resuspended in fresh media by vortexing and placed back into the flask to incubate for another 4 days. At day 8 post transfection, cells were spun down, and the supernatant was taken and placed with the previous supernatant and cells were discarded. The supernatant was filtered through a 0.45 µm filter and ran over a gravity flow column containing sepharose beads with protein A to bind antibody. After binding, the column was washed with wash/bind buffer (0.15 M NaCl, 20 mM Na₂HPO₄, pH 7.0). The beads were treated with elution buffer (0.1 M glycine, pH 3.0) and this was eluted into a tube containing neutralization buffer (1 M Tris-HCl, pH 8.5) at roughly 1:10 the volume of elution. Eluted protein was then concentrated using a centrifuge filter (Amicon) (3,000 MWCO) in a swing bucket rotor according to manufacturer recommendation. Once the volume was reduced to 1 mL, an aliquot was tested using the 280nm reading on a nanodrop and protein purity was analyzed by blot analysis.

Confocal Microscopy. HAE tissues were removed from trans-wells and frozen in O.C.T compounding embedding media (EM Sciences). 10-20 μm tissue sections were cut using a MICROM HM525cryostat and collected on Superfrost Plus slides and heat fixed at 55°C for 30 min. Sections were permeabilized in 0.5% Triton X-100 for 15 min at 4°C followed by blocking in 1% normal goat serum. Sections were incubated with primary antibodies for RSV F (1:600), N (1:200), P (1:600) (Abcam) or Keratan Sulfate (1:1,200) (EMD Millipore) overnight at 4°C. The following day, tissues were washed with 0.05% tween-PBS, secondary antibodies (Jackson) and TRITC-Phalloidin (1:1,000) (Invitrogen) were added at room temperature for 1 h, washed and mounted using SloFade plus DAPI (Invitrogen). Pictures were taken using a Nikon A1 confocal microscope and analyzed with NIS-Elements software (Nikon).

Stellaris Fluorescent in situ hybridization (FISH) for viral RNA detection.

Forty-eight DNA probes targeting the HMPV and RSV vRNA genome between nt 1-5,467 were obtained from BioSearch Technologies (Novato, CA) and designed using the software provided by the company. Each probe is 20 nt long and linked at the 3' end to Quasar fluorophore. Cells were fixed for 10-30 min with 4% PFA and then permeabilized overnight with 70% ethanol at 4°C. The next day cells were washed once with 2x SSC-10% formamide buffer, and then incubated overnight at 25°C in hybridization buffer (4x SSC, 1x Denhardt's solution, 150 $\mu\text{g}/\text{mL}$ ssDNA, 2 mM EDTA, 50% formamide in DEPC treated water) containing the probes at a concentration of 2.5 mM. After 24 h, cells were washed two times for 20 min with 2x SSC-10% formamide buffer and slides were then mounted using Vectashield mounting media.

Fluorescence threshold analysis. GFP cells present within infected tissues, were quantified with either NIS elements "object count" or ImageJ (FIJI) using the "adaptive threshold" analysis plugin. Briefly for ImageJ quantification, fluorescent microscopy images of HAE tissues were imported, background subtracted for each image and converted B&W. Using several test images, the adaptive threshold was

set to ensure that all data points with minimal background were obtained, and this macro was used for all images within that replicate. Finally, particle density was quantified using “analyze particles” and total density was quantified as percent area. GFP expression was also analyzed using NIS elements software using threshold analysis based on area coverage using the “object count” plug-in and selecting a fluorescence threshold. All counts were taken as percent area coverage.

Infection of Human Airway Epithelial (HAE) tissues. Human tracheal bronchial differentiated airway (EpiAirway) tissues were purchased from Mattek and maintained in 3 mL of Air-100 media at 37°C for one week prior to infection, with the media changed and the apical surface washed with 0.9% NaCl every other day to remove mucus. Prior to infection, the basal surface was washed with hepes buffered saline (HBS) for 30 min and the apical surface was washed three times with 0.9% NaCl every 10 min with incubation. For HMPV, the apical surface washes were completed using alpha-lysophosphatidylcholine (Sigma) in HBS (75 µg/mL). Tissues were infected with either rgRSV or rgHMPV on the apical surface and incubated for 3 h at 37°C. The apical side of tissues were then washed once with HBS and incubated at 37°C. Media containing 0.3 µg/mL TPCK-trypsin was added to rgHMPV infected tissues and replenished daily. Images were obtained using a Zeiss Axiovert-100 or a Nikon Ti-2. After the final time point, both apical and basal sides were washed with PBS and fixed in 4% paraformaldehyde for 20 min at room temperature.

Microneutralization and spread in HAE tissues. For microneutralization, rgRSV (MOI 1) was preincubated with MEDI8897 or Palivizumab for 1 h at 37°C. rgHMPV (MOI 3) was preincubated with 54G10 for one hour at room temperature. Both rgRSV and rgHMPV incubations were completed in a total volume of 150 µL TEER buffer (Mattek). For spread, HAE tissues were infected with rgRSV (MOI 0.3) or rgHMPV (MOI 3.0). Antibody dilutions were completed in 50 µL of TEER buffer

and added to the apical surface. The initial antibody was added at 6 hpi and replenished every 24 h post inoculation until experiments were completed.

Statistical analysis. Statistical analysis was performed using Prism7 for Windows (Graphpad). A p-value of less than 0.05 was considered statistically significant. Multiple comparisons tests were generated using a one-way ANOVA with a Bonferroni multiple comparison correction. P values are indicated as defined: * $P < 0.05$, ** $P < 0.005$, *** $P < 0.0005$, **** $P < 0.0001$.

Chapter 3: Human metapneumovirus fusion protein triggering: Increasing complexities by analysis of new strains

*This work was completed with the help of Andres Chang and Edita Klimyte, who both contributed intellectually to this work. Andres generated the HMPV F clones from the viral stocks used during all experiments. Edita Klimyte conducted syncytia and luciferase assays used in this chapter (shown in Fig 3.1, I generate the figures for this data). I performed protein expression and cleavage shown in figure 3.2, the protein model for figure 3.3, and the co-expression syncytia and luciferase fusion experiments in figure 3.4. This chapter is adapted from a manuscript (Kinder et al. *Virology*. 2019 May;531: 248-254)

Introduction

Human metapneumovirus (HMPV) is a recently discovered enveloped, negative-sense, single-stranded RNA virus. Although first identified in 2001, HMPV has now been shown to be a cause for respiratory tract infections in humans worldwide since at least 1958 (30-32). Nearly everyone is initially infected by five years of age and reinfection is common throughout life (34). Infection leads to a variety of symptoms ranging from coughing and wheezing to pneumonia and bronchiolitis, potentially requiring hospitalization in severe cases. In addition, infants, immunocompromised, and elderly patients are most likely to develop severe infections (31, 36, 37, 42-46). While HMPV is ubiquitous and responsible for severe upper and lower respiratory tract infections, there is still no FDA approved antiviral treatment or vaccination available. Therefore, a more thorough understanding of the viral lifecycle and molecular mechanisms required for infection are needed to discover novel antiviral targets.

HMPV is phylogenetically classified into two genetic lineages (A and B) and further characterized into sub-lineages (A1, A2, B1 and B2) based on the sequences of two surface glycoproteins: the fusion protein (F) and the attachment protein (G) (78). To infect cells, enveloped viruses fuse their membrane with host cell membranes, a process mediated by one or more viral surface glycoproteins.

In the instance of HMPV, this process is mediated by F alone *in vitro* and *in vivo*, whereas closely related paramyxoviruses require both F and G (157, 189, 334). F is a homo-trimeric class I fusion protein present within viral membranes as well as membranes of infected host cells. To become activated, F is proteolytically cleaved from the precursor form (F₀), into the metastable, disulfide-linked heterodimer (F₁+F₂) (158, 159). Cleavage can be accomplished by the addition of exogenous trypsin *in vitro* (189), although *in vivo* it is thought that F is cleaved by secreted or cell surface proteases present in the host. Once cleaved, HMPV F can be triggered to undergo an essentially irreversible and energetically favorable conformational change from the pre-fusion form to the post-fusion state with released potential energy driving membrane fusion (189, 240-242).

HMPV particles have been shown to be internalized via clathrin mediated endocytosis in human bronchial epithelial cells through a dynamin dependent mechanism (242, 335). Further evidence demonstrated that for HMPV, viral and host membrane fusion takes place within the endosomes (335). Some strains of HMPV, mainly within clade A, utilize low pH generated through endosomal acidification as a mechanism to trigger the fusion protein, similar to HA from influenza. However, this is proposed to not be true for all strains of HMPV (189, 240-242, 335). For fusion proteins that are triggered by low pH, it is hypothesized that repulsive electrostatic forces between critical residues lead to global protein destabilization, initiating the conformational transition from the pre-fusion to post-fusion state (336-338). It has been proposed that specific histidine (H) residues become protonated at low pH and subsequently interact with neighboring basic residues to destabilize the pre-fusion state and initiate membrane fusion. In HMPV F, H435 within the globular head is thought to serve as a pH sensor (241, 242). Recently, a high-resolution structure of a stabilized pre-fusion HMPV F [NL/1/00(A1)] was solved [PDB: 5WB0] (205). This structure revealed that lysine (K) 20 and glutamic acid (E) 433 interact to form a potential salt bridge. Under low pH conditions, protonation of the neighboring H435 may lead to cation electrostatic repulsion driving conformational changes and promotes membrane fusion. Studies with recombinant HMPV containing mutations in this region have confirmed its

importance for viral infectivity (239, 241). Additional residues have been identified as playing a role in low pH triggered fusion, including K296, W396, and N404. Furthermore, studies using F proteins from prototype strains from each clade have suggested that fusion induced by low pH is restricted to clade A virus fusion proteins, and glycine (G) 294 is critical for low pH triggered fusion (240, 241). However, few HMPV F proteins have been studied in each clade and therefore additional analysis is needed to further understand this mechanism.

In this study, we examined three previously uncharacterized HMPV F proteins for their fusion activity, protein expression, and cleavage activation levels. The first F protein, cloned from TN83-1211, contained a unique H434 residue, adjacent to a previously characterized histidine at 435 demonstrated to be critical for low pH fusion. Protein mutagenesis in our reference strain supports its contribution to increased fusion at low pH and more efficient cleavage by trypsin. The second F protein, cloned from TN94-49, is able to promote low pH mediated fusion without G294, although this residue was previously identified as critical for this mechanism of membrane fusion. The third HMPV F protein, cloned from TN96-12, contains E at position 294. Interestingly, TN96-12 was unable to mediate fusion at either neutral or low pH conditions, or in the presence of the attachment protein, G. This finding suggests additional factors are necessary to trigger the F protein. Taken together, these results further demonstrate the complexity of HMPV F mediated membrane fusion and the significant phenotypic differences observed with only a few amino acid changes.

Results

To examine HMPV fusion, F protein genes were cloned from three available HMPV strains: TN94-49, TN96-12 and TN83-1211, all isolated in the Williams laboratory and propagated and stored at BEI resources. These F isolates were sequenced and compared to a low pH prototype strain, CAN97-83, used as a positive control in these studies. HMPV F is highly conserved, and therefore few

amino acid changes were detected between strains. The TN94-49 F clone differed from CAN97-83 F by only 6 amino acids (Fig 3.1D). One notable difference was residue 294, which contained K294 instead of G294, a glycine residue previously suggested as essential for low pH triggered fusion for clade A HMPV F proteins (240). When comparing TN96-12 F clone to CAN97-83 F, 9 amino acid changes were present, including E294 instead of G294. Lastly, the F isolate from TN83-1211 only differed from CAN97-83 by two amino acids, S175 and H434, and did not match the published isolate sequence of TN83-1211. However, this mutation was present in several clones analyzed, suggesting the viral stock may have had a heterogeneous population of virus present. For clarity, we refer to this protein as S175H434 F. The presence of a unique amino acid in S175H434, H434, instead of the highly conserved Q434 in all other published strains, led us to further study this F isolate. The neighboring residue H435 is hypothesized to play a critical role in electrostatic repulsion with neighboring residues after protonation at low pH, acting as a physiologic timing sensor to promote fusion. Based on these findings, we hypothesized that the second histidine at position 434 could potentially be involved in fusion of S175H434 after exposure to low pH, similar to the function observed for H435. In addition, TN94-49 containing K294 and TN96-12 containing E294 were of interest to assess the role of these amino acids in low pH mediated fusion compared to G294.

To determine whether these F isolates were able to promote neutral or low pH- mediated membrane fusion, we first conducted a syncytia assay. As previously reported, CAN97-83 F promoted fusion when exposed to low pH and was therefore used as a positive control for low pH triggered fusion (Fig. 3.1A). TN94-49 F generated syncytia following low pH treatment, similar to CAN97-83 F, but no syncytia formation was observed at neutral pH. Interestingly, TN96-12 F was unable to generate cell-to-cell fusion at both neutral and low pH, whereas S175H434 F generated minimal background syncytia at neutral pH and robust syncytia formation after exposure to low pH that was significantly higher than the syncytia observed with CAN97-83 F (Fig 3.1A, quantified in 3.1B). To confirm our findings in the syncytia assay, we utilized a luciferase reporter assay as a second

cell-to-cell fusion assay metric. Consistent with the syncytia assay, TN94-49 F exhibited no fusion above background at neutral pH, and low pH induced activity similar to that of CAN97-83 F, while S175H434 F exhibited significantly higher (nearly 500%) low pH-induced fusion activity compared to CAN97-83 F. Again, TN96-12 F-mediated fusion was undetectable above background levels (Fig 3.1C).

F S175H434 differs from CAN97-83 F by only two amino acids yet demonstrates significantly increased low pH-induced membrane fusion (Fig 3.1 A-C). H435 has been implicated in low pH-mediated triggering, so it appeared that H434 might serve a similar role. To examine the contribution of H434 in fusion, we generated a point mutation in CAN97-83 WT F using site-directed mutagenesis, changing Q at position 434 to H (CAN97-83 Q434H). We then conducted both syncytia and luciferase reporter assays to examine fusion activity of this mutant. Interestingly, syncytia assays demonstrated that CAN97-83 Q434H was able to recapitulate the high level of fusion observed for S175H434 (Fig 3.1A), and quantification of the fusion activity demonstrated a similar fusion profile to that of S175H434 (Fig 3.1B). The luciferase reporter assay again confirmed that CAN97-83 Q434H demonstrated fusion activity similar to S175H434 and significantly higher than WT CAN97-83 F (Fig 3.1C). Together, these results demonstrate that the hyperfusogenic phenotype observed in S175H434 is primarily mediated by a single amino acid change, Q434H.

Fusion mediated by F requires that the protein is synthesized, trafficked to the surface and proteolytically processed. As fusion is correlated with cell surface expression and cleavage activation, we utilized radioactive metabolic labelling coupled with surface biotinylation to examine both total and surface protein expression and cleavage activation profiles for each F isolate. Interestingly, we identified significant differences in the total and surface protein expression levels between the F proteins. Compared to CAN97-83 WT F, TN94-49 F had similar levels of total (F_0+F_1) and surface expression, (Fig 3.2A and quantified in 3.2B), which correlated with the similar fusion activities found for these proteins (Fig 3.1C). The two F proteins shown to promote high levels of fusion, S175H434 and

CAN97-83 Q434H, both displayed higher average total protein expression (approximately 6-fold and 3-fold, respectively, compared to CAN97-83 F; Fig 3.2A and 3.2B), though this difference was only statistically significant for S175H434 F. The two highly fusing F proteins also displayed higher average surface protein expression (approximately 10-fold and 7-fold, compared to CAN97-83), though again statistical significance was only reached for S175H434 F. These results suggest that higher surface expression levels may be at least partially responsible for the higher levels of fusion observed for S175H434. However, TN96-12 F failed to promote fusion, despite similarly high surface expression, demonstrating that surface expression is only one factor contributing to overall fusion (Fig 3.1B). These findings demonstrate that a single amino acid change was able to increase the fusion protein expression compared to WT, suggesting that this area of the protein is involved in protein stability or turnover and offering a potential explanation for the phenotypes observed.

HMPV F is synthesized as an inactive, monomeric protein that must be proteolytically processed into the heterodimeric, disulfide linked F₁ and F₂, in order to mediate fusion. *In vitro*, exogenous trypsin cleaves the protein within the cleavage motif to generate the fusogenically active form. Due to the requirement of cleavage for fusion, we examined the relative amount of trypsin cleavage for each F variant. To identify a potential role for proteolytic activation by trypsin on fusion activity, percent cleavage $\left[\left(\frac{F_1}{F_0+F_1}\right) \times 100\right]$ was quantified for the surface population of F (Fig 3.2C). Interestingly, F variants that were more highly expressed, S175H434, TN96-12, and CAN97-83 Q434H were cleaved at significantly higher levels than CAN97-83 or TN94-49, potentially contributing to the observed hyperfusogenic phenotypes (Fig 3.2C). Though the higher levels of CAN97-83 Q434H protein expression did not reach statistical significance, this protein displayed significantly higher levels of protein cleavage compared to CAN97-83 WT F.

These findings suggest the hyperfusogenic phenotypes observed for S175H434 F were due in part to the presence of higher levels of F at the surface

as well as increased cleavage activation. The finding that CAN97-83 Q434H yielded significantly increased membrane fusion and cleavage suggests H434 is important for this phenotype. Conversely, TN96-12, which failed to mediate cell-to-cell fusion in both syncytia and luciferase reporter assays, was significantly more abundant in total, and approaching significantly higher surface populations ($p=0.0685$). In addition, it was cleaved significantly higher when compared to CAN97-83 F. Although cleaved significantly higher when compared to CAN97-83 F, TN96-12 F was unable to mediate fusion in cell-to-cell fusion assays suggesting there may be other factors necessary for triggering of this F isolate which are not present on the cell surface.

Discussion

In this study we examined the fusion activity, expression, and cleavage of three previously uncharacterized F proteins. Previously, we have reported low pH-promoted membrane fusion for CAN97-83, and others have reported this phenomenon only within clade A strains of HMPV (189, 240-242), with a glycine residue at position 294 (G294) described as a requirement for low pH-promoted fusion (240). However, TN94-49 F contains a lysine (K) at this position and promotes fusion after exposure to low pH, indicating that either of these residues can be present at position 294 in an HMPV F protein which promotes low pH-induced fusion (Fig 3.3). Genetic variability analysis of HMPV F proteins demonstrated that position 294 is one of two positively selected sites with relaxed selective constraints for the amino acids G, K or E, indicating that when one of these are present at this position, viral fitness is unaffected (339). Analyses from the Melero group (240, 241) indicated that E294 was present with neutral pH fusing F proteins, while previous results from several groups showed low pH fusion with F proteins containing G294. Our findings demonstrate that K294 can also be present in a low pH induced F protein. Additional amino acids at positions 296, 396 and 404 (Fig 3.3) have been described to modulate low pH fusion sensitivity (241). However, these amino acids are completely conserved in the strains of HMPV examined in this study.

HMPV F S175H434 displayed a hyperfusogenic phenotype and significantly increased protein expression of both total and surface populations compared to CAN97-83 F, but only two amino acid changes were present between the two proteins. One notable amino acid difference was H434, which is in close proximity to a previously identified amino acid, H435, shown to be important for low pH triggered fusion. We generated a CAN97-83 mutant, containing Q434H, and demonstrated this single amino acid mutation could recapitulate the hyperfusogenic phenotype and expression patterns observed for S175H434 F. Due to its close proximity, H434 may contribute to low pH mediated fusion through a similar mechanism to H435, which has been hypothesized to interact with surrounding residues and, upon protonation, destabilize the pre-fusion form to initiate refolding to the post-fusion form. Recently, a high-resolution pre-fusion structure of HMPV F was published. Examination of the structure suggests the need for destabilization in the heptad repeat B region to trigger the refolding event to the post-fusion conformation (205). This structure also suggests a model for the role of H435 in fusion, as a potential electrostatic disruption between E433 and K20 by protonated H435 upon acidification could provide this destabilization (Fig 3.3A and 3.3C). Additionally, K438 could play a role given the close proximity of the residue to the H434 and H435 amino acid positions, potentially enhancing this destabilization and increasing fusion activity (Fig 3.3A and 3.3D) (239). Lastly, there are significant differences in the overall protein expression of F from the examined strains, suggesting a potential role in protein folding, overall stability, or turnover rates for H434. When examining known sequences of HMPV F proteins, H434 was not present, which suggests that the hyperfusogenicity conferred by this amino acid may not be beneficial to HMPV infectivity. For parainfluenza virus 3 (PIV3), a closely related paramyxovirus, enhancement of receptor binding and fusion within the monolayer was detrimental for replication in human airway epithelium and *in vivo* during infection in cotton rats (328). However, when examining a hyperfusogenic F protein mutant from a more closely related pneumovirus, respiratory syncytial virus, there were increased viral loads, severe lung pathology and weight loss in mice compared to controls (301), so whether

hyper-fusogenicity is preferentially selected by HMPV during infection is not well understood. Interestingly, when HMPV was incubated with the neutralizing monoclonal antibody 54G10, one of the detected escape mutations was Q434H. No changes in binding affinity of 54G10 for the Q434H mutant were detected, suggesting that this mutation may introduce structural changes into the F protein which provide some potential benefit (340).

Our results show that TN96-12 was also highly expressed in both total and surface populations but does not mediate fusion in cell-to-cell fusion assays. Co-expression of TN96-12 F with G at neutral or low pH was not sufficient to induce syncytia formation in cell culture (Fig 3.4A and 3.4B), indicating that lack of the G protein is not the reason for the absence of fusion. TN96-12 HMPV is a clinical isolate, able to initiate infection in patients as well as propagate in cell culture, and thus must have a functional fusion protein. Therefore, our findings point toward the need for other host factors required for fusion of some HMPV strains in order to escape the endosome and initiate infection, and the lack of fusion in our assays suggests these factors may not be present on the cell surface. Currently, heparan sulfate proteoglycans and RGD binding integrins are proposed cellular factors for association and entry of HMPV through endocytosis (123, 243, 335, 341). It is possible that there are other critical factor(s) within the endosome that interact with HMPV F and trigger the fusion protein, similar to the use of the endosomal receptor NPC-1 by Ebola virus GP (234).

Taken together, the results in this study highlight the diversity of HMPV F activity and the complexity associated with fusion. Our results indicate that the contribution of a single amino acid can be responsible for observed phenotypes, demonstrating that minor evolutionary changes can lead to significant phenotypic differences that alter HMPV infection and tropism. Further studies are necessary to better understand and elucidate key contributing factors of fusion protein stability, cleavage and host factor interaction required for HMPV infection, as well as which key residues and regions of the F protein are vital for fusion and entry of the virus.

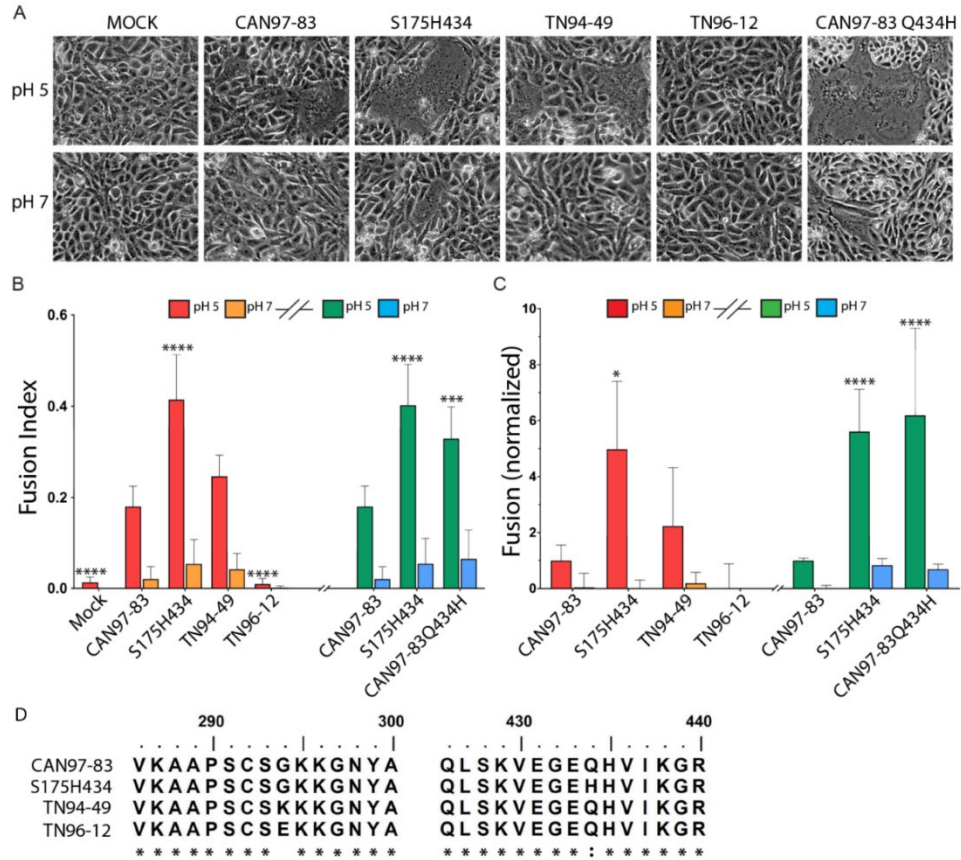


Figure 3.1. HMPV F proteins from different strains exhibit variable fusion activity promoted by low pH. (A) Representative images of syncytia formation of cells expressing the HMPV F proteins after pulses at pH 5 or pH 7 ($n = 3$). (B) The fusion index was calculated using the equation $f = [1 - (C/N)]$ where C is the number of cells in a field after fusion and N, the number of nuclei. Six fields were scored per condition representative of 3 independent experiments. “*”s indicate statistical significance compared to fusion for CAN97-83 (A2) F after pH 5 pulses ($n=3$) [* $p<0.05$, ** $p<0.005$, *** $p<0.0005$ and **** $p<0.0001$]. Graph was broken into two experiments (denoted by the graph break and colors: red/orange bars represent independent experiment from green/blue). Statistical significance within these assays is compared to CAN97-83 within each independent experiment. (C) Luciferase reporter gene assay of Vero cells transfected with HMPV F upon which BSR cells were overlaid and subjected to two pH pulses. Data are presented and normalized to CAN97-83 (A2) F luminescence (fusion) at pH 5 ($n = 3$) +/- standard deviation. * Indicates statistical significance compared to CAN97-83 F after pH 5 pulses. Graphical representation and statistics were conducted as described in B. (D) Partial protein sequence analysis of F from 4 strains of HMPV surrounding key residues at positions 294 and 435. Sequence alignment was generated using ClustalW. The asterisk “*” indicates identical residues and the colon “:” indicates conserved substitutions.

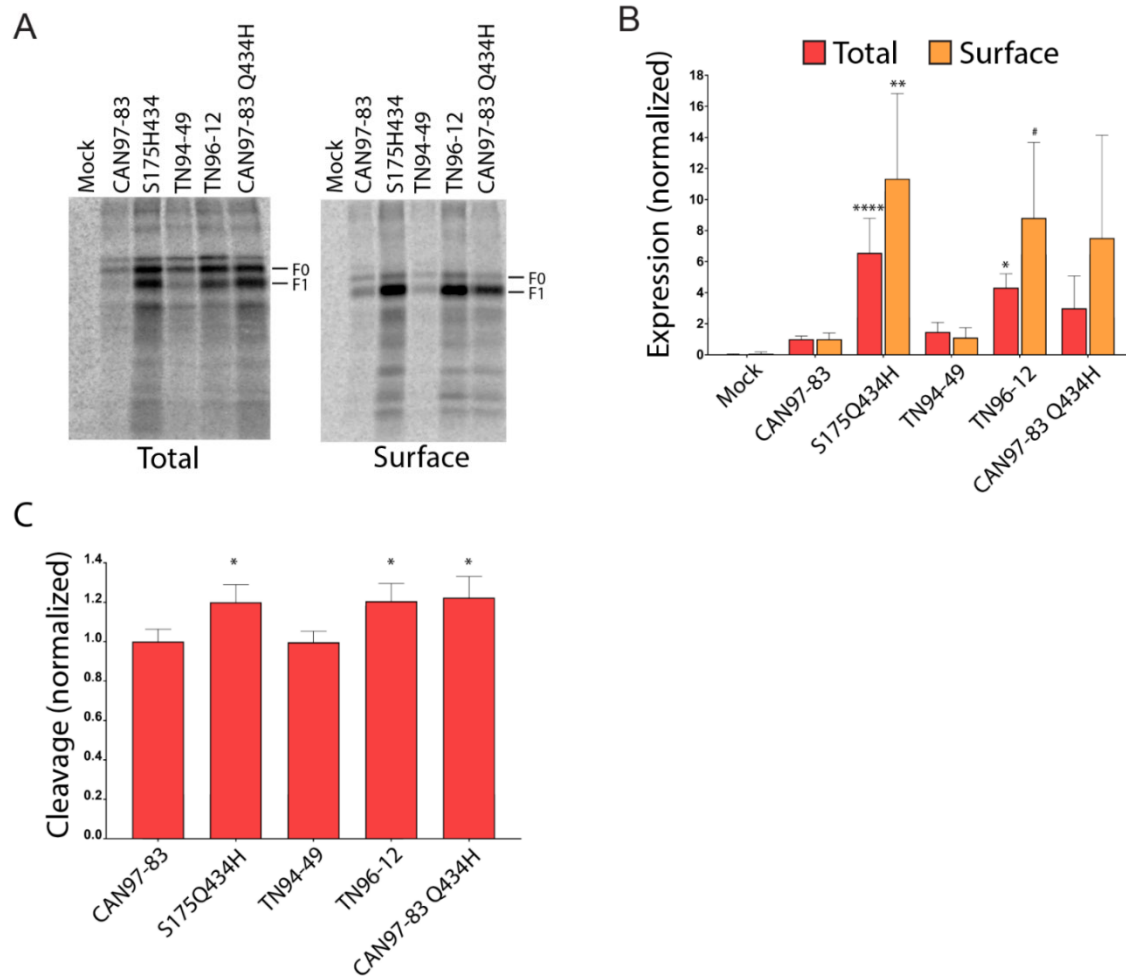


Figure 3.2. HMPV F protein expression and cleavage by exogenous trypsin. (A) Representative gels of total and surface protein expression in metabolically labeled Vero cells expressing empty vector pCAGGS-MCS (Mock), CAN97-83 F, S175H434 F, TN94-49 F, TN96-12 F, and mutant CAN97-83 Q434H F in the presence of 3.0 μ g/ml of TPCK-trypsin. **(B)** Quantification of the total and surface protein populations for F (F₀ and F₁ forms) in metabolically labeled Vero cells. Data are presented as normalization to CAN97-83 (A2) F expression, which was set to 1 (n = 4). “*”s Indicate statistical significance compared to F for CAN97-83 F (n= 4) [# P<0.07, * p<0.05, ** p<0.005, *** p<0.0005 and **** p<0.0001]. **(C)** Quantification of the relative amount of fusion protein cleavage within the surface population of F calculated using F₁/(F₁ + F₀) and normalized to CAN97-83, set as 1.

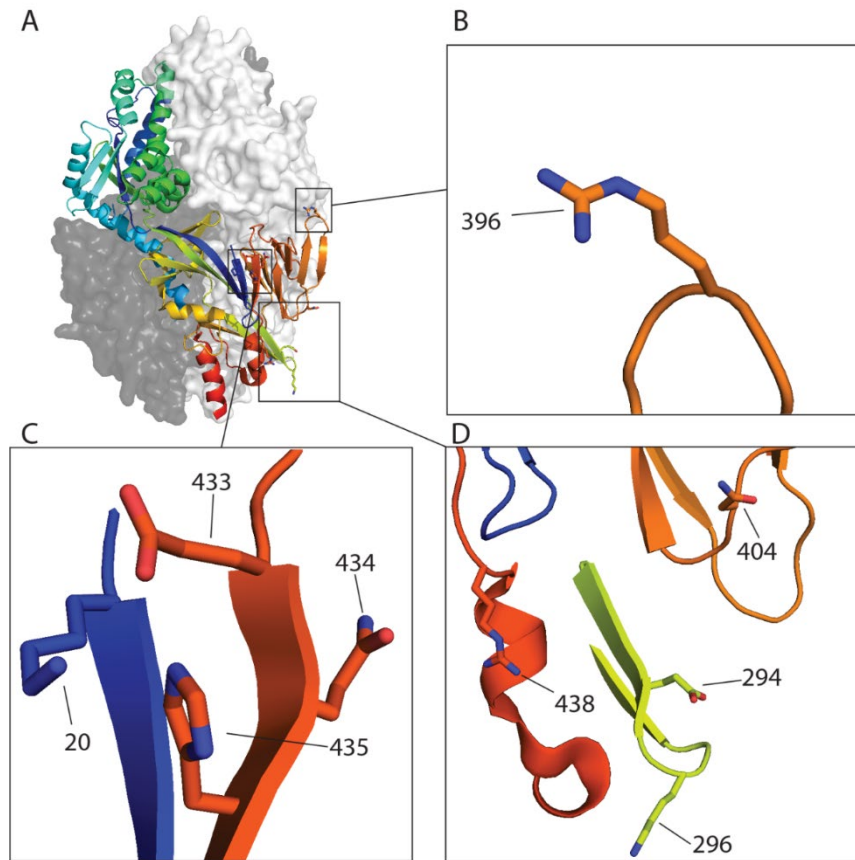


Figure 3.3: HMPV residues identified thus far involved in low pH mediated fusion. A) The pre-fusion homo-trimeric structure of HMPV F of NL/1/00 (pdb: 5WB0) with residue positions identified for low pH fusion highlighted including **(B)** 396 **(C)** 20, 433, 434, 435 **(D)** 294, 296, 396, 404 and 438. Images generated using Pymol protein structure software.

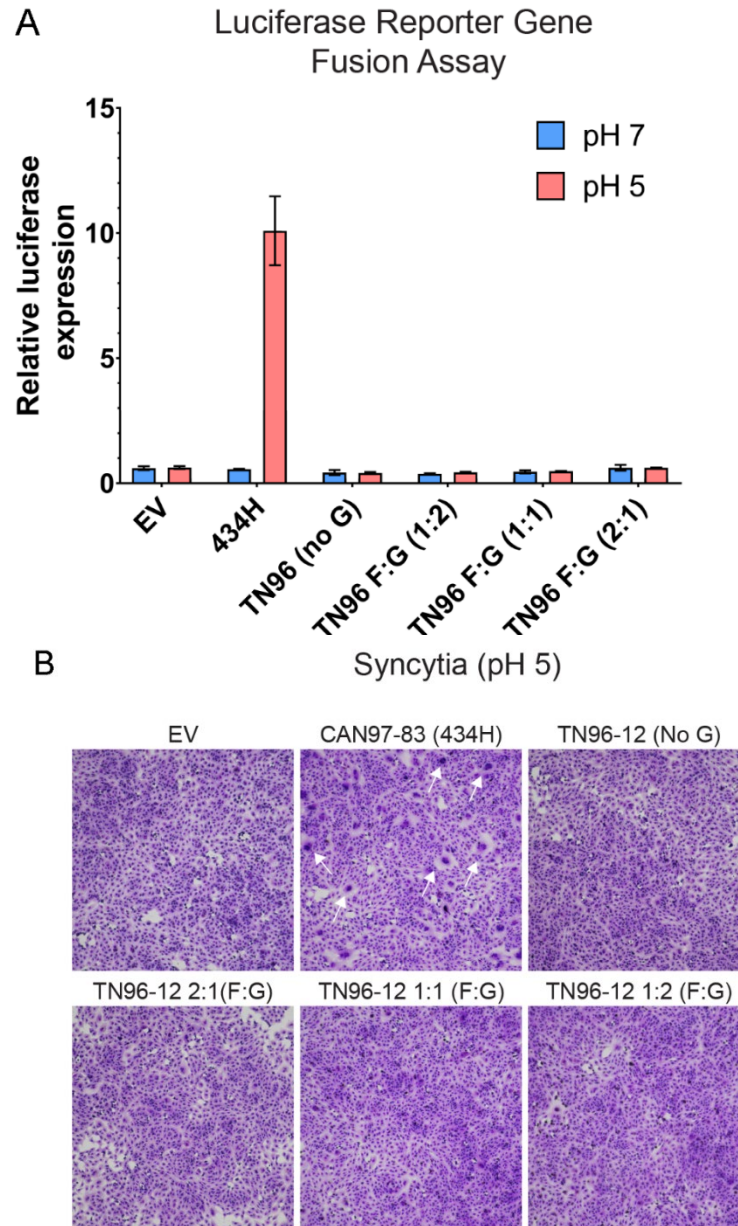


Figure 3.4: Addition of HMPV G to TN96-12 F is unable to mediate fusion at low pH. A) HMPV F (TN 96-12) was co-transfected with or without G at various ratios in VERO cells and fusion activity was measured in a luciferase reporter assay. B) Co-transfected cells were subjected to H&E staining and bright field microscopy to examine syncytia formation. White arrows indicate presence of multinucleated syncytia present in the representative field. Error bars represent the standard deviation of two independent replicates completed in duplicate.

Chapter 4: SPINT2 inhibits proteases involved in activation of both influenza viruses and metapneumoviruses

* This work was completed in collaboration with Dr. Marco Strauss and Dr. Gary Whittaker (Cornell University) who provided constructs for TMPRSS2, HAT and Matriptase enzymes as well as completing the peptide cleavage assay and kinetics for HMPV F (Table 4.1). In addition, they conducted all of the influenza assays and corresponding figures (Figures 4.1, 4.2, 4.4, 4.5, and 4.7). I performed all other experiments and generated the associated figures (Figures 4.3 and 4.6). This chapter was adapted from a co-written manuscript (Kinder and Straus et al 2020. *Virology*. 543:43-53).

Introduction

Influenza-like illnesses (ILIs) represent a significant burden on public health and can be caused by a range of respiratory viruses in addition to influenza virus itself (342). An ongoing goal of anti-viral drug discovery is to develop broadly acting therapeutics that can be used in the absence of definitive diagnosis, such as in the case of ILIs. For such strategies to succeed, drug targets that are shared across virus families need to be identified.

One common cause of influenza, which shaped the term ILI, are influenza A viruses (IAV), including H1N1 and H3N2, that cross species barriers from their natural avian hosts and infect humans (343, 344). Novel emerging viruses such as H7N9 that has caused hundreds of deaths since its appearance in China in 2013 pose an additional concern (345). The World Health Organization (WHO) estimates that each year about 1 billion suffer from flu infections, 3 to 5 million people worldwide are hospitalized with severe illness and approximately 290,000 to 650,000 people die from the disease (346). Mortality rates can dramatically rise during influenza pandemics as observed with the Spanish flu of 1918, the Asian pandemic of 1957 and the Hong Kong pandemic of 1968 (344, 347). Vaccinations can provide an effective protection against seasonal and pandemic outbreaks but provide limited or no protection when viruses evolve and/or acquire mutations

resulting in antigenically distinct viruses. This antigenic drift or shift requires that new vaccines be produced quickly and in vast amounts which can be problematic especially during pandemics. In addition to vaccines, several antiviral therapies have been applied to treat influenza A infections such as adamantanes acting as M2 ion channel blockers (amantadine, rimantadine) and neuraminidase inhibitors which block the cleavage of sialic acid in newly formed virions (oseltamivir, zanamivir) (348). However, several influenza subtypes including the most common H1N1 and H3N2 have emerged globally that are resistant against adamantanes and similar observations were made with respect to oseltamivir (348). More recently, baloxavir marboxil (BXM) which is an inhibitor of the influenza polymerase acidic subunit (PA) was approved as an antiviral therapy (349). Although it is fully effective against currently circulating influenza A and B viruses clinical trial studies have already shown that treatment with BXM selects for influenza virus with specific amino acid substitutions in PA resulting in reduced susceptibility to the drug (350, 351).

Another common cause of ILI are pneumo- and paramyxoviruses, including human metapneumovirus (HMPV), respiratory syncytial virus, and parainfluenza viruses. Clinical presentation of these viruses resembles many of the symptoms of influenza, where they cause significant morbidity and mortality as well as a large economic burden (352, 353). HMPV is ubiquitous, with nearly everyone infected by the age of 5 and reinfection is common throughout life, impacting children, the elderly and immunocompromised individuals (30, 36, 354). While HMPV is a common cause of ILI, there are currently no approved vaccines or antiviral therapeutics. Further research is needed to establish targets for intervention, and factors required for infection need to be examined in more detail.

Certain influenza viruses and HMPV appear to share common activating proteases. The influenza fusion protein hemagglutinin (HA) is synthesized as a precursor that needs to be cleaved by host cell proteases to exert its fusogenic activity (355, 356). Cleavage separates the precursor HA₀ into HA₁ and HA₂, which remain associated via disulfide bonds and leads to exposure of the fusion peptide

at the N-terminus of HA₂ (355, 356). Low pathogenicity avian influenza (LPAI) usually possess a monobasic cleavage site which consists of 1 – 2 non-consecutive basic amino acids and which is generally cleaved by trypsin-like serine proteases such trypsin, as well as members of the type II transmembrane serine protease (TTSP) family including TMPRSS2, TMPRSS4, HAT (TMPRSS11D) and matriptase (355-357). In addition, some other proteases such as KLK5 and KLK 12 have been implicated in influenza pathogenicity (177). In humans these proteases are localized in the respiratory tract and therefore influenza infections are usually confined to this tissue. In contrast, highly pathogenic avian influenza (HPAI) viruses are defined by a polybasic cleavage site which consists of 6 – 7 basic residues allowing them to be activated by members of the proprotein convertase (PC) family such as furin and PC6 (358). These proteases are not confined to a specific tissue and dramatically increase the risk of a systemic infection.

Similar to influenza HA, HMPV requires the fusion protein (F) to be proteolytically processed at a single basic residue to generate the active, metastable form. Without this cleavage process, the F protein is unable to mediate viral entry into the target cell. However, to date, only trypsin and TMPRSS2 have been shown to effectively cleave HMPV F and other proteases have yet to be identified (189, 192).

In addition, other respiratory viruses have been reported to utilize similar proteases for activation, including SARS-CoV and MERS-CoV, demonstrating that targeting these proteases would inhibit multiple respiratory pathogens (359). The fact that proteolytic activation is such a crucial step for several respiratory viruses that predominately require a specific class of proteases makes these proteases a viable target for the development of novel antiviral therapies (360). Earlier studies described the administration of the serine protease inhibitor aprotinin to inhibit influenza replication and demonstrated that aprotinin successfully inhibited IAV activation and replication (361). However, when targeting host specific factors there are potential off target effects, and therefore the potential side effects of

targeting host proteases requires further investigation. Hamilton et al. reported that the hepatocyte growth activator inhibitor 2 (HAI-2) effectively inhibited trypsin-mediated cleavage of H1N1 and H3N2 *in vitro* and *in vivo* (362). HAI-2 is encoded by the SPINT2 gene and hereafter we will also refer to the protein as SPINT2. SPINT2 is 225 KDa plasma membrane-localized serine protease inhibitor found in epithelial cells of various tissues including the respiratory tract and all major organs (363). In most tissues, SPINT2 co-localizes with matriptase suggesting a regulatory role of SPINT2 on matriptase-mediated cleavage events. However, the finding that SPINT2 is also expressed in brain and lymph node cells indicates that it might regulate other proteases than matriptase (363). Recent reports associated the physiological role of SPINT2 with the inhibition of human serine-type proteases such as matriptase, plasmin, kallikreins (KLK) and coagulation factor Xia (364-367). SPINT2 possesses one transmembrane domain and two kunitz-type inhibitor domains that are exposed to the extracellular space and which are believed to facilitate a potent inhibition of target proteases. Wu et al. recently described that the kunitz-type domain 1 of SPINT2 is responsible for matriptase inhibition (367). A major function of SPINT2 is its role as a tumor suppressor because down-regulation diminishes the prospect of survival of several cancers such as hepatocellular carcinoma, gastric cancer, prostate cancer or melanoma (368-371). However, SPINT2 was also associated with placenta development and epithelial homeostasis (372, 373).

A previous study from our lab described the effective inhibition of trypsin by SPINT2 resulting in dramatically reduced cleavage of influenza A HA using a model protease and subsequently reduced viral growth in cell culture and mouse studies (362). Here, we report that purified SPINT2 protein inhibits several host proteases found in the human respiratory tract, such as matriptase and TMPRSS2, that are relevant for the activation of influenza viruses currently circulating and causing significant disease outbreaks. To demonstrate broad applicability, we also tested the potential of SPINT2 to inhibit the activation of the fusion protein (F) from human metapneumovirus (HMPV), a member of the pneumovirus family. We confirm the original findings that HMPV F is proteolytically processed by trypsin

and TMPRSS2. In addition, we found that HAT, KLK5 and matriptase were able to cleave F, but KLK12 could not. Our results show that SPINT2 can inhibit the activation of proteases that are responsible for the activation of influenza H1N1, H3N2 and H7N9 HA as well as HMPV F. In a cell culture model, we demonstrate that viral loads are significantly reduced in the presence of SPINT2 when infections were conducted with A/CA/04/09 and A/X31. Moreover, the application of SPINT2 24 h post infection inhibited the activation of influenza A viruses with the same efficacy as when SPINT2 was added to cell culture medium at the time of infection. Thus, SPINT2 exhibits the potential to serve as a novel and efficient antiviral therapeutic to relieve patients from influenza A, human metapneumovirus, SARS-CoV and potentially other respiratory viruses that require these host factors for entry.

Results

SPINT2 inhibits recombinant human respiratory tract proteases that cleave HMPV F and HA cleavage site peptide mimics

Using a fluorogenic peptide cleavage assay that utilizes fluorogenic peptides mimicking the HA cleavage site we previously tested the ability of SPINT2 to inhibit proteases shown to cleave HAs from seasonal and pandemic influenza A strains that infected humans (171, 374). We found that certain HA subtypes such as H1, H2 and H3 are cleaved by a wide variety of human respiratory proteases while others such as H5, H7 and H9 displayed more variability in cleavage by proteases and seemed less well adapted to proteases present in the human respiratory tract (171). Here, we extended our previous study and tested a peptide mimicking the cleavage site of the pneumovirus fusion protein of HMPV F using a variety of proteases known for their ability to cleave the peptide mimic (Table 4.1A) (189, 190). When we tested the cleavage of a peptide mimicking the HMPV F cleavage site using trypsin, matriptase, KLK5, KLK12, HAT or plasmin we found that all proteases except KLK12 were able to proteolytically cleave the peptide (Table 4.1A). However, the V_{max} values for matriptase (9.24 RFU/min), KLK5 (5.8

RFU/min) and HAT (2.99 RFU/min) were very low compared to trypsin (135.2 RFU/min) suggesting that the three proteases have a low affinity interaction and processivity for HMPV F.

Next, trypsin, matriptase and KLK5 were selected for the SPINT2 inhibition assays as described below. For the SPINT2 inhibition assays, trypsin (which typically resides in the intestinal tract and expresses a very broad activity towards different HA subtypes and HMPV F) served as a control (375). In addition, furin was used as a negative control that is not inhibited by SPINT2. As none of the peptides used in combination with the aforementioned proteases has a furin cleavage site we tested furin-mediated cleavage on a peptide with a H5N1 HPAI cleavage motif in the presence of 500 nM SPINT2. We continued by measuring the V_{max} values for each protease/peptide combination in the presence of different SPINT2 concentrations and plotted the obtained V_{max} values against the SPINT2 concentrations on a logarithmic scale. Using Prism7 software, we then determined the IC_{50} that reflects at which concentration the V_{max} of the respective reaction is inhibited by half. SPINT2 cleavage inhibition of a representative H1N1 cleavage site by trypsin results in an IC_{50} value of 70.6 nM (Table 4.1B) while the inhibition efficacy of SPINT2 towards matriptase, HAT, KLK5 and KLK12 ranged from 11 nM to 25 nM (Table 4.1B). However, inhibition was much less efficient for plasmin compared with trypsin (122 nM). We observed a similar trend when testing peptides mimicking the H3N2 and H7N9 HA cleavage sites using trypsin, HAT, KLK5, plasmin and trypsin, matriptase, plasmin, respectively (Table 4.1B). With the exception of plasmin, we found that human respiratory tract proteases are inhibited with a higher efficacy compared to trypsin. We expanded our analysis to peptides mimicking HA cleavage sites of H2N2, H5N1 (LPAI and HPAI), H6N1 and H9N2 that all reflected the results described above (Table 4.1B). Only cleavage inhibition of H6N1 HA by KLK5 did not significantly differ from the observation made with trypsin (Table 4.1B). When we tested the inhibition of HMPV cleavage by trypsin, matriptase and KLK5, SPINT2 demonstrated high inhibition efficacy for all three tested proteases with measured IC_{50} for trypsin, matriptase and KLK5 of 0.04 nM, 0.0003 nM and 0.95 nM, respectively (Table 4.1C). Compared to the IC_{50}

values observed with the peptides mimicking influenza HA cleavage site motifs the IC₅₀ values for the HMPV F peptide were very low.

Cleavage of distinct full-length HA subtypes and HMPV F is efficiently inhibited by SPINT

Cleavage of peptides mimicking cleavage sites of viral fusion proteins do not always reflect the *in vivo* situation and requires validation by expressing the full-length fusion proteins in a cell culture model to test cleavage and cleavage inhibition of the respective protease (171). However, before conducting these experiments we wanted to ensure that SPINT2 does not have a cytotoxic effect on cells. Therefore, 293T cells were incubated with various concentrations of SPINT2 over a time period of 24 hours. PBS and 500µM H₂O₂ served as cytotoxic negative and positive controls respectively. We observed a slight reduction of about 10 -15 % in cell viability when SPINT2 was added to the cells (Fig 4.1).

To test SPINT2-mediated cleavage inhibition of full-length HA we expressed the HAs of A/CA/04/09 (H1N1), A/x31 (H3N2) and A/Shanghai/2/2013 (H7N9) in 293T cells and added recombinant matriptase or KLK5 protease that were pre-incubated with 10nM or 500nM SPINT2. Trypsin and the respective protease without SPINT2 incubation were used as controls. Cleavage of HA₀ was analyzed via Western Blot and the signal intensities of the HA₁ bands were quantified using the control sample without SPINT2 incubation as a reference point to illustrate the relative cleavage of HA with and without inhibitor (Fig 4.2A and 4.2D). Trypsin cleaved all tested HA proteins with very high efficiency that was not observed with matriptase or KLK5 (Fig 4.2B- 4.2D). However, H1N1 HA was cleaved by matriptase and KLK5 to a similar extent without and with 10nM SPINT2. 500nM SPINT2 led to a relative cleavage reduction of about 70% and 50% for matriptase and KLK5, respectively (Fig 4.2A and 4.2B). KLK5-mediated cleavage of H3N2 HA was reduced by about 10% when KLK5 was pre-incubated with 10nM SPINT2 and by about 60% when 500nM SPINT2 was used (Fig 4.2A and 4.2C). When we tested the cleavage inhibition of matriptase with H7N9 HA as a substrate

we found that 10nM and 500nM SPINT reduced the cleavage to 40% and 10% cleavage, respectively, compared to the control. (Fig 4.2A and 4.2D). In contrast, 10nM SPINT2 had no effect on KLK5-mediated cleavage of H7N9 HA while 500nM reduced relative cleavage by approximately 70% (Fig 4.2A and 4.2D).

In order to determine whether SPINT2 also prevented cleavage of HMPV F we first examined which proteases, in addition to trypsin and TMPRSS2, were able to cleave HMPV F. First, we co-transfected the full length TMPRSS2, HAT and matriptase with HMPV F in VERO cells. The F protein was then radioactively labeled with ³⁵S methionine and cleavage was examined by quantifying the F₀ full length protein and the F₁ cleavage product. We found that TMPRSS2 and HAT were able to efficiently cleave HMPV F while matriptase decreased the expression of F, though it is not clear if this was due to general degradation of protein or lower initial expression. However, matriptase demonstrated potential low-level cleavage when co-transfected (Fig 4.3A and 4.3B). We then examined cleavage by the exogenous proteases KLK5, KLK12 and matriptase. Compared with the trypsin control, KLK5 and matriptase were able to cleave HMPV F, while KLK12 was not (Fig 4.3C and 4.3D). In agreement with the peptide assay, cleavage of HMPV F by KLK5 and matriptase was less efficient than for trypsin and both peptide, and full-length protein assays demonstrate that KLK12 does not cleave HMPV F. This also serves as confirmation that matriptase likely cleaves HMPV F, but co-expression with matriptase may alter protein synthesis, stability or turnover if co-expressed during synthesis and transport to the cell surface. Next, we tested SPINT2 inhibition of exogenous proteases trypsin, KLK5 and matriptase. We pre-incubated SPINT2 with each protease, added it to VERO cells expressing HMPV F and analyzed cleavage product formation. SPINT2 pre- incubation minimally affected cleavage at a concentration of 10nM but addition of 500nM SPINT2 resulted in inhibition of trypsin, KLK5 and matriptase-mediated cleavage of HMPV, similar to our findings for HA (Fig 4.3E and 4.3F).

SPINT2 inhibits HA mediated cell-cell fusion

The above presented biochemical experiments demonstrate that SPINT2 is able to efficiently inhibit proteolytic cleavage of HMPV F and several influenza A HA subtypes by a variety of proteases. For a functional analysis to determine whether SPINT2 inhibition prevents cells to cell fusion and viral growth, we examined influenza A infection in cell culture. While HMPV is an important human pathogen, Influenza grows significantly better in cell culture compared with HMPV. First, we tested whether cleavage inhibition by SPINT2 resulted in the inhibition of cell-cell fusion. As described above, matriptase and KLK5 were pre-incubated with 10nM and 500nM SPINT2 and subsequently added to VERO cells expressing A/CA/04/09 (H1N1) HA or A/Shanghai/2/2013 (H7N9) HA. Cells were then briefly exposed to a low pH buffer to induce fusion and subsequently analyzed using an immune fluorescence assay. When matriptase and KLK5 were tested with 10nM SPINT2 and incubated with VERO cells expressing H1N1 HA, we still observed syncytia formation (Fig 4.4A). However, 500 mM SPINT2 resulted in the abrogation of syncytia formation triggered by cleavage of the respective HA by matriptase and KLK5. We made the same observation when we tested KLK5 and H7N9 HA (Fig 4.4B). Matriptase-mediated H7N9 HA syncytia formation was inhibited by the addition of 10nM SPINT2 (Fig 4.4B). To ensure that cell-cell fusion inhibition is a result of HA cleavage inhibition through SPINT2 but not a side effect of SPINT2 treatment *per se* we expressed A/Vietnam/1204/2004 (H5N1) HA in VERO cells and treated them with the inhibitor. H5N1 HA possesses a HPAI cleavage site and is cleaved intracellularly by furin during its maturation process. SPINT2 does not inhibit furin and is not able to cross cell membranes. Thus, SPINT2 can not interfere with the proteolytic processing of H5N1 HA and therefore this control allows to examine whether SPINT2 interferes with cell-cell fusion. Figure 4.4C shows that H5N1 HA forms large syncytia in the absence of SPINT2 as well as in the presence of 500 nM SPINT2. Hence, we conclude that SPINT2 does not have a direct inhibitory effect on cell-cell fusion.

SPINT2 reduces viral growth in cell culture

To understand whether SPINT2 was able to inhibit or reduce the growth of virus in a cell culture model over the course of 48 hours we transfected cells with human TMPRSS2 and human matriptase, two major proteases that have been shown to be responsible for the activation of distinct influenza A subtype viruses. TMPRSS2 is essential for H1N1 virus propagation in mice and plays a major role in the activation of H7N9 and H9N2 viruses (176, 376, 377). Matriptase cleaves H1N1 HA in a sub-type specific manner, is involved in the *in vivo* cleavage of H9N2 HA and our results described above suggest a role for matriptase in the activation of H7N9 (177, 376). At 18 hours post transfection we infected MDCK cells with A/CA/04/09 (H1N1) at a MOI of 0.1 and subsequently added SPINT2 protein at different concentrations. Non-transfected cells served as a control and exogenous trypsin was added to facilitate viral propagation. The supernatants were harvested 48 hours post infection and viral titers were subsequently analyzed using an immuno-plaque assay.

SPINT2 initially mitigated trypsin-mediated growth of H1N1 at a concentration of 50nM and the extent of inhibition slightly increased with higher concentrations (Fig 4.5A). The highest tested SPINT2 concentration of 500nM reduced viral growth by about 1 log (Fig 4.5A). We observed a similar pattern with cells transfected with human matriptase (Fig 4.5B). Growth inhibition started at a SPINT2 concentration of 50nM and with the application of 500nM growth was reduced by approximately 1.5 logs (Fig 4.5B). When we infected cells expressing TMPRSS2 with H1N1 and added SPINT2, viral growth was significantly reduced at a concentration of 150nM. Addition of 500nM SPINT2 led to a reduction of viral growth of about 1.5 logs (Fig 4.5C). We also tested whether SPINT2 could reduce the growth of a H3N2 virus because it is major circulating seasonal influenza subtype. However, TMPRSS2 and matriptase do not seem to activate H3N2 viruses (175, 177). Hence, trypsin and SPINT2 were added to the growth medium of cells infected with A/X31 H3N2. Compared to control cells without added inhibitor SPINT2 significantly inhibited trypsin mediated H3N2 growth at a concentration of 50nM (Fig 4.5D). At the highest SPINT2 concentration of 500nM viral growth was reduced by about 1 log (Fig 4.5D).

We also examined the effect of SPINT2 inhibition of HMPV spread over time. VERO cells were infected with rgHMPV at MOI 1 and subsequently treated with 500nM of SPINT2 and 0.3µg/mL of TPCK-trypsin. Every 24 hours, cells were scraped, and the amount of virus present was titered up to 96hpi with SPINT2 and trypsin replenished daily. We find that un-treated cells are infected and demonstrate significant spread through 96hpi. Conversely, cells infected and treated with SPINT2 had no detectible virus up to 48hpi and very minimal virus detected at 72 and 96hpi, demonstrating that SPINT2 significantly inhibition HMPV viral replication and spread (Fig 4.6).

Antiviral therapies are often applied when patients already show signs of disease. Therefore, we tested if SPINT2 was able to reduce viral growth when added to cells 24 hours after the initial infection. Cells were infected with 0.1 MOI of A/CA/04/09 (H1N1) and trypsin was added to promote viral growth. At the time of infection, we also added 500nM SPINT2 to one sample. A second sample received 500nM SPINT2 24 hours post infection. Growth supernatants were harvested 24 hours later, and viral growth was analyzed. We found that viral growth was significantly reduced by regardless whether SPINT2 was added at the time of infection or 24 hours later (Fig 4.7).

Discussion

Influenza A virus has caused four pandemics since the early 20th century and infects millions of people each year as seasonal 'flu, resulting in up to 690,000 deaths annually (346) . Vaccination efforts have proven to be challenging due to the antigenic drift of the virus and emerging resistance phenotypes (378). Moreover, the efficacy of vaccines seems to be significantly reduced in certain high-risk groups (379). Prevalent antiviral therapies to treat influenza A virus-infected patients such as adamantanes and neuraminidase inhibitors target viral proteins but there is increasing number of reports about circulating influenza A subtypes that are resistant to these treatments(348). HMPV causes infections in the upper and lower respiratory tract expressing very similar symptoms as

influenza infections and resulting in significant morbidity and mortality (352, 353). The most susceptible groups are young children, older adults and people that are immunocompromised (30, 36, 354). Currently, there are not treatment against HMPV infections available. In this study we focused on a novel approach that uses antiviral therapies targeting host factors rather than viral proteins offering a more broad and potentially more effective therapeutic approach (360). We demonstrate that SPINT2, a potent inhibitor of serine-type proteases, can significantly inhibit cleavage of HMPV F and HA, impair HA-triggered fusion of cells and hence, reduce the growth of various influenza A strains in cell culture.

We assessed cleavage of the HMPV fusion protein in vitro using a peptide cleavage assay modified from previously work on other viral fusion proteins (171, 374). The HMPV F peptide was cleaved by trypsin, plasmin, matriptase and KLK5 but was unable to be cleaved by KLK12. To confirm these findings in a system in which the entire HMPV F protein was subject to cleavage, we co-expressed the fusion protein with TMPRSS2, HAT and matriptase proteases, or treated F with exogenous proteases KLK5, KLK12 and matriptase. These findings are the first to identify proteases besides trypsin and TMPRSS2 that are able to cleave HMPV F. In addition, HMPV appears to utilize many of the serine proteases that influenza uses for HA processing and therefore, offers strong potential for an antiviral target.

SPINT2 demonstrates greater advantage over other inhibitors of host proteases such as e.g. aprotinin that was shown to be an effective antiviral but also seemed to be specific only for a subset of proteases (361). It can be argued that a more specific protease inhibitor which inhibits only one or very few proteases might be more advantageous because it may result in less side effects. With respect to influenza A infections, TMPRSS2 could represent such a specific target as it was shown to a major activating proteases for H1N1 and H7N9 in mice and human airway cells (176, 376, 377, 380, 381). However, there is no evidence that that application of a broad-spectrum protease inhibitor results in more severe side effects than a specific one as side effects may not be a consequence of the protease inhibition but the compound itself may act against different targets in the

body. The reports demonstrating that TMPRSS2 is crucial for H1N1 and H7N9 virus propagation in mice and cell culture suggest that it also plays a major role in the human respiratory tract. So far, however, it is unclear whether the obtained results translate to humans and other studies have shown that for example human matriptase is able to process H1N1 and H7N9 (177, 382).

Our peptide assay suggests that SPINT2 has a wide variety of host protease specificity. With the exception of plasmin, all the tested proteases in combination with peptides mimicking the cleavage site of different HA subtypes expressed IC_{50} values in the nanomolar range. Interestingly, the IC_{50} values obtained for cleavage inhibition of HMPV F were substantially lower, in the picomolar range. This suggests that the HMPV cleavage may be more selectively inhibited by SPINT2. However, the western blot data showed that addition of the lowest concentration (10 nM) of SPINT2 did not result in cleavage inhibition of HMPV F by the tested proteases. Differences in sensitivity of SPINT2 between influenza HA and HMPV require further investigation.

SPINT2 poses several potential advantages over other inhibitors that target host proteases. Cell culture studies showed that, for example, matriptase-mediated H7N9 HA cleavage was efficiently inhibited at a concentration of 10nM SPINT2. In contrast, the substrate range for aprotinin, a serine protease inhibitor shown to reduce influenza A infections by targeting host proteases, seemed to be more limited (361). Other synthetic and peptide-like molecules designed to inhibit very specific serine proteases such as TMPRSS2, TMPRSS4 and TMPRSS11D (HAT) were only tested with those proteases and their potential to inhibit other proteases relevant for influenza A activation remains unclear (383-385). Currently, the most promising antiviral protein inhibitor is camostat which is already approved in Japan for the treatment of chronic pancreatitis (386). Recently, it was demonstrated that camostat inhibited influenza replication in cell culture and prevented the viral spread and pathogenesis of SARS-CoV in mice by inhibition of serine proteases (385, 387). However, camostat was applied prior to the virus infection and it was administered into the mice via oral gavage (387).

A previous study showed that SPINT2 significantly attenuated influenza A infections in mice using a concentration that was 40x lower than the described camostat concentration and intranasal administration was sufficient (362). Our current study suggests that SPINT2 is able to significantly inhibit viral spread during an ongoing infection and does not need to be applied prior or at the start of an infection. The mouse study also showed that SPINT2 can be applied directly to the respiratory tract while camostat that is currently distributed as a pill and therefore less organ specific. In addition, camostat is synthetic whereas SPINT2 is a naturally occurring molecule which may attenuate potential adverse effects due to non-native compounds activating the immune system. Future research will be conducted to test if SPINT2 can be applied more efficiently via an inhaler and to explore potential side effects in mice studies. However, when we tested the potential of SPINT2 to inhibit viral replication in a cell culture model we were only able to achieve growth reductions of approximately 1 -1.5 logs after 48 hours with a concentration of 500nM SPINT2. One potential explanation is that 500nM SPINT2 was unable to saturate the proteases present in the individual experiments and was not sufficient to prevent viral growth. In addition, the continuous overexpression of matriptase and TMPRSS2 may have produced an artificially high quantity of protein that exceeded the inhibitory capacities of SPINT2. This problem could be solved either by using higher concentration of SPINT2 or by optimizing its inhibitory properties. However, the data also demonstrates that SPINT2 has the ability to inhibit proteases that expressed on the cell surface and that inhibition is not limited to proteases that were added exogenously and pre-incubated with the inhibitor (Fig 4.5). SPINT2 did not express any cytotoxic effects up to a concentration of 10 mM, significantly above the therapeutic dosage required for inhibition. In comparison with other studies, the SPINT2 concentration we used here were in the nanomolar range while other published inhibitors require micromolar concentrations (383-385). However, we believe that future research will allow to fully utilize the potential of SPINT2 as a broad-spectrum antiviral therapy. Wu et al., recently described that the Kunitz domain I of SPINT2 is responsible for the inhibition of matriptase (367). In future studies we will explore

whether the inhibitory capabilities of SPINT2 can be condensed into small peptides that may improve its efficacy. Its ability to inhibit a broad range of serine proteases that are involved in the activation of influenza A suggest that a SPINT2 based antiviral therapy could be efficient against other pathogens too. TMPRSS2, for example, not only plays a major role in the pathogenesis of H1N1 but is also required for the activation of SARS-CoV and MERS-CoV and HMPV (388, 389). Currently, treatment options for these viruses are very limited and therefore SPINT2 could become a viable option if its potential as an antiviral therapeutic can be fully exploited.

However, while SPINT2 has a therapeutic potential to treat ILIs caused by viruses that require activation by trypsin-like serine proteases it may have its limitation to provide a treatment option for infections caused by influenza HPAI viruses, such as H5N1 (390) . These viruses are believed to be activated by furin and pro-protein convertases that belong to the class of subtilisin-like proteases (358) . Preliminary data from our lab demonstrated that SPINT2 did not inhibit furin-mediated cleavage of HPAI cleavage site peptide mimics as well as peptides carrying described furin cleavage sites (data not shown). In addition, furin acts intracellularly and we have no evidence that SPINT2 is able to penetrate the cell membrane and thus inhibiting proteases located in intracellular compartments. Therefore, it seems unlikely that SPINT2 is able to inhibit furin in cell culture-based studies or *in vivo* experiments.

In conclusion we believe SPINT2 has potential to be developed into a novel antiviral therapy. In contrast to most similar drugs that are synthetic, SPINT2 is an endogenously expressed protein product that confers resistance to a variety of pathogenic viruses which can potentially be delivered directly into the respiratory tract as an aerosol. Most importantly, SPINT2 demonstrated the ability to significantly attenuate an ongoing viral infection in cell culture and further research will be conducted to explore the time period during which SPINT2 demonstrates the highest efficacy.

A	VMAX (RFU/MIN)	STDEV
TRYPsin	135.25	17.55
MATRIPTASE	9.24	0.39
KLK5	5.80	0.12
HAT	2.99	0.41
KLK12	0.00	0.00
PLASMIN	37.86	2.07

B	IC ₅₀ values (nM)					
IAV HA	Trypsin	Matriptase	HAT	KLK5	KLK12	Plasmin
H1N1 HA	70.57	25.00	24.08	28.34	11.70	122.10
H2N2 HA	155.40	NT	34.74	8.27	6.88	NT
H3N2 HA	207.90	NT	15.33	9.54	NT	106.00
H5N1 HPAI HA	1135.00	194.10	NT	NT	NT	1166.00
H5N1 LPAI HA	145.80	5.32	23.56	6.38	3.66	160.10
H6N1 HA	30.52	NT	NT	29.93	14.04	NT
H7N9 HA	20.97	8.00	NT	NT	NT	77.59
H9N2 HA	99.16	9.02	12.74	11.79	NT	134.00
C	IC ₅₀ values (nM)					
	Trypsin	Matriptase	HAT	KLK5	KLK12	Plasmin
HMPV F	0.04	0.0003	NT	0.95	NT	NT

Table 4.1: Cleavage of HMPV F and SPINT2 inhibition of peptide cleavage of various proteases: (A) A fluorogenic peptide mimicking the cleavage site of HMPV F was incubated with the indicated proteases and cleavage was monitored by the increase of fluorescence at 390 nm. RFU = relative fluorescence units. StDev = Standard Deviation. Fluorogenic peptides mimicking the cleavage sites of A/CA/04/09 H1N1, A/Japan/305/1957 H2N2 HA, A/Aichi/2/68 H3N2 HA, A/Vietnam/1203/2004 H5N1 LPAI HA, A/Vietnam/1204/2004 H5N1 HPAI HA, A/Taiwan/2/2013 H6N1 HA, A/Shanghai/2/2013 H7N9 HA, A/Hong Kong/2108/2003 H9N2 HA and HMPV F were incubated with the indicated proteases and different SPINT2 concentrations. Cleavage was monitored by the increase of fluorescence at 390 nm and the resulting Vmax values were used to calculate the IC₅₀ values. **(B)** IC₅₀ values of influenza A fluorogenic cleavage site peptide mimics. Concentrations are in nanomolar. **(C)** IC₅₀ values of the HMPV F cleavage site peptide mimic. Concentrations are in picomolar. NT = Not tested.

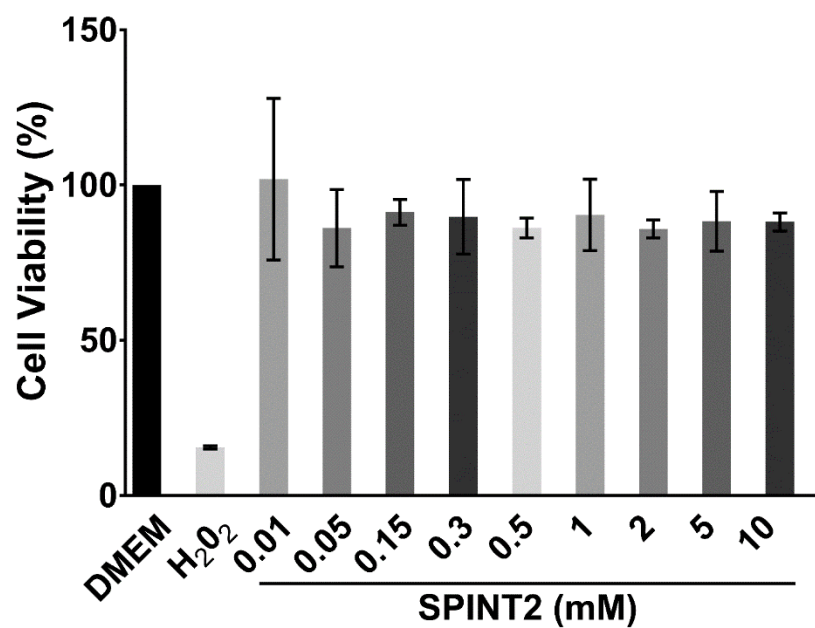


Figure 4.1: Cytotoxicity assay to evaluate the cytotoxic effect of SPINT2. 293T cells were incubated with indicated SPINT2 concentrations for 24 hours. DMEM and 500 μ M H₂O₂ served as controls. After 24 hours cell viability was determined via a spectrophotometric assay.

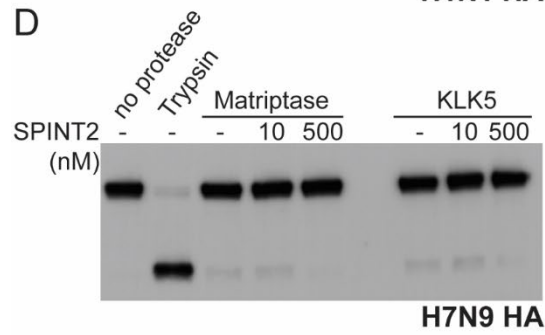
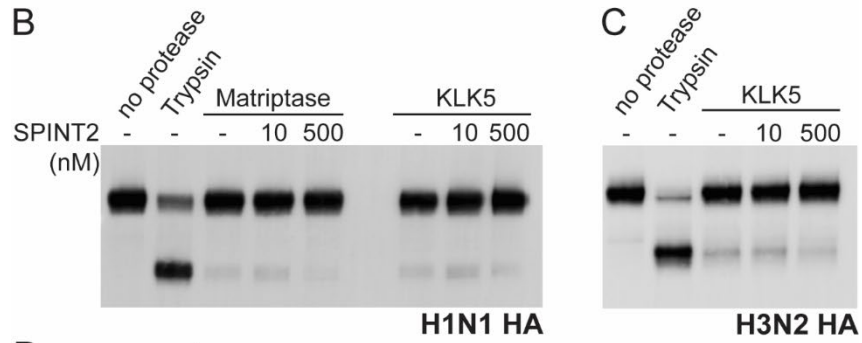
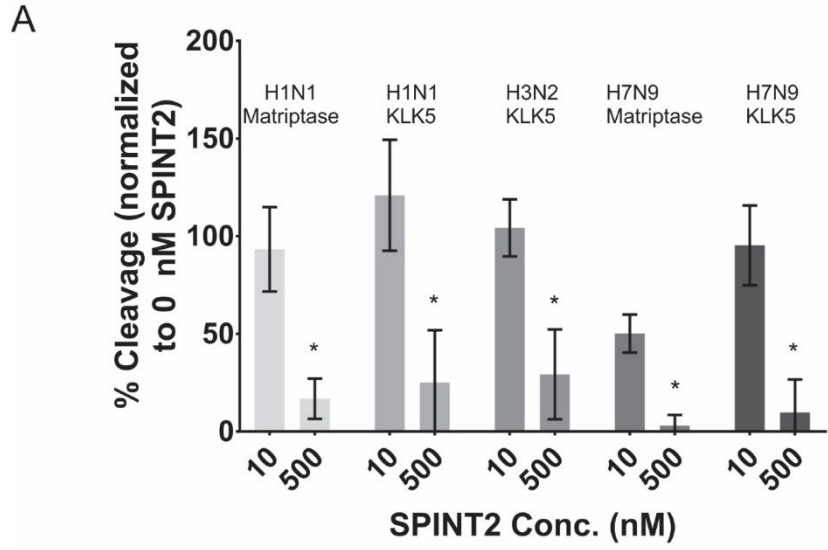


Figure 4.2: SPINT2 inhibits cleavage of HA protein expressed in 293T cells. Cells were transfected with plasmids encoding for the indicated HA and allowed to express the protein for ~18 hours. The recombinant proteases were incubated for 15 minutes with the indicated SPINT2 concentrations and subsequently added to the cells for 10 minutes (trypsin) or 90 minutes (matriptase and KLK5). Western blots were performed and the HA₁ band was quantified using ImageJ. **(A)** Quantification of the HA₁ band comparing the signal intensity of the 0 nM SPINT2 samples against 10 nM and 500 nM SPINT2 of the respective HA/protease combination. Three independent experiments were carried out and the western blots of each experiment were analyzed. Quantifications were conducted as described in the methods section. **(B – D)** Western blots showing the cleavage of **(B)** A/CA/04/09 H1N1 HA by matriptase and KLK5 at different SPINT2 concentration, **(C)** A/Aichi/2/68 H3N2 HA by KLK5 at different SPINT2 concentration and **(D)** A/Shanghai/2/2013 H7N9 HA by matriptase and KLK5 at different SPINT2 concentrations. Statistical analysis was performed using a non-paired student's t-test comparing the samples tested with 10 nM SPINT2 against the respective sample incubated with 500 nM SPINT2. Error bars indicate standard deviation. * indicates $p = < 0.05$.

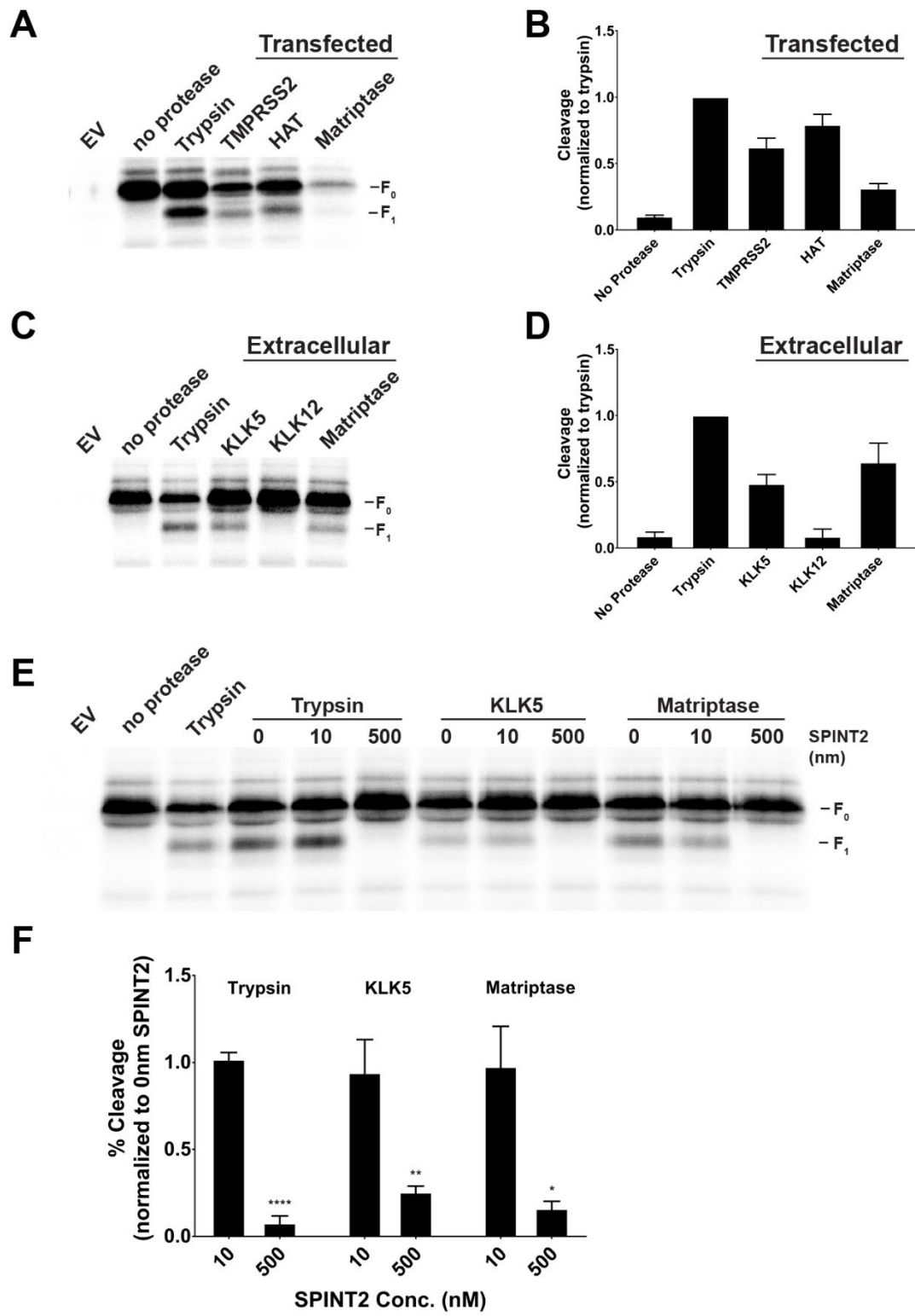


Figure 4.3: TMPRSS2, HAT, matriptase and KLK5 cleave HMPV F and SPINT2 is able to prevent cleavage by exogenous proteases. HMPV F was either expressed alone or co-transfected with protease and allowed to express for ~ 18 hours. Cells were then metabolically starved of cysteine and methionine followed by radioactive S35 labeling of protein for 4 hours in the presence of TPCK-trypsin or specified protease. SPINT2 treated proteases were incubated at room temperature for 10 minutes and placed onto cells for 4 hours. Radioactive gels were quantified using ImageQuant software with percent cleavage equal to $\left[\left(\frac{F_1}{F_0+F_1}\right) \times 100\right]$. **(A)** and **(B)** Co-transfected proteases TMPRSS2, HAT and matriptase are able to cleave HMPV F (n=4) while **(C)** and **(D)** exogenous proteases KLK5 and matriptase but not KLK12 are able to cleave HMPV F (n=5). **(E)** and **(F)** SPINT2 prevented cleavage of HMPV F by trypsin, KLK5 and matriptase at nm concentrations demonstrated by the loss of the F₁ cleavage product (n=3). Statistical analysis was performed using a one-way ANOVA followed by a student's t-test with a bonferroni multiple comparisons test correction. P<0.05 *, P<0.005 **, P<0.005 ***, P<0.001 ****. N values represent independent replicates for each treatment group. Error bars represent SD.

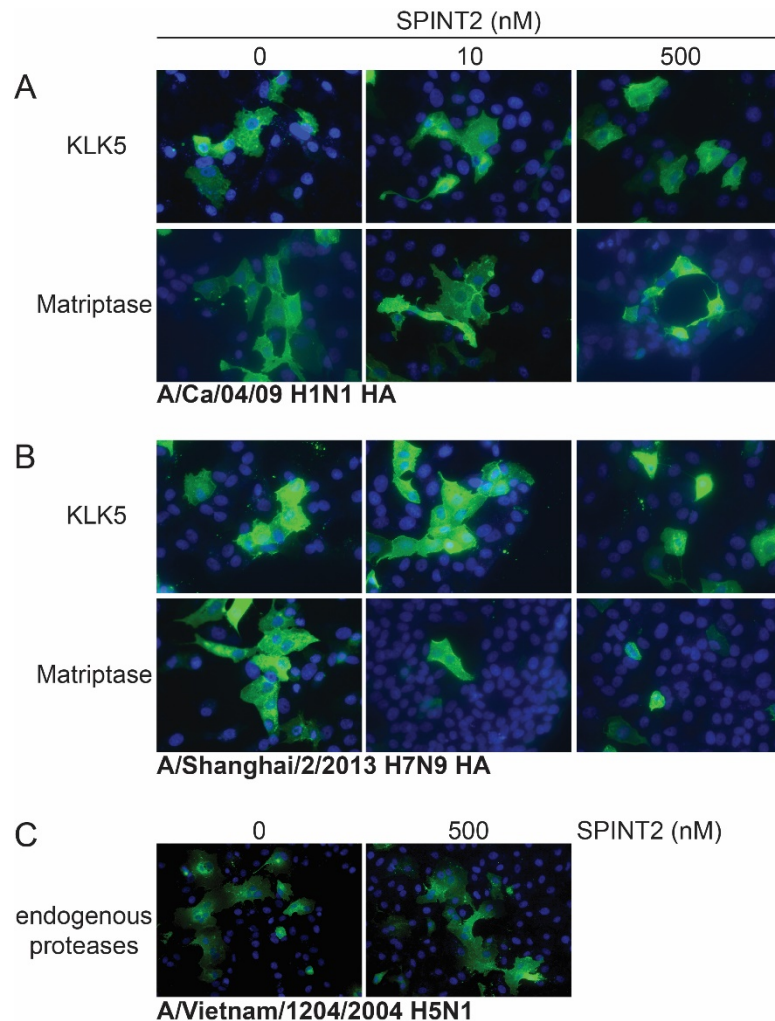


Figure 4.4: SPINT2 inhibits HA-mediated cell-cell fusion. VERO cells were transfected with plasmids encoding for **(A)** A/CA/04/09 H1N1 HA or **(B)** A/Shanghai/2/2013 H7N9 HA and allowed to express the protein for ~18 hours. Recombinant matriptase and KLK5 were incubated with different SPINT2 concentrations for 15 minutes and then added to the HA-expressing cells for 3 hours. After 3 hours the cells were briefly treated with cell fusion buffer at pH5, washed, supplemented with growth medium and returned to the incubator for 1 hour to allow fusion. HA protein was detected using HA-specific primary antibodies and a secondary fluorogenic Alexa488 antibody. Nuclei were stained using DAPI. Magnification 40x. **(C)** VERO cells expressed A/Vietnam/1204/2004 H5N1 HA that was cleaved during its maturation process in the cell. SPINT2 was added at 0 nM or 500 nM at the time of transfection. Magnification 25x.

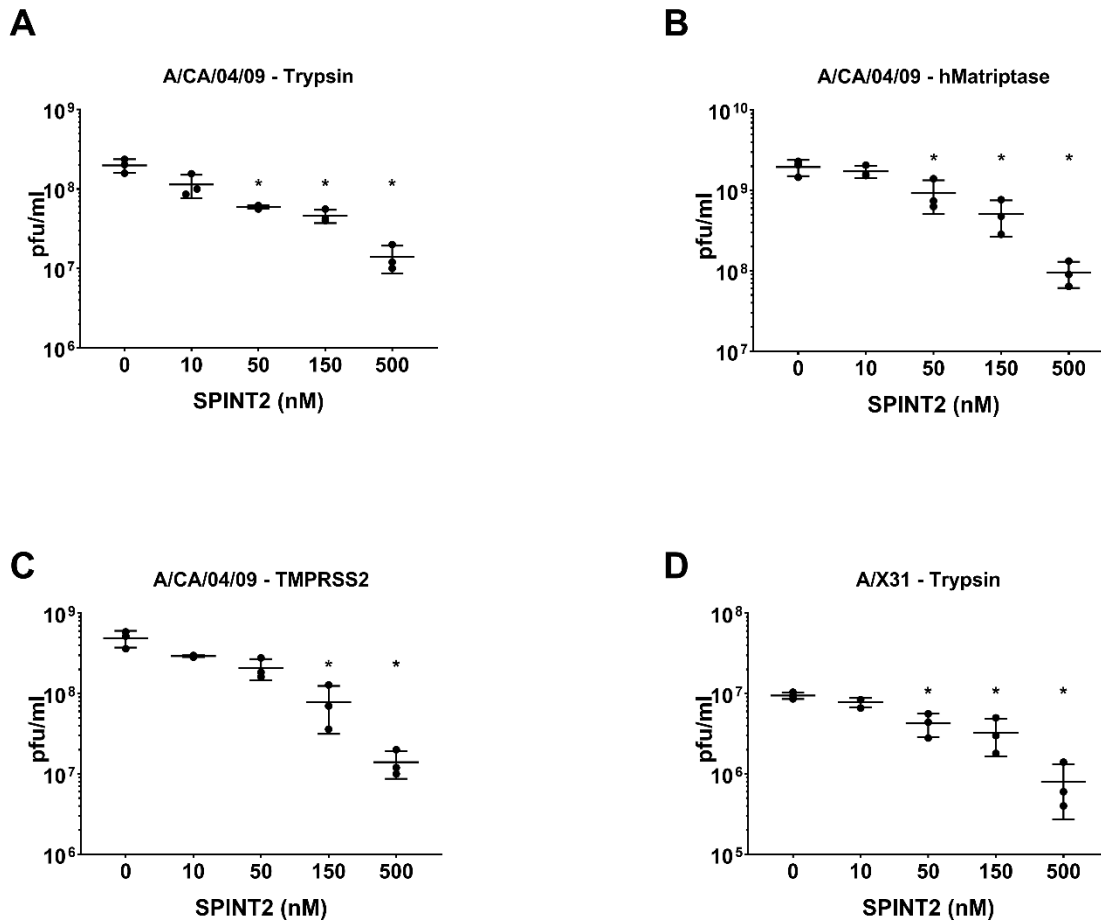


Figure 4.5: SPINT2 reduces IAV growth in cell culture. MDCK cells were transfected with plasmids encoding for human matriptase or human TMPRSS2 and allowed to express the proteins for ~18 hours. Cells expressing human matriptase (**B**) or human TMPRSS2 (**C**) were then infected with A/CA/04/09 H1N1 at a MOI of 0.1 and different SPINT2 concentration were added to each well. Non-transfected cells to which trypsin was added served as a control (**A**). (**D**) MDCK cells were infected with A/X31 H3N2 at a MOI of 0.1 and trypsin was added to assist viral propagation. Different SPINT2 concentration was added as indicated. After 48 hours of infection the supernatants were collected and used for an immuno-plaque assay to determine the viral loads. Experiment was repeated three times and each dot represents the viral titer of a single experiment. Statistical analysis was performed using a non-paired student's t-test comparing the control (0 h) against the respective sample. Error bars indicate standard deviation. * indicates $p = < 0.05$. Extended horizontal line within the error bars represents mean value of the three independent replicates.

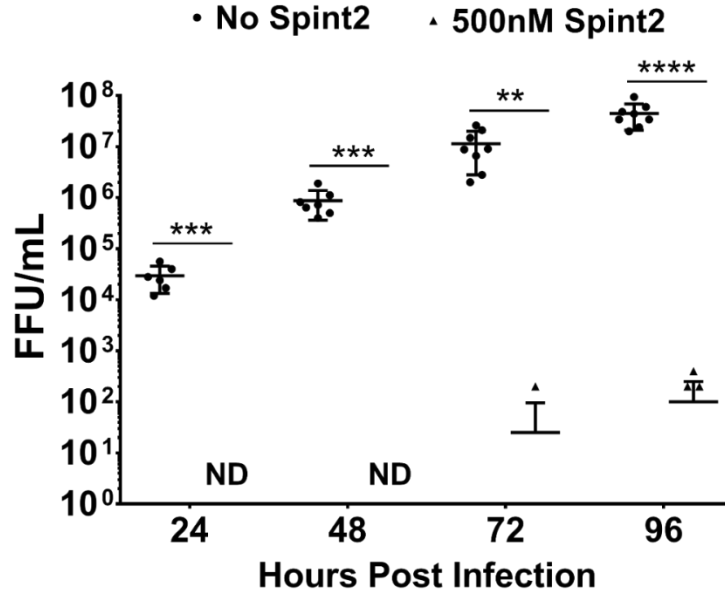


Figure 4.6: SPINT2 mitigates the spread of HMPV in cell culture. VERO cells were infected with a MOI 1 of rgHMPV. SPINT2 and TPCK-trypsin were added at 500nM and 0.3µg/mL respectively and spread was monitored up to 96hpi. Cells not treated with SPINT2 demonstrated significant spread up through 96hpi whereas treated samples did not show any detectable virus up to 48hpi. However, there was minimal detected virus at 72 and 96hpi. Error bars indicate standard deviation of 4 independent samples completed in duplicate (all data points plotted within the graph). Statistical analysis was performed using a student's t-test. P <0.05 *, P <0.005 **, P <0.005 ***, P <0.001 ****. ND indicates that the sample was below the limit of detection.

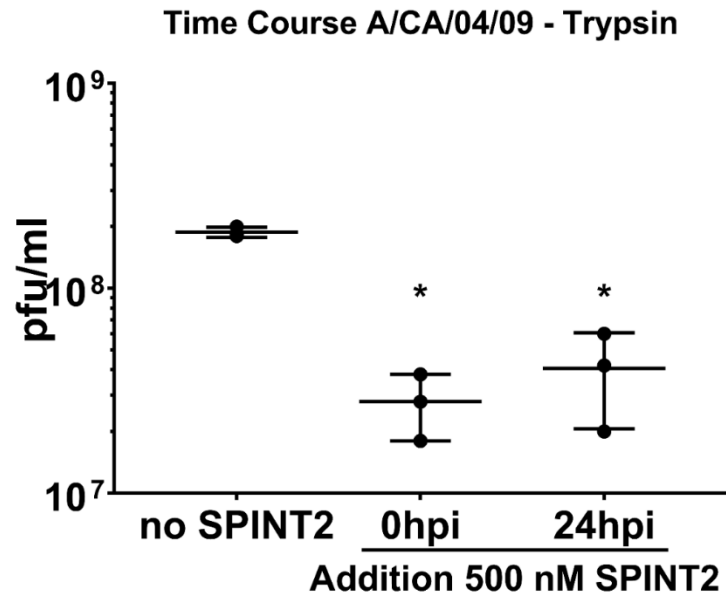


Figure 4.7: SPINT2 reduces viral growth when added 24 hours post infection. MDCK cells were infected with A/CA/04/09 H1N1 at a MOI of 0.1 and trypsin was added. 500nM SPINT2 were added at the time of infection or 24 hours post infection. Supernatants were collected 48 hours post infection and used for an immuno-plaque assay to determine the viral titers. Statistical analysis was performed using a non-paired student's t-test comparing the control (0 h) against the respective sample. Error bars indicate standard deviation. * indicates $p = < 0.001$. Extended horizontal line within the error bars represents mean value of the three independent replicates.

Chapter 5: Respiratory syncytial virus and human metapneumovirus infections in 3-D airway tissues expose an interesting dichotomy in viral replication, spread, and inhibition by neutralizing antibodies

* This work was completed in collaboration with Medimmune/Astrazeneca who provided the RSV virus and RSV antibodies used during these studies. I performed all experiments, data analysis, and figure creation. Dr. Carole Moncman helped with imaging and image processing, post fixation processing of HAE tissues, and data acquisition. This section was adapted from a manuscript (Kinder et al J Virol, 2020: JVI.01068-20)

Introduction

Respiratory syncytial virus (RSV) and human metapneumovirus (HMPV) are single-stranded, negative-sense RNA (nsRNA) enveloped viruses in the *Pneumoviridae* family (18). As leading causes for respiratory infections in children, 95% of children by the age of two are infected with RSV (21) and nearly all are seropositive for HMPV by the age of 5 (30, 354). Children, immunocompromised, and elderly populations are at significant risk for contracting and developing severe lower respiratory tract infection, with infants at the greatest risk (21-23, 26, 27, 30, 354, 391-397). While both RSV and HMPV cause severe morbidity and mortality, no vaccines are available and only limited treatment options exist. For RSV, the only FDA -approved therapy is palivizumab, a humanized monoclonal antibody given prophylactically to high risk infants during the infectious season (28, 29). To better understand how to target these viruses therapeutically, a deeper understanding of viral infection in physiologically relevant model systems is needed.

Pneumoviruses initiate infection by attaching to target cells via their surface glycoproteins, the fusion protein (F) and /or the attachment protein (G), which interact with host receptors and attachment factors. Subsequently, F undergoes a large conformational change to mediate membrane fusion, after which the viral nucleocapsids are released into the cytoplasm of the infected cell (99, 398). This

membrane fusion process is critical, and inhibition of the fusion protein blocks entry and infection. Interestingly, both HMPV and RSV mutants lacking surface glycoproteins G and SH but containing F can mediate entry and infection, albeit attenuated to some degree (121, 123, 399, 400), demonstrating that F has a critical role for entry and is involved in attachment. Based on its critical role for infection, targeting the fusion protein is one of the most common strategies for developing therapeutics against HMPV and RSV (100-102, 401).

After entering the target cell, HMPV and RSV nucleocapsids are released and used as templates for synthesis of viral mRNAs and genomic RNA (vRNA) by the viral RNA dependent RNA polymerase. Research from our lab and others suggests these processes occur in punctate cytosolic structures, termed inclusion bodies (IBs), which are minimally composed of the nucleoprotein (N), the phosphoprotein (P), and vRNA (251, 255). IB-like structures have also been described for other nsRNA viruses, including ebola virus (261, 402), marburg virus (262), rabies virus (256, 403), vesicular stomatitis virus (263), parainfluenza virus 3 (264) and parainfluenza virus 5 (266), suggesting a broadly conserved mechanism for viral transcription and genome replication. Once newly synthesized-nucleocapsids assemble in IBs, they traffic to assembly sites at the plasma membrane. For HMPV, it has been suggested that the actin cytoskeleton might play a crucial role in nucleocapsid transport and inclusion body coalescence during infection (251), similar to what has been reported for ebola virus (404). In addition, the actin cytoskeleton has been reported to have a role in movement of ribonucleocapsids to sites of assembly in RSV and measles virus-infected cells, further supporting the importance of the cytoskeleton for viral infection and spread (320, 405, 406). After transport, the nucleocapsids coalesce with other viral proteins at the plasma membrane, the proposed assembly site for pneumoviruses, although recent research suggests a cell-to-cell dependent mechanism may play an important role in pneumovirus spread (407). This mechanism allows for the transfer of infectious particles via *en bloc* transmission by forming syncytia (395, 396, 408, 409), intercellular extensions (288, 298) or polyploid viruses (30, 84,

410-412) to allow for transmission of multiple genomes from one cell to another, compared with the traditional method of single particle release and reentry.

HMPV has been shown to be primarily cell-associated and induce the formation of long, actin-based filamentous extensions, which are important for direct cell-to-cell spread *in vitro*, even in the presence of neutralizing antibodies (288). RSV has also been shown to form actin-based extensions involving Actin Related Protein-2 (ARP2), suggesting a potential role for these structures during budding and spread in cell culture monolayers (298). RSV additionally induces cell-to-cell fusion in immortalized cell monolayers, generating multinucleated cells termed syncytia which are also a hallmark of other enveloped virus infections (396). Similarly, HMPV has been shown to generate syncytia, although to a much lesser extent compared to RSV (413, 414). While RSV replication is enhanced through the formation of syncytia *in vitro* (301), the formation of these structures in animal models and patients is not well understood. A few reports have described the presence of syncytia in postmortem autopsies of patients infected with either RSV or HMPV (395, 409). Currently, the roles of intercellular extensions and syncytia have yet to be fully elucidated in more physiologically relevant model systems in order to further understand how viruses enter and spread within infected tissue.

Human airway epithelial (HAE) tissues have been used previously as model systems to examine respiratory biology and pathogen interactions in cell culture (136, 143, 144, 313, 315, 316, 321-325, 327, 415-419). This model system utilizes primary human cells differentiated on a trans-well with an air-liquid interface to generate polarized bronchial epithelial tissue composed of multilayered epithelial cells including basal, apical ciliated, and goblet cells. This composition allows for a more accurate recapitulation of the lung environment including cellular 3-D structural organization, functional cilia, and mucus production. This method provides a more accurate model system to study respiratory viruses *in vitro*, offering significant advantages compared to traditional 2-D cell monolayers (312, 313, 319, 415, 417-420). These tissue models have been used to study both RSV

(143, 144, 314, 316, 319, 323-326, 420, 421) and HMPV (135, 136, 318, 333) infections. For RSV, HAE models have demonstrated that apical ciliated cells are the primary target cell, although occasional infection of non-ciliated cells was also observed (323, 324, 326, 421). RSV-induced syncytia, a hallmark in 2-D cell culture, have been observed in several HAE studies, but with varied results. No syncytia were reported in several studies, even up to 36 days post infection (323, 324), whereas another study observed infrequent syncytia (326). For HMPV, very few studies have been conducted using HAE tissues as a model system (135, 136, 318, 333). Consistent with findings from RSV, the primary target for HMPV is also apical ciliated cells (136). However, there are limited studies examining viral and host interactions for both HMPV and RSV in HAE tissues.

In this work, we performed a detailed analysis of RSV and HMPV infection in 3-D HAE cultures, exploring aspects of the viral lifecycles that have not been examined previously in HAE tissues. RSV demonstrated significantly higher rates of infection, spread, and apical release than HMPV. Apical ciliated cells infected with either RSV or HMPV generated large cytosolic IBs, consisting of at least N, P, and vRNA, suggesting that these structures are critical replication complexes formed during viral infection *in vivo*. No syncytia formation was observed for either virus in our HAE studies. Interestingly, HMPV efficiently induced the formation of filamentous extensions in HAE cultures, while RSV formed significantly fewer extensions.

Lastly, we examined monoclonal antibody inhibition of entry and spread in HAE tissues for RSV and HMPV. The only approved FDA treatment against RSV, palivizumab, was able to inhibit RSV entry and spread. We also tested nirsevimab, a novel monoclonal antibody against RSV that has demonstrated potent efficacy against RSV in 2-D cell culture and animal models (422-424). We find that in HAE tissues, nirsevimab is able to block entry and spread of RSV with greater potency than palivizumab, supporting the findings in other model systems and supports its potential as a novel antiviral therapeutic against RSV. The anti-HMPV antibody 54G10 effectively inhibited the entry of HMPV but only modestly, though

significantly, reduced viral spread. Together, our results highlight the conserved and varied aspects of entry, replication, and assembly between two closely related pneumoviruses within HAE tissues and demonstrate an interesting dichotomy between HMPV and RSV and their lifecycles.

Results

Both HMPV and RSV have been studied extensively in 2-D non-polarized monolayers to analyze virus-host interactions. RSV has also been studied in 3-D HAE tissues to assess viral infection and pathology (143, 144, 314, 316, 321, 324-326, 421). In contrast, only a few reports examined HMPV in 3-D model systems (135, 136, 318, 333). While many important aspects of infection have been identified in 2-D cell studies, additional analysis in more physiologically relevant model systems is needed to further our understanding of the viral lifecycle. To address this, we utilized HAE tissues, a 3-D tissue model system which more accurately recapitulates the lung environment, including cellular polarization, mucus production, and functional cilia.

To compare the two pneumoviruses, we first assessed RSV and HMPV infection, spread, and apical release side-by-side in HAE tissues. Tissues were infected with recombinant green fluorescent protein (GFP) expressing RSV-A2 (rgRSV) or HMPV-A2 CAN97-83 (rgHMPV). At 24 hours post infection (hpi), GFP expression was analyzed, and showed that both HMPV and RSV initiated infection in this model system (Fig 5.1A). Initial infection was equivalent between both viruses, but HMPV infection was less efficient compared to RSV, requiring a MOI of 3 and 0.3 respectively to generate a comparable infection at 24 hpi (Fig 5.1B). We then examined viral spread within tissues as well as release from the apical surface up to 144 hpi. Using fluorescence threshold analysis (NIS elements) to quantify GFP expression, we found that RSV efficiently spreads from 24 hpi through 144 hpi, with the largest increase in infection seen from 24 to 48 hpi. However, minimal changes in spread were observed past 72 hpi, suggesting spread has plateaued (Fig 5.1A, quantified in 5.1C). In contrast, HMPV infected

cells increased significantly, but modestly, from 24 hpi to 48 hpi, followed by a decrease from 72 hpi to 144 hpi, with minimal infection remaining at later time points (Fig 5.1A, quantified in 5.1C). Analysis of apical release of viral particles showed a 3-log difference in the amount of released virus at 24 hpi between HMPV and RSV, even though the number of infected cells were similar between the two viruses (Fig 5.1B and 5.1D). In addition, there was no detectable release of HMPV after 24 hpi. This result demonstrates a rapid spread and sustained release of high titers of RSV particles from the apical surface whereas HMPV spread and particle release was minimal at all time points with a decrease in spread after 48 hpi.

Previously, both RSV (323, 324, 326, 421) and HMPV (136) were reported to primarily infect apical ciliated cells in HAE cultures. To verify this in our side-by-side analysis, infected tissues were cryo-sectioned and stained for keratan sulfate (KS), a marker for ciliated airway cells. RSV and HMPV both exclusively infected ciliated cells, confirming this as the primary target cell type for both pneumoviruses (Fig 5.1E). In a few instances, infected cells appeared below the apical surface. However, staining with KS demonstrated that these cells were ciliated, though they had not yet reached the apical surface. Based on these findings, the minimal spread and release of HMPV compared to RSV cannot be attributed to a difference in the type of cells infected, or the initial rates of infection. Therefore, we examined other aspects of the viral lifecycle to better understand how both viruses interact with host cells during infection.

HMPV and RSV induce the formation of replicative inclusion bodies

The formation of inclusion bodies (IBs) in 2-D cell monolayers has been shown to be critical for viral genome replication and transcription for HMPV and RSV (251, 255). However, to our knowledge, the presence of IBs has not been examined in 3-D HAE tissues or *in vivo*. To verify these structures are found in HAE infected tissues and to assess whether differences in the early stages of infection were observed for RSV and HMPV, we examined the formation of IBs by fluorescently staining RSV or HMPV N and P proteins, the minimal components

required for IB-like structure formation (252, 253). Co-localization of both N and P proteins was observed in cytoplasmic structures for RSV (Fig 5.2A and 5.2B) and HMPV (Fig 5.3A and 5.3B) suggesting that IBs form in infected HAE tissues.

To confirm these structures were IBs, we conducted fluorescence *in situ* hybridization (FISH) staining for vRNA, known to be localized to IBs during infection of 2-D cells (251, 255). We observed strong co-localization of N and P for both RSV (Fig 5.2C- 5.2F) and HMPV (Fig. 5.3C-5.3F) with their respective signal of vRNA, confirming the formation of IBs in infected tissues for both viruses. These findings are, to our knowledge, the first report of the formation of these structures in 3-D HAE tissues for both RSV and HMPV, and thus strongly support the hypothesis that these structures are critical for replication and spread of the viruses in 3-D models and likely *in vivo*, thus providing a viable therapeutic target for pneumoviruses.

N, P and vRNA had strong colocalization at inclusion bodies and at the plasma membrane, suggesting the coalescence of these viral factors at sites of assembly for both RSV and HMPV. In addition, P also demonstrated localization at the plasma membrane independently of N and vRNA, often associated with cilia-like structures at the apical surface for both RSV and HMPV infected cells. However, the presence of P at these sites was much stronger for RSV compared to HMPV. P has been previously reported to associate with IBs and the plasma membrane to form extensions for HMPV (288) and in proposed assembly complexes for RSV (425), which is supported by our findings. These suggest that differences seen in spread dynamics of the viruses are not a result of differences in the ability to cause initial infection or generate replicative structures.

HMPV and RSV form extensions but no syncytia in HAE tissues

There are numerous reports of actin cytoskeletal involvement in infectious cycles for both HMPV (288, 335, 426) and RSV (298, 427-431). We have previously shown that HMPV forms actin-based extensions, which were identified as a mechanism for direct cell-to-cell spread in BEAS-2B bronchial epithelial cells

(288). HMPV P co-localized with actin, and transient expression of P alone recapitulated some extension formation. Recent reports examining RSV demonstrated that viral infection leads to the formation of actin-based extensions in A549 cells (298). RSV-induced extensions were suggested to be filopodia and could be induced by the expression of F alone. Additionally, disruption of actin architecture in RSV infected cells decreased viral spread, suggesting that these extensions are critical for infecting new cells.

To compare the formation of actin-based extensions between the two pneumoviruses in different cell types, we infected Vero (monkey kidney), HEP-2 (human laryngeal carcinoma) and BEAS-2B (human bronchial epithelial, non-diseased) cells and analyzed extension formation. For all three cell types, both RSV (Fig 5.4A) and HMPV (Fig 5.4B) induced the formation of filamentous extensions at 24 hpi. Interestingly, a previous study did not observe extension formation in RSV-infected Vero cells (298). These differences may be, due in part, to other factors such as reagents or cell culture methodology.

We next examined extension formation of RSV and HMPV in 3-D HAE tissues. When phenotypically examining cross-sections of HAE tissues, HMPV-infected cells demonstrated a high percentage of extensions compared with RSV, where only a small number of infected cells with extensions were observed for RSV (Fig 5.4C). RSV and HMPV-induced extensions had similar morphology, but were infrequent in RSV-infected HAE tissues. The presence of extensions in HAE tissues was further confirmed by microtome sectioning two full tissues at the peak of infection with either HMPV (48 hpi) or RSV (72 hpi). Extensions were defined and counted as thin protrusions extending from the cell body which were ≥ 0.5 of the cell body diameter. For HMPV, 35.8% of infected cells contained extensions (1541 total infected cells counted), while only 4.4% of RSV infected cells had extensions (3859 total infected cells counted) (Fig 5.4D). Although both RSV and HMPV have been shown to extensively modify the actin cytoskeleton in non-polarized cell monolayers, RSV rarely forms extensions in HAE tissues, suggesting these extensions are less important for infection and propagation *in vivo*.

Conversely, HMPV generated intercellular extensions in both 2-D and 3-D model systems, supporting the idea that HMPV is primarily cell-associated and may utilize extensions for direct cell-to-cell spread (288).

A hallmark characteristic of RSV infection is the formation of multinucleated cells, termed syncytia, which has been shown to be prominent in 2-D cell monolayers. For HMPV, syncytia formation is less common compared with RSV, but is observed in 2-D culture (241, 413). Studies on RSV-mediated syncytia formation in HAE tissues have been inconclusive (321), while for HMPV, no reports have reported formation in HAE models for HMPV. At the peak of infection for both RSV (72 hpi) and HMPV (48 hpi), we examined syncytia formation in two fully microtome sectioned HAE tissues. Interestingly, no syncytia were observed for HMPV or RSV in either tissue examined nor was syncytia visible from the apical side. However, the lack of syncytia did not hinder the infectivity or spread of RSV. Since cell-to-cell fusion for both viruses is mediated by the fusion glycoprotein, we examined the localization of F in cryo-sections using immunofluorescence staining to determine if this finding was due to the localization of the F proteins. RSV F was predominantly localized to the apical surface of infected cells but was also present within extensions and throughout the infected cell, with a similar staining pattern observed for HMPV F (Fig 5.4C). Since both viral fusion proteins were present at locations beyond the apical surface, there are likely other variables that may contribute to the lack of syncytia formation for HMPV and RSV. Further investigation into the mechanisms that underlie fusion in tissues is required to better understand the factors that contribute to this phenomenon and whether syncytia formation impacts viral replication and spread *in vivo*.

Nirsevimab, palivizumab and 54G10 block viral entry and spread in HAE tissues

Recently, a novel monoclonal anti-F antibody, nirsevimab, showed significantly more potent neutralizing capacity in 2-D cultures and animal models with an extended serum half-life compared with palivizumab (422, 423, 432).

Conversely, no FDA approved anti-F antibodies are available against HMPV, but a neutralizing monoclonal antibody, 54G10, has been described that has sub-nanomolar efficacy *in vitro* against all clades of HMPV and also has cross reactivity to RSV, although efficacy against RSV is 6x less potent compared with palivizumab (340). To better understand how HMPV and RSV infection might be targeted in HAE tissues, we compared nirsevimab and palivizumab for RSV, and 54G10 for HMPV, for their ability to inhibit viral entry and spread in 3-D HAE tissues.

We first conducted a microneutralization assay to assess the neutralizing capacity of palivizumab and nirsevimab on RSV in HAE tissues. We pre-incubated the virus in the presence or absence of neutralizing antibody for 1 hour and then inoculated tissues at the apical surface. As expected, both nirsevimab and palivizumab were able to completely neutralize RSV entry at a concentration of 0.5 $\mu\text{g}/\text{mL}$ and 10 $\mu\text{g}/\text{mL}$ respectively (Fig 5.5A and 5.5B). Congruent with previous findings, nirsevimab demonstrated significantly higher neutralizing potency compared with palivizumab (approximately 20-fold) (Fig 5.5C). Similarly, 54G10 demonstrated a complete block of infection at 10 $\mu\text{g}/\text{mL}$ (Fig 5.6A and 5.6B, quantified in 5.6C), indicating therapeutic potential for 54G10 against HMPV.

The effect of neutralizing antibodies on RSV and HMPV spread at the apical surface of tissues after infection was examined. We inoculated tissues at the apical surface with RSV or HMPV and then monitored fluorescence after infection. RSV infection alone had a significant increase in spread from 24 hpi through 72 hpi (Fig 5.1A, 5.1B, 5.7A-5.7C). In the presence of palivizumab and nirsevimab, RSV spread was almost completely inhibited compared with the 24 hpi time point, demonstrating that RSV spread occurs mostly through apical release and reentry which can be blocked by antibody present at the apical surface. Our results also confirm previous observations for palivizumab and its ability to prevent spread in HAE tissues (324). Nirsevimab again demonstrated a significantly higher potency (approximately 10-fold) compared with palivizumab, showing similar inhibition of spread at lower concentrations (Fig 5.7A-5.7C).

We also examined 54G10 inhibition of HMPV spread from 24 hpi through 48 hpi. There was a modest, but statistically significant inhibition in HMPV spread with increasing amounts of 54G10 (Fig. 5.8A-5.8C). Spread in the presence of 2.5 $\mu\text{g}/\text{mL}$ and 25 $\mu\text{g}/\text{mL}$ of neutralizing antibody was only reduced by 25%, suggesting that a large fraction of HMPV spread likely still occurs via a direct cell-to-cell transmission mechanism likely utilizing extensions as shown in 2-D cell monolayers (288). Further investigation into the mechanisms for HMPV cell-to-cell spread in 3-D tissues will help to elucidate how HMPV spread can be targeted therapeutically. Altogether, our results indicate the mechanisms by which neutralizing antibodies act to prevent RSV infections, although, a different strategy may be needed to fully inhibit HMPV spread.

Discussion

In this study, we conducted a comparative analysis of HMPV and RSV infection in HAE tissues. Altogether, our results demonstrate that two closely related human respiratory pathogens may utilize significantly different mechanisms of spread in a 3-D model system. RSV can infect, replicate, and release large amounts of virus apically, resulting in very efficient spread. In striking contrast, HMPV is also able to infect ciliated cells in the HAE tissue, and productive establishment of replication centers is seen, as judged by production of viral RNA, but little apical release of virus was observed, leading to poor spread in this system.

Initial infection mediated by HMPV required higher MOIs to achieve similar infection rates, suggesting that RSV infects HAE tissues more efficiently than HMPV. RSV spread in HAE tissues increased significantly from 24 hpi up to 72 hpi, compared with HMPV which reached a peak of infection at 48 hpi and significantly decreased thereafter. HMPV has been demonstrated to establish persistent infection (75, 433-437). Thus, it is possible that the low replication rates of HMPV in HAE tissues may drive the virus toward persistence rather than an acute infection. In support of this, HMPV peaked at 48 hpi but a low, residual infection was present up to 144 hpi. When examining infected tissues, both HMPV

and RSV primarily infected apical ciliated cells, as previously demonstrated (136, 319, 321, 324). Therefore, the differences observed in entry and replication between HMPV and RSV do not appear to be due to the cell types infected. A recent publication utilized HMPV CAN97-82 (B strain) infection in human airway epithelium obtained from nasal biopsies and showed limited apical release up to five days post-infection (318). These studies and ours suggest strain differences may affect how HAE tissues release and spread virus to some degree. The presence of both the HMPV SH and G proteins, as well as the strain used, was recently reported to impact spread in HAE tissues (135), with the deletion of HMPV G especially deleterious. Interestingly, HMPV infection occurred at a higher level in these studies and further investigation is needed to understand differences involved in efficient HMPV entry in 3-D tissues (135, 136, 318, 333).

Once cells have been infected, both HMPV and RSV form IBs. The formation and characterization of these replication organelles in 2-D model systems have been previously reported (251, 255), but IB formation has not been previously examined in 3-D tissues. We showed that these IB structures form within HAE-infected cells and contain markers for IBs, including P, N and viral RNA. This is the first report of the formation of these structures in 3-D HAE tissues for both RSV and HMPV, and suggests these structures are broadly important for pneumovirus infection. As these structures appear in 2-D models for a number of negative-sense, single-stranded RNA viruses (251, 256, 261-264, 266, 402, 403), identifying and understanding critical host and viral components of these organelles may provide a unique anti-viral approach against a wide range of human viral pathogens.

Recent reports have shown both RSV and HMPV form actin-based filamentous structures, important for viral spread within 2-D monolayers (288, 298). Viral titer for RSV was significantly reduced when these structures were inhibited (298). For HMPV, these filamentous structures were shown to be involved in cell-to-cell spread of the virus, independent of neutralizing antibodies in BEAS-2B cells.

Similar to RSV, when these cytoskeletal structures are inhibited, viral spread was significantly reduced (288).

To assess the importance of cellular polarization on extension formation in 2-D monolayers, we examined extensions formation in 3-D HAE tissues. Interestingly, extensions similar to those observed in 2-D cells were also detected in approximately a third of HMPV-infected cells within HAE tissues, whereas RSV-infected cells had few extensions. Thus, we hypothesize that infection by RSV relies primarily on abundant release of particles from the apical side of tissues and re-infection of new target cells. However, the low apical release of virus and high percentage of cells with extensions suggests that HMPV infection of new target cells is likely dependent primarily on direct cell-to-cell contacts, similar to previous findings in 2-D models. Furthermore, HMPV was also demonstrated to be primarily associated with minimal release, and therefore extensions may be the primary mechanism of spread (288). However, even with the formation of extensions, spread of HMPV was minimal, suggesting that additional factors may be needed for efficient cell-to-cell spread in HAE tissues.

RSV forms large, multinucleated cells termed syncytia, which are a hallmark of infection in 2-D monolayers. In addition, while not as prominent, HMPV also mediates cell-to-cell fusion during monolayer infection (413, 414). Some studies have indicated that RSV can form minimal and infrequent syncytia in HAE tissues; however, there are conflicting results (314, 321). Analysis of lung autopsy specimens for both viruses suggested that syncytia formation can occur *in vivo* (395, 409). We were unable to identify any syncytia in either the fully sectioned tissues or apical images for RSV or HMPV. Studies in polarized cell monolayers or in HAE tissues demonstrated that RSV F was primarily localized to the apical surface (321, 438). Here, we also found that RSV and HMPV F were primarily localized to the apical surface. In addition, we also observed the presence of staining at the basolateral portion of infected cells. Other factors for cell-to-cell fusion may be required in order to mediate the formation of syncytia in addition to the cellular distribution of F. It is also unknown if syncytia formation is beneficial

for viral replication. A RSV strain containing a hyperfusogenic fusion protein led to larger syncytia in 2-D monolayers and higher pathogenesis *in vivo*, suggesting that higher fusion is beneficial for viral replication and spread (301).

One caveat in HAE tissues that is different from *in vivo* studies is the lack of immune cells, which play a major role during infection. Their absence may contribute to our observations related to initial infection rate, apical release, spread kinetics, and lack of cytopathic effects. The inflammatory response has been suggested to be important for RSV infection (439), and may also play roles in HMPV infection as well. The inflammatory response yields damage to the lung epithelium layer, which may expose proteins and other factors present in tight junctions, not normally accessible to the virus (440, 441), and this could aid in HMPV spread. Further experiments are needed to understand how immune cells and the inflammatory response could modulate HMPV infection of airways.

Lastly, therapeutic monoclonal antibodies against RSV and HMPV were evaluated for their inhibition of viral infection and spread in this study. Pre-incubation of RSV with palivizumab or nirsevimab showed neutralization and spread inhibition for RSV in HAE tissues. Nirsevimab demonstrated a significantly higher neutralizing capacity compared to palivizumab (423). These results confirm the potential for nirsevimab, which is currently in late stage clinical study, for immunoprophylaxis against RSV. Studies in 2-D *in vitro* cultures and *in vivo* studies has demonstrated increased efficacy and potency against RSV compared with the only available therapeutic, palivizumab (422, 423, 432), which are further supported by the results of this study.

We also examined the effect of 54G10, a potent neutralizing monoclonal antibody against HMPV F (340) for inhibition HMPV infection and spread in HAE. Pre-incubation of HMPV with 54G10 at a concentration of 5 $\mu\text{g}/\text{mL}$ completely inhibited viral entry. However, spread was only modestly, but significantly at 2.5 $\mu\text{g}/\text{mL}$ and increasing the concentration of 54G10 to 25 $\mu\text{g}/\text{mL}$ did not result in further spread reduction. These results suggest that at least a portion of HMPV

spread in HAE tissues may occur by a neutralizing antibody-independent cell-to-cell mechanism. Thus, targeting the F protein of HMPV may not be the most effective antiviral therapy. The RSV and HMPV antibodies have different potencies in 2-D cell culture and bind the F protein at different sites (palivizumab: site II, nirsevimab: site 0 and 54G10: site IV). It is unclear if the modest inhibition of spread by 54G10 is related to a certain F binding mechanism of action. Future studies evaluating a large panel of antibodies could help to determine if this phenomenon is specific for HMPV or related to F protein binding.

While this study furthers our understanding of two important respiratory pathogens in a more physiologically relevant model, there is further research needed to characterize pneumovirus infection. Here, we utilize A2 subtypes of both HMPV and RSV to model viral replication in HAE tissues. However, it is possible there is strain-to-strain variation which can only be determined with additional studies in this model system. We also exploited monoclonal antibodies to understand entry and spread of RSV and HMPV in HAE tissues and examined the efficacy these antibodies as potential antiviral therapeutics. However, additional antibodies against both RSV and HMPV should be analyzed to determine which viral protein sites are more important to entry and spread and use this information to identify optimal sites for antiviral targets. HAE tissues offer a unique model system to better understand viral infection in 3-D human tissue using an *in vitro* culture method, with caveats. An important role of the respiratory tract is a protective barrier for invading pathogens. In response, the lung signals the immune system to fight infection. This results in the inhibition and clearance of infection, but also generates tissue damage as a result of inflammation and infection. This critical aspect is absent in the HAE system and therefore, this level of complexity is inaccessible using this method.

Altogether, these results demonstrate a significant dichotomy between two very closely related pneumoviruses and illustrate important aspects of their viral lifecycles. RSV spreads primarily through release and re-entry of viral particles. Current approaches to combat RSV entry and spread by targeting the F protein

are a promising avenue for RSV antiviral therapeutics. However, HMPV spread is poorly affected via this approach, suggesting other aspects of viral lifecycle may be more effective. Both RSV and HMPV, in addition to other nsRNA viruses, form punctate replication organelles in the cytoplasm of infected cells. It is possible that targeting components involved in the formation and maintenance of these viral organelles may prove to be a potent, broad spectrum antiviral for many significant viral pathogens. As there are limited studies analyzing these structures, more research is needed to better understand their formation, function, and key role in viral replication.

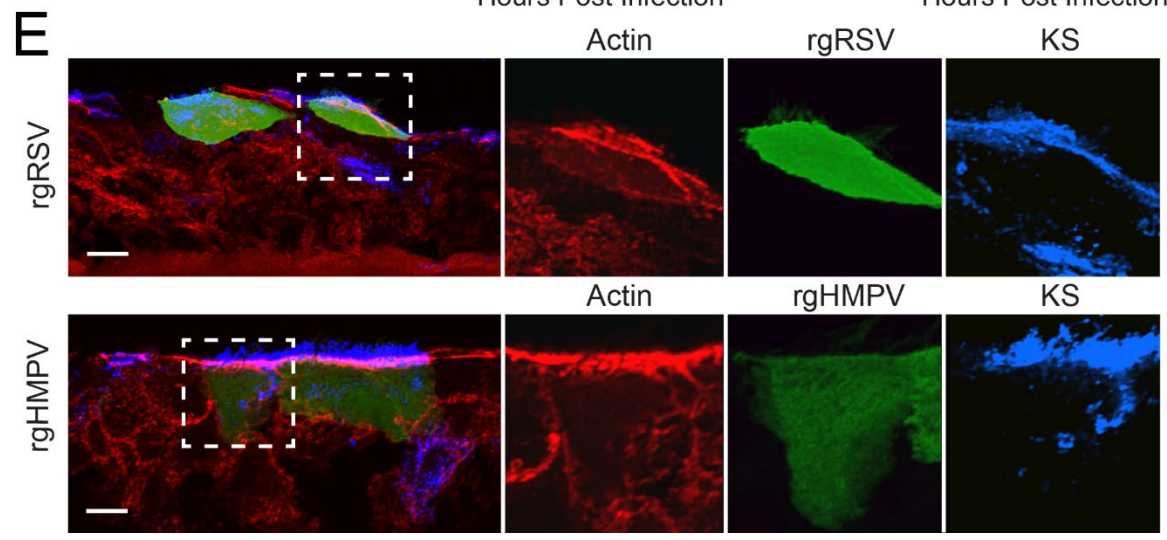
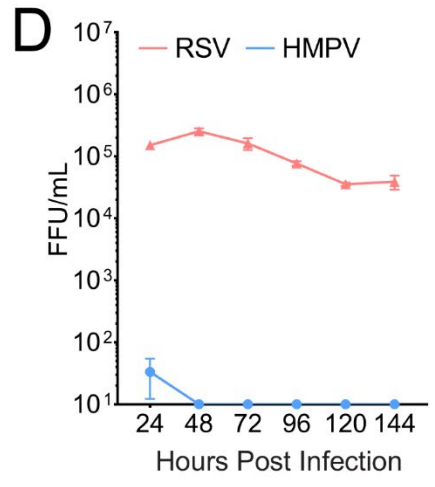
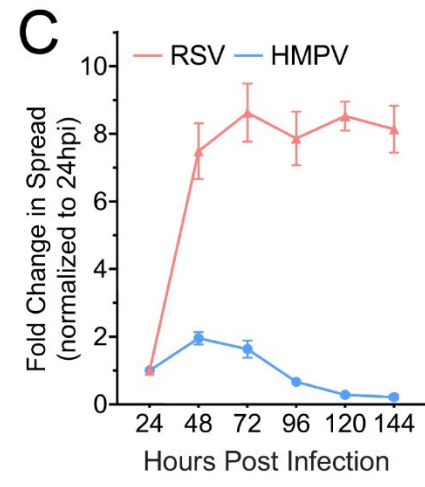
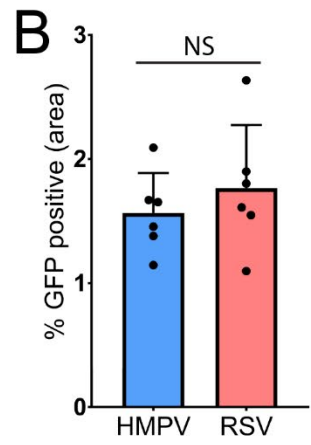
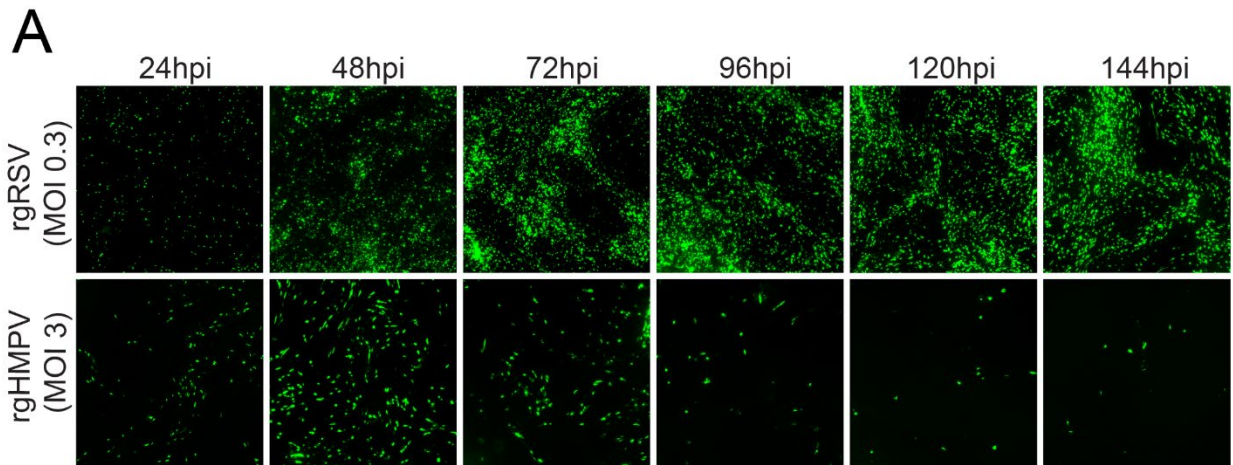


Figure 5.1: RSV and HMPV infection, spread and release in HAE tissues. **(A)** HAE tissues were infected with MOI 0.3 of rgRSV or MOI 3.0 of rgHMPV, and initial infection and spread was examined up to 144 hours post infection (HPI). **(B)** RSV and HMPV infection at 24hpi time point **(C)** Spread analysis of HMPV and RSV were determined using fluorescence threshold analysis. **(D)** Apical release of virus was determined by washing the apical surface of HAE tissues, titrating the viral wash in 2-D monolayers, and calculating fluorescence-forming units (FFU). **(E)** Infected cells for HMPV (48hpi) and RSV (72hpi) were stained for actin cytoskeleton, as well as keratan sulfate (KS) to stain for ciliated cells. Error bars represent SEM of 6 different tissues. Scale bar = 10 μ m.

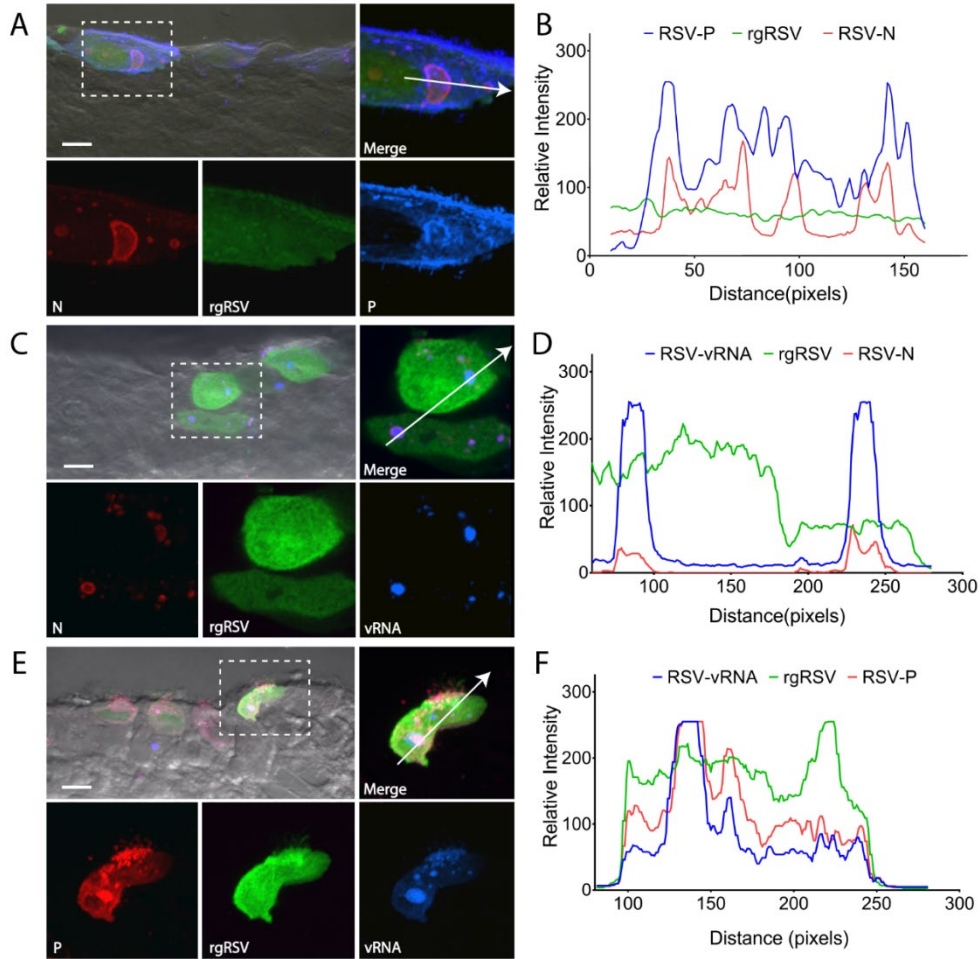


Figure 5.2: RSV inclusion body formation in HAE. (A) HAE tissues were infected with rgRSV and stained for the nucleoprotein, N, and phosphoprotein, P, to assess the formation of inclusion bodies in HAE tissues. **(B)** Co-localization of N and P was analyzed using co-localization chromatography from NIS elements. **(C)** To confirm inclusion body formation in HAE tissues, FISH analysis was conducted to label vRNA. **(D)** Both vRNA and RSV N colocalize to cytosolic punctate structures in infected cells. **(E)** vRNA was also assessed in relation to RSV using fluorescence microscopy. **(F)** Chromatogram analysis demonstrates that P and vRNA co-localize with one another in infected cells. Scale bar = 10 μ m for combined images with DIC and 5 μ m for fluorescence insets. Arrows indicate the cross-section measurement for the corresponding chromatograms.

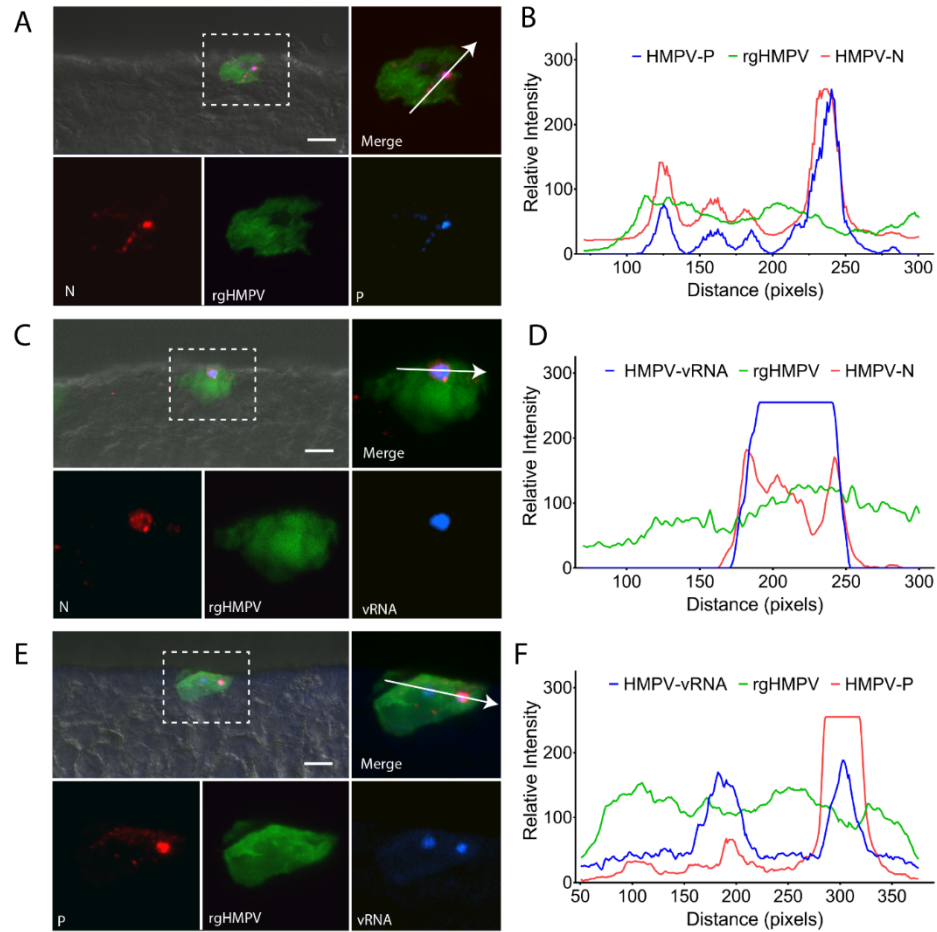


Figure 5.3: HMPV inclusion body formation in HAE. (A) HAE tissues were infected with rgHMPV and stained for the nucleoprotein, N, and phosphoprotein, P, to determine the formation of inclusion bodies in HAE tissues. (B) Co-localization of N and P was analyzed using co-localization chromatography from NIS elements. (C) To confirm inclusion body formation in HAE tissues, FISH analysis was conducted to label vRNA. (D) Both vRNA and HMPV N colocalize to cytosolic punctate structures in infected cells. (E) vRNA was also assessed in relation to HMPV using fluorescence microscopy. (F) Chromatogram analysis demonstrates that P and vRNA co-localize with one another in infected cells. Scale bar = 10 μ m for combined images with DIC and 5 μ m for fluorescence insets. Arrows indicate the cross-section measurement for the corresponding chromatograms.

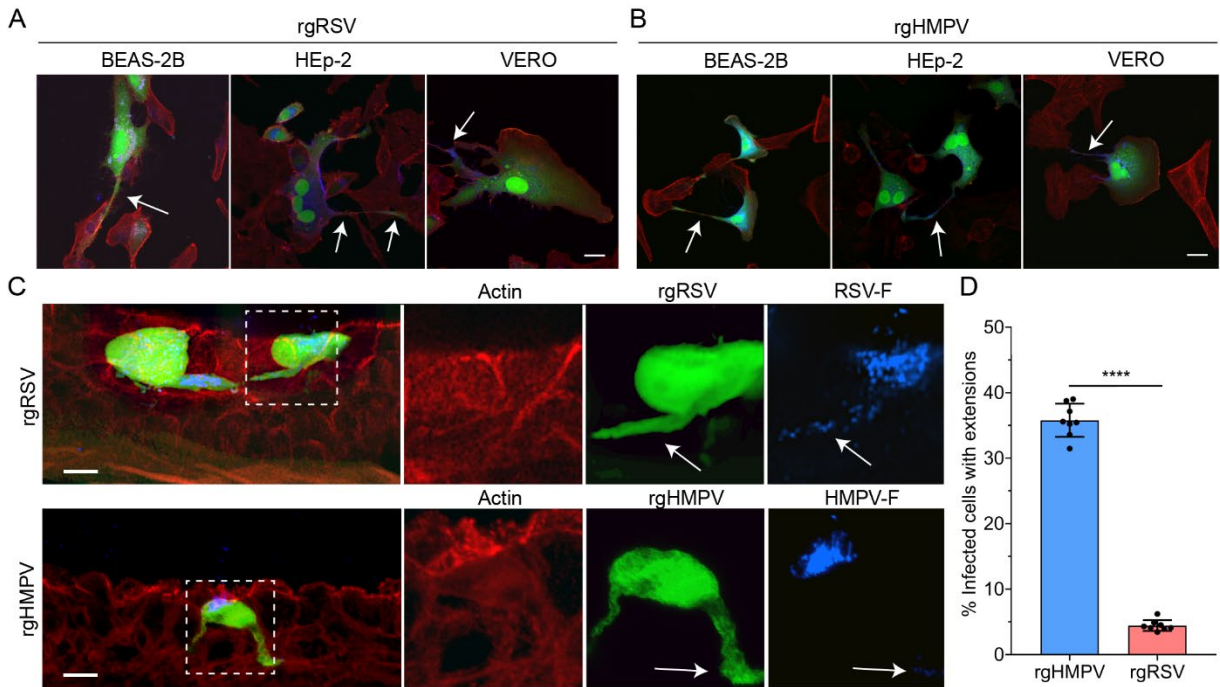


Figure 5.4: HMPV forms intercellular extensions significantly more than RSV. BEAS-2B, Vero and HEp-2 cells infected with rgRSV (**A**) or rgHMPV (**B**) demonstrate the formation of long filamentous extensions. (**C**) HAE tissues infected with either rgRSV or rgHMPV demonstrate the formation of these filamentous extensions in a 3-D model system. (**D**) Extension formation is significantly more common in rgHMPV infected tissues compared with those infected with rgRSV. Statistical significance represented with $p < 0.05$ *, $P < 0.005$ **, $P < 0.0005$ *** and $P < 0.0001$ ****. Scale bar = 25 μ m for 2-D cell culture and 10 μ m for HAE tissues, 5 μ m for higher magnification insets.

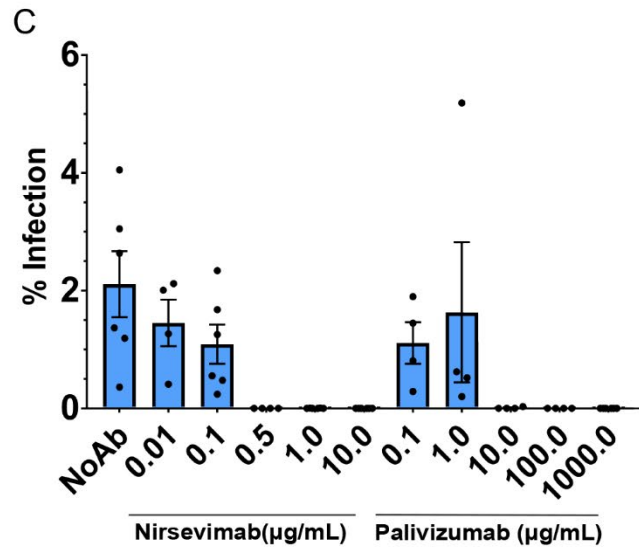
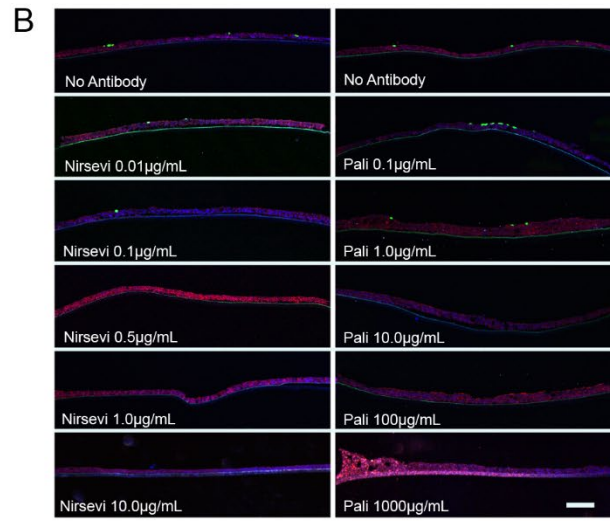
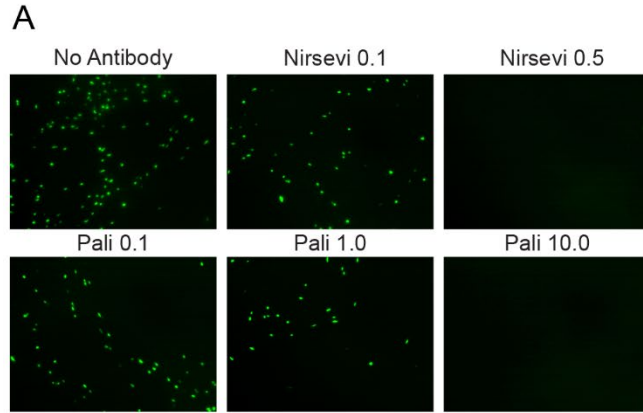


Figure 5.5: Nirsevimab and palivizumab inhibition of RSV entry. (A) HAE tissues were infected with rgRSV at MOI 1.0 preincubated with or without palivizumab (pali) or nirsevimab (nirsevi) for 1 hour at 37°C. After 48hours post infection, fluorescence was examined by inverted or confocal microscopy to determine inhibition of infection as well as microtome cross sections **(B)** of infected tissues to examine infection inhibition. **(C)** Threshold analysis of inverted fluorescence microscopy images were quantified using ImageJ adaptive threshold analysis. Scale bar = 10µm. Error bars represent SEM of 4-6 tissues for each treatment group.

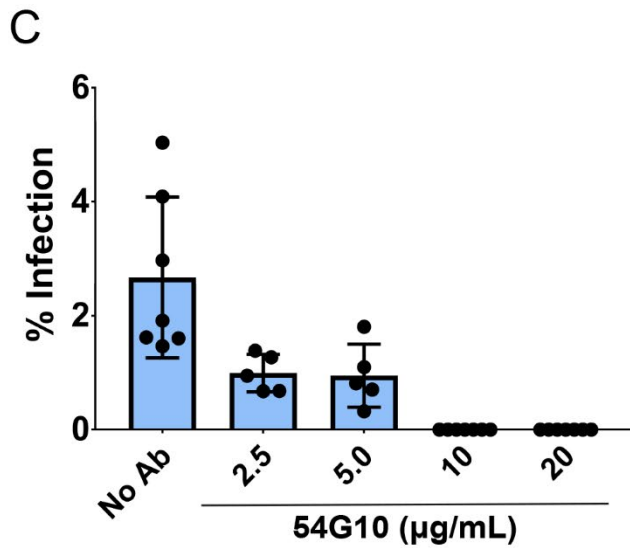
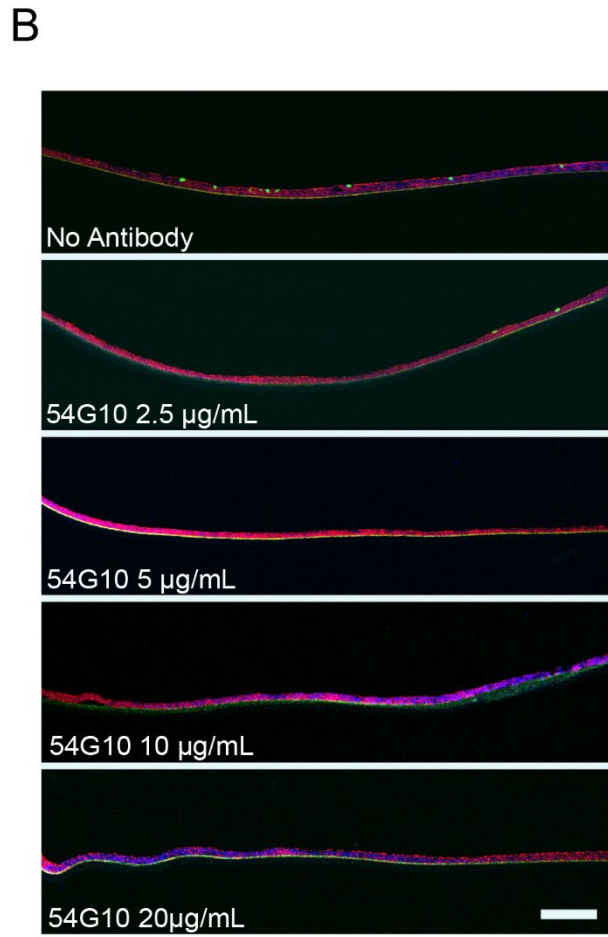
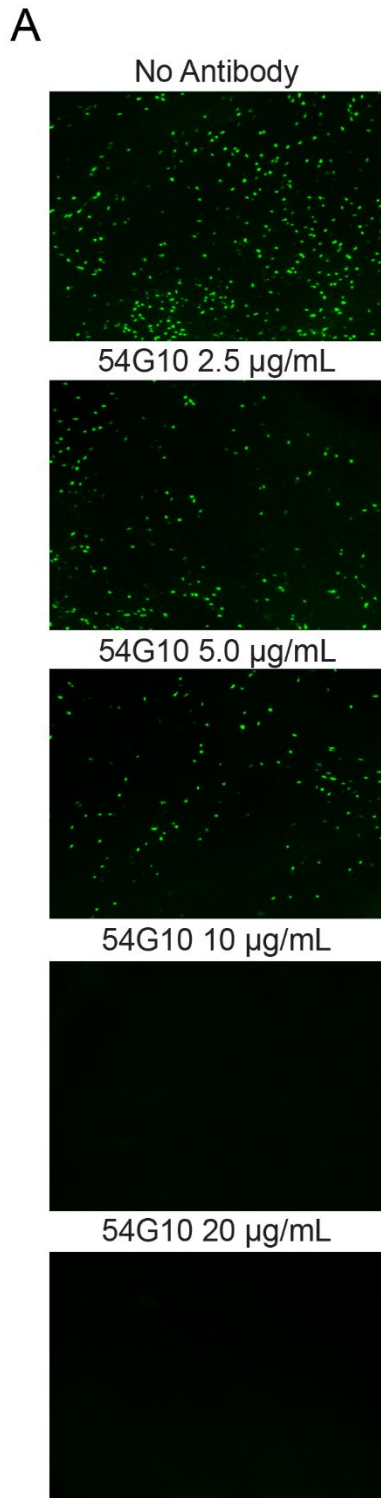


Figure 5.6: 54G10 inhibition of HMPV entry. (A) HAE tissues were infected with rgHMPV at MOI 3.0 preincubated with or without 54G10 for 1 hour at 25°C. After 48hours post infection, fluorescence was examined by inverted or confocal microscopy to determine inhibition of infection **(B)** as well as microtome cross sections of infected tissues to examine infection inhibition. **(C)** Threshold analysis of inverted fluorescence microscopy images were quantified using ImageJ adaptive threshold analysis. Scale bar = 10µm. Error bars represent SEM of 4-6 tissues for each treatment group.

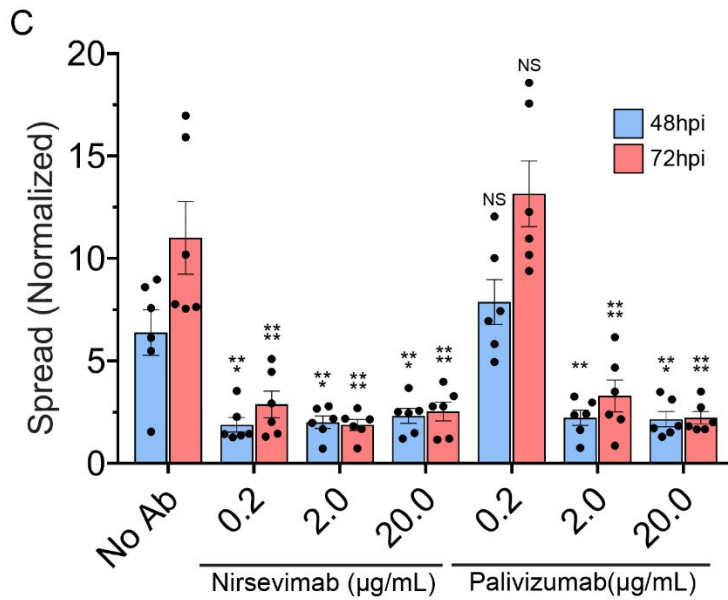
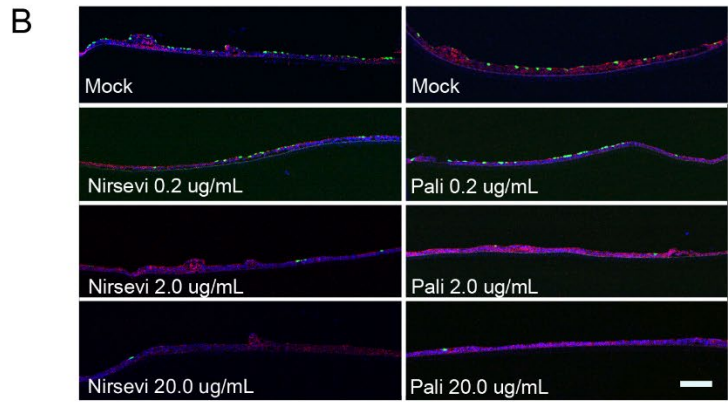
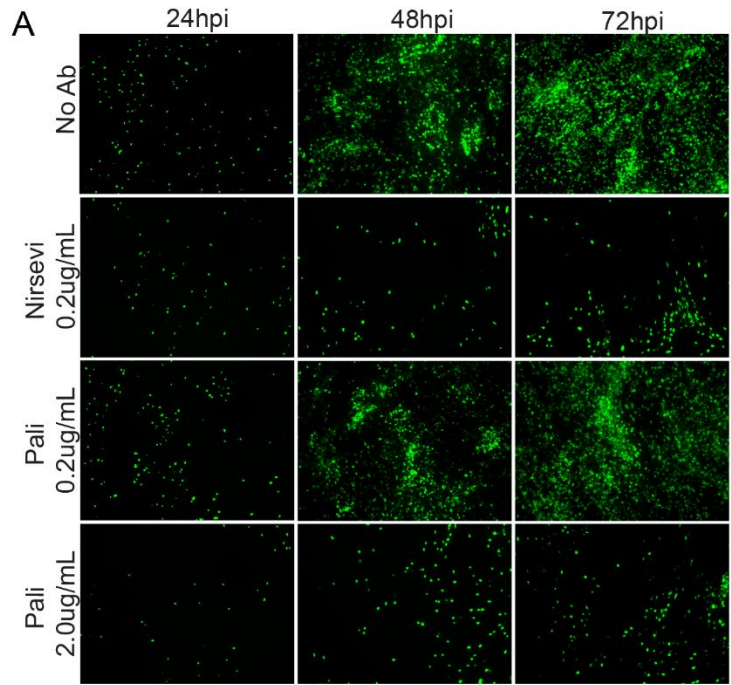


Figure 5.7: Nirsevimab inhibits spread significantly more potently than palivizumab. (A) HAE tissues were infected with rgRSV at MOI of 0.3. Tissues were treated apically with either palivizumab or nirsevimab 6 hours post inoculation in 50µL of TEER buffer. Fluorescence microscopy images were taken up to 72 hours post infection. **(B)** Tissues were fixed at 72hpi and microtome-sectioned for each treatment group and examined for viral spread. **(C)** Fluorescence threshold analysis of inverted fluorescence microscopy images demonstrate that both pali and nirsevi are able to prevent the spread of rgRSV in HAE-infected tissues, with nirsevi able to inhibit spread at lower concentrations compared with pali. Scale bar = 10µm. Error bars represent SEM of 6 tissues per treatment group. Statistical significance represented with $p < 0.05$ *, $P < 0.005$ **, $P < 0.0005$ *** and $P < 0.0001$ ****.

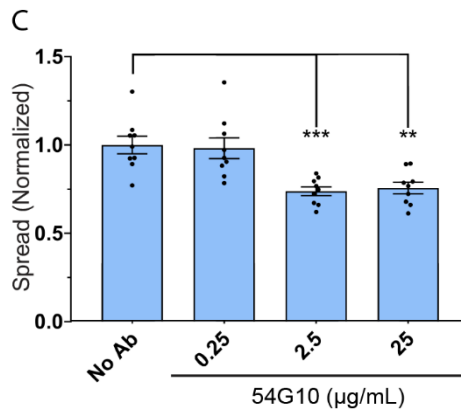
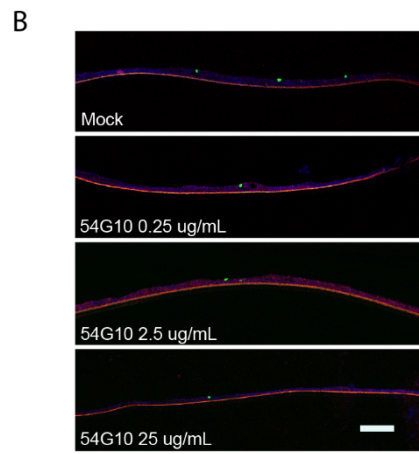
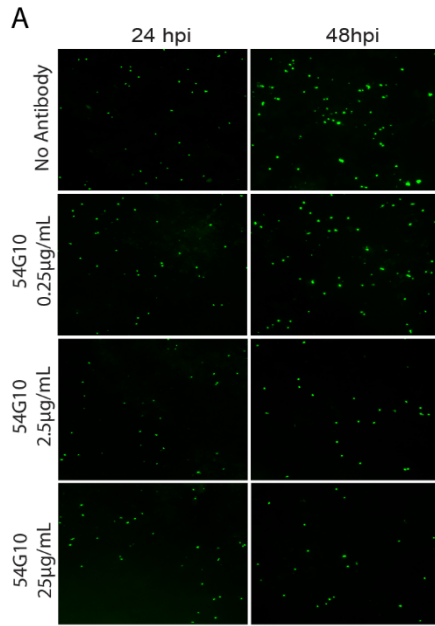


Figure 5.8: 54G10 significantly inhibits spread of HMPV. (A) HAE tissues were infected with rgHMPV at MOI of 3.0. Tissues were treated apically with 54G10 6 hours post inoculation in 50 μ L of TEER buffer. Fluorescence microscopy images were taken up to 72 hours post infection. **(B)** Tissues were fixed at 48hpi and microtome-sectioned for each treatment group and examined for viral spread. **(C)** Fluorescence threshold analysis of inverted fluorescence microscopy images demonstrate that 54G10 modestly but significantly prevents the spread of rgHMPV in HAE infected tissues. Scale bar = 10 μ m. Error bars represent SEM of 6 tissues per treatment group. Statistical significance represented with $p < 0.05$ *, $P < 0.005$ **, $P < 0.0005$ *** and $P < 0.0001$ ****.

Chapter 6: RSV and HMPV viral co-infections

* This chapter was completed with the help of Dr. Nicolas Cifuentes and Rachel Thompson. Nicolas and Rachel generated the transfection inclusion body counts (Figure 6.5) and Nicolas generated the recombinant mCherry virus for HMPV, examined the co-infection potential over time, and conducted microscopy (Figure 6.1-6.4). I generated all figures as well as performed experiments in figure 6.6. Nicolas contributed to the initial drafts of the written portion.

Introduction

The *Pneumoviridae* is a recently created viral family that harbors two important pediatric respiratory pathogens, human metapneumovirus (HMPV) and respiratory syncytial virus (RSV) (18). Pneumoviruses cause upper and lower respiratory tract infections, symptomatically presenting as a mild cold-like disease which can progress to severe pneumonia and bronchiolitis (21-23, 26, 27, 30, 354, 391-397). Despite the high prevalence of these viruses, no FDA-approved vaccines are available against either RSV or HMPV. Only one prophylactic therapeutic, palivizumab, is available for RSV (28, 29), and none are available against HMPV. However, palivizumab is given only to high risk infants born during the infectious season. An important, yet highly understudied feature of pneumoviruses is the occurrence of viral co-infections, which have been associated in some cases with a more severe outcome of the disease for these two viruses (38, 40).

Pneumovirus particles are enveloped and contain a non-segmented, negative-sense single-stranded RNA genome (nsNSV) coated by the nucleoprotein (N), giving rise to helical nucleocapsids (442, 443). The nucleoprotein interacts with the viral phosphoprotein (P), which recruits both the large RNA-dependent RNA-polymerase (L) and the M2-1 protein onto nucleocapsids forming the replication complex. During initial infection, a membrane fusion step mediated by the viral surface glycoproteins allows entry into target cells, releasing the viral nucleocapsids into the cell cytoplasm. The viral

RNA-dependent RNA polymerase then initiates transcription and replication of the viral genome to generate messenger RNA (mRNAs) as well as the genomic RNA (vRNA) (444). An important feature observed in pneumovirus infected cells is the formation of perinuclear structures named inclusion bodies (IBs) (251, 445). The available evidence indicates that IBs are the sites of pneumovirus genome transcription and replication, producing both genomic material for viral particle formation and mRNA for viral protein production (251, 254, 255, 445, 446). Additional robust evidence linking IBs to genome transcription and replication has been reported for other nsNSVs including rhabdoviruses (256, 263), filoviruses (261, 262, 447) and paramyxoviruses (264, 266), further supporting an important role for IBs in viral infections within the negative sense RNA viruses.

Here, we explored the dynamics of co-infections by RSV and HMPV in immortalized cell lines. Infection experiments using both viruses showed the population of HMPV-RSV co-infected cells was only a minor fraction of the total infected cells and required significantly more HMPV compared to RSV. However, the fraction of co-infected cells did show increases over time. Interestingly in co-infected cells, we found the presence of IBs with positive co-localizing signal for both HMPV and RSV genomes, suggesting that replication and transcription of both viruses can occur in the same specialized compartment. We recapitulated IB formation by homologous and heterologous co-expression of pneumovirus N and P proteins and found that HMPV P can complement RSV N to facilitate IB formation. However, various permutations of N and P proteins yielded changes in the minigenome replication efficiency for both viruses. Furthermore, using a minigenome replication assay, we find that RSV N and P are able to partially complement replication in addition to HMPV proteins and genome, but are less efficient compared with homologous HMPV protein expression only. Conversely, RSV again showed significant replication deficiency when HMPV N and P are present, supporting a potential dominant negative phenotype where HMPV interferes with RSV replication. To our knowledge, this is the first demonstration of pneumovirus coinfections at a cellular level, providing new insights into the consequences of viral coinfections *in vivo*.

Results and Discussion

HMPV and RSV coinfections in immortalized cell lines

To quantitatively evaluate the frequency of HMPV-RSV co-infections by flow cytometry, we created a recombinant HMPV carrying a mCherry cassette, located between the N and P genes (Fig 6.1A). The recombinant virus, named rJPS02-76mCherry (denoted rmcHMPV), was grown in the presence of TPCK-trypsin to titers comparable to the previously reported rJPS02-76EGFP (192) (Fig 6.1B). Human bronchial epithelial cells (BEAS2B) were infected with the rmcHMPV, with a recombinant RSV carrying a GFP cassette (denoted rgRSV), or with combinations of both at different multiplicities of infection (MOI), with infection by both viruses carried out at the same time. The presence of coinfecting cells was initially evaluated by microscopy at 24, 48 and 72 hpi and subsequently analysed by flow cytometry. Initially, we evaluated singly infected cells in three different cell types: LLC-MK2, Vero, and BEAS-2B, to understand infection and spread kinetics for each virus. rmcHMPV demonstrated a more robust infection and spread in LLC-MK2 cells compared with both BEAS-2B or Vero cells, and the percent of infected cells increased through 72hpi (Fig 6.2A). This result was not surprising since HMPV has been described as a poor growing virus *in vitro*, and some cell lines including BEAS2B are not as suitable for viral growth and Veros show lower kinetics compared with LLC-MK2 (448). For RSV, LLC-MK2 and Vero cells demonstrated similar percentage of infection and rates of spread, but BEAS-2B cells again showed decreased permissiveness to infection and increased cell death was observed at late times of infection when high MOIs were used (Fig 6.2B).

To examine for cells co-infected with HMPV and RSV, the levels of HMPV were kept at a constant MOI of 1, and RSV was used at MOIs of 0.01, 0.1 or 1. The highest levels of co-infected cells were observed when using infection ratios of 1:1 of HMPV to RSV in BEAS-2B cells, but with much lower percentages of co-

infected cells observed when less RSV was used (Fig 6.3A). When examining infection in Vero and LLC-MK2 cells, we observed a relatively low number of co-infected cells similar to that observed in BEAS-2B, although more abundant in comparison. (Fig 6.3A). By 48 and 72 hpi, the number of co-infected cells increased significantly, indicative of viral spread through infection a naïve cell or entry of one virus into a cell previously infected by another virus (Fig 6.3B). In addition, singly infected HMPV cells were almost undetectable at 72hpi, but the total number of co-infected cells observed suggests that HMPV is still able to spread, but eventually, almost all HMPV infected cells are present in a co-infection.

When analysing co-infections of singly vs co-infected cells infected at the same time, RSV demonstrated a decrease in the number of infected cells at 24hpi. This suggests that the presence of HMPV significantly alters initial entry and replication of RSV, but is unaffected at later times post infection. Conversely, HMPV appears to be unaffected and the infection percentage at 24hpi remains largely unchanged. This phenomenon of viral interference has been reported for other viruses and remains poorly understood (449-451), but offers one explanation for our observations during co-infection. Similar reductions in viral loads were reported clinically for co-infections of RSV and HMPV as well, further supporting our observations *in vitro* (452-454)..

HMPV and RSV heterologous protein complementation

In order to better understand how these viruses are interacting, we first examined co-infected cells in detail beginning with effects on replication. We conducted fluorescence *in situ* hybridization (FISH), using probes that hybridize to either the vRNA from HMPV or the vRNA from RSV. Different patterns of vRNA signals were found in co-infected cells, the most striking being the colocalization of signals in structures that resemble what has been described as IBs (Fig 6.4). Z-stack analysis demonstrated that signals of vRNA from both viruses occupied the same location within co-infected cells (Fig 6.4). One intriguing possibility for the

observed co-localization is the heterologous complementation of viral proteins for IB formation and/or RNA synthesis.

For pneumoviruses, IB formation can be minimally recapitulated by homologous expression of P and N (254, 455), therefore, we decided to test if heterologous protein expression between viruses would complement IB formation. As a control, HMPV N and P, as well as RSV N and P, were verified to induce formation of IBs when co-expressed in Vero cells. Interestingly, a significant percentage of cells expressing HMPV P and RSV N still formed IBs, while cells expressing HMPV N and RSV P formed no IB-like structures (Fig 6.5). In order to test if heterologous proteins could be incorporated into already formed IBs, triple transfections were performed. Upon HMPV N and P co-expression, the additional expression of either RSV N or P had a strong deleterious effect on IB formation, appearing to act in a dominant negative mechanism (Fig 6.5). Instead of large IBs (>500nm), cells displayed speckles, consisting of small and abundant cytosolic puncta for both signals but significantly smaller in size (<500nm) compared to normal IBs. In contrast, RSV N and P still formed IBs in the presence of either HMPV N or P, though to reduced levels (Fig 6.5). However, these experiments are preliminary, and more investigation is needed to better understand the effects of protein complementation for both viruses on IB formation.

To further examine the functional consequences of heterologous IB formation, we employed HMPV and RSV mini-replicon assays. Here, the 3' leader region from the viral genomic RNA is placed in front of a luciferase reporter. Successful binding and initiation by the viral replication complex results in the production of luciferase transcript, resulting in luciferase protein production which can be measured quantitatively. Heterologous expression of RSV N or P in place of HMPV proteins in the mini-replicon assay resulted no replication, suggesting these are not able to take the place of the cognate protein of HMPV. However, expression of both RSV N and P did result in a 10% increase in luciferase activity, which indicates that heterologous IBs were functional, but significantly less than cognate protein expression (Fig 6.6A). Similarly, when examining HMPV N or P

expression in the RSV mini-replicon assay, single complementation of N or P resulted in no luciferase activity whereas both HMPV N and P expression resulted in a 10% increase in luciferase activity (Fig 6.6B). Lastly, we conducted mini-replicon assays using all HMPV proteins and co-expressed RSV N, P or all 4 of the RSV proteins (including M2-1 and L) to determine if there were synergistic or dominant negative effects on replication. Compared with the HMPV proteins alone, addition of RSV P mildly decreased replication by 20%, whereas the addition of N decreased it to nearly 50%. Co-expression of N/P from RSV or the addition of all mini-genome components resulted in only 30% reduction in replication, suggesting that RSV proteins do not completely inhibit HMPV replication, but these components are less efficient in comparison. Conversely, the addition of any HMPV components to the RSV mini-replicon resulted in significant reduction of RSV replication to 20% compared with RSV components alone, suggesting HMPV proteins are able to act in a dominant negative fashion instead of complementation, where they inhibit the function of RSV proteins by competing for substrate and prevent replication.

HMPV P (294 aa) and RSV P (241 aa) share only 37% amino acid identity. However, their overall domain structure is highly similar and includes the presence of N- and C-terminal intrinsically disordered regions (IDRs) and a central α -helical tetramerization domain (456, 457). Most of the identical amino acids between HMPV P and RSV P are in the tetramerization domain, but our results suggest that these proteins are unlikely to form heteromeric protein complexes that complement replication. Additionally, the deleterious effect of RSV N or P over HMPV IBs could be explained by their higher affinity for critical cellular components, including actin and/or actin related proteins which are important for virus lifecycle (251, 288, 406, 431, 458-460), but this remains to be further examined.

From 24 to 72hpi, singly infected HMPV cells are almost completely gone and instead, only found in co-infected cells. However, the number of infected cells that contain HMPV increased, suggesting that HMPV is able to spread, but also results in more co-infected cells. One possibility is that RSV is able to infect nearly

100% of cells, and although the initial infection rates are altered when both viruses are present, they are unaffected at later times post infection. This allows HMPV to spread but permissiveness of RSV entry gives rise to an increase in both HMPV positive and co-infected cells. Another explanation is a cooperative effect of these viruses at the cell surface. RSV and HMPV proteins and nucleic acids move to the plasma, aggregating at viral assembly sites. As both pneumoviruses bud, there may be an interaction occurring, where HMPV and RSV particles travel closely associated, leading to entry of both viruses into a single cell. Another purely speculative idea is the presence of chimeric viruses. HMPV and RSV demonstrate high similarity, with homologous proteins performing similar functions during the viral lifecycle. We have also shown that there are some potential interactions of replication components from one virus interacting with the genetic material of another using the mini-replicon system. Therefore, as nucleic acids are being packed into virions for spread, there could be a heterologous nucleic acid population, containing genomes from both RSV and HMPV in newly formed virions. This chimeric virus then delivers both genomes to a naïve cell, which increases the number of HMPV and subsequently, co-infected cells. However, there needs to be further investigation of assembly and spread to better understand spread kinetics in co-infected populations and how this increase in co-infected cells is occurring and how it affects the replication efficiency of each virus. In addition, there is no current evidence for the presence of chimeric viruses and therefore, this mechanism needs to be examined further to identify if this is possible.

The RSV genome is 2 kb larger than the HMPV genome, and contains two non-structural proteins NS1 and NS2, absent in HMPV. Both proteins have anti-interferon activities, representing an additional advantage of RSV infections over HMPV. However, while purely speculative, in the event that viral chimeras were generated from co-infected cells, this offers a potential explanation of why co-infections between these two viruses are able to generate a worse clinical outcome in patients, although this severity varies (39, 41, 44, 452-454, 461-472). It may also offer one potential explanation for why co-infected cells are more prevalent at later

times post infection and singly infected HMPV cells are absent. Our current data suggests that HMPV and RSV have a potentially reduced synergy, but these are examined in transfection and not infection experiments, where a host of other viral proteins may interact to favour replication and spread for both viruses. However, one study examined the amounts of RSV and HMPV viral loads in co-infected patients and saw no change for HMPV but a small, significant decrease in RSV titer (452), similar to our findings using the mini-replicon assay and suggested by other studies as well (453, 454). In addition, there may be synergistic crossover of HMPV and RSV proteins involved in other aspects of viral lifecycle, but further studies examining key components needs to be conducted to better understand interactions between pneumoviruses. Future work will define if these co-infections are beneficial for viral infection and spread and the molecular mechanisms underlying this phenomenon.

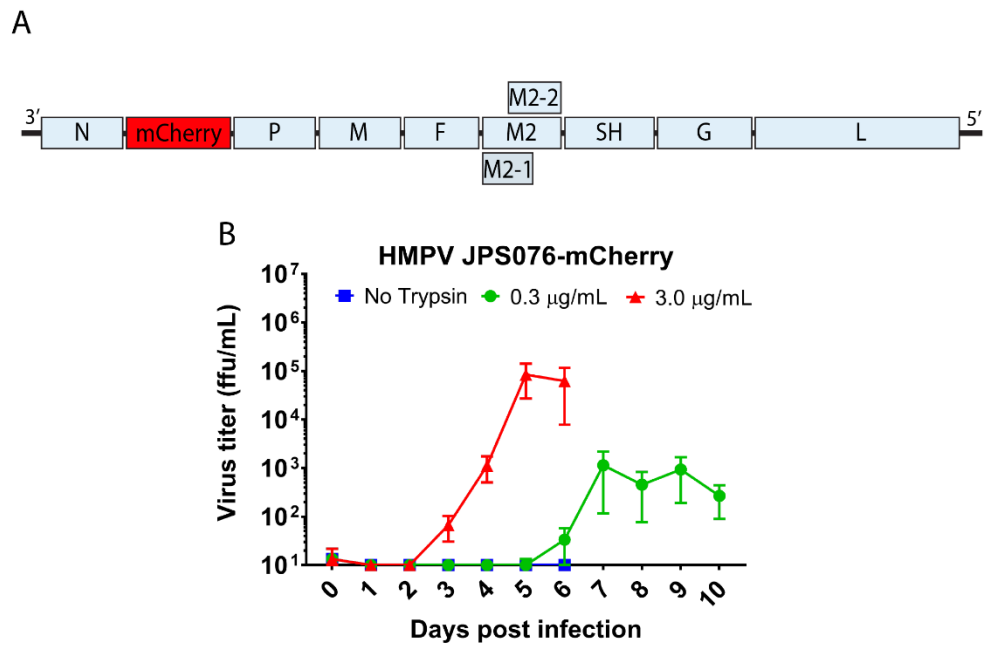


Figure 6.1: Recombinant mCherry HMPV shows efficient growth. (A) Recombinant mCherry-expressing HMPV strain JPS07E2 (rmcHMPV) was created by placing the gene for the fluorophore between the N and P gene segments. **(B)** rmcHMPV growth kinetics were similar to those observed for the JPS07E2 strain expressing GFP. Growth was seen when exogenous trypsin was added at 3 and 0.3µg/mL but no growth when trypsin was not present (n=3).

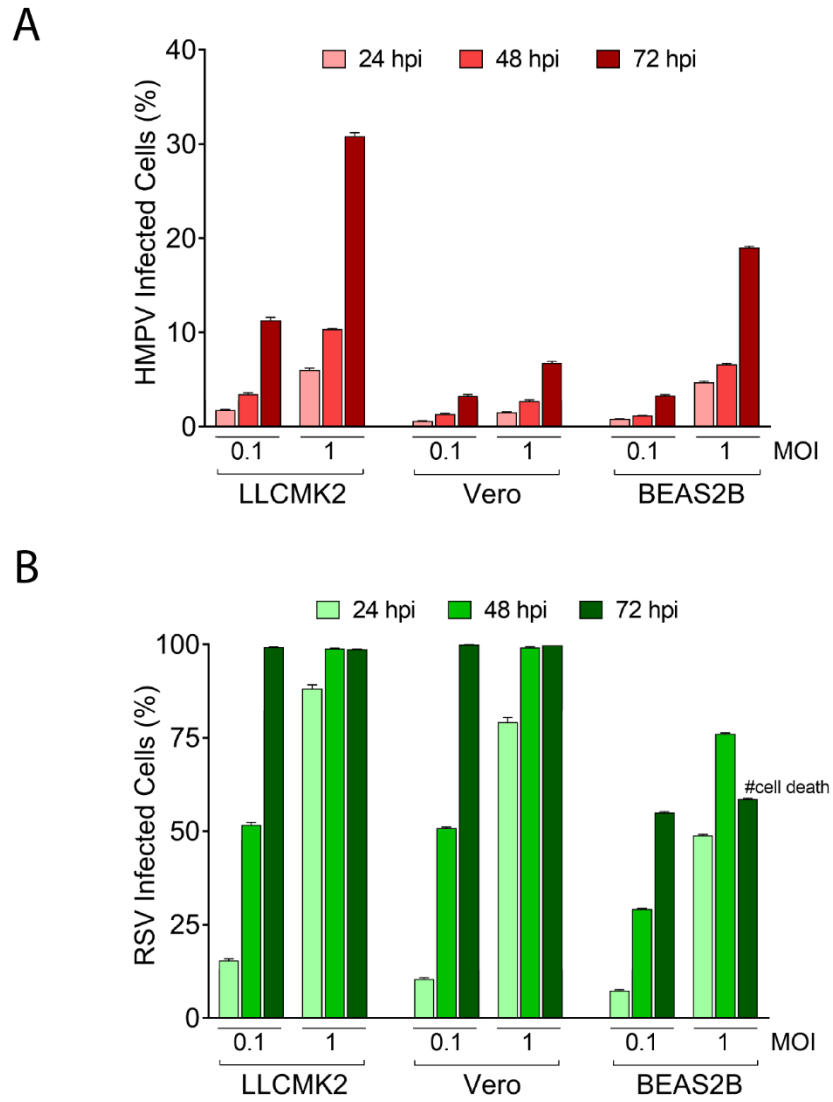


Figure 6.2: HMPV and RSV growth in infected cells. LLC-MK2, Vero, and BEAS-2B cells were infected with **(A)** rmHMPV and **(B)** rgRSV to observe infection and growth over time. LLC-MK2 cells demonstrated the highest infection and growth rate for both viruses (n=3).

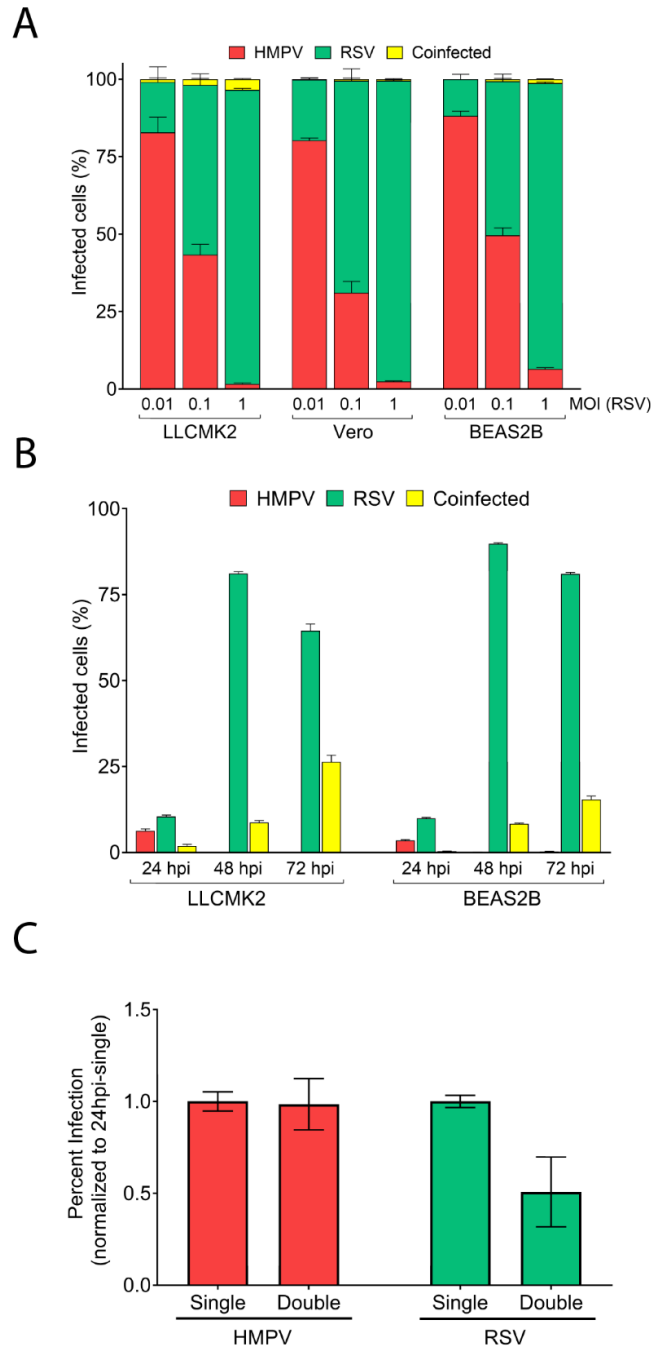
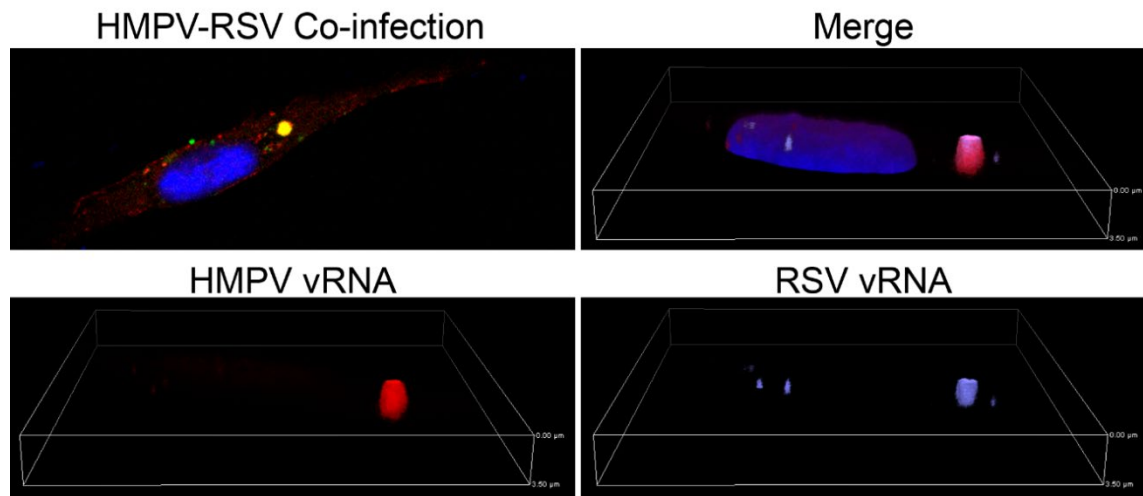


Figure 6.3: Analysis of HMPV and RSV co-infections. (A) rgRSV (MOI 0.01, 0.1 or 1) and rmHMPV (MOI 1) were added simultaneously to LLC-MK2, Vero, or BEAS-2B. At 24 hpi, the percent of co-infected cells was determined using flow cytometry. **(B)** Co-infected cells were then

analysed over time up to 72 hpi, showing that co-infected cells increase over time. (C)



Simultaneous infection of pneumoviruses affects RSV but not HMPV at 24hpi (n=3).

Figure 6.4: HMPV and RSV in co-infected cells can occupy the same IB. Vero cells infected with rgRSV and wild type HMPV. Co-infected cells were examined using FISH against the RSV and HMPV genomes which demonstrated co-localization within inclusion body like structures.

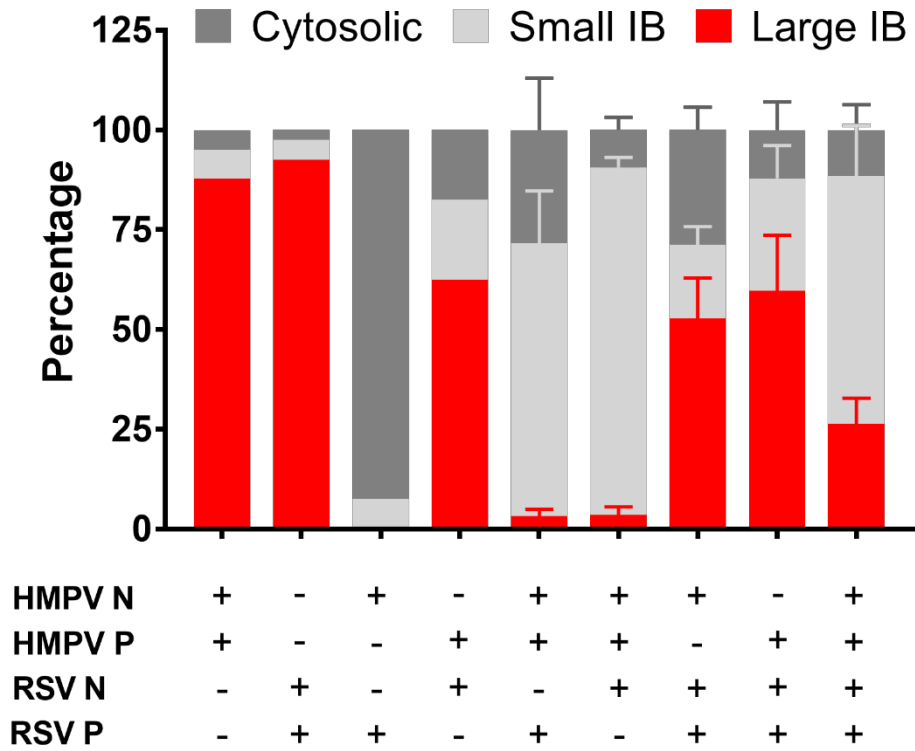


Figure 6.5: Recombinant RSV or HMPV N and P expression alter inclusion body formation. Permutations of RSV and HMPV N and P were co-expressed in Vero cells and inclusion bodies were examined using fluorescence microscopy. Both RSV N and P contained an HA tag used for staining. HA tagged HMPV P was used in conditions 1,4 and 9. Untagged HMPV P was used in conditions 5,6, and 8. 100 cells were counted per transfection group and each was categorized as containing large inclusion bodies (>500 nm), small inclusion bodies (<500 nm), or cytosolic protein distribution.

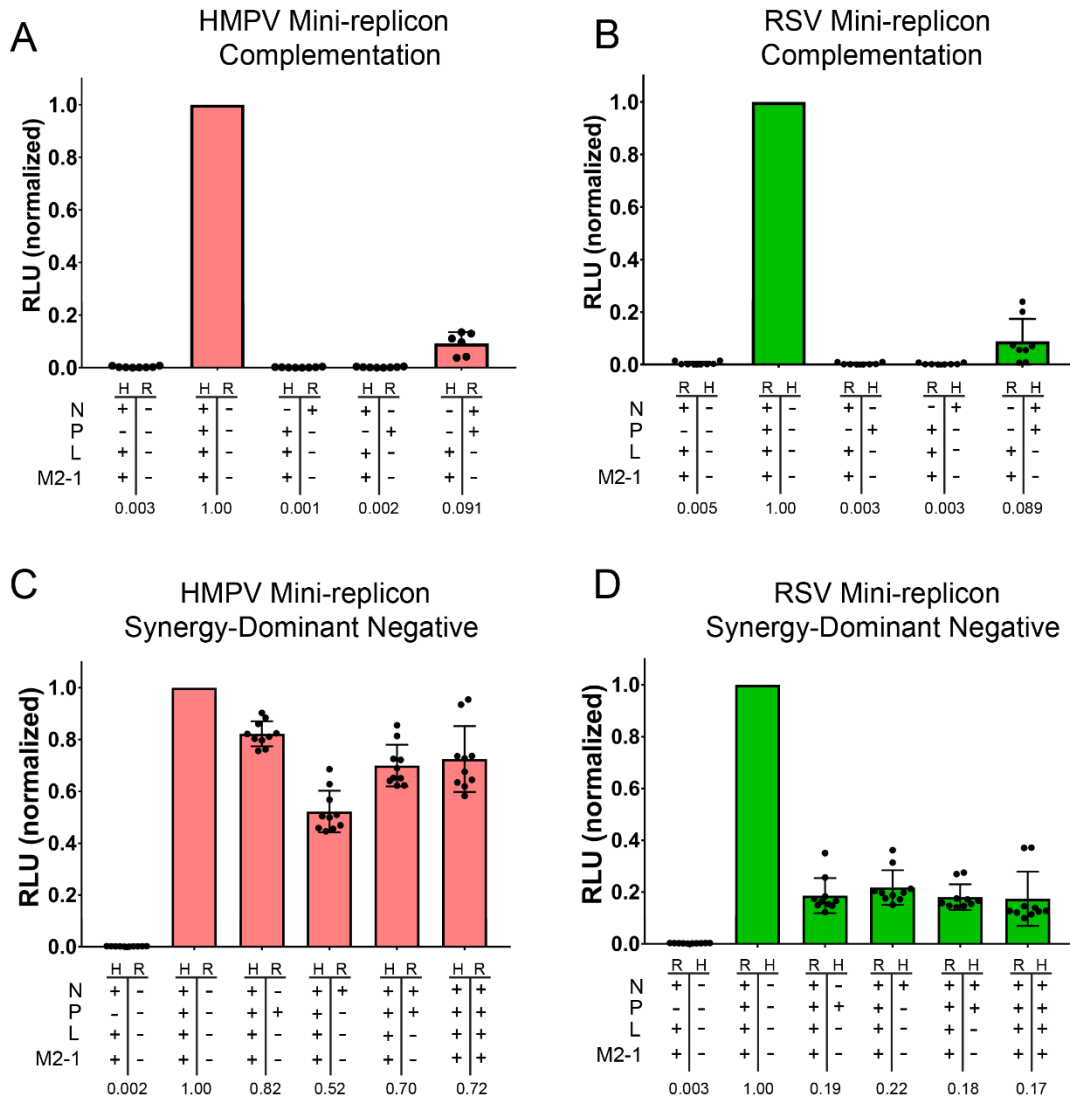


Figure 6.6: HMPV and RSV mini-replicon complementation, synergy, and dominant negative effects. The HMPV (H) or RSV (R) mini-replicon plasmids along with genes for viral proteins in the indicated permutations were transfected into BSR cells. Luciferase activity was measured 24 hours post transfection for each of the complementation and synergy/dominant negative groups (n=3-5).

Chapter 7: Discussion and Future Directions

The topics covered in this dissertation create a better understanding of key molecular interactions for pneumovirus entry, spread, and inhibition. We identified novel information about how HMPV strains can utilize low pH as a timing mechanism for triggering and what residues within the protein contribute to this phenomenon (Chapter 3). We further analyzed other known aspects of HMPV lifecycle, identifying previously unknown proteases that process HMPV F and using this new information to target multiple viruses therapeutically (Chapter 4). Further exploring pneumovirus lifecycles, we employed a 3-D human airway tissue model system to directly compare and contrast infection, spread, and phenotypes associated with infection, identifying important information for potential therapeutic development (Chapter 5). Lastly, we explored the phenomenon of viral co-infections, allowing us to better understand how these closely related pneumoviruses co-occupy replication compartments in co-infected cells and explore a potential synergy for these *in vitro* (Chapter 6). While our results generate interesting and novel information about pneumovirus lifecycles, there remain many more research questions that need to be explored.

Low pH mediate triggering of HMPV F: Analysis of new strains reveals complex requirements for fusion

Understanding requirements for viral entry is an important aspect for preventing entry as a therapeutic approach. Prior to research conducted during this thesis, only a few fusion proteins from different HMPV strains had been shown to promote low pH triggered fusion (189, 240-242). However, other HMPV F proteins had been found to promote membrane fusion independent of pH while others are unable to mediate fusion at all in cell-based assays. Analysis of specific residues that contribute to low pH-mediated fusion had been examined using site directed mutagenesis, recombinant viral strains, or viral strains with conserved amino acid sequences reported for fusion phenotypes. Together, these results led to the hypothesis that low pH fusion requires a glycine (G) at position 294, as well as

lysine (K) at 296, tryptophan (W) at 396, asparagine (N) at 404, and histidine (H) at 435, which are primarily associated with the A2 viral strain subtype and therefore, a rare strain dependent phenomenon (189, 240-242). However, work presented in this thesis has examined newly available strains of HMPV to better understand low pH mediated fusion and the role for specific residues in this process (chapter 3).

Fusion protein triggering is a complex phenomenon and its temporal and spatial regulation is vital for viral spread. For many viruses, interactions between the attachment protein and a cellular receptor trigger the fusion protein. Alternatively, the fusion protein can directly interact with cellular factors to promote fusion. For viruses that are neither triggered by receptor binding or signaling by the cognate attachment protein, they must utilize some environmental signal, often using low pH present in cellular endosomes (154). Low pH triggering is utilized by the fusion proteins from many viruses, including members of *Orthomyxoviridae*, *Flaviviridae*, *Togaviridae*, *Rhabdoviridae*, *Bunyaviridae*, *Filoviridae*, and *Arenaviridae*, although there are families containing members with mixed requirements (154). These fusion proteins utilize specific residues, typically involving a histidine salt bridge, to disrupt electrostatic interactions to promote the conformational changes needed for fusion. In addition, there are direct, indirect, or a combination of factors required to trigger fusion and entry. This process becomes more complicated when factoring in the complex lipid membrane environment, which is both a barrier for viruses to cross and subsequently a hijacked resource to produce enveloped viral progeny.

For the closely related paramyxoviruses, it has been hypothesized that many members enter at the plasma membrane due to pH-independent entry (94, 145, 157). When examining the pneumovirus family, results describe a more complex entry pathway. RSV has been shown to mediate cell-to-cell fusion independent of the other surface glycoproteins, G and SH (91, 399, 400). Reports suggest RSV is also able to utilize multiple cellular factors for attachment and entry, including CX3CR1, heparan sulfate, L-sign, DC-Sign, nucleolin, and TLR4

(316, 473-478). These interactions subsequently allow RSV to enter via micropinocytosis where it fuses with the endosomal compartment for genome release (479). For HMPV, the fusion protein is able to mediate infection without G or SH as well (121, 123), similar to RSV. However, HMPV lacking G or SH still spreads in animal models whereas no detectable virus is recovered from animals infected with RSV lacking G or SH, suggesting HMPV is more independent of other surface glycoproteins, requiring only F for infection. While no receptor has been reported, there have been two attachment factors that are critical for HMPV entry: heparan sulfate and $\alpha\beta 1$ integrin (123, 243, 398). Subsequent entry of HMPV is mediated by endocytosis in a dynamin- and clathrin-dependent manner in bronchial epithelial cells (335). For the subtypes of HMPV that utilize low pH as a trigger, this trafficking pathway provides a trigger for fusion. However, it remains unexplored what factors are important for strains that do not use this mechanism.

Using chemicals, such as ammonium chloride, to prevent endosomal acidification blocks entry of viruses such as influenza and VSV which require low pH for triggering (480-482). When endosomal acidification was blocked prior to addition of HMPV, TN94-49 (A1) about 50% inhibition in infection was observed, whereas TN96-12 (A2) was still able to mediate efficient infection independent of pH (335). The observation that TN94-49 requires low pH was recapitulated using the isolated F protein, where low pH mediated cell-to-cell fusion was demonstrated. However, we did not observe any fusion activity for TN96-12 F, suggesting that other requirements are required independent of pH. TN96-12 was also examined in the presence of the homotypic attachment protein, G, but failed to promote fusion suggesting a further level of unexplored regulation (Fig 3.4). Despite entry being mediated by F, independent of other viral surface glycoproteins, strains of both HMPV and RSV have recently been identified that contain a duplication site in the attachment protein, hypothesized to increase the number of glycosylation sites present, potentially aiding in attachment to promote viral fitness (138, 142). In addition, G is still retained in all clinical strains of HMPV, suggesting an essential role that has not been fully understood *in vivo*.

Both HMPV F S174H434 and HMPV F TN96-12 demonstrated significantly higher overall and surface expression but showed significantly different fusion phenotypes. The addition of a histidine at 434, in addition to the previously reported 435, appeared to enhance the fusogenic activity when exposed to low pH. H434 may therefore act to enhance de-stabilization, creating interactions that are more sensitive to pH changes. Despite the significantly higher expression of TN96-12, fusion was still unable to be mediated under any conditions, suggesting other important factors required for fusion are still to be discovered.

Future experiments should explore the potential of a cellular receptor for HMPV, potentially elucidating a common factor needed for strains not requiring low pH for entry. Such a receptor would likely be present within the endosome, as strains that do not require low pH are also taken in by endocytosis, similar to the multistep entry process required for Ebola (234, 236). There is currently limited information on and resources available for clinical isolates of HMPV. Further analysis of strain sequences and phenotypic characterization of HMPV F would lead to a deeper understanding of which amino acids are important for fusion and establish if low pH mediated fusion is a rare, strain dependent phenomenon or part of a more complex regulatory interaction during infection for some strains.

Identifying and targeting proteases for antiviral treatment of HMPV

Viruses containing class I and II fusion glycoproteins require a cleavage event of the fusion protein or accessory protein, respectively, during the infectious process. This cleavage event allows priming of the fusion complex, creating a metastable form to promote fusion upon appropriate signaling (483). One of the most well studied respiratory viruses, influenza A, requires cleavage at a single basic amino acid residue to prime its class I fusion protein, HA. Historically, trypsin is used to promote cleavage *in vitro* (484, 485). Endogenous proteases required for activation were not reported until recently when a variety of serine proteases present in the lung that mediate cleavage of HA were identified (170, 173, 174, 176, 177, 376, 377, 380, 381, 383). Studies examining *in vitro* and animal model

systems further demonstrated that influenza subtypes also have variable protease specificity depending on the strain, but why this preference is present requires more research (173, 176, 375, 377, 381). Highly pathogenic influenza strains have a mutation in this cleavage site, converting it to a multi-basic stretch. This allows recognition and cleavage by more abundant, non-tissue specific intracellular proteases like furin (355). Identifying and understanding these proteases is important for characterizing pathogenicity and tropism during infection and spread. Similar to influenza, all HMPV strains contain a cleavage motif where a single basic amino acid is cleaved to release the fusion peptide (189). There is only one reported variation in the consensus sequence and these strains are considered trypsin independent, but few strains harbor this modification (190, 193). Trypsin independent strains did not grow to higher titers compared to strains requiring trypsin or those with an inserted furin cleavage motif, suggesting that this mutation does not enhance pathogenicity (190, 193).

Prior to our studies, it was known that trypsin and TMPRSS2 were able to cleave HMPV F (189, 192). The hypothesis that other proteases could also promote HMPV F cleavage led us to investigate other proteases identified for influenza which may also be utilized by HMPV or other respiratory viruses that have similar cleavage requirements. Other human respiratory viruses with class I fusion proteins requiring cleavage at a basic amino acid include paramyxoviruses such as parainfluenza virus 1-4 (486) and Sendai virus (486). In addition, TMPRSS2 was shown to cleave one of the two cleavage sites present in coronaviruses (CoV) such as 229-E (487), EMC (488), SARS-CoV (489, 490), MERS-CoV (491) and the novel SARS-CoV-2 (492). SARS-CoV and MERS-CoV have both been shown to be cleaved by TMPRSS2 and this protease plays an important role in infection. One cleavage site of MERS-CoV has the basic furin recognition motif (RXXR) for proteases recognizing multi-basic cleavage motifs, suggesting some potential cleavage by more abundant, endogenous proteases such as furin. However, HMPV shares a similar basic motif (RQSR) and is unable to be cleaved by furin, suggesting a more restricted motif requirement for efficient cleavage. The novel SARS-CoV-2 has a similar mutation compared with highly

pathogenic influenza (493), where an addition of basic amino acids residues at one of the cleavage sites (RRAR) which has a higher affinity for proteases that recognize a multi-basic amino acid stretch for cleavage, ultimately leading to more efficient processing. This mutation is a major contributing factor that led to a global pandemic that emerged in late 2019. Studies also support the use of TMPRSS2 by SARS-CoV-2, but studies also suggest cleavage by furin and other proteases that cleave at multi-basic amino acid motifs (494). However, there are limited options available to target this specific aspect of the viral life cycle. Therefore, a better understanding of how these respiratory viruses utilize host proteases to activate their fusion proteins and initiate infection is important for developing novel therapeutic targets against a broad range of viruses requiring this class of proteases.

Targeting pathogen specific factors often leads to the development of drug resistance. Using an approach that targets a broadly used host factor not only prevents drug resistance from developing, but also could identify broad-spectrum inhibitors of multiple pathogens using a single chemical and dosage. In our studies, we used HAI-2 (362) (referred to as SPINT2) as a broad-spectrum serine protease inhibitor that prevents spread of influenza and HMPV and therefore, inhibits the cleavage of HA and F, respectively (Chapter 4). Inhibiting serine proteases has been explored previously including aprotinin (361, 495, 496) and camostat (385, 491, 495, 497). While aprotinin was able to inhibit entry and is an approved therapy in Russia, the pharmacokinetics as a competitive inhibitor of several serine proteases makes it an unfavorable treatment (496). Camostat has been approved for use in Japan for the treatment of pancreatitis and postoperative reflux esophagitis (386, 498). This protease inhibitor also demonstrates significant potential for other morbidities, including some viral infections, but the limited availability makes it difficult to rapidly achieve the use of camostat on a global scale. Recently, the SARS-CoV-2 pandemic led to emergency drug repurposing where camostat was a highly sought-after contender for treating SARS-CoV-2 patients (492). Camostat has been shown to inhibit SAR-CoV-2 infection in vitro and there are several on-going clinical trials examining this protease inhibitor for

effectiveness against SARS-CoV-2. However, a significant amount of research needs to be conducted to better understand efficacy and safety. This unprecedented time has allowed for the use of camostat world-wide which could result in its use against influenza, CoV, and HMPV soon.

Identifying proteases involved in HMPV infection has revealed novel and very important information about this ubiquitous pathogen. We show that targeting cleavage is a significant mechanism for developing antivirals. However, other proteases need to be identified and examined in more physiologically relevant model systems to better understand how our findings translate to more complex systems of infection. In addition, analyzing SPINT2 compared to camostat in various model systems would help understand how advantageous this method would be in comparison. The advantage of SPINT2 is that it is endogenously expressed in humans, whereas camostat is a synthetic compound. This offers the potential for less side effects and administration of higher, more efficacious doses that may be needed to prevent infection. However, the generation of a protein inhibitor on a large scale presents a significant challenge that must be overcome. Identification of novel naturally occurring and synthetic protease inhibitors that inhibit viral infection would provide for broad protection and prevention of viral spread while simultaneously mitigating side effects to prevent and treat multiple respiratory pathogens. Some of this research has already begun, but there is significantly more needed to ensure an effective treatment (495, 496).

Complex 3-D human airway epithelial tissues as a model system of infection.

Historically, RSV and HMPV infections have been studied using 2-D cell monolayers, leading to a better understanding of infection. Because these viruses are evolutionarily similar and share several key characteristics during the lifecycle, we examined previous 2-D findings using a complex, more physiologically relevant 3-D human airway epithelial (HAE) model system. RSV has had multiple reports using HAE tissues (143, 144, 314, 316, 319, 323-326, 420, 421), but only four

HMPV studies have utilized HAE tissues (135, 136, 318, 333). However, none of these reports have done extensive molecular characterization of these viruses during the stages of infection. Using these models, other reports have suggested that viruses grown in 2-D culture undergo adaptations, altering infection dynamics in more complex models. For RSV, there is evidence suggesting growth of virus in monolayers results in less infection when the virus is subsequently added to HAE tissues (143, 144, 421), compared to virus initially grown on tissues which infects with higher efficiency. These observations are true for many other viruses including measles and PIV, where studying them out of context prevents important, tissue specific information from being obtained (294, 297, 499-501). It is possible that growth of RSV and HMPV in HAE tissues could alter the infectivity and spread kinetics compared with strains grown in 2-D monolayers. Growing viruses in HAE tissues would generate strains with more physiologically relevant adaptations and these studies would be important for understanding how this contributes to entry, spread, and replication as well as how to target these more effectively. However, growth of virus in these complex models is costly and therefore difficult to achieve with current methods.

Other reports have demonstrated that cell polarity is an important factor for determining where viral factors localize during infection. Polarized cell monolayers infected with RSV showed F localized to the apical surface and this was recapitulated using 3-D tissues. In comparison, 2-D cells demonstrate a general localization to the plasma membrane (438). Having F localized at the apical surface is consistent with proposed locations for viral assembly and budding sites *in vivo*, which has been difficult to characterize using non-polarized models. Similarly, RSV and HMPV have been demonstrated to form actin-based extensions in 2-D cultures and chemically inhibiting actin dynamics in these systems profoundly affects viral replication and spread (288, 298). However, when we examined infection in our 3-D model, we found that these extensions were significantly less prevalent in RSV infected cells compared to HMPV (Fig 5.4). Therefore, it is possible that RSV-induced extensions in 2-D monolayers are a result of cells lacking polarization, where the actin cytoskeleton is important for

other functions not found in this system. Previous unpublished work in our lab studying HMPV examined the effect of actin cytoskeletal inhibitors on HAE infected tissues. We found that inhibition, similar to 2-D cells, significantly inhibited replication and spread (El Najjar and Dutch, unpublished results), but further analysis is needed to understand how it affects extension formation. Both HMPV and RSV proteins are able to interact with the actin cytoskeleton, supporting a critical role for viral function (288, 427, 502). Actin and actin-related proteins are present in isolated virus when analyzed by mass spectrometry, further supporting the role of actin in viral assembly and spread (288, 503, 504). The role of extensions during HMPV and RSV infection in HAE tissues needs to be analyzed to understand what the purpose of these extensions is during assembly and spread.

We used this HAE system to analyze the therapeutic potential of monoclonal antibodies (mAbs) for entry and spread inhibition. While both HMPV and RSV were neutralized to prevent viral entry, there was a large difference observed in the effect of neutralizing antibodies on spread kinetics (Fig 5.5 - 5.8). RSV spread was completely inhibited when mAbs were added to the apical surface after infection, but HMPV spread was only inhibited approximately 25%. These findings were also shown for both viruses in 2-D monolayers where RSV entry and spread were blocked but only entry was inhibited for HMPV and an approximately 50% reduction was seen for spread. These observations in both 2-D and 3-D models highlight an interesting dichotomy between RSV and HMPV infections. Our results support previous work that shows HMPV can spread directly from cell-to-cell in monolayers, independent of neutralizing mAbs (288). Interestingly, HMPV infection peaked at 48 hours, and spread was only observed within this 24-hour window. HMPV is primarily cell associated and therefore, sloughing of apical cells carrying infected HMPV may result in loss of infectious particles, potentially explaining why limited spread was seen at later times post infection. In addition to RSV and HMPV, there have been other respiratory viruses studied including influenza, parainfluenza, measles virus, and adenoviruses and while our results are preliminary, comparing and contrasting other well studied viruses also allows for understanding how previously identified phenotypes in pneumoviruses may

manifest in our model system (136, 143, 144, 313, 315, 316, 321-325, 327, 415-419).

Even though using tissue systems allows for understanding infection in a more physiologic context, there are some pitfalls. RSV spread inhibition was observed for both palivizumab and nirsevimab in 2-D and 3-D models. However, palivizumab is only effective when given prophylactically, but is not effective when given during an already active infection. Therefore, this work suggests the antibodies have strong potential as novel therapeutics, but the complexity of systems present in other models is needed to fully explore the potential window for therapeutic intervention. One major drawback of the HAE model is the lack of an immune system, which is critical for understanding infection progression, clearance, and treatment. Establishing more complex model systems that incorporate both organ and immune system specific constituents would aid our understanding of viral infections and the antiviral response. Further studying pneumovirus infections in the presence of other important factors present within lung tissue will be critical for understanding how the phenotypes reported here are altered with increasing model system complexity.

Viral co-infections: Potential synergy for HMPV and RSV co-infected cells

Co-infections occur when opportunistic hosts are susceptible to one or more pathogens which infect a specific organ system. Often, there combination of fungal-bacterial-viral co-infections which result in one pathogen invading while creating an environment that allows another pathogen to thrive in a synergetic manner (505-507). There is a significant number of reports documenting the simultaneous presence of one or more respiratory viruses that can result in significant morbidity compared with single species infections. However, there is also evidence of viral interference, infection with where one virus prevents the entry of another. This phenomenon suggests co-infections often cannot occur and therefore they have been infrequently studied so they remain poorly understood (449-451). However, there is likely a benefit that arises from co-infection which

promotes some fitness advantage for both viruses instead of competition, which would only promote the growth and spread of one species.

More specifically, RSV and HMPV have been reported to co-infect individuals, leading to increased disease severity as a result (38, 40), though co-infection at a cellular level has not been examined. These viruses also share many similarities both genetically and in protein function during infection. We aimed to better understand how RSV and HMPV were resulting in more severe pathology by examining viral co-infected cells and the potential for synergy during infection. We observed minimal amounts of co-infected cells initially, but these population increased over time (Fig 6.3). We observed the phenomenon of viral interference where initial infection with one virus affected the entry of another. Upon closer examination, IB formation was observed, minimally composed of N, P and viral RNA. Interestingly, RSV and HMPV vRNA and proteins co-localized to the same inclusion bodies in co-infected cells, suggesting the potential for viral protein complementation. The N and P proteins of each virus serve similar functions and the overall structures compared with one another are quite similar, despite minimal sequence conservation. However, testing various combinations of N and P resulted in mixed results for IB formation (Fig 6.5). More interestingly, using a minigenome replicon system, only 10% of replication efficiency was retained when swapping out N and P from both viruses, but adding them in addition to all cognate replication proteins suggests that HMPV is primarily unaffected whereas RSV still has a significant reduction (Fig 6.7).

Our observations generate more questions about why RSV and HMPV proteins and viral RNA in co-infected cells would occupy the same replication organelle given that we currently observe minimal synergy for replication. We primarily studied co-infections using protein expression in eukaryotic cells, which takes away the complexity of other viral factors that may be important during infection in addition to the replication complex. This could offer an explanation as to why co-infected cells show IB co-habitation, but transfection experiments resulted in minimal functionality. Both RSV and HMPV hijack cellular factors, many

of which have not been identified, and these may promote a synergistic environment within these cells. This suggests another potential scenario where sequestration of these host factors into inclusion bodies draws HMPV and RSV proteins together into these replication organelles and not be driven by viral synergy which would explain the limited synergy observed in replication. However, this still leaves the question of whether co-infections are a consequence of chance, or if there is a benefit of two viruses co-infecting the same cell.

To examine this further, co-infected samples will need to be analyzed to characterize replication and spread compared to singly infected cells. More interestingly though, is the potential for the formation of viral chimeras, where budding viruses contain multiple genomes from both viruses that can pass on and co-infect other cells. Our time course data supports that at 72 hours, singly infected HMPV appears to decrease and overall co-infected cells increase. However, more analysis will need to be conducted to determine if this is due to chimera formation or other potential mechanisms of spread. Additionally, critical host factors utilized by both RSV and HMPV to form inclusion bodies is poorly understood due to the high volatility and dynamic nature. Identifying key viral and host factors that are critical for the formation and function of IBs would be critical to help elucidate the interactions that govern the coalescence of both RSV and HMPV genomes in the same IB and whether this is driven by a synergistic interaction or a co-dependence on specific host factors that are critical for both viruses during infection.

Appendix 1: Designing a clinical testing platform for the merging SARS-CoV-2 (COVID-19) pandemic

* This chapter was completed with the help of David B. Cobb and Dr. Morgan McCoy from the University of Kentucky microbiology clinic, who assisted with validation and testing in the clinic. In addition, Dr. Kate Wolf from the University of Kentucky, Department of Microbiology, Immunology, and Molecular Genetics helped with design, testing, and troubleshooting. All data and graphs presented here were generated by me.

Introduction

The emergence of viral epidemics and pandemics is difficult to predict, leading to devastating and unforeseen outcomes (508). Historical viral pandemics include smallpox (509), measles (510), yellow fever (511), Zika (512), Ebola hemorrhagic fever (513), severe acute respiratory syndrome/Middle Eastern respiratory syndrome (514, 515), human immunodeficiency virus (516, 517), and influenza virus (518-521). However, there have been significant advances in scientific research that have allowed us to combat some potential outbreaks. Historically, both smallpox and measles viruses were a significant health burden. This ultimately led to the development of vaccines resulting in the complete eradication of smallpox in 1979 (509). For measles, worldwide vaccination efforts led to a significant decrease of infections and subsequent hospitalizations and death. However, recent movements in the modern era challenging vaccinations have generated a severe threat for the re-emergence of measles (5, 510, 522).

Vaccines are not available for every pathogenic virus, so the development and use of antivirals is critical (523-530). This is especially true for those viruses that circulate in non-human reservoirs and re-emerge in human populations periodically. However, effective antivirals can be

challenging to maintain, as many viruses have high mutation rates and multiple species transmission which makes these chances of resistance even higher (518, 521, 527). These factors can contribute to the generation of highly pathogenic viruses resulting in outbreaks, epidemics, and in some cases leading to pandemics. This is particularly dangerous for viruses that have high mutation rates, which can result in vaccines or antiviral therapies losing the ability to combat the pathogen effectively (530-533). For IAV, these evolutionary changes result in the need for yearly vaccinations (534). Although the annual flu vaccine offers protection, with the levels varying by year, it is difficult to predict which strain will dominate and which epitopes are important for eliciting an immune response. In addition, mutations that enhance the infection and spread can occur and result in significant morbidity and mortality, such as those seen in the IAV pandemics (519, 535, 536). Altogether, pandemic viruses can generate extreme morbidity and mortality and are difficult to prepare for given the vast number of variables that are unable to be controlled.

Some viruses that have strong potential to cause outbreaks are poorly understood and others are likely still to be discovered. Bat species in particular harbor many viruses that have generated zoonotic transmission from an intermediate host, eventually infecting humans (537, 538). These viruses include Hendra (HeV) and Nipah (NiV), which cause deadly respiratory disease and encephalitis in horses and pigs respectively (7, 11, 13, 539-541). While HeV and NiV are only responsible for a small amount of morbidity, the mortality rates of those infected range from 50-100%. Due to the small amount of cases and rapid epidemiologic analysis, further cases and outbreaks have been avoided and some treatment and prevention options are available (14, 15). Outbreaks like these bring up interesting questions as to what potential viruses are lying dormant in nature that have high potential for outbreaks in humans that can ultimately lead to novel a global pandemic.

One viral family, Coronaviridae, has been involved in several global pandemics in recent years. Coronaviruses (CoV) are enveloped, single stranded, positive sense RNA viruses that infects both animals and humans (542). The conserved components of CoV are the RNA-dependent-RNA polymerase (RdRp), membrane protein (M), envelope protein (E), spike protein (S), and nucleocapsid protein (N). Many strains also encode other accessory proteins that are less conserved, serving roles specific to the needs of the specific strain. The first reports of endemic CoV in humans dates back to the 1960s (543, 544), when HCoV-OC43 and HCoV-229E were first described, followed by HCoV-NL63 and HCoV-HKU1 which were described in the early 2000s (545, 546). All four of these CoV strains cause mild to moderate cold-like symptoms in humans and typically follow a seasonal distribution (542). However, in late 2002, a novel CoV called severe acute respiratory syndrome (SARS-CoV) arose in China due zoonotic transmission from bat to civet, and from civet to human, likely due to exposure within food markets. SARS-CoV ultimately caused an epidemic affecting approximately 8,000 individuals, demonstrating a mortality rate of up to 10%, with individuals over 55 years of age significantly affected (547, 548). Since 2004, no cases of SARS have been reported and therefore the threat for a global pandemic was mitigated. A second novel coronavirus caused an epidemic which began in 2014 in the Middle East. Middle East respiratory syndrome (MERS-CoV) came from a zoonotic transmission from camels to humans, likely originating from bat species. This initially infected around 400 individuals and yielded a fatality rate of up to 35% (549, 550). Subsequently, in 2015, a large secondary outbreak was detected in South Korea, suggesting the potential for spread, but has not been detected outside of the Middle East and Asia due to the requirement of camels as the intermediate species. Unlike SARS, there have been annual cases reported in the Middle East every year since the initial epidemic, establishing a cyclical infectious cycle (550). While both SARS-CoV and MERS-CoV are regarded as significant pathogens, both of these CoV epidemics were relatively small and short lived, and therefore, lack of funding for continued research resulted in no approved therapeutics or vaccines available.

In late 2019, another novel CoV emerged in Wuhan, China, presenting with respiratory distress symptoms (551-554). Genetic analysis suggested this viral strain shared high homology with SARS-CoV, but contained important genetic differences that lead to changes in spread and infection (554). Epidemiologic surveillance found that some CoV strains present in both bats and pangolins demonstrated high genetic similarity and may explain the point of origin (553, 555, 556). Since the first case was reported, COVID19, caused by the virus SARS-CoV-2, has spread to almost every country and the virus has infected millions of people, with cases increasing daily. Initially, the death rate was suspected to be close to that reported for SARS-CoV (557, 558). Similarly, the death rate associated with elderly individuals was significantly higher as well (553, 557, 558). Initial cases were diagnosed using lab developed tests (LDT) that utilize reverse transcriptase real-time polymerase chain reaction (RT-qPCR) against RNA isolated from patient samples, and the U.S. put forth FDA guidelines to aid diagnostic potential (559). However, there are currently no standard test kits available worldwide and therefore, detection of the virus as well as nucleic acid extraction platforms are being examined for emergency use. In addition, there are some commercially available kits from several companies that are highly sensitive and automated. However, these are either extremely long processes, have limited testing capacity, or are unavailable in many places, all of which decrease the high throughput testing needed for the current pandemic.

In this chapter, we develop a RT-qPCR based testing platform for the diagnosis of SARS-CoV-2 for use in the University of Kentucky clinic. We used the Lyra, a currently available RT-qPCR platform for SARS-CoV-2 in conjunction with a magnetic bead based nucleic acid extraction kit to purify viral genetic material from patient samples. We determined that our lab developed test is both sensitive and precise and demonstrates a limit of detection of 400 copies/mL. In addition, when used with patient samples, we are able to accurately detect the presence of virus with similar sensitivity to currently approved diagnostic platforms.

Material and Methods

Thermocycler and PCR kit: The Lyra SARS-CoV-2 RT-qPCR assay kit (Quidel) was used to complete the PCR testing on the QuantStudio 7 Flex (Thermofisher). The kit contains a positive control that was used for the accuracy and precision tests.

RNA isolation: RNA from either patient samples or standard control was isolated using the Thermofisher MagMax viral and pathogen nucleic acid isolation kit (A42352) according to the manufacturer's protocol. Briefly, 380 μ L of patient sample or standard with 20 μ L of process control was placed into 550 μ L of the binding buffer and bead slurry then treated with 10 μ L of proteinase K. The positive control was 50 μ L of Lyra kit positive control into 330 μ L of saline buffer and 20 μ L of process control. Sample mixing was completed at 1050 rpm for all steps. Samples were mixed for 2 min, incubated at 65°C for 5 min and mixed for 5 min then allowed to sit on a magnetic stand for 10 min or until the beads collected and the supernatant was aspirated. The beads were then washed with 1mL of wash buffer followed by mixing for 2 min, incubated until beads settled and supernatant was removed. This was completed two more times with 1mL and 0.5mL of 80% ethanol. After the second wash, the beads were dried by mixing for 2 min. 50 μ L of elution buffer was placed in each sample, mixed for 5 min, incubated at 65°C for 5 min and then mixed for 5 additional min. Beads were collected on the magnetic stand for 3 min and the eluate was taken and moved into a new plate for RT-qPCR.

Lyra RT-qPCR: The Lyra RT-qPCR was set up as designed by Quidel in the emergency use authorization for the Thermofisher quant studio 7 pro. Briefly, 135 μ L of rehydration buffer was added to each vial of dehydrated master mix (8 samples/vial). 5 μ L of isolated RNA was placed into each well with rehydrated PCR master mix and subsequently sealed and spun down. The PCR was performed using the 96-well fast insert at 20 μ L total volume with the following settings: 1) 55°C for 5 min 2) 60°C for 5 min 3) 65°C for 5 min 4) 92°C for 5 sec and 57°C for

40 sec 5) repeat step 4 for 10 cycles without capture 6) 92°C for 5 sec and 57°C for 40 sec 7) repeat step 6 for 30 cycles with capture. The threshold was set to automatic detection based on cycle 3-15 of the PCR.

Limit of detection analysis: The limit of detection was established for the Quidel Lyra SARS-CoV-2 assay using heat inactivated virus at a stock concentration of 1.7e7/mL in TE from BEI resources (NRC-52281 lot 70033641). Initial limit of detection ranges was completed in triplicate diluting the initial stock to 1e5/mL doing 1:2 dilutions from 100,000 copies/mL to 781 copies/mL. Subsequent LOD testing was completed using serial dilutions from 1.7e7/mL to 1.7e5/mL in DEPC water followed by diluting this stock into saline (0.9% NaCl) for 1600, 800, and 400 copies/mL of genome into a total volume of 8mL of saline. 380 µL of this dilution was run 20 times through independent RNA isolation for RT-qPCR analysis.

Results and Discussion:

To generate a lab developed testing (LDT) platform for SARS-CoV-2, we combined the Lyra SARSCoV-2 RT-qPCR kit with the MagMax nucleic acid extraction platform. In order to achieve emergency use authorization (EUA) approval for our kit, there are several test metrics that must be conducted to ensure the platform is sensitive and accurate. First, we conducted an initial accuracy test of replicates within the sample experimental procedure to ensure that there was minimal variation. This accuracy test was composed of 10 positive and 10 negative samples independently isolated and analyzed using RT-qPCR. All positive control samples were detected at expected Ct values, with an average Ct value of 21.05 while no negative samples showed signal for the SARS-CoV-2 (Fig A-1A). In addition, the internal isolation control standards were picked up at an average Ct value of 17 for both the positive and negative samples, confirming the isolation was successful and consistent.

Next, we conducted a precision assay that assessed the consistency between runs completed over multiple days. To do this, 5 positive samples and 5 negative

samples were prepared on 5 separate days, followed by RNA isolation and analysis by PCR. The positive samples again showed an average Ct value of 21.42, 20.93, 20.95, 20.81, and 20.16, consistent with the initial accuracy measurement (Fig A-1A and A-1B). There were no negative controls that demonstrated any signal for SARS-CoV-2 nucleic acids. Additionally, the internal controls showed high consistency with a Ct value of 17.68, 17.32, 17.35, 17.39, and 17.11 (Fig A-1B). These results suggest that the current testing platform is both accurate and precise while also demonstrating high sensitivity for detection.

To ensure our findings were consistent with previous studies conducted during the initial Lyra test development, we examined a panel of four verification samples that contained nucleic acid material at known concentrations. These samples were provided to us blinded for testing purposes from Quidel. We isolated each member of this panel in duplicate and analyzed them by RT-qPCR. The expected values for members 1 and 3 were 24 +/- 1 and members 2 and 4 were expected at 27 +/- 1. During our nucleic acid isolation and RT-qPCR, we detected member 1 at a ct value of 19.44, member 2 at 22.50, member 3 at 20.95, and member 4 at 23.24, all of which were lower than the expected values for detection, suggesting that the current testing and extraction platform was operating with greater sensitivity than previously reported by the current Lyra testing platform (Fig A-1C).

Lastly, in order to ensure that the test is sensitive and able to detect minimal amounts of viral nucleic acids present in the samples, we conducted a limit of detection (LOD) assay using gamma irradiated SARS-CoV-2 virus. Previously, this method was utilized by Quidel to determine the LOD on a variety of thermocycler platforms, including the Thermofisher Quantstudio 7 Pro, which is closely related to the QuantStudio 7 Flex used in these studies. The LOD established on these platforms demonstrated a detection limit at 800 copies/mL and were able to detect 20/20 isolations with an average Ct value of 27.3 (Fig

A-2A). Initially, we generated a stock of gamma irradiated virus at 100,000 copies/mL and conducted a 1:2 dilution down to 781 copies/mL in triplicate. We were able to detect dilutions all the way down to 781 copies/mL which had an average Ct value of 24.2 (Fig A-2A). Data from the 6,250 and 1,562 copies/mL only yielded two data points per group due to loading error and internal control failure.

Based on this initial LOD, we then proceeded to dilute gamma-irradiated virus at 2x LOD (1600 copies/mL), 1x LOD (800 copies/mL) and 0.5x LOD (400 copies/mL) compared with the current established detection level. At 2x LOD, we were able to pick up all 20 replicates at an average Ct value of 20.96. We were also able to pick up all 20 replicates 1x LOD with an average Ct value of 22.37, which is 5 Ct values lower than the current assays detection. At 0.5x the LOD, we were able to detect 19/20 samples with an average Ct value of 23.02 which is still 4 Ct values lower than the current Lyra assay LOD (Fig A-2B). One sample from the 400 copies/mL group was lost during the extraction processes and therefore, only 19/20 samples were detected. However, based on the other datapoints within the set, the LOD may potentially be lower than 400 copies/mL.

In this chapter, we developed a testing platform for the detection of the novel SARS-CoV-2 virus using a combination of a commercially available RT-qPCR kit coupled with a magnetic bead-based nucleic extraction platform for emergency use authorization. We were able to demonstrate that this test is able to deliver consistent results with minimal variation between tests confirming both accuracy and precision of detection. In addition, testing standards generated by Quidel specifically for the Lyra platform were detected at lower Ct values when compared to expected values, suggesting that this mechanism was more sensitive than the currently approved Lyra platform. Further supporting this, we were able to establish a LOD of 400 copies/mL compared with the current Lyra platform which has an LOD of 800 copies/mL. Our current testing capacity was initially limited by the time and capacity of currently available testing platforms. The LDT generated in this

study is able to utilize another platform to increase the testing capacity while ensuring that sensitivity, accuracy, and precision are conserved.

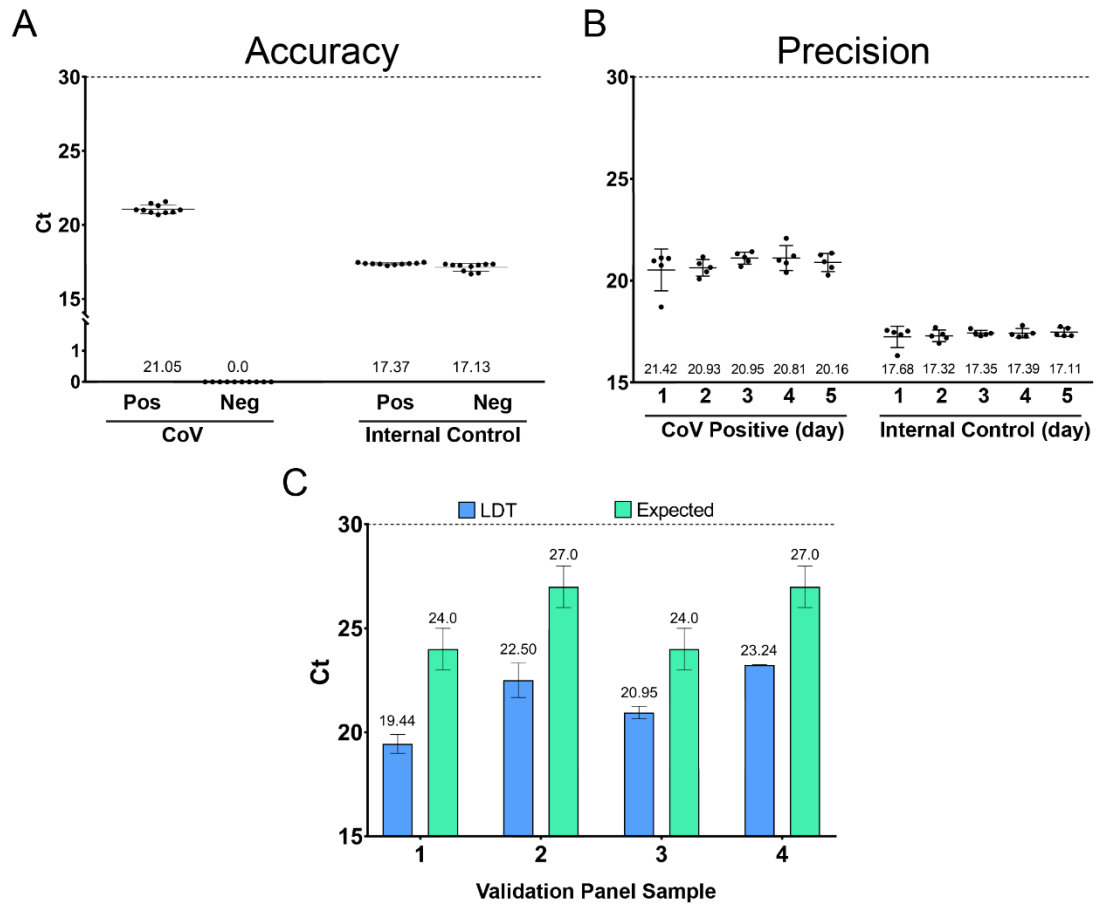


Figure A-1: The LDT demonstrates high precision and accuracy for SARS CoV 2 detection. The current LDT was able to detect the positive control both **(A)** accurately and **(B)** precisely, with minimal variation between samples within a single run or over multiple days of testing. **(C)** Validation samples (1-4) were provided in a blinded fashion for analysis and compared with expected outcomes from previous studies demonstrating that the LDT is more sensitive than the current testing platform.

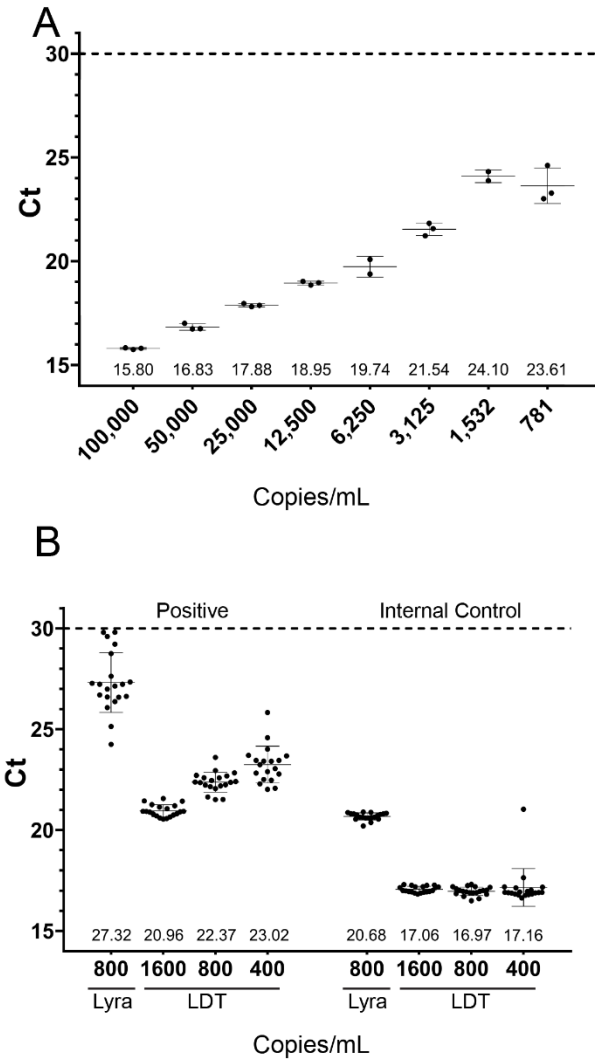


Figure A-2: The limit of detection of SARS CoV 2 is highly sensitive. (A) The initial limit of detection was able to be determined using a 2-fold serial dilution starting from 100,000 copies/mL down to 781 copies/mL. **(B)** 20 replicates of 1600, 800, and 400 copies/mL were independently isolated and analyzed by RT-qPCR demonstrating a 95% confidence in the limit of detection at 400 copies/mL.

Appendix 2: List of Abbreviations

HMPV	Human metapneumovirus
RSV	Respiratory syncytial virus
IAV	Influenza A virus
RNP	Ribonucleoprotein
N	Nucleoprotein
F	Fusion protein
P	Phosphoprotein
L	Large polymerase
M	Matrix protein
SH	Small hydrophobic protein
G	Attachment Protein
IB(s)	Inclusion Body/Bodies
FISH	Fluorescence in situ hybridization
HAE	Human airway epithelium
GFP	Green fluorescent protein
HRA	Heptad repeat A
HRB	Heptad repeat B
WT	Wild type

References

1. Rima B, Balkema-Buschmann A, Dundon WG, Duprex P, Easton A, Fouchier R, Kurath G, Lamb R, Lee B, Rota P, Wang L, Ictv Report C. 2019. ICTV Virus Taxonomy Profile: Paramyxoviridae. *J Gen Virol* 100:1593-1594.
2. Knipe DM, Howley PM. 2013. *Fields Virology*, 6th Edition. Lippincott Williams & Wilkins.
3. Hotez PJ, Nuzhath T, Colwell B. 2020. Combating vaccine hesitancy and other 21st century social determinants in the global fight against measles. *Curr Opin Virol* 41:1-7.
4. Bankamp B, Hickman C, Icenogle JP, Rota PA. 2019. Successes and challenges for preventing measles, mumps and rubella by vaccination. *Curr Opin Virol* 34:110-116.
5. Phadke VK, Bednarczyk RA, Salmon DA, Omer SB. 2016. Association Between Vaccine Refusal and Vaccine-Preventable Diseases in the United States: A Review of Measles and Pertussis. *Jama* 315:1149-58.
6. Young PL, Halpin K, Selleck PW, Field H, Gravel JL, Kelly MA, Mackenzie JS. 1996. Serologic evidence for the presence in Pteropus bats of a paramyxovirus related to equine morbillivirus. *Emerg Infect Dis* 2:239-40.
7. Olson JG, Rupprecht C, Rollin PE, An US, Niezgodna M, Clemins T, Walston J, Ksiazek TG. 2002. Antibodies to Nipah-like virus in bats (*Pteropus lylei*), Cambodia. *Emerg Infect Dis* 8:987-8.
8. Selvey LA, Wells RM, McCormack JG, Ansford AJ, Murray K, Rogers RJ, Lavercombe PS, Selleck P, Sheridan JW. 1995. Infection of humans and horses by a newly described morbillivirus. *Med J Aust* 162:642-5.
9. Rockx B, Winegar R, Freiberg AN. 2012. Recent progress in henipavirus research: molecular biology, genetic diversity, animal models. *Antiviral Res* 95:135-49.

10. Bellini WJ, Harcourt BH, Bowden N, Rota PA. 2005. Nipah virus: an emergent paramyxovirus causing severe encephalitis in humans. *J Neurovirol* 11:481-7.
11. Sherrini BA, Chong TT. 2014. Nipah encephalitis - an update. *Med J Malaysia* 69 Suppl A:103-11.
12. Weatherman S, Feldmann H, de Wit E. 2018. Transmission of henipaviruses. *Curr Opin Virol* 28:7-11.
13. Sharma V, Kaushik S, Kumar R, Yadav JP, Kaushik S. 2019. Emerging trends of Nipah virus: A review. *Rev Med Virol* 29:e2010.
14. Broder CC, Xu K, Nikolov DB, Zhu Z, Dimitrov DS, Middleton D, Pallister J, Geisbert TW, Bossart KN, Wang LF. 2013. A treatment for and vaccine against the deadly Hendra and Nipah viruses. *Antiviral Res* 100:8-13.
15. Middleton D, Pallister J, Klein R, Feng YR, Haining J, Arkininstall R, Frazer L, Huang JA, Edwards N, Wareing M, Elhay M, Hashmi Z, Bingham J, Yamada M, Johnson D, White J, Foord A, Heine HG, Marsh GA, Broder CC, Wang LF. 2014. Hendra virus vaccine, a one health approach to protecting horse, human, and environmental health. *Emerg Infect Dis* 20:372-9.
16. Apalsch AM, Green M, Ledesman-Medina J, Nour B, Wald ER. 1995. Parainfluenza and influenza virus infections in pediatric organ transplant recipients. *Clin Infectious Disease* 20:394-399.
17. Vainionpää R, Hyypiä T. 1994. Biology of parainfluenza viruses. *Clinical microbiology reviews* 7:265-275.
18. Afonso CL, Amarasinghe GK, Banyai K, Bao Y, Basler CF, Bavari S, Bejerman N, Blasdell KR, Briand FX, Briese T, Bukreyev A, Calisher CH, Chandran K, Cheng J, Clawson AN, Collins PL, Dietzgen RG, Dolnik O, Domier LL, Durrwald R, Dye JM, Easton AJ, Ebihara H, Farkas SL, Freitas-Astua J, Formenty P, Fouchier RA, Fu Y, Ghedin E, Goodin MM, Hewson R, Horie M, Hyndman TH, Jiang D, Kitajima EW, Kobinger GP, Kondo H, Kurath G, Lamb RA, Lenardon S, Leroy EM, Li CX, Lin XD, Liu L, Longdon B, Marton S, Maisner A, Muhlberger E, Netesov SV, Nowotny

- N, et al. 2016. Taxonomy of the order Mononegavirales: update 2016. *Arch Virol* 161:2351-60.
19. Blount RE, Jr., Morris JA, Savage RE. 1956. Recovery of cytopathogenic agent from chimpanzees with coryza. *Proc Soc Exp Biol Med* 92:544-9.
 20. Chanock R, Roizman B, Myers R. 1957. Recovery from infants with respiratory illness of a virus related to chimpanzee coryza agent (CCA). I. Isolation, properties and characterization. *Am J Hyg* 66:281-90.
 21. Hall CB, Weinberg GA, Iwane MK, Blumkin AK, Edwards KM, Staat MA, Auinger P, Griffin MR, Poehling KA, Erdman D, Grijalva CG, Zhu Y, Szilagyi P. 2009. The burden of respiratory syncytial virus infection in young children. *N Engl J Med* 360:588-98.
 22. Nair H, Nokes DJ, Gessner BD, Dherani M, Madhi SA, Singleton RJ, O'Brien KL, Roca A, Wright PF, Bruce N, Chandran A, Theodoratou E, Sutanto A, Sedyaningsih ER, Ngama M, Munywoki PK, Kartasasmita C, Simoes EA, Rudan I, Weber MW, Campbell H. 2010. Global burden of acute lower respiratory infections due to respiratory syncytial virus in young children: a systematic review and meta-analysis. *Lancet* 375:1545-55.
 23. Abraha HY, Lanctot KL, Paes B. 2015. Risk of respiratory syncytial virus infection in preterm infants: reviewing the need for prevention. *Expert Rev Respir Med* 9:779-99.
 24. Bont L, Checchia PA, Fauroux B, Figueras-Aloy J, Manzoni P, Paes B, Simões EA, Carbonell-Estrany X. 2016. Defining the Epidemiology and Burden of Severe Respiratory Syncytial Virus Infection Among Infants and Children in Western Countries. *Infect Dis Ther* 5:271-98.
 25. Kodama F, Nace DA, Jump RLP. 2017. Respiratory Syncytial Virus and Other Noninfluenza Respiratory Viruses in Older Adults. *Infect Dis Clin North Am* 31:767-790.
 26. Falsey AR, Hennessey PA, Formica MA, Cox C, Walsh EE. 2005. Respiratory Syncytial Virus Infection in Elderly and High-Risk Adults. *New England Journal of Medicine* 352:1749-1759.

27. Matias G, Taylor R, Haguinet F, Schuck-Paim C, Lustig R, Shinde V. 2017. Estimates of hospitalization attributable to influenza and RSV in the US during 1997-2009, by age and risk status. *BMC Public Health* 17:271.
28. Johnson S, Oliver C, Prince GA, Hemming VG, Pfarr DS, Wang SC, Dormitzer M, O'Grady J, Koenig S, Tamura JK, Woods R, Bansal G, Couchenour D, Tsao E, Hall WC, Young JF. 1997. Development of a humanized monoclonal antibody (MEDI-493) with potent in vitro and in vivo activity against respiratory syncytial virus. *J Infect Dis* 176:1215-24.
29. Subramanian KN, Weisman LE, Rhodes T, Ariagno R, Sanchez PJ, Steichen J, Givner LB, Jennings TL, Top FH, Jr., Carlin D, Connor E. 1998. Safety, tolerance and pharmacokinetics of a humanized monoclonal antibody to respiratory syncytial virus in premature infants and infants with bronchopulmonary dysplasia. MEDI-493 Study Group. *Pediatr Infect Dis J* 17:110-5.
30. van den Hoogen BG, de Jong JC, Groen J, Kuiken T, de Groot R, Fouchier RA, Osterhaus AD. 2001. A newly discovered human pneumovirus isolated from young children with respiratory tract disease. *Nat Med* 7:719-24.
31. van den Hoogen BG, Bestebroer TM, Osterhaus AD, Fouchier RA. 2002. Analysis of the genomic sequence of a human metapneumovirus. *Virology* 295:119-32.
32. van den Hoogen BG, Osterhaus DM, Fouchier RA. 2004. Clinical impact and diagnosis of human metapneumovirus infection. *Pediatr Infect Dis J* 23:S25-32.
33. Panda S, Mohakud NK, Pena L, Kumar S. 2014. Human metapneumovirus: review of an important respiratory pathogen. *Int J Infect Dis* 25:45-52.
34. Don M, Korppi M, Valent F, Vainionpaa R, Canciani M. 2008. Human metapneumovirus pneumonia in children: results of an Italian study and mini-review. *Scand J Infect Dis* 40:821-6.

35. Papenburg J, Boivin G. 2010. The distinguishing features of human metapneumovirus and respiratory syncytial virus. *Rev Med Virol* 20:245-60.
36. Kahn JS. 2006. Epidemiology of human metapneumovirus. *Clin Microbiol Rev* 19:546-57.
37. Deffrasnes C, Hamelin ME, Boivin G. 2007. Human metapneumovirus. *Semin Respir Crit Care Med* 28:213-21.
38. Greensill J, McNamara PS, Dove W, Flanagan B, Smyth RL, Hart CA. 2003. Human metapneumovirus in severe respiratory syncytial virus bronchiolitis. *Emerg Infect Dis* 9:372-5.
39. McNamara PS, Flanagan BF, Smyth RL, Hart CA. 2007. Impact of human metapneumovirus and respiratory syncytial virus co-infection in severe bronchiolitis. *Pediatr Pulmonol* 42:740-3.
40. Semple MG, Cowell A, Dove W, Greensill J, McNamara PS, Halfhide C, Shears P, Smyth RL, Hart CA. 2005. Dual infection of infants by human metapneumovirus and human respiratory syncytial virus is strongly associated with severe bronchiolitis. *J Infect Dis* 191:382-6.
41. Williams JV, Harris PA, Tollefson SJ, Halburnt-Rush LL, Pingsterhaus JM, Edwards KM, Wright PF, Crowe JE, Jr. 2004. Human metapneumovirus and lower respiratory tract disease in otherwise healthy infants and children. *N Engl J Med* 350:443-50.
42. Feuillet F, Lina B, Rosa-Calatrava M, Boivin G. 2012. Ten years of human metapneumovirus research. *J Clin Virol* 53:97-105.
43. Boivin G, De Serres G, Cote S, Gilca R, Abed Y, Rochette L, Bergeron MG, Dery P. 2003. Human metapneumovirus infections in hospitalized children. *Emerg Infect Dis* 9:634-40.
44. Esper F, Boucher D, Weibel C, Martinello RA, Kahn JS. 2003. Human metapneumovirus infection in the United States: clinical manifestations associated with a newly emerging respiratory infection in children. *Pediatrics* 111:1407-10.

45. Esper F, Martinello RA, Boucher D, Weibel C, Ferguson D, Landry ML, Kahn JS. 2004. A 1-year experience with human metapneumovirus in children aged <5 years. *J Infect Dis* 189:1388-96.
46. van den Hoogen BG, van Doornum GJ, Fockens JC, Cornelissen JJ, Beyer WE, de Groot R, Osterhaus AD, Fouchier RA. 2003. Prevalence and clinical symptoms of human metapneumovirus infection in hospitalized patients. *J Infect Dis* 188:1571-7.
47. Boivin G, Abed Y, Pelletier G, Ruel L, Moisan D, Cote S, Peret TC, Erdman DD, Anderson LJ. 2002. Virological features and clinical manifestations associated with human metapneumovirus: a new paramyxovirus responsible for acute respiratory-tract infections in all age groups. *J Infect Dis* 186:1330-4.
48. Falsey AR, Erdman D, Anderson LJ, Walsh EE. 2003. Human metapneumovirus infections in young and elderly adults. *J Infect Dis* 187:785-90.
49. Laham FR, Israele V, Casellas JM, Garcia AM, Lac Prugent CM, Hoffman SJ, Hauer D, Thumar B, Name MI, Pascual A, Taratutto N, Ishida MT, Balduzzi M, Maccarone M, Jackli S, Passarino R, Gaivironsky RA, Karron RA, Polack NR, Polack FP. 2004. Differential production of inflammatory cytokines in primary infection with human metapneumovirus and with other common respiratory viruses of infancy. *J Infect Dis* 189:2047-56.
50. Nicholson KG, Kent J, Hammersley V, Cancio E. 1997. Acute viral infections of upper respiratory tract in elderly people living in the community: comparative, prospective, population based study of disease burden. *Bmj* 315:1060-4.
51. Liao RS, Appelgate DM, Pelz RK. 2012. An outbreak of severe respiratory tract infection due to human metapneumovirus in a long-term care facility for the elderly in Oregon. *J Clin Virol* 53:171-3.
52. Osbourn M, McPhie KA, Ratnamohan VM, Dwyer DE, Durrheim DN. 2009. Outbreak of human metapneumovirus infection in a residential aged care facility. *Commun Dis Intell Q Rep* 33:38-40.

53. Louie JK, Schnurr DP, Pan CY, Kiang D, Carter C, Tougaw S, Ventura J, Norman A, Belmusto V, Rosenberg J, Trochet G. 2007. A summer outbreak of human metapneumovirus infection in a long-term-care facility. *J Infect Dis* 196:705-8.
54. Boivin G, De Serres G, Hamelin ME, Cote S, Argouin M, Tremblay G, Maranda-Aubut R, Sauvageau C, Ouakki M, Boulianne N, Couture C. 2007. An outbreak of severe respiratory tract infection due to human metapneumovirus in a long-term care facility. *Clin Infect Dis* 44:1152-8.
55. Falsey AR. 2008. Human metapneumovirus infection in adults. *Pediatr Infect Dis J* 27:S80-3.
56. Kearney MT, Cotton JM, Richardson PJ, Shah AM. 2001. Viral myocarditis and dilated cardiomyopathy: mechanisms, manifestations, and management. *Postgrad Med J* 77:4-10.
57. Weinreich MA, Jabbar AY, Malguria N, Haley RW. 2015. New-Onset Myocarditis in an Immunocompetent Adult with Acute Metapneumovirus Infection. *Case Rep Med* 2015:814269.
58. Zwaans WA, Mallia P, van Winden ME, Rohde GG. 2014. The relevance of respiratory viral infections in the exacerbations of chronic obstructive pulmonary disease-a systematic review. *J Clin Virol* 61:181-8.
59. Ilvan A, Aslan G, Serin MS, Calikoglu M, Yilmaz FM, Tezcan S, Tas D, Ayrik C, Uygungul E, Sezer O, Emekdas G. 2013. [Investigation of the presence of human metapneumovirus in patients with chronic obstructive pulmonary disease and asthma and its relationship with the attacks]. *Mikrobiyol Bul* 47:636-49.
60. Asner S, Waters V, Solomon M, Yau Y, Richardson SE, Grasemann H, Gharabaghi F, Tran D. 2012. Role of respiratory viruses in pulmonary exacerbations in children with cystic fibrosis. *J Cyst Fibros* 11:433-9.
61. de Boer K, Vandemheen KL, Tullis E, Doucette S, Fergusson D, Freitag A, Paterson N, Jackson M, Loughheed MD, Kumar V, Aaron SD. 2011. Exacerbation frequency and clinical outcomes in adult patients with cystic fibrosis. *Thorax* 66:680-5.

62. Garcia DF, Hiatt PW, Jewell A, Schoonover SL, Cron SG, Riggs M, Grace S, Oermann CM, Piedra PA. 2007. Human metapneumovirus and respiratory syncytial virus infections in older children with cystic fibrosis. *Pediatr Pulmonol* 42:66-74.
63. Hamelin ME, Prince GA, Gomez AM, Kinkead R, Boivin G. 2006. Human metapneumovirus infection induces long-term pulmonary inflammation associated with airway obstruction and hyperresponsiveness in mice. *J Infect Dis* 193:1634-42.
64. Tsukagoshi H, Ishioka T, Noda M, Kozawa K, Kimura H. 2013. Molecular epidemiology of respiratory viruses in virus-induced asthma. *Front Microbiol* 4:278.
65. Madhi SA, Ludewick H, Kuwanda L, van Niekerk N, Cutland C, Klugman KP. 2007. Seasonality, incidence, and repeat human metapneumovirus lower respiratory tract infections in an area with a high prevalence of human immunodeficiency virus type-1 infection. *Pediatr Infect Dis J* 26:693-9.
66. Ali M, Baker JM, Richardson SE, Weitzman S, Allen U, Abba O. 2013. Human metapneumovirus (hMPV) infection in children with cancer. *J Pediatr Hematol Oncol* 35:444-6.
67. Schildgen O, Glatzel T, Geikowski T, Scheibner B, Matz B, Bindl L, Born M, Viazov S, Wilkesmann A, Knopfle G, Roggendorf M, Simon A. 2005. Human metapneumovirus RNA in encephalitis patient. *Emerg Infect Dis* 11:467-70.
68. Hata M, Ito M, Kiyosawa S, Kimpara Y, Tanaka S, Yamashita T, Hasegawa A, Kobayashi S, Koyama N, Minagawa H. 2007. A fatal case of encephalopathy possibly associated with human metapneumovirus infection. *Jpn J Infect Dis* 60:328-9.
69. Jeannot N, van den Hoogen BG, Schefold JC, Suter-Riniker F, Sommerstein R. 2017. Cerebrospinal Fluid Findings in an Adult with Human Metapneumovirus-Associated Encephalitis. *Emerg Infect Dis* 23:370.

70. Dokos C, Masjosthusmann K, Rellensmann G, Werner C, Schuler-Luttmann S, Muller KM, Schiborr M, Ehlert K, Groll AH. 2013. Fatal human metapneumovirus infection following allogeneic hematopoietic stem cell transplantation. *Transpl Infect Dis* 15:E97-e101.
71. Williams JV, Martino R, Rabella N, Otegui M, Parody R, Heck JM, Crowe JE, Jr. 2005. A prospective study comparing human metapneumovirus with other respiratory viruses in adults with hematologic malignancies and respiratory tract infections. *J Infect Dis* 192:1061-5.
72. Alvarez R, Harrod KS, Shieh WJ, Zaki S, Tripp RA. 2004. Human metapneumovirus persists in BALB/c mice despite the presence of neutralizing antibodies. *J Virol* 78:14003-11.
73. Kolli D, Bataki EL, Spetch L, Guerrero-Plata A, Jewell AM, Piedra PA, Milligan GN, Garofalo RP, Casola A. 2008. T lymphocytes contribute to antiviral immunity and pathogenesis in experimental human metapneumovirus infection. *J Virol* 82:8560-9.
74. Liu Y, Haas DL, Poore S, Isakovic S, Gahan M, Mahalingam S, Fu ZF, Tripp RA. 2009. Human metapneumovirus establishes persistent infection in the lungs of mice and is reactivated by glucocorticoid treatment. *J Virol* 83:6837-48.
75. Marsico S, Caccuri F, Mazzuca P, Apostoli P, Roversi S, Lorenzin G, Zani A, Fiorentini S, Giagulli C, Caruso A. 2018. Human lung epithelial cells support human metapneumovirus persistence by overcoming apoptosis. *Pathog Dis* 76.
76. Chow WZ, Chan YF, Oong XY, Ng LJ, Nor'E SS, Ng KT, Chan KG, Hanafi NS, Pang YK, Kamarulzaman A, Tee KK. 2016. Genetic diversity, seasonality and transmission network of human metapneumovirus: identification of a unique sub-lineage of the fusion and attachment genes. *Scientific Reports* 6:27730.
77. Haynes AK, Fowlkes AL, Schneider E, Mutuc JD, Armstrong GL, Gerber SI. 2016. Human Metapneumovirus Circulation in the United States, 2008 to 2014. *Pediatrics* 137.

78. van den Hoogen BG, Herfst S, Sprong L, Cane PA, Forleo-Neto E, de Swart RL, Osterhaus AD, Fouchier RA. 2004. Antigenic and genetic variability of human metapneumoviruses. *Emerg Infect Dis* 10:658-66.
79. Boivin G, Mackay I, Sloots TP, Madhi S, Freymuth F, Wolf D, Shemer-Avni Y, Ludewick H, Gray GC, LeBlanc E. 2004. Global genetic diversity of human metapneumovirus fusion gene. *Emerg Infect Dis* 10:1154-7.
80. Kim JI, Park S, Lee I, Park KS, Kwak EJ, Moon KM, Lee CK, Bae J-Y, Park M-S, Song K-J. 2016. Genome-Wide Analysis of Human Metapneumovirus Evolution. *PLOS ONE* 11:e0152962.
81. Bouscambert-Duchamp M, Lina B, Trompette A, Moret H, Motte J, Andréoletti L. 2005. Detection of human metapneumovirus RNA sequences in nasopharyngeal aspirates of young French children with acute bronchiolitis by real-time reverse transcriptase PCR and phylogenetic analysis. *Journal of clinical microbiology* 43:1411-1414.
82. Huck B, Scharf G, Neumann-Haefelin D, Puppe W, Weigl J, Falcone V. 2006. Novel human metapneumovirus sublineage. *Emerging infectious diseases* 12:147-150.
83. Mackay IM, Bialasiewicz S, Jacob KC, McQueen E, Arden KE, Nissen MD, Sloots TP. 2006. Genetic diversity of human metapneumovirus over 4 consecutive years in Australia. *J Infect Dis* 193:1630-3.
84. Peret TC, Boivin G, Li Y, Couillard M, Humphrey C, Osterhaus AD, Erdman DD, Anderson LJ. 2002. Characterization of human metapneumoviruses isolated from patients in North America. *J Infect Dis* 185:1660-3.
85. McAdam AJ, Hasenbein ME, Feldman HA, Cole SE, Offermann JT, Riley AM, Lieu TA. 2004. Human metapneumovirus in children tested at a tertiary-care hospital. *J Infect Dis* 190:20-6.
86. Walsh EE, Peterson DR, Falsey AR. 2008. Human metapneumovirus infections in adults: another piece of the puzzle. *Arch Intern Med* 168:2489-96.

87. Navaratnarajah CK, Generous AR, Yousaf I, Cattaneo R. 2020. Receptor-mediated cell entry of paramyxoviruses: Mechanisms, and consequences for tropism and pathogenesis. *J Biol Chem* 295:2771-2786.
88. Cox RM, Plemper RK. 2017. Structure and organization of paramyxovirus particles. *Curr Opin Virol* 24:105-114.
89. Lamb RA, Kolakofsky D. 2001. *Paramyxoviridae*: The viruses and their replication, p 1305-1340. *In* Knipe DM, Howley PM (ed), *Fields Virology* (Fourth Edition). Lippincott-Raven Press, New York.
90. Biacchesi S, Skiadopoulos MH, Boivin G, Hanson CT, Murphy BR, Collins PL, Buchholz UJ. 2003. Genetic diversity between human metapneumovirus subgroups. *Virology* 315:1-9.
91. Karron RA, Buonagurio DA, Georgiu AF, Whitehead SS, Adamus JE, Clements-Mann ML, Harris DO, Randolph VB, Udem SA, Murphy BR, Sidhu MS. 1997. Respiratory syncytial virus (RSV) SH and G proteins are not essential for viral replication *in vitro*: Clinical evaluation and molecular characterization of a cold-passaged, attenuated RSV subgroup B mutant. *Proceedings of the National Academy of Sciences* 94:13961-13966.
92. Shafagati N, Williams J. 2018. Human metapneumovirus - what we know now. *F1000Research* 7:135-135.
93. Schildgen V, van den Hoogen B, Fouchier R, Tripp RA, Alvarez R, Manoha C, Williams J, Schildgen O. 2011. Human Metapneumovirus: lessons learned over the first decade. *Clinical microbiology reviews* 24:734-754.
94. Porotto M, Devito I, Palmer SG, Jurgens EM, Yee JL, Yokoyama CC, Pessi A, Moscona A. 2011. Spring-loaded model revisited: paramyxovirus fusion requires engagement of a receptor binding protein beyond initial triggering of the fusion protein. *Journal of virology* 85:12867-12880.
95. Farzan SF, Palermo LM, Yokoyama CC, Orefice G, Fornabaio M, Sarkar A, Kellogg GE, Greengard O, Porotto M, Moscona A. 2011. Premature activation of the paramyxovirus fusion protein before target cell

- attachment with corruption of the viral fusion machinery. *J Biol Chem* 286:37945-54.
96. Outlaw VK, Lemke JT, Zhu Y, Gellman SH, Porotto M, Moscona A. 2020. Structure-Guided Improvement of a Dual HPIV3/RSV Fusion Inhibitor. *Journal of the American Chemical Society* 142:2140-2144.
 97. Battles MB, Langedijk JP, Furmanova-Hollenstein P, Chaiwatpongsakorn S, Costello HM, Kwanten L, Vranckx L, Vink P, Jaensch S, Jonckers THM, Koul A, Arnoult E, Peeples ME, Roymans D, McLellan JS. 2016. Molecular mechanism of respiratory syncytial virus fusion inhibitors. *Nature chemical biology* 12:87-93.
 98. Huang J, Diaz D, Mousa JJ. 2019. Antibody Epitopes of Pneumovirus Fusion Proteins. *Front Immunol* 10:2778.
 99. Battles MB, McLellan JS. 2019. Respiratory syncytial virus entry and how to block it. *Nat Rev Microbiol* 17:233-245.
 100. Kumar P, Srivastava M. 2018. Prophylactic and therapeutic approaches for human metapneumovirus. *Virusdisease* 29:434-444.
 101. Villafana T, Falloon J, Griffin MP, Zhu Q, Esser MT. 2017. Passive and active immunization against respiratory syncytial virus for the young and old. *Expert Rev Vaccines* 16:1-13.
 102. Mejias A, Garcia-Maurino C, Rodriguez-Fernandez R, Peeples ME, Ramilo O. 2017. Development and clinical applications of novel antibodies for prevention and treatment of respiratory syncytial virus infection. *Vaccine* 35:496-502.
 103. Piacentini S, La Frazia S, Riccio A, Pedersen JZ, Topai A, Nicolotti O, Rossignol J-F, Santoro MG. 2018. Nitazoxanide inhibits paramyxovirus replication by targeting the Fusion protein folding: role of glycoprotein-specific thiol oxidoreductase ERp57. *Scientific Reports* 8:10425.
 104. Barrett CT, Webb SR, Dutch RE. 2019. A Hydrophobic Target: Using the Paramyxovirus Fusion Protein Transmembrane Domain To Modulate Fusion Protein Stability. *J Virol* 93.

105. Aguilar HC, Matreyek KA, Choi DY, Filone CM, Young S, Lee B. 2007. Polybasic KKR Motif in the Cytoplasmic Tail of Nipah Virus Fusion Protein Modulates Membrane Fusion by Inside-Out Signaling. *J Virol* 81:4520-4532.
106. Lee JK, Prussia A, Paal T, White LK, Snyder JP, Plemper RK. 2008. Functional Interaction between Paramyxovirus Fusion and Attachment Proteins. *Journal of Biological Chemistry* 283:16561-16572.
107. Palermo LM, Porotto M, Yokoyama CC, Palmer SG, Mungall BA, Greengard O, Niewiesk S, Moscona A. 2009. Human parainfluenza virus infection of the airway epithelium: viral hemagglutinin-neuraminidase regulates fusion protein activation and modulates infectivity. *J Virol* 83:6900-8.
108. Plemper RK, Brindley MA, Iorio RM. 2011. Structural and Mechanistic Studies of Measles Virus Illuminate Paramyxovirus Entry. *PLoS Pathog* 7:e1002058.
109. Plemper RK, Hammond AL, Gerlier D, Fielding AK, Cattaneo R. 2002. Strength of envelope protein interaction modulates cytopathicity of measles virus. *Journal of virology* 76:5051-5061.
110. Porotto M, Murrell M, Greengard O, Moscona A. 2003. Triggering of Human Parainfluenza Virus 3 Fusion Protein (F) by the Hemagglutinin-Neuraminidase (HN) Protein: an HN Mutation Diminishes the Rate of F Activation and Fusion. *J Virol* 77:3647-3654.
111. Porotto M, Palmer SG, Palermo LM, Moscona A. 2012. Mechanism of fusion triggering by human parainfluenza virus type III: communication between viral glycoproteins during entry. *J Biol Chem* 287:778-93.
112. Stone-Hulslander J, Morrison TG. 1997. Detection of an interaction between the HN and F proteins in Newcastle disease virus-infected cells. *J Virol* 71:6287-6295.
113. Yao Q, Hu X, Compans RW. 1997. Association of the parainfluenza virus fusion and hemagglutinin-neuraminidase glycoproteins on cell surfaces. *J Virol* 71:650-656.

114. Bao X, Kolli D, Liu T, Shan Y, Garofalo RP, Casola A. 2008. Human metapneumovirus small hydrophobic protein inhibits NF-kappaB transcriptional activity. *Journal of virology* 82:8224-8229.
115. Bao X, Liu T, Shan Y, Li K, Garofalo RP, Casola A. 2008. Human metapneumovirus glycoprotein G inhibits innate immune responses. *PLoS pathogens* 4:e1000077-e1000077.
116. Bukreyev A, Yang L, Collins PL. 2012. The secreted G protein of human respiratory syncytial virus antagonizes antibody-mediated restriction of replication involving macrophages and complement. *Journal of virology* 86:10880-10884.
117. Bukreyev A, Yang L, Fricke J, Cheng L, Ward JM, Murphy BR, Collins PL. 2008. The secreted form of respiratory syncytial virus G glycoprotein helps the virus evade antibody-mediated restriction of replication by acting as an antigen decoy and through effects on Fc receptor-bearing leukocytes. *J Virol* 82:12191-204.
118. Le Nouen C, Hillyer P, Brock LG, Winter CC, Rabin RL, Collins PL, Buchholz UJ. 2014. Human metapneumovirus SH and G glycoproteins inhibit macropinocytosis-mediated entry into human dendritic cells and reduce CD4+ T cell activation. *J Virol* 88:6453-69.
119. Shingai M, Azuma M, Ebihara T, Sasai M, Funami K, Ayata M, Ogura H, Tsutsumi H, Matsumoto M, Seya T. 2008. Soluble G protein of respiratory syncytial virus inhibits Toll-like receptor 3/4-mediated IFN-beta induction. *Int Immunol* 20:1169-80.
120. Teng MN, Whitehead SS, Collins PL. 2001. Contribution of the respiratory syncytial virus G glycoprotein and its secreted and membrane-bound forms to virus replication in vitro and in vivo. *Virology* 289:283-96.
121. Biacchesi S, Skiadopoulou MH, Yang L, Lamirande EW, Tran KC, Murphy BR, Collins PL, Buchholz UJ. 2004. Recombinant human Metapneumovirus lacking the small hydrophobic SH and/or attachment G glycoprotein: deletion of G yields a promising vaccine candidate. *J Virol* 78:12877-87.

122. He B, Leser GP, Paterson RG, Lamb RA. 1998. The paramyxovirus SV5 small hydrophobic (SH) protein is not essential for virus growth in tissue culture cells. *Virology* 250:30-40.
123. Chang A, Masante C, Buchholz UJ, Dutch RE. 2012. Human metapneumovirus (HMPV) binding and infection are mediated by interactions between the HMPV fusion protein and heparan sulfate. *J Virol* 86:3230-43.
124. Whitehead SS, Bukreyev A, Teng MN, Firestone CY, St Claire M, Elkins WR, Collins PL, Murphy BR. 1999. Recombinant respiratory syncytial virus bearing a deletion of either the NS2 or SH gene is attenuated in chimpanzees. *J Virol* 73:3438-42.
125. de Graaf M, Herfst S, Aarbiou J, Burgers PC, Zaaraoui-Boutahar F, Bijl M, van Ijcken W, Schrauwen EJA, Osterhaus ADME, Luidert TM, Scholte BJ, Fouchier RAM, Andeweg AC. 2013. Small hydrophobic protein of human metapneumovirus does not affect virus replication and host gene expression in vitro. *PloS one* 8:e58572-e58572.
126. Ling R, Sinkovic S, Toquin D, Guionie O, Etteradossi N, Easton AJ. 2008. Deletion of the SH gene from avian metapneumovirus has a greater impact on virus production and immunogenicity in turkeys than deletion of the G gene or M2-2 open reading frame. *J Gen Virol* 89:525-33.
127. Buchholz UJ, Biacchesi S, Pham QN, Tran KC, Yang L, Luongo CL, Skiadopoulou MH, Murphy BR, Collins PL. 2005. Deletion of M2 gene open reading frames 1 and 2 of human metapneumovirus: effects on RNA synthesis, attenuation, and immunogenicity. *Journal of virology* 79:6588-6597.
128. Fuentes S, Tran KC, Luthra P, Teng MN, He B. 2007. Function of the respiratory syncytial virus small hydrophobic protein. *Journal of virology* 81:8361-8366.
129. He B, Lin GY, Durbin JE, Durbin RK, Lamb RA. 2001. The SH Integral Membrane Protein of the Paramyxovirus Simian Virus 5 Is Required To Block Apoptosis in MDBK Cells. *Journal of Virology* 75:4068.

130. Xu P, Li Z, Sun D, Lin Y, Wu J, Rota PA, He B. 2011. Rescue of wild-type mumps virus from a strain associated with recent outbreaks helps to define the role of the SH ORF in the pathogenesis of mumps virus. *Virology* 417:126-36.
131. Masante C, El Najjar F, Chang A, Jones A, Moncman CL, Dutch RE. 2014. The human metapneumovirus small hydrophobic protein has properties consistent with those of a viroporin and can modulate viral fusogenic activity. *J Virol* 88:6423-33.
132. Gan SW, Tan E, Lin X, Yu D, Wang J, Tan GM, Vararattanavech A, Yeo CY, Soon CH, Soong TW, Pervushin K, Torres J. 2012. The small hydrophobic protein of the human respiratory syncytial virus forms pentameric ion channels. *J Biol Chem* 287:24671-89.
133. Gonzalez ME, Carrasco L. 2003. Viroporins. *FEBS Lett* 552:28-34.
134. Biacchesi S, Pham QN, Skiadopoulos MH, Murphy BR, Collins PL, Buchholz UJ. 2005. Infection of nonhuman primates with recombinant human metapneumovirus lacking the SH, G, or M2-2 protein categorizes each as a nonessential accessory protein and identifies vaccine candidates. *J Virol* 79:12608-13.
135. Dubois J, Pizzorno A, Cavanagh M-H, Padey B, Nicolas de Lamballerie C, Uyar O, Venable M-C, Carbonneau J, Traversier A, Julien T, Lavigne S, Couture C, Lina B, Hamelin M-È, Terrier O, Rosa-Calatrava M, Boivin G. 2019. Strain-Dependent Impact of G and SH Deletions Provide New Insights for Live-Attenuated HMPV Vaccine Development. *Vaccines* 7:164.
136. de Graaf M, Herfst S, Aarbiou J, Burgers PC, Zaaraoui-Boutahar F, Bijl M, van Ijcken W, Schrauwen EJA, Osterhaus ADME, Luiders TM, Scholte BJ, Fouchier RAM, Andeweg AC. 2013. Small Hydrophobic Protein of Human Metapneumovirus Does Not Affect Virus Replication and Host Gene Expression In Vitro. *PLOS ONE* 8:e58572.
137. Schobel SA, Stucker KM, Moore ML, Anderson LJ, Larkin EK, Shankar J, Bera J, Puri V, Shilts MH, Rosas-Salazar C, Halpin RA, Fedorova N,

- Shrivastava S, Stockwell TB, Peebles RS, Hartert TV, Das SR. 2016. Respiratory Syncytial Virus whole-genome sequencing identifies convergent evolution of sequence duplication in the C-terminus of the G gene. *Scientific reports* 6:26311-26311.
138. Saikusa M, Nao N, Kawakami C, Usuku S, Sasao T, Toyozawa T, Takeda M, Okubo I. 2017. A novel 111-nucleotide duplication in the G gene of human metapneumovirus. *Microbiol Immunol* 61:507-512.
139. Eshaghi A, Duvvuri VR, Lai R, Nadarajah JT, Li A, Patel SN, Low DE, Gubbay JB. 2012. Genetic variability of human respiratory syncytial virus A strains circulating in Ontario: a novel genotype with a 72 nucleotide G gene duplication. *PloS one* 7:e32807-e32807.
140. Hotard AL, Laikhter E, Brooks K, Hartert TV, Moore ML. 2015. Functional Analysis of the 60-Nucleotide Duplication in the Respiratory Syncytial Virus Buenos Aires Strain Attachment Glycoprotein. *Journal of Virology* 89:8258.
141. Ahmed A, Haider SH, Parveen S, Arshad M, Alsenaidy HA, Baaboud AO, Mobaireek KF, AlSaadi MM, Alsenaidy AM, Sullender W. 2016. Co-Circulation of 72bp Duplication Group A and 60bp Duplication Group B Respiratory Syncytial Virus (RSV) Strains in Riyadh, Saudi Arabia during 2014. *PLOS ONE* 11:e0166145.
142. Saikusa M, Kawakami C, Nao N, Takeda M, Usuku S, Sasao T, Nishimoto K, Toyozawa T. 2017. 180-Nucleotide Duplication in the G Gene of Human metapneumovirus A2b Subgroup Strains Circulating in Yokohama City, Japan, since 2014. *Frontiers in microbiology* 8:402-402.
143. Kwilas S, Liesman RM, Zhang L, Walsh E, Pickles RJ, Peeples ME. 2009. Respiratory syncytial virus grown in Vero cells contains a truncated attachment protein that alters its infectivity and dependence on glycosaminoglycans. *J Virol* 83:10710-8.
144. Corry J, Johnson SM, Cornwell J, Peeples ME. 2016. Preventing Cleavage of the Respiratory Syncytial Virus Attachment Protein in Vero

- Cells Rescues the Infectivity of Progeny Virus for Primary Human Airway Cultures. *J Virol* 90:1311-20.
145. Azarm KD, Lee B. 2020. Differential Features of Fusion Activation within the Paramyxoviridae. *Viruses* 12.
 146. Colman PM, Lawrence MC. 2003. The structural biology of type I viral membrane fusion. *Nature Reviews Molecular Cell Biology* 4:309-319.
 147. Blijleven JS, Boonstra S, Onck PR, van der Giessen E, van Oijen AM. 2016. Mechanisms of influenza viral membrane fusion. *Semin Cell Dev Biol* 60:78-88.
 148. Chen B. 2019. Molecular Mechanism of HIV-1 Entry. *Trends Microbiol* 27:878-891.
 149. Millet JK, Whittaker GR. 2018. Physiological and molecular triggers for SARS-CoV membrane fusion and entry into host cells. *Virology* 517:3-8.
 150. Walls AC, Xiong X, Park Y-J, Tortorici MA, Snijder J, Quispe J, Cameroni E, Gopal R, Dai M, Lanzavecchia A, Zambon M, Rey FA, Corti D, Veessler D. 2019. Unexpected Receptor Functional Mimicry Elucidates Activation of Coronavirus Fusion. *Cell* 176:1026-1039.e15.
 151. Du L, Yang Y, Zhou Y, Lu L, Li F, Jiang S. 2017. MERS-CoV spike protein: a key target for antivirals. *Expert Opin Ther Targets* 21:131-143.
 152. Salata C, Calistri A, Alvisi G, Celestino M, Parolin C, Palù G. 2019. Ebola Virus Entry: From Molecular Characterization to Drug Discovery. *Viruses* 11:274.
 153. Pallesen J, Murin CD, de Val N, Cottrell CA, Hastie KM, Turner HL, Fusco ML, Flyak AI, Zeitlin L, Crowe JE, Andersen KG, Saphire EO, Ward AB. 2016. Structures of Ebola virus GP and sGP in complex with therapeutic antibodies. *Nature Microbiology* 1:16128.
 154. White JM, Delos SE, Brecher M, Schornberg K. 2008. Structures and mechanisms of viral membrane fusion proteins: multiple variations on a common theme. *Critical reviews in biochemistry and molecular biology* 43:189-219.

155. Lamb RA, Jardetzky TS. 2007. Structural basis of viral invasion: lessons from paramyxovirus F. *Curr Opin Struct Biol* 17:427-36.
156. El Najjar F, Schmitt AP, Dutch RE. 2014. Paramyxovirus glycoprotein incorporation, assembly and budding: a three way dance for infectious particle production. *Viruses* 6:3019-3054.
157. Chang A, Dutch RE. 2012. Paramyxovirus fusion and entry: multiple paths to a common end. *Viruses* 4:613-36.
158. Smith EC, Popa A, Chang A, Masante C, Dutch RE. 2009. Viral entry mechanisms: the increasing diversity of paramyxovirus entry. *Febs j* 276:7217-27.
159. Lamb RA, Parks GD. 2007. *Paramyxoviridae*: The viruses and their replication, p 1449-1496. *In* Knipe DM, Howley PM (ed), *Fields Virology*, Fifth ed. Lippincott, Williams and Wilkins, Philadelphia.
160. Lamb RA, Paterson RG, Jardetzky TS. 2006. Paramyxovirus membrane fusion: lessons from the F and HN atomic structures. *Virology* 344:30-7.
161. Russell CJ, Jardetzky TS, Lamb RA. 2001. Membrane fusion machines of paramyxoviruses: capture of intermediates of fusion. *Embo J* 20:4024-34.
162. Lamb RA, Joshi SB, Dutch RE. 1999. The paramyxovirus fusion protein forms an extremely stable core trimer: structural parallels to influenza virus haemagglutinin and HIV-1 gp41. *Molec Membr Biol* 16:11-19.
163. Morrison T, Portner A. 1991. Structure, function, and intracellular processing of the glycoproteins of *Paramyxoviridae*, p 347-382. *In* Kingsbury DW (ed), *The Paramyxoviruses*. Plenum Press, New York.
164. Morrison TG. 1988. Structure, function, and intracellular processing of paramyxovirus membrane proteins. *Virus Res* 10:113-136.
165. Kordyukova L. 2017. Structural and functional specificity of Influenza virus haemagglutinin and paramyxovirus fusion protein anchoring peptides. *Virus Research* 227:183-199.
166. Fung TS, Liu DX. 2018. Post-translational modifications of coronavirus proteins: roles and function. *Future virology* 13:405-430.

167. Arslan A, van Noort V. 2016. Evolutionary conservation of Ebola virus proteins predicts important functions at residue level. *Bioinformatics* 33:151-154.
168. Watanabe Y, Bowden TA, Wilson IA, Crispin M. 2019. Exploitation of glycosylation in enveloped virus pathobiology. *Biochimica et Biophysica Acta (BBA) - General Subjects* 1863:1480-1497.
169. Peitsch C, Klenk H-D, Garten W, Böttcher-Friebertshäuser E. 2014. Activation of influenza A viruses by host proteases from swine airway epithelium. *Journal of virology* 88:282-291.
170. Böttcher E, Matrosovich T, Beyerle M, Klenk H-D, Garten W, Matrosovich M. 2006. Proteolytic Activation of Influenza Viruses by Serine Proteases TMPRSS2 and HAT from Human Airway Epithelium. *Journal of Virology* 80:9896-9898.
171. Straus MR, Whittaker GR. 2017. A peptide-based approach to evaluate the adaptability of influenza A virus to humans based on its hemagglutinin proteolytic cleavage site. *PLOS ONE* 12:e0174827.
172. Straus MR, Kinder JT, Segall M, Dutch RE, Whittaker GR. 2020. SPINT2 inhibits proteases involved in activation of both influenza viruses and metapneumoviruses. *Virology* 543:43-53.
173. Lambertz RLO, Pippel J, Gerhauser I, Kollmus H, Anhlan D, Hrinčius ER, Krausze J, Kuhn N, Schughart K. 2018. Exchange of amino acids in the H1-haemagglutinin to H3 residues is required for efficient influenza A virus replication and pathology in Tmprss2 knock-out mice. *J Gen Virol* 99:1187-1198.
174. Zmora P, Hoffmann M, Kollmus H, Moldenhauer AS, Danov O, Braun A, Winkler M, Schughart K, Pohlmann S. 2018. TMPRSS11A activates the influenza A virus hemagglutinin and the MERS coronavirus spike protein and is insensitive against blockade by HAI-1. *J Biol Chem* 293:13863-13873.
175. Kuhn N, Bergmann S, Kosterke N, Lambertz RLO, Keppner A, van den Brand JMA, Pohlmann S, Weiss S, Hummler E, Hatesuer B, Schughart K.

2016. The Proteolytic Activation of (H3N2) Influenza A Virus Hemagglutinin Is Facilitated by Different Type II Transmembrane Serine Proteases. *J Virol* 90:4298-4307.
176. Hatesuer B, Bertram S, Mehnert N, Bahgat MM, Nelson PS, Pohlmann S, Schughart K. 2013. Tmprss2 is essential for influenza H1N1 virus pathogenesis in mice. *PLoS Pathog* 9:e1003774.
177. Hamilton BS, Whittaker GR. 2013. Cleavage activation of human-adapted influenza virus subtypes by kallikrein-related peptidases 5 and 12. *J Biol Chem* 288:17399-407.
178. Magnen M, Gueugnon F, Guillon A, Baranek T, Thibault VC, Petit-Courty A, de Veer SJ, Harris J, Humbles AA, Si-Tahar M, Courty Y. 2017. Kallikrein-Related Peptidase 5 Contributes to H3N2 Influenza Virus Infection in Human Lungs. *Journal of virology* 91:e00421-17.
179. Suguitan AL, Jr., Matsuoka Y, Lau Y-F, Santos CP, Vogel L, Cheng LI, Orandle M, Subbarao K. 2012. The multibasic cleavage site of the hemagglutinin of highly pathogenic A/Vietnam/1203/2004 (H5N1) avian influenza virus acts as a virulence factor in a host-specific manner in mammals. *Journal of virology* 86:2706-2714.
180. Monne I, Fusaro A, Nelson MI, Bonfanti L, Mulatti P, Hughes J, Murcia PR, Schivo A, Valastro V, Moreno A, Holmes EC, Cattoli G. 2014. Emergence of a Highly Pathogenic Avian Influenza Virus from a Low-Pathogenic Progenitor. *Journal of Virology* 88:4375-4388.
181. Bolt G, Pedersen LO, Birkeslund HH. 2000. Cleavage of the respiratory syncytial virus fusion protein is required for its surface expression: role of furin. *Virus Res* 68:25-33.
182. González-Reyes L, Ruiz-Argüello MB, García-Barreno B, Calder L, López JA, Albar JP, Skehel JJ, Wiley DC, Melero JA. 2001. Cleavage of the human respiratory syncytial virus fusion protein at two distinct sites is required for activation of membrane fusion. *Proceedings of the National Academy of Sciences* 98:9859-9864.

183. Wang C, Horby PW, Hayden FG, Gao GF. 2020. A novel coronavirus outbreak of global health concern. *Lancet* 395:470-473.
184. Zhu N, Zhang D, Wang W, Li X, Yang B, Song J, Zhao X, Huang B, Shi W, Lu R, Niu P, Zhan F, Ma X, Wang D, Xu W, Wu G, Gao GF, Tan W. 2020. A Novel Coronavirus from Patients with Pneumonia in China, 2019. *N Engl J Med* 382:727-733.
185. Munster VJ, Koopmans M, van Doremalen N, van Riel D, de Wit E. 2020. A Novel Coronavirus Emerging in China - Key Questions for Impact Assessment. *N Engl J Med* 382:692-694.
186. Belouzard S, Chu VC, Whittaker GR. 2009. Activation of the SARS coronavirus spike protein via sequential proteolytic cleavage at two distinct sites. *Proceedings of the National Academy of Sciences* 106:5871-5876.
187. Reinke LM, Spiegel M, Plegge T, Hartleib A, Nehlmeier I, Gierer S, Hoffmann M, Hofmann-Winkler H, Winkler M, Pohlmann S. 2017. Different residues in the SARS-CoV spike protein determine cleavage and activation by the host cell protease TMPRSS2. *PLoS One* 12:e0179177.
188. Coutard B, Valle C, de Lamballerie X, Canard B, Seidah NG, Decroly E. 2020. The spike glycoprotein of the new coronavirus 2019-nCoV contains a furin-like cleavage site absent in CoV of the same clade. *Antiviral Research* 176:104742.
189. Schowalter RM, Smith SE, Dutch RE. 2006. Characterization of human metapneumovirus F protein-promoted membrane fusion: critical roles for proteolytic processing and low pH. *J Virol* 80:10931-41.
190. Biacchesi S, Pham QN, Skiadopoulos MH, Murphy BR, Collins PL, Buchholz UJ. 2006. Modification of the trypsin-dependent cleavage activation site of the human metapneumovirus fusion protein to be trypsin independent does not increase replication or spread in rodents or nonhuman primates. *J Virol* 80:5798-806.
191. Thomas G. 2002. Furin at the cutting edge: from protein traffic to embryogenesis and disease. *Nature reviews Molecular cell biology* 3:753-766.

192. Shirogane Y, Takeda M, Iwasaki M, Ishiguro N, Takeuchi H, Nakatsu Y, Tahara M, Kikuta H, Yanagi Y. 2008. Efficient multiplication of human metapneumovirus in Vero cells expressing the transmembrane serine protease TMPRSS2. *J Virol* 82:8942-6.
193. Schickli JH, Kaur J, Ulbrandt N, Spaete RR, Tang RS. 2005. An S101P substitution in the putative cleavage motif of the human metapneumovirus fusion protein is a major determinant for trypsin-independent growth in vero cells and does not alter tissue tropism in hamsters. *J Virol* 79:10678-89.
194. Biacchesi S, Pham QN, Skiadopoulos MH, Murphy BR, Collins PL, Buchholz UJ. 2006. Modification of the trypsin-dependent cleavage activation site of the human metapneumovirus fusion protein to be trypsin independent does not increase replication or spread in rodents or nonhuman primates. *Journal of virology* 80:5798-5806.
195. Ogata M, Fryling CM, Pastan I, FitzGerald DJ. 1992. Cell-mediated cleavage of Pseudomonas exotoxin between Arg279 and Gly280 generates the enzymatically active fragment which translocates to the cytosol. *J Biol Chem* 267:25396-401.
196. Kumar S, Sarkar A, Pugach P, Sanders RW, Moore JP, Ward AB, Wilson IA. 2019. Capturing the inherent structural dynamics of the HIV-1 envelope glycoprotein fusion peptide. *Nature communications* 10:763-763.
197. Gilman MSA, Furmanova-Hollenstein P, Pascual G, B van 't Wout A, Langedijk JPM, McLellan JS. 2019. Transient opening of trimeric prefusion RSV F proteins. *Nature communications* 10:2105-2105.
198. Dutch RE, Leser GP, Lamb RA. 1999. Paramyxovirus fusion protein: characterization of the core trimer, a rod-shaped complex with helices in anti-parallel orientation. *Virology* 254:147-159.
199. Xu K, Chan YP, Bradel-Tretheway B, Akyol-Ataman Z, Zhu Y, Dutta S, Yan L, Feng Y, Wang LF, Skinotis G, Lee B, Zhou ZH, Broder CC, Aguilar HC, Nikolov DB. 2015. Crystal Structure of the Pre-fusion Nipah Virus

- Fusion Glycoprotein Reveals a Novel Hexamer-of-Trimers Assembly.
PLoS Pathog 11:e1005322.
200. Wong JJW, Paterson RG, Lamb RA, Jardetzky TS. 2015. Structure and stabilization of the Hendra virus F glycoprotein in its prefusion form. *Proceedings of the National Academy of Sciences* doi:10.1073/pnas.1523303113:201523303.
 201. Hashiguchi T, Fukuda Y, Matsuoka R, Kuroda D, Kubota M, Shirogane Y, Watanabe S, Tsumoto K, Kohda D, Plemper RK, Yanagi Y. 2018. Structures of the prefusion form of measles virus fusion protein in complex with inhibitors. *Proceedings of the National Academy of Sciences* 115:2496-2501.
 202. Welch BD, Liu Y, Kors CA, Leser GP, Jardetzky TS, Lamb RA. 2012. Structure of the cleavage-activated prefusion form of the parainfluenza virus 5 fusion protein. *Proceedings of the National Academy of Sciences* 109:16672-16677.
 203. Yin H-S, Wen X, Paterson RG, Lamb RA, Jardetzky TS. 2006. Structure of the parainfluenza virus 5 F protein in its metastable, prefusion conformation. *Nature* 439:38-44.
 204. McLellan JS, Chen M, Joyce MG, Sastry M, Stewart-Jones GB, Yang Y, Zhang B, Chen L, Srivatsan S, Zheng A, Zhou T, Graepel KW, Kumar A, Moin S, Boyington JC, Chuang GY, Soto C, Baxa U, Bakker AQ, Spits H, Beaumont T, Zheng Z, Xia N, Ko SY, Todd JP, Rao S, Graham BS, Kwong PD. 2013. Structure-based design of a fusion glycoprotein vaccine for respiratory syncytial virus. *Science* 342:592-8.
 205. Battles MB, Mas V, Olmedillas E, Cano O, Vazquez M, Rodriguez L, Melero JA, McLellan JS. 2017. Structure and immunogenicity of pre-fusion-stabilized human metapneumovirus F glycoprotein. *Nat Commun* 8:1528.
 206. Swanson K, Wen X, Leser GP, Paterson RG, Lamb RA, Jardetzky TS. 2010. Structure of the Newcastle disease virus F protein in the post-fusion conformation. *Virology* 402:372-9.

207. McLellan JS, Yang Y, Graham BS, Kwong PD. 2011. Structure of Respiratory Syncytial Virus Fusion Glycoprotein in the Postfusion Conformation Reveals Preservation of Neutralizing Epitopes. *Journal of Virology* 85:7788-7796.
208. Más V, Rodriguez L, Olmedillas E, Cano O, Palomo C, Terrón MC, Luque D, Melero JA, McLellan JS. 2016. Engineering, Structure and Immunogenicity of the Human Metapneumovirus F Protein in the Postfusion Conformation. *PLOS Pathogens* 12:e1005859.
209. Das DK, Govindan R, Nikić-Spiegel I, Krammer F, Lemke EA, Munro JB. 2018. Direct Visualization of the Conformational Dynamics of Single Influenza Hemagglutinin Trimers. *Cell* 174:926-937.e12.
210. Kim YH, Donald JE, Grigoryan G, Leser GP, Fadeev AY, Lamb RA, DeGrado WF. 2011. Capture and imaging of a prehairpin fusion intermediate of the paramyxovirus PIV5. *Proceedings of the National Academy of Sciences* 108:20992-20997.
211. Connolly SA, Leser GP, Yin HS, Jardetzky TS, Lamb RA. 2006. Refolding of a paramyxovirus F protein from prefusion to postfusion conformations observed by liposome binding and electron microscopy. *Proc Natl Acad Sci U S A* 103:17903-8.
212. Baker RW, Hughson FM. 2016. Chaperoning SNARE assembly and disassembly. *Nat Rev Mol Cell Biol* 17:465-79.
213. Wesolowski J, Paumet F. 2010. SNARE motif: a common motif used by pathogens to manipulate membrane fusion. *Virulence* 1:319-324.
214. Skehel JJ, Wiley DC. 1998. Coiled coils in both intracellular vesicle and viral membrane fusion. *Cell* 95:871-4.
215. Yang ST, Kiessling V, Simmons JA, White JM, Tamm LK. 2015. HIV gp41-mediated membrane fusion occurs at edges of cholesterol-rich lipid domains. *Nat Chem Biol* 11:424-31.
216. Yang ST, Kiessling V, Tamm LK. 2016. Line tension at lipid phase boundaries as driving force for HIV fusion peptide-mediated fusion. *Nat Commun* 7:11401.

217. Bukrinsky MI, Mukhamedova N, Sviridov D. 2019. Lipid Rafts and Pathogens: The Art of Deception and Exploitation. *J Lipid Res* doi:10.1194/jlr.TR119000391.
218. Kollmitzer B, Heftberger P, Rappolt M, Pabst G. 2013. Monolayer spontaneous curvature of raft-forming membrane lipids. *Soft matter* 9:10877-10884.
219. Biswas S, Yin SR, Blank PS, Zimmerberg J. 2008. Cholesterol promotes hemifusion and pore widening in membrane fusion induced by influenza hemagglutinin. *J Gen Physiol* 131:503-13.
220. Yang X, Kurteva S, Ren X, Lee S, Sodroski J. 2005. Stoichiometry of Envelope Glycoprotein Trimers in the Entry of Human Immunodeficiency Virus Type 1. *Journal of Virology* 79:12132-12147.
221. Bentz J. 2000. Minimal aggregate size and minimal fusion unit for the first fusion pore of influenza hemagglutinin-mediated membrane fusion. *Biophys J* 78:227-45.
222. Blumenthal R, Sarkar DP, Durell S, Howard DE, Morris SJ. 1996. Dilation of the influenza hemagglutinin fusion pore revealed by the kinetics of individual cell-cell fusion events. *Journal of Cell Biology* 135:63-71.
223. Danieli T, Pelletier SL, Henis YI, White JM. 1996. Membrane fusion mediated by the influenza virus hemagglutinin requires the concerted action of at least three hemagglutinin trimers. *Journal of Cell Biology* 133:559-569.
224. Fontana J, Steven AC. 2015. Influenza virus-mediated membrane fusion: Structural insights from electron microscopy. *Arch Biochem Biophys* 581:86-97.
225. Li S, Sieben C, Ludwig K, Hofer CT, Chiantia S, Herrmann A, Eghiaian F, Schaap IA. 2014. pH-Controlled two-step uncoating of influenza virus. *Biophys J* 106:1447-56.
226. Sieczkarski SB, Whittaker GR. 2005. Characterization of the host cell entry of filamentous influenza virus. *Arch Virol* 150:1783-96.

227. Rust MJ, Lakadamyali M, Zhang F, Zhuang X. 2004. Assembly of endocytic machinery around individual influenza viruses during viral entry. *Nature structural & molecular biology* 11:567-573.
228. Takada A, Robison C, Goto H, Sanchez A, Murti KG, Whitt MA, Kawaoka Y. 1997. A system for functional analysis of Ebola virus glycoprotein. *Proc Natl Acad Sci U S A* 94:14764-9.
229. Sanchez A, Yang Z-Y, Xu L, Nabel GJ, Crews T, Peters CJ. 1998. Biochemical analysis of the secreted and virion glycoproteins of Ebola virus. *J Virol* 72:6442-6447.
230. Volchkov VE, Feldmann H, Volchkova VA, Klenk HD. 1998. Processing of the Ebola virus glycoprotein by the proprotein convertase furin. *Proc Natl Acad Sci U S A* 95:5762-7.
231. Weissenhorn W, Carfi A, Lee KH, Skehel JJ, Wiley DC. 1998. Crystal structure of the Ebola virus membrane fusion subunit, GP2, from the envelope glycoprotein ectodomain. *Mol Cell* 2:605-616.
232. Chandran K, Sullivan NJ, Felbor U, Whelan SP, Cunningham JM. 2005. Endosomal Proteolysis of the Ebola Virus Glycoprotein Is Necessary for Infection. *Science*.
233. Schornberg K, Matsuyama S, Kabsch K, Delos S, Bouton A, White J. 2006. Role of endosomal cathepsins in entry mediated by the Ebola virus glycoprotein. *J Virol* 80:4174-8.
234. Carette JE, Raaben M, Wong AC, Herbert AS, Obernosterer G, Mulherkar N, Kuehne AI, Kranzusch PJ, Griffin AM, Ruthel G, Dal Cin P, Dye JM, Whelan SP, Chandran K, Brummelkamp TR. 2011. Ebola virus entry requires the cholesterol transporter Niemann-Pick C1. *Nature* 477:340-3.
235. Yu D-S, Weng T-H, Wu X-X, Wang FXC, Lu X-Y, Wu H-B, Wu N-P, Li L-J, Yao H-P. 2017. The lifecycle of the Ebola virus in host cells. *Oncotarget* 8:55750-55759.
236. Fénéant L, Szymańska-de Wijs KM, Nelson EA, White JM. 2019. An exploration of conditions proposed to trigger the Ebola virus glycoprotein for fusion. *PLOS ONE* 14:e0219312.

237. Das D, Bulow U, Diehl W, Durham N, Senjobe F, Chandran K, Luban J, Munro J. 2020. Conformational changes in the Ebola virus membrane fusion machine induced by pH, Ca²⁺, and receptor binding. *PLOS Biology* 18:e3000626.
238. Markosyan RM, Miao C, Zheng YM, Melikyan GB, Liu SL, Cohen FS. 2016. Induction of Cell-Cell Fusion by Ebola Virus Glycoprotein: Low pH Is Not a Trigger. *PLoS Pathog* 12:e1005373.
239. Chang A, Hackett BA, Winter CC, Buchholz UJ, Dutch RE. 2012. Potential electrostatic interactions in multiple regions affect human metapneumovirus F-mediated membrane fusion. *J Virol* 86:9843-53.
240. Herfst S, Mas V, Ver LS, Wierda RJ, Osterhaus AD, Fouchier RA, Melero JA. 2008. Low-pH-induced membrane fusion mediated by human metapneumovirus F protein is a rare, strain-dependent phenomenon. *J Virol* 82:8891-5.
241. Mas V, Herfst S, Osterhaus AD, Fouchier RA, Melero JA. 2011. Residues of the human metapneumovirus fusion (F) protein critical for its strain-related fusion phenotype: implications for the virus replication cycle. *J Virol* 85:12650-61.
242. Schowalter RM, Chang A, Robach JG, Buchholz UJ, Dutch RE. 2009. Low-pH Triggering of Human Metapneumovirus Fusion: Essential Residues and Importance in Entry. *J Virol* 83:1511-1522.
243. Cox RG, Livesay SB, Johnson M, Ohi MD, Williams JV. 2012. The human metapneumovirus fusion protein mediates entry via an interaction with RGD-binding integrins. *J Virol* 86:12148-60.
244. Noton SL, Fearn R. 2015. Initiation and regulation of paramyxovirus transcription and replication. *Virology* 479-480:545-554.
245. Wignall-Fleming EB, Hughes DJ, Vattipally S, Modha S, Goodbourn S, Davison AJ, Randall RE. 2019. Analysis of Paramyxovirus Transcription and Replication by High-Throughput Sequencing. *Journal of Virology* 93:e00571-19.

246. Jordan PC, Liu C, Raynaud P, Lo MK, Spiropoulou CF, Symons JA, Beigelman L, Deval J. 2018. Initiation, extension, and termination of RNA synthesis by a paramyxovirus polymerase. *PLOS Pathogens* 14:e1006889.
247. Cressey TN, Noton SL, Nagendra K, Braun MR, Fearn R. 2018. Mechanism for de novo initiation at two sites in the respiratory syncytial virus promoter. *Nucleic acids research* 46:6785-6796.
248. Fearn R. 2019. The Respiratory Syncytial Virus Polymerase: A Multitasking Machine. *Trends Microbiol* 27:969-971.
249. Noton SL, Tremaglio CZ, Fearn R. 2019. Killing two birds with one stone: How the respiratory syncytial virus polymerase initiates transcription and replication. *PLoS Pathog* 15:e1007548.
250. Fearn R, Plemper RK. 2017. Polymerases of paramyxoviruses and pneumoviruses. *Virus Res* 234:87-102.
251. Cifuentes-Munoz N, Branttie J, Slaughter KB, Dutch RE. 2017. Human Metapneumovirus Induces Formation of Inclusion Bodies for Efficient Genome Replication and Transcription. *J Virol* 91.
252. Derdowski A, R Peters T, Glover N, Qian R, Utley T, Burnett A, Williams J, Spearman P, Crowe J. 2008. Human metapneumovirus nucleoprotein and phosphoprotein interact and provide the minimal requirements for inclusion body formation, vol 89.
253. Lifland AW, Jung J, Alonas E, Zurla C, Crowe JE, Jr., Santangelo PJ. 2012. Human respiratory syncytial virus nucleoprotein and inclusion bodies antagonize the innate immune response mediated by MDA5 and MAVS. *J Virol* 86:8245-58.
254. Garcia J, Garcia-Barreno B, Vivo A, Melero JA. 1993. Cytoplasmic inclusions of respiratory syncytial virus-infected cells: formation of inclusion bodies in transfected cells that coexpress the nucleoprotein, the phosphoprotein, and the 22K protein. *Virology* 195:243-7.
255. Rincheval V, Lelek M, Gault E, Bouillier C, Sitterlin D, Blouquit-Laye S, Galloux M, Zimmer C, Eleouet JF, Rameix-Welti MA. 2017. Functional

- organization of cytoplasmic inclusion bodies in cells infected by respiratory syncytial virus. *Nat Commun* 8:563.
256. Lahaye X, Vidy A, Pomier C, Obiang L, Harper F, Gaudin Y, Blondel D. 2009. Functional characterization of Negri bodies (NBs) in rabies virus-infected cells: Evidence that NBs are sites of viral transcription and replication. *J Virol* 83:7948-58.
 257. Nikolic J, Le Bars R, Lama Z, Scrima N, Lagaudrière-Gesbert C, Gaudin Y, Blondel D. 2017. Negri bodies are viral factories with properties of liquid organelles. *Nature Communications* 8:58.
 258. Goodin MM, Chakrabarty R, Yelton S, Martin K, Clark A, Brooks R. 2007. Membrane and protein dynamics in live plant nuclei infected with *Sonchus yellow net virus*, a plant-adapted rhabdovirus. *J Gen Virol* 88:1810-20.
 259. Tripathi D, Raikhy G, Goodin MM, Dietzgen RG, Pappu HR. 2015. In vivo localization of iris yellow spot tospovirus (Bunyaviridae)-encoded proteins and identification of interacting regions of nucleocapsid and movement proteins. *PLoS One* 10:e0118973.
 260. Deng M, Bragg JN, Ruzin S, Schichnes D, King D, Goodin MM, Jackson AO. 2007. Role of the *Sonchus Yellow Net Virus* N Protein in Formation of Nuclear Viroplasms. *Journal of Virology* 81:5362-5374.
 261. Hoenen T, Shabman RS, Groseth A, Herwig A, Weber M, Schudt G, Dolnik O, Basler CF, Becker S, Feldmann H. 2012. Inclusion bodies are a site of ebolavirus replication. *J Virol* 86:11779-88.
 262. Kolesnikova L, Muhlberger E, Ryabchikova E, Becker S. 2000. Ultrastructural organization of recombinant Marburg virus nucleoprotein: comparison with Marburg virus inclusions. *J Virol* 74:3899-904.
 263. Heinrich BS, Cureton DK, Rahmeh AA, Whelan SP. 2010. Protein expression redirects vesicular stomatitis virus RNA synthesis to cytoplasmic inclusions. *PLoS Pathog* 6:e1000958.
 264. Zhang S, Jiang Y, Cheng Q, Zhong Y, Qin Y, Chen M. 2017. Inclusion Body Fusion of Human Parainfluenza Virus Type 3 Regulated by Acetylated alpha-Tubulin Enhances Viral Replication. *J Virol* 91.

265. Li Z, Guo D, Qin Y, Chen M. 2019. PI4KB on Inclusion Bodies Formed by ER Membrane Remodeling Facilitates Replication of Human Parainfluenza Virus Type 3. *Cell Reports* 29:2229-2242.e4.
266. Carlos TS, Young DF, Schneider M, Simas JP, Randall RE. 2009. Parainfluenza virus 5 genomes are located in viral cytoplasmic bodies whilst the virus dismantles the interferon-induced antiviral state of cells. *J Gen Virol* 90:2147-56.
267. Romero-Brey I, Bartenschlager R. 2016. Endoplasmic Reticulum: The Favorite Intracellular Niche for Viral Replication and Assembly. *Viruses* 8:160.
268. Romero-Brey I, Bartenschlager R. 2014. Membranous replication factories induced by plus-strand RNA viruses. *Viruses* 6:2826-57.
269. Alenquer M, Vale-Costa S, Etibor TA, Ferreira F, Sousa AL, Amorim MJ. 2019. Influenza A virus ribonucleoproteins form liquid organelles at endoplasmic reticulum exit sites. *Nature communications* 10:1629-1629.
270. Zhou Y, Su JM, Samuel CE, Ma D. 2019. Measles Virus Forms Inclusion Bodies with Properties of Liquid Organelles. *J Virol* 93.
271. Heinrich BS, Maliga Z, Stein DA, Hyman AA, Whelan SPJ. 2018. Phase Transitions Drive the Formation of Vesicular Stomatitis Virus Replication Compartments. *mBio* 9:e02290-17.
272. Garcia-Jove Navarro M, Kashida S, Chouaib R, Souquere S, Pierron G, Weil D, Gueroui Z. 2019. RNA is a critical element for the sizing and the composition of phase-separated RNA–protein condensates. *Nature Communications* 10:3230.
273. Hyman AA, Weber CA, Julicher F. 2014. Liquid-liquid phase separation in biology. *Annu Rev Cell Dev Biol* 30:39-58.
274. Langdon EM, Gladfelter AS. 2018. A New Lens for RNA Localization: Liquid-Liquid Phase Separation. *Annu Rev Microbiol* 72:255-271.
275. Peran I, Mittag T. 2019. Molecular structure in biomolecular condensates. *Curr Opin Struct Biol* 60:17-26.

276. Nayak DP, Hui EK, Barman S. 2004. Assembly and budding of influenza virus. *Virus Res* 106:147-65.
277. Pornillos O, Garrus JE, Sundquist WI. 2002. Mechanisms of enveloped RNA virus budding. *Trends Cell Biol* 12:569-79.
278. Mothes W, Sherer NM, Jin J, Zhong P. 2010. Virus Cell-to-Cell Transmission. *Journal of Virology* 84:8360-8368.
279. Sattentau Q. 2008. Avoiding the void: cell-to-cell spread of human viruses. *Nat Rev Microbiol* 6:815-26.
280. Cifuentes-Munoz N, Ellis Dutch R. 2019. To assemble or not to assemble: The changing rules of pneumovirus transmission. *Virus Res* 265:68-73.
281. Dadonaite B, Vijayakrishnan S, Fodor E, Bhella D, Hutchinson EC. 2016. Filamentous influenza viruses. *J Gen Virol* 97:1755-1764.
282. Vijayakrishnan S, Loney C, Jackson D, Suphamungmee W, Rixon FJ, Bhella D. 2013. Cryotomography of Budding Influenza A Virus Reveals Filaments with Diverse Morphologies that Mostly Do Not Bear a Genome at Their Distal End. *PLOS Pathogens* 9:e1003413.
283. Calder LJ, Wasilewski S, Berriman JA, Rosenthal PB. 2010. Structural organization of a filamentous influenza A virus. *Proceedings of the National Academy of Sciences* 107:10685-10690.
284. Shaikh FY, Utley TJ, Craven RE, Rogers MC, Lapierre LA, Goldenring JR, Crowe JE, Jr. 2012. Respiratory syncytial virus assembles into structured filamentous virion particles independently of host cytoskeleton and related proteins. *PloS one* 7:e40826-e40826.
285. Ke Z, Dillard RS, Chirkova T, Leon F, Stobart CC, Hampton CM, Strauss JD, Rajan D, Rostad CA, Taylor JV, Yi H, Shah R, Jin M, Hartert TV, Peebles RS, Jr., Graham BS, Moore ML, Anderson LJ, Wright ER. 2018. The Morphology and Assembly of Respiratory Syncytial Virus Revealed by Cryo-Electron Tomography. *Viruses* 10:446.
286. Hamelin ME, Abed Y, Boivin G. 2004. Human metapneumovirus: a new player among respiratory viruses. *Clin Infect Dis* 38:983-90.

287. Blasco R, Moss B. 1992. Role of cell-associated enveloped vaccinia virus in cell-to-cell spread. *J Virol* 66:4170-9.
288. El Najjar F, Cifuentes-Muñoz N, Chen J, Zhu H, Buchholz UJ, Moncman CL, Dutch RE. 2016. Human metapneumovirus Induces Reorganization of the Actin Cytoskeleton for Direct Cell-to-Cell Spread. *PLoS Pathog* 12:e1005922.
289. Yanagi Y, Takeda M, Ohno S, Hashiguchi T. 2009. Measles Virus Receptors, p 13-30. *In* Griffin DE, Oldstone MBA (ed), *Measles: History and Basic Biology* doi:10.1007/978-3-540-70523-9_2. Springer Berlin Heidelberg, Berlin, Heidelberg.
290. Hashimoto K, Ono N, Tatsuo H, Minagawa H, Takeda M, Takeuchi K, Yanagi Y. 2002. SLAM (CD150)-Independent Measles Virus Entry as Revealed by Recombinant Virus Expressing Green Fluorescent Protein. *Journal of Virology* 76:6743-6749.
291. Takeuchi K, Miyajima N, Nagata N, Takeda M, Tashiro M. 2003. Wild-type measles virus induces large syncytium formation in primary human small airway epithelial cells by a SLAM(CD150)-independent mechanism. *Virus Res* 94:11-6.
292. Noyce RS, Richardson CD. 2012. Nectin 4 is the epithelial cell receptor for measles virus. *Trends Microbiol* 20:429-39.
293. Noyce RS, Bondre DG, Ha MN, Lin L-T, Sisson G, Tsao M-S, Richardson CD. 2011. Tumor Cell Marker PVRL4 (Nectin 4) Is an Epithelial Cell Receptor for Measles Virus. *PLOS Pathogens* 7:e1002240.
294. Singh BK, Pfaller CK, Cattaneo R, Sinn PL. 2019. Measles Virus Ribonucleoprotein Complexes Rapidly Spread across Well-Differentiated Primary Human Airway Epithelial Cells along F-Actin Rings. *mBio* 10.
295. Cattaneo R, Donohue RC, Generous AR, Navaratnarajah CK, Pfaller CK. 2019. Stronger together: Multi-genome transmission of measles virus. *Virus Res* 265:74-79.
296. Singh BK, Li N, Mark AC, Mateo M, Cattaneo R, Sinn PL. 2016. Cell-to-Cell Contact and Nectin-4 Govern Spread of Measles Virus from Primary

- Human Myeloid Cells to Primary Human Airway Epithelial Cells. *J Virol* 90:6808-6817.
297. Singh BK, Hornick AL, Krishnamurthy S, Locke AC, Mendoza CA, Mateo M, Miller-Hunt CL, Cattaneo R, Sinn PL. 2015. The Nectin-4/Afadin Protein Complex and Intercellular Membrane Pores Contribute to Rapid Spread of Measles Virus in Primary Human Airway Epithelia. *J Virol* 89:7089-96.
 298. Mehedi M, McCarty T, Martin SE, Le Nouen C, Buehler E, Chen YC, Smelkinson M, Ganesan S, Fischer ER, Brock LG, Liang B, Munir S, Collins PL, Buchholz UJ. 2016. Actin-Related Protein 2 (ARP2) and Virus-Induced Filopodia Facilitate Human Respiratory Syncytial Virus Spread. *PLoS Pathog* 12:e1006062.
 299. Cifuentes-Muñoz N, Dutch RE, Cattaneo R. 2018. Direct cell-to-cell transmission of respiratory viruses: The fast lanes. *PLoS pathogens* 14:e1007015-e1007015.
 300. Sanjuan R. 2017. Collective Infectious Units in Viruses. *Trends Microbiol* 25:402-412.
 301. Hotard AL, Lee S, Currier MG, Crowe JE, Jr., Sakamoto K, Newcomb DC, Peebles RS, Jr., Plemper RK, Moore ML. 2015. Identification of residues in the human respiratory syncytial virus fusion protein that modulate fusion activity and pathogenesis. *J Virol* 89:512-22.
 302. Loney C, Mottet-Osman G, Roux L, Bhella D. 2009. Paramyxovirus Ultrastructure and Genome Packaging: Cryo-Electron Tomography of Sendai Virus. *Journal of Virology* 83:8191-8197.
 303. Rager M, Vongpunsawad S, Duprex WP, Cattaneo R. 2002. Polypliod measles virus with hexameric genome length. *The EMBO Journal* 21:2364-2372.
 304. Dahlberg JE, Simon EH. 1969. Physical and genetic studies of Newcastle disease virus: Evidence for multiploid particles. *Virology* 38:666-678.
 305. French CA. 2009. Chapter 2 - Respiratory Tract, p 65-103. *In* Cibas ES, Ducatman BS (ed), *Cytology (Third Edition)*

doi:<https://doi.org/10.1016/B978-1-4160-5329-3.00002-5>. W.B. Saunders, Philadelphia.

306. Kini SR. 2002. Anatomy, Histology, and Cytology of Normal Components of the Lower Respiratory Tract, p 27-37. *In* Kini SR (ed), Color Atlas of Pulmonary Cytopathology doi:10.1007/978-0-387-21641-6_3. Springer New York, New York, NY.
307. Iwasaki A, Foxman EF, Molony RD. 2017. Early local immune defences in the respiratory tract. *Nature reviews Immunology* 17:7-20.
308. Newton AH, Cardani A, Braciale TJ. 2016. The host immune response in respiratory virus infection: balancing virus clearance and immunopathology. *Seminars in immunopathology* 38:471-482.
309. Sharma L, Feng J, Britto CJ, Dela Cruz CS. 2020. Mechanisms of Epithelial Immunity Evasion by Respiratory Bacterial Pathogens. *Frontiers in Immunology* 11.
310. Nicod LP. 2005. Lung defences: an overview. *European Respiratory Review* 14:45-50.
311. Lloyd CM, Marsland BJ. 2017. Lung Homeostasis: Influence of Age, Microbes, and the Immune System. *Immunity* 46:549-561.
312. Dvorak A, Tilley AE, Shaykhiev R, Wang R, Crystal RG. 2011. Do airway epithelium air-liquid cultures represent the in vivo airway epithelium transcriptome? *Am J Respir Cell Mol Biol* 44:465-73.
313. Pezzulo AA, Starner TD, Scheetz TE, Traver GL, Tilley AE, Harvey BG, Crystal RG, McCray PB, Jr., Zabner J. 2011. The air-liquid interface and use of primary cell cultures are important to recapitulate the transcriptional profile of in vivo airway epithelia. *Am J Physiol Lung Cell Mol Physiol* 300:L25-31.
314. Broadbent L, Villenave R, Guo-Parke H, Douglas I, Shields MD, Power UF. 2016. In Vitro Modeling of RSV Infection and Cytopathogenesis in Well-Differentiated Human Primary Airway Epithelial Cells (WD-PAECs). *Methods Mol Biol* 1442:119-39.

315. Hasan S, Sebo P, Osicka R. 2018. A guide to polarized airway epithelial models for studies of host-pathogen interactions. *Febs j* 285:4343-4358.
316. Johnson SM, McNally BA, Ioannidis I, Flano E, Teng MN, Oomens AG, Walsh EE, Peeples ME. 2015. Respiratory Syncytial Virus Uses CX3CR1 as a Receptor on Primary Human Airway Epithelial Cultures. *PLoS Pathog* 11:e1005318.
317. Liesman RM, Buchholz UJ, Luongo CL, Yang L, Proia AD, DeVincenzo JP, Collins PL, Pickles RJ. 2014. RSV-encoded NS2 promotes epithelial cell shedding and distal airway obstruction. *J Clin Invest* 124:2219-33.
318. Nicolas de Lamballerie C, Pizzorno A, Dubois J, Julien T, Padey B, Bouveret M, Traversier A, Legras-Lachuer C, Lina B, Boivin G, Terrier O, Rosa-Calatrava M. 2019. Characterization of cellular transcriptomic signatures induced by different respiratory viruses in human reconstituted airway epithelia. *Scientific Reports* 9:11493.
319. Pickles RJ. 2013. Human airway epithelial cell cultures for modeling respiratory syncytial virus infection. *Curr Top Microbiol Immunol* 372:371-87.
320. Singh BK, Pfaller CK, Cattaneo R, Sinn PL. 2019. Measles Virus Ribonucleoprotein Complexes Rapidly Spread across Well-Differentiated Primary Human Airway Epithelial Cells along F-Actin Rings. *mBio* 10:e02434-19.
321. Villenave R, Shields MD, Power UF. 2013. Respiratory syncytial virus interaction with human airway epithelium. *Trends Microbiol* 21:238-44.
322. Zhang L, Bukreyev A, Thompson CI, Watson B, Peeples ME, Collins PL, Pickles RJ. 2005. Infection of ciliated cells by human parainfluenza virus type 3 in an in vitro model of human airway epithelium. *J Virol* 79:1113-24.
323. Zhang L, Collins PL, Lamb RA, Pickles RJ. 2011. Comparison of differing cytopathic effects in human airway epithelium of parainfluenza virus 5 (W3A), parainfluenza virus type 3, and respiratory syncytial virus. *Virology* 421:67-77.

324. Zhang L, Peeples ME, Boucher RC, Collins PL, Pickles RJ. 2002. Respiratory syncytial virus infection of human airway epithelial cells is polarized, specific to ciliated cells, and without obvious cytopathology. *J Virol* 76:5654-66.
325. Kwilas AR, Yednak MA, Zhang L, Liesman R, Collins PL, Pickles RJ, Peeples ME. 2010. Respiratory syncytial virus engineered to express the cystic fibrosis transmembrane conductance regulator corrects the bioelectric phenotype of human cystic fibrosis airway epithelium in vitro. *J Virol* 84:7770-81.
326. Villenave R, Thavagnanam S, Sarlang S, Parker J, Douglas I, Skibinski G, Heaney LG, McKaigue JP, Coyle PV, Shields MD, Power UF. 2012. In vitro modeling of respiratory syncytial virus infection of pediatric bronchial epithelium, the primary target of infection in vivo. *Proc Natl Acad Sci U S A* 109:5040-5.
327. Bhowmick R, Derakhshan T, Liang Y, Ritchey J, Liu L, Gappa-Fahlenkamp H. 2018. A Three-Dimensional Human Tissue-Engineered Lung Model to Study Influenza A Infection. *Tissue Eng Part A* 24:1468-1480.
328. Palmer SG, Porotto M, Palermo LM, Cunha LF, Greengard O, Moscona A. 2012. Adaptation of human parainfluenza virus to airway epithelium reveals fusion properties required for growth in host tissue. *MBio* 3.
329. Alkhatib G, Massie B, Briedis DJ. 1988. Expression of bicistronic measles virus P/C mRNA by using hybrid adenoviruses: levels of C protein synthesized in vivo are unaffected by the presence or absence of the upstream P initiator codon. *J Virol* 62:4059-4069.
330. Bellini WJ, Englund G, Richardson CD, Rozenblatt S, Lazzarini RA. 1986. Matrix genes of measles virus and canine distemper virus: cloning, nucleotide sequences, and deduced amino acid sequences. *J Virol* 58:408-416.
331. Fujinami RS, Oldstone MBA, Wroblewska Z, Frankel ME, Koprowski H. 1983. Molecular mimicry in virus infection: Crossreaction of measles virus

- phosphorprotein or of herpes simplex virus protein with human intermediate filaments. *Immunology* 80:2346-2350.
332. Sissons JGP, Schreiber RD, Perrin LH, Cooper NR, Muller-Eberhard HJ, Oldstone MBA. 1979. Lysis of measles virus-infected cells by the purified cytolytic alternative complement pathway and antibody. *J Exp Med* 150:445-454.
333. Klimyte EM, Smith SE, Oreste P, Lembo D, Dutch RE. 2016. Inhibition of Human Metapneumovirus Binding to Heparan Sulfate Blocks Infection in Human Lung Cells and Airway Tissues. *J Virol* 90:9237-50.
334. Naylor CJ, Brown PA, Edworthy N, Ling R, Jones RC, Savage CE, Easton AJ. 2004. Development of a reverse-genetics system for Avian pneumovirus demonstrates that the small hydrophobic (SH) and attachment (G) genes are not essential for virus viability. *Journal of General Virology* 85:3219-3227.
335. Cox RG, Mainou BA, Johnson M, Hastings AK, Schuster JE, Dermody TS, Williams JV. 2015. Human Metapneumovirus Is Capable of Entering Cells by Fusion with Endosomal Membranes. *PLoS Pathog* 11:e1005303.
336. Harrison SC. 2008. Viral membrane fusion. *Nat Struct Mol Biol* 15:690-8.
337. Huang Q, Sivaramakrishna RP, Ludwig K, Korte T, Bottcher C, Herrmann A. 2003. Early steps of the conformational change of influenza virus hemagglutinin to a fusion active state: stability and energetics of the hemagglutinin. *Biochim Biophys Acta* 1614:3-13.
338. Kampmann T, Mueller DS, Mark AE, Young PR, Kobe B. 2006. The Role of histidine residues in low-pH-mediated viral membrane fusion. *Structure* 14:1481-7.
339. Lo Presti A, Cammarota R, Apostoli P, Cella E, Fiorentini S, Babakir-Mina M, Ciotti M, Ciccozzi M. 2011. Genetic variability and circulation pattern of human metapneumovirus isolated in Italy over five epidemic seasons. *New Microbiol* 34:337-44.
340. Schuster JE, Cox RG, Hastings AK, Boyd KL, Wadia J, Chen Z, Burton DR, Williamson RA, Williams JV. 2015. A broadly neutralizing human

- monoclonal antibody exhibits in vivo efficacy against both human metapneumovirus and respiratory syncytial virus. *J Infect Dis* 211:216-25.
341. Wei Y, Zhang Y, Cai H, Mirza AM, Iorio RM, Peeples ME, Niewiesk S, Li J. 2014. Roles of the putative integrin-binding motif of the human metapneumovirus fusion (f) protein in cell-cell fusion, viral infectivity, and pathogenesis. *J Virol* 88:4338-52.
342. World, Health, Organization. 2014. Global Epidemiological Surveillance Standards for Influenza.
343. Fouchier RAM, Guan Y. Ecology and evolution of influenza viruses in wild and domestic birds, p 173-189, *Textbook of Influenza* doi:10.1002/9781118636817.ch11.
344. Yen HL, Webster RG. 2009. Pandemic influenza as a current threat. *Curr Top Microbiol Immunol* 333:3-24.
345. World, Health, Organization. 2017. Human infection with avian influenza A(H7N9) virus - China.
346. World, Health, Organization. 2018. Influenza fact sheet.
347. Kilbourne ED. 2006. Influenza pandemics of the 20th century. *Emerg Infect Dis* 12:9-14.
348. Hussain M, Galvin HD, Haw TY, Nutsford AN, Husain M. 2017. Drug resistance in influenza A virus: the epidemiology and management. *Infect Drug Resist* 10:121-134.
349. Takashita E, Morita H, Ogawa R, Nakamura K, Fujisaki S, Shirakura M, Kuwahara T, Kishida N, Watanabe S, Odagiri T. 2018. Susceptibility of Influenza Viruses to the Novel Cap-Dependent Endonuclease Inhibitor Baloxavir Marboxil. *Front Microbiol* 9:3026.
350. Hayden FG, Sugaya N, Hirotsu N, Lee N, de Jong MD, Hurt AC, Ishida T, Sekino H, Yamada K, Portsmouth S, Kawaguchi K, Shishido T, Arai M, Tsuchiya K, Uehara T, Watanabe A. 2018. Baloxavir Marboxil for Uncomplicated Influenza in Adults and Adolescents. *N Engl J Med* 379:913-923.

351. Omoto S, Speranzini V, Hashimoto T, Noshi T, Yamaguchi H, Kawai M, Kawaguchi K, Uehara T, Shishido T, Naito A, Cusack S. 2018. Characterization of influenza virus variants induced by treatment with the endonuclease inhibitor baloxavir marboxil. *Sci Rep* 8:9633.
352. Li Y, Reeves RM, Wang X, Bassat Q, Brooks WA, Cohen C, Moore DP, Nunes M, Rath B, Campbell H, Nair H. 2019. Global patterns in monthly activity of influenza virus, respiratory syncytial virus, parainfluenza virus, and metapneumovirus: a systematic analysis. *Lancet Glob Health* 7:e1031-e1045.
353. Taylor S, Lopez P, Weckx L, Borja-Tabora C, Ulloa-Gutierrez R, Lazcano-Ponce E, Kerdpanich A, Angel Rodriguez Weber M, Mascarenas de Los Santos A, Tinoco JC, Safadi MA, Lim FS, Hernandez-de Mezerville M, Faingezicht I, Cruz-Valdez A, Feng Y, Li P, Durviaux S, Haars G, Roy-Ghanta S, Vaughn DW, Nolan T. 2017. Respiratory viruses and influenza-like illness: Epidemiology and outcomes in children aged 6 months to 10 years in a multi-country population sample. *J Infect* 74:29-41.
354. Leung J, Esper F, Weibel C, Kahn JS. 2005. Seroepidemiology of Human Metapneumovirus (hMPV) on the Basis of a Novel Enzyme-Linked Immunosorbent Assay Utilizing hMPV Fusion Protein Expressed in Recombinant Vesicular Stomatitis Virus. *Journal of Clinical Microbiology* 43:1213-1219.
355. Steinhauer DA. 1999. Role of hemagglutinin cleavage for the pathogenicity of influenza virus. *Virology* 258:1-20.
356. Taubenberger JK. 1998. Influenza virus hemagglutinin cleavage into HA₁, HA₂: No laughing matter. *Proc Natl Acad Sci USA* 95:9713-9715.
357. Bottcher-Friebertshauser E, Klenk HD, Garten W. 2013. Activation of influenza viruses by proteases from host cells and bacteria in the human airway epithelium. *Pathog Dis* 69:87-100.
358. Horimoto T, Nakayama K, Smeekens SP, Kawaoka Y. 1994. Proprotein-processing endoproteases PC6 and furin both activate hemagglutinin of virulent avian influenza viruses. *J Virol* 68:6074-8.

359. Millet JK, Whittaker GR. 2015. Host cell proteases: Critical determinants of coronavirus tropism and pathogenesis. *Virus Res* 202:120-34.
360. Laporte M, Naesens L. 2017. Airway proteases: an emerging drug target for influenza and other respiratory virus infections. *Curr Opin Virol* 24:16-24.
361. Zhirnov OP, Matrosovich TY, Matrosovich MN, Klenk HD. 2011. Aprotinin, a protease inhibitor, suppresses proteolytic activation of pandemic H1N1v influenza virus. *Antivir Chem Chemother* 21:169-74.
362. Hamilton BS, Chung C, Cyphers SY, Rinaldi VD, Marcano VC, Whittaker GR. 2014. Inhibition of influenza virus infection and hemagglutinin cleavage by the protease inhibitor HAI-2. *Biochem Biophys Res Commun* 450:1070-5.
363. Szabo R, Hobson JP, List K, Molinolo A, Lin CY, Bugge TH. 2008. Potent inhibition and global co-localization implicate the transmembrane Kunitz-type serine protease inhibitor hepatocyte growth factor activator inhibitor-2 in the regulation of epithelial matriptase activity. *J Biol Chem* 283:29495-504.
364. Delaria KA, Muller DK, Marlor CW, Brown JE, Das RC, Rocznik SO, Tamburini PP. 1997. Characterization of placental bikunin, a novel human serine protease inhibitor. *J Biol Chem* 272:12209-14.
365. Roversi FM, Olalla Saad ST, Machado-Neto JA. 2018. Serine peptidase inhibitor Kunitz type 2 (SPINT2) in cancer development and progression. *Biomed Pharmacother* 101:278-286.
366. Wu SR, Lin CH, Shih HP, Ko CJ, Lin HY, Lan SW, Lin HH, Tu HF, Ho CC, Huang HP, Lee MS. 2019. HAI-2 as a novel inhibitor of plasmin represses lung cancer cell invasion and metastasis. *Br J Cancer* 120:499-511.
367. Wu SR, Teng CH, Tu YT, Ko CJ, Cheng TS, Lan SW, Lin HY, Lin HH, Tu HF, Hsiao PW, Huang HP, Chen CH, Lee MS. 2017. The Kunitz Domain I of Hepatocyte Growth Factor Activator Inhibitor-2 Inhibits Matriptase Activity and Invasive Ability of Human Prostate Cancer Cells. *Sci Rep* 7:15101.

368. Dong W, Chen X, Xie J, Sun P, Wu Y. 2010. Epigenetic inactivation and tumor suppressor activity of HAI-2/SPINT2 in gastric cancer. *Int J Cancer* 127:1526-34.
369. Fukai K, Yokosuka O, Chiba T, Hirasawa Y, Tada M, Imazeki F, Kataoka H, Saisho H. 2003. Hepatocyte growth factor activator inhibitor 2/placental bikunin (HAI-2/PB) gene is frequently hypermethylated in human hepatocellular carcinoma. *Cancer Res* 63:8674-9.
370. Hwang S, Kim HE, Min M, Raghunathan R, Panova IP, Munshi R, Ryu B. 2015. Epigenetic Silencing of SPINT2 Promotes Cancer Cell Motility via HGF-MET Pathway Activation in Melanoma. *J Invest Dermatol* 135:2283-2291.
371. Tsai CH, Teng CH, Tu YT, Cheng TS, Wu SR, Ko CJ, Shyu HY, Lan SW, Huang HP, Tzeng SF, Johnson MD, Lin CY, Hsiao PW, Lee MS. 2014. HAI-2 suppresses the invasive growth and metastasis of prostate cancer through regulation of matriptase. *Oncogene* 33:4643-52.
372. Szabo R, Hobson JP, Christoph K, Kosa P, List K, Bugge TH. 2009. Regulation of cell surface protease matriptase by HAI2 is essential for placental development, neural tube closure and embryonic survival in mice. *Development* 136:2653-63.
373. Wu CJ, Feng X, Lu M, Morimura S, Udey MC. 2017. Matriptase-mediated cleavage of EpCAM destabilizes claudins and dysregulates intestinal epithelial homeostasis. *J Clin Invest* 127:623-634.
374. Jaimes JA, Millet JK, Goldstein ME, Whittaker GR, Straus MR. 2019. A Fluorogenic Peptide Cleavage Assay to Screen for Proteolytic Activity: Applications for coronavirus spike protein activation. *J Vis Exp* doi:10.3791/58892.
375. Galloway SE, Reed ML, Russell CJ, Steinhauer DA. 2013. Influenza HA subtypes demonstrate divergent phenotypes for cleavage activation and pH of fusion: implications for host range and adaptation. *PLoS Pathog* 9:e1003151.

376. Baron J, Tarnow C, Mayoli-Nussle D, Schilling E, Meyer D, Hammami M, Schwalm F, Steinmetzer T, Guan Y, Garten W, Klenk HD, Bottcher-Friebertshauser E. 2013. Matriptase, HAT, and TMPRSS2 activate the hemagglutinin of H9N2 influenza A viruses. *J Virol* 87:1811-20.
377. Sakai K, Ami Y, Tahara M, Kubota T, Anraku M, Abe M, Nakajima N, Sekizuka T, Shirato K, Suzaki Y, Ainai A, Nakatsu Y, Kanou K, Nakamura K, Suzuki T, Komase K, Nobusawa E, Maenaka K, Kuroda M, Hasegawa H, Kawaoka Y, Tashiro M, Takeda M. 2014. The host protease TMPRSS2 plays a major role in in vivo replication of emerging H7N9 and seasonal influenza viruses. *J Virol* 88:5608-16.
378. Houser K, Subbarao K. 2015. Influenza vaccines: challenges and solutions. *Cell Host Microbe* 17:295-300.
379. Karlsson EA, Meliopoulos VA, van de Velde NC, van de Velde LA, Mann B, Gao G, Rosch J, Tuomanen E, McCullers J, Vogel P, Schultz-Cherry S. 2017. A Perfect Storm: Increased Colonization and Failure of Vaccination Leads to Severe Secondary Bacterial Infection in Influenza Virus-Infected Obese Mice. *mBio* 8.
380. Limburg H, Harbig A, Bestle D, Stein DA, Moulton HM, Jaeger J, Janga H, Harges K, Koepke J, Schulte L, Koczulla AR, Schmeck B, Klenk HD, Bottcher-Friebertshauser E. 2019. TMPRSS2 Is the Major Activating Protease of Influenza A Virus in Primary Human Airway Cells and Influenza B Virus in Human Type II Pneumocytes. *J Virol* 93.
381. Tarnow C, Engels G, Arendt A, Schwalm F, Sediri H, Preuss A, Nelson PS, Garten W, Klenk HD, Gabriel G, Bottcher-Friebertshauser E. 2014. TMPRSS2 is a host factor that is essential for pneumotropism and pathogenicity of H7N9 influenza A virus in mice. *J Virol* 88:4744-51.
382. Whittaker GR, Straus MR. 2019. Human matriptase/ST 14 proteolytically cleaves H7N9 hemagglutinin and facilitates the activation of influenza A/Shanghai/2/2013 virus in cell culture. *Influenza Other Respir Viruses* doi:10.1111/irv.12707.

383. Meyer D, Sielaff F, Hammami M, Bottcher-Friebertshauser E, Garten W, Steinmetzer T. 2013. Identification of the first synthetic inhibitors of the type II transmembrane serine protease TMPRSS2 suitable for inhibition of influenza virus activation. *Biochem J* 452:331-43.
384. Sielaff F, Bottcher-Friebertshauser E, Meyer D, Saupe SM, Volk IM, Garten W, Steinmetzer T. 2011. Development of substrate analogue inhibitors for the human airway trypsin-like protease HAT. *Bioorg Med Chem Lett* 21:4860-4.
385. Yamaya M, Shimotai Y, Hatachi Y, Lusamba Kalonji N, Tando Y, Kitajima Y, Matsuo K, Kubo H, Nagatomi R, Hongo S, Homma M, Nishimura H. 2015. The serine protease inhibitor camostat inhibits influenza virus replication and cytokine production in primary cultures of human tracheal epithelial cells. *Pulm Pharmacol Ther* 33:66-74.
386. Sai JK, Suyama M, Kubokawa Y, Matsumura Y, Inami K, Watanabe S. 2010. Efficacy of camostat mesilate against dyspepsia associated with non-alcoholic mild pancreatic disease. *J Gastroenterol* 45:335-41.
387. Zhou Y, Vedantham P, Lu K, Agudelo J, Carrion R, Jr., Nunneley JW, Barnard D, Pohlmann S, McKerrow JH, Renslo AR, Simmons G. 2015. Protease inhibitors targeting coronavirus and filovirus entry. *Antiviral Res* 116:76-84.
388. Gierer S, Bertram S, Kaup F, Wrensch F, Heurich A, Kramer-Kuhl A, Welsch K, Winkler M, Meyer B, Drosten C, Dittmer U, von Hahn T, Simmons G, Hofmann H, Pohlmann S. 2013. The spike protein of the emerging betacoronavirus EMC uses a novel coronavirus receptor for entry, can be activated by TMPRSS2, and is targeted by neutralizing antibodies. *J Virol* 87:5502-11.
389. Matsuyama S, Nagata N, Shirato K, Kawase M, Takeda M, Taguchi F. 2010. Efficient activation of the severe acute respiratory syndrome coronavirus spike protein by the transmembrane protease TMPRSS2. *J Virol* 84:12658-64.

390. Beigel JH, Farrar J, Han AM, Hayden FG, Hyer R, de Jong MD, Lochindarat S, Nguyen TK, Nguyen TH, Tran TH, Nicoll A, Touch S, Yuen KY. 2005. Avian influenza A (H5N1) infection in humans. *N Engl J Med* 353:1374-85.
391. Jain S, Williams DJ, Arnold SR, Ampofo K, Bramley AM, Reed C, Stockmann C, Anderson EJ, Grijalva CG, Self WH, Zhu Y, Patel A, Hymas W, Chappell JD, Kaufman RA, Kan JH, Dansie D, Lenny N, Hillyard DR, Haynes LM, Levine M, Lindstrom S, Winchell JM, Katz JM, Erdman D, Schneider E, Hicks LA, Wunderink RG, Edwards KM, Pavia AT, McCullers JA, Finelli L. 2015. Community-acquired pneumonia requiring hospitalization among U.S. children. *N Engl J Med* 372:835-45.
392. Kahn JS. 2006. Epidemiology of Human Metapneumovirus. *Clinical Microbiology Reviews* 19:546-557.
393. Ebihara T, Endo R, Kikuta H, Ishiguro N, Yoshioka M, Ma X, Kobayashi K. 2003. Seroprevalence of human metapneumovirus in Japan. *J Med Virol* 70:281-3.
394. Wolf DG, Zakay-Rones Z, Fadeela A, Greenberg D, Dagan R. 2003. High seroprevalence of human metapneumovirus among young children in Israel. *J Infect Dis* 188:1865-7.
395. Vargas SO, Kozakewich HP, Perez-Atayde AR, McAdam AJ. 2004. Pathology of human metapneumovirus infection: insights into the pathogenesis of a newly identified respiratory virus. *Pediatr Dev Pathol* 7:478-86; discussion 421.
396. Hamelin M-È, Abed Y, Boivin G. 2004. Human Metapneumovirus: A New Player among Respiratory Viruses. *Clinical Infectious Diseases* 38:983-990.
397. Hall CB, Weinberg GA, Iwane MK, Blumkin AK, Edwards KM, Staat MA, Auinger P, Griffin MR, Poehling KA, Erdman D, Grijalva CG, Zhu Y, Szilagyi P. 2009. The Burden of Respiratory Syncytial Virus Infection in Young Children. *New England Journal of Medicine* 360:588-598.

398. Cox RG, Williams JV. 2013. Breaking in: human metapneumovirus fusion and entry. *Viruses* 5:192-210.
399. Techaarpornkul S, Barretto N, Peeples ME. 2001. Functional analysis of recombinant respiratory syncytial virus deletion mutants lacking the small hydrophobic and/or attachment glycoprotein gene. *J Virol* 75:6825-34.
400. Bukreyev A, Whitehead SS, Murphy BR, Collins PL. 1997. Recombinant respiratory syncytial virus from which the entire SH gene has been deleted grows efficiently in cell culture and exhibits site-specific attenuation in the respiratory tract of the mouse. *J Virol* 71:8973-82.
401. Wen SC, Williams JV. 2015. New Approaches for Immunization and Therapy against Human Metapneumovirus. *Clinical and Vaccine Immunology* 22:858-866.
402. Nelson EV, Schmidt KM, Deflube LR, Doganay S, Banadyga L, Olejnik J, Hume AJ, Ryabchikova E, Ebihara H, Kedersha N, Ha T, Muhlberger E. 2016. Ebola Virus Does Not Induce Stress Granule Formation during Infection and Sequesters Stress Granule Proteins within Viral Inclusions. *J Virol* 90:7268-7284.
403. Nikolic J, Civas A, Lama Z, Lagaudriere-Gesbert C, Blondel D. 2016. Rabies Virus Infection Induces the Formation of Stress Granules Closely Connected to the Viral Factories. *PLoS Pathog* 12:e1005942.
404. Schudt G, Dolnik O, Kolesnikova L, Biedenkopf N, Herwig A, Becker S. 2015. Transport of Ebolavirus Nucleocapsids Is Dependent on Actin Polymerization: Live-Cell Imaging Analysis of Ebolavirus-Infected Cells. *J Infect Dis* 212 Suppl 2:S160-6.
405. Dietzel E, Kolesnikova L, Maisner A. 2013. Actin filaments disruption and stabilization affect measles virus maturation by different mechanisms. *Virology journal* 10:249-249.
406. Santangelo PJ, Bao G. 2007. Dynamics of filamentous viral RNPs prior to egress. *Nucleic Acids Res* 35:3602-11.

407. Cifuentes-Muñoz N, Ellis Dutch R. 2019. To assemble or not to assemble: The changing rules of pneumovirus transmission. *Virus Research* 265:68-73.
408. Sattentau Q. 2008. Avoiding the void: cell-to-cell spread of human viruses. *Nature Reviews Microbiology* 6:815-826.
409. Neilson KA, Yunis EJ. 1990. Demonstration of Respiratory Syncytial Virus in an Autopsy Series. *Pediatric Pathology* 10:491-502.
410. Liljeroos L, Krzyzaniak MA, Helenius A, Butcher SJ. 2013. Architecture of respiratory syncytial virus revealed by electron cryotomography. *Proceedings of the National Academy of Sciences* 110:11133-11138.
411. Bächli T, Howe C. 1973. Morphogenesis and Ultrastructure of Respiratory Syncytial Virus. *Journal of Virology* 12:1173-1180.
412. Loo LH, Jumat MR, Fu Y, Ayi TC, Wong PS, Tee NWS, Tan BH, Sugrue RJ. 2013. Evidence for the interaction of the human metapneumovirus G and F proteins during virus-like particle formation. *Virology Journal* 10:294.
413. Dubois J, Cavanagh MH, Terrier O, Hamelin ME, Lina B, Shi R, Rosa-Calatrava M, Boivin G. 2017. Mutations in the fusion protein heptad repeat domains of human metapneumovirus impact on the formation of syncytia. *J Gen Virol* 98:1174-1180.
414. Aerts L, Cavanagh M-H, Dubois J, Carbonneau J, Rhéaume C, Lavigne S, Couture C, Hamelin M-È, Boivin G. 2015. Effect of in vitro syncytium formation on the severity of human metapneumovirus disease in a murine model. *PloS one* 10:e0120283-e0120283.
415. Ravi M, Paramesh V, Kaviya SR, Anuradha E, Solomon FD. 2015. 3D cell culture systems: advantages and applications. *J Cell Physiol* 230:16-26.
416. Mertens TCJ, Karmouty-Quintana H, Taube C, Hiemstra PS. 2017. Use of airway epithelial cell culture to unravel the pathogenesis and study treatment in obstructive airway diseases. *Pulm Pharmacol Ther* 45:101-113.
417. Parker J, Sarlang S, Thavagnanam S, Williamson G, O'Donoghue D, Villenave R, Power U, Shields M, Heaney L, Skibinski G. 2010. A 3-D

- well-differentiated model of pediatric bronchial epithelium demonstrates unstimulated morphological differences between asthmatic and nonasthmatic cells. *Pediatr Res* 67:17-22.
418. Gray TE, Guzman K, Davis CW, Abdullah LH, Nettesheim P. 1996. Mucociliary differentiation of serially passaged normal human tracheobronchial epithelial cells. *Am J Respir Cell Mol Biol* 14:104-12.
419. Whitcutt MJ, Adler KB, Wu R. 1988. A biphasic chamber system for maintaining polarity of differentiation of cultured respiratory tract epithelial cells. *In Vitro Cell Dev Biol* 24:420-8.
420. Kwilas S, Liesman RM, Zhang L, Walsh E, Pickles RJ, Peeples ME. 2009. Respiratory Syncytial Virus Grown in Vero Cells Contains a Truncated Attachment Protein That Alters Its Infectivity and Dependence on Glycosaminoglycans. *Journal of Virology* 83:10710-10718.
421. Wright PF, Ikizler MR, Gonzales RA, Carroll KN, Johnson JE, Werkhaven JA. 2005. Growth of respiratory syncytial virus in primary epithelial cells from the human respiratory tract. *J Virol* 79:8651-4.
422. Zhu Q, Lu B, McTamney P, Palaszynski S, Diallo S, Ren K, Ulbrandt ND, Kallewaard N, Wang W, Fernandes F, Wong S, Svabek C, Moldt B, Esser MT, Jing H, Suzich JA. 2018. Prevalence and Significance of Substitutions in the Fusion Protein of Respiratory Syncytial Virus Resulting in Neutralization Escape From Antibody MEDI8897. *J Infect Dis* 218:572-580.
423. Zhu Q, McLellan JS, Kallewaard NL, Ulbrandt ND, Palaszynski S, Zhang J, Moldt B, Khan A, Svabek C, McAuliffe JM, Wrapp D, Patel NK, Cook KE, Richter BWM, Ryan PC, Yuan AQ, Suzich JA. 2017. A highly potent extended half-life antibody as a potential RSV vaccine surrogate for all infants. *Sci Transl Med* 9.
424. Griffin MP, Khan AA, Esser MT, Jensen K, Takas T, Kankam MK, Villafana T, Dubovsky F. 2017. Safety, Tolerability, and Pharmacokinetics of MEDI8897, the Respiratory Syncytial Virus Prefusion F-Targeting

- Monoclonal Antibody with an Extended Half-Life, in Healthy Adults.
Antimicrob Agents Chemother 61.
425. Shaikh FY, Cox RG, Lifland AW, Hotard AL, Williams JV, Moore ML, Santangelo PJ, Crowe JE, Jr. 2012. A critical phenylalanine residue in the respiratory syncytial virus fusion protein cytoplasmic tail mediates assembly of internal viral proteins into viral filaments and particles. *mBio* 3.
 426. Jumat MR, Nguyen Huong T, Wong P, Loo LH, Tan BH, Fenwick F, Toms GL, Sugrue RJ. 2014. Imaging analysis of human metapneumovirus-infected cells provides evidence for the involvement of F-actin and the raft-lipid microdomains in virus morphogenesis. *Virology* 11:198.
 427. Shahriari S, Wei K-J, Ghildyal R. 2018. Respiratory Syncytial Virus Matrix (M) Protein Interacts with Actin In Vitro and in Cell Culture. *Viruses* 10:535.
 428. Shaikh FY, Utley TJ, Craven RE, Rogers MC, Lapierre LA, Goldenring JR, Crowe JE, Jr. 2012. Respiratory Syncytial Virus Assembles into Structured Filamentous Virion Particles Independently of Host Cytoskeleton and Related Proteins. *PLOS ONE* 7:e40826.
 429. Gower TL, Peeples ME, Collins PL, Graham BS. 2001. RhoA is activated during respiratory syncytial virus infection. *Virology* 283:188-96.
 430. Burke E, Mahoney NM, Almo SC, Barik S. 2000. Profilin is required for optimal actin-dependent transcription of respiratory syncytial virus genome RNA. *J Virol* 74:669-75.
 431. Ulloa L, Serra R, Asenjo A, Villanueva N. 1998. Interactions between cellular actin and human respiratory syncytial virus (HRSV). *Virus Res* 53:13-25.
 432. Domachowske JB, Khan AA, Esser MT, Jensen K, Takas T, Villafana T, Dubovsky F, Griffin MP. 2018. Safety, Tolerability and Pharmacokinetics of MEDI8897, an Extended Half-life Single-dose Respiratory Syncytial Virus Prefusion F-targeting Monoclonal Antibody Administered as a Single Dose to Healthy Preterm Infants. *Pediatr Infect Dis J* 37:886-892.

433. Soto JA, Gálvez NMS, Benavente FM, Pizarro-Ortega MS, Lay MK, Riedel C, Bueno SM, Gonzalez PA, Kalergis AM. 2018. Human Metapneumovirus: Mechanisms and Molecular Targets Used by the Virus to Avoid the Immune System. *Frontiers in immunology* 9:2466-2466.
434. Liu Y, Haas DL, Poore S, Isakovic S, Gahan M, Mahalingam S, Fu ZF, Tripp RA. 2009. Human Metapneumovirus Establishes Persistent Infection in the Lungs of Mice and Is Reactivated by Glucocorticoid Treatment. *Journal of Virology* 83:6837-6848.
435. Yacine A, Guy B. 2008. Persistent Human Metapneumovirus Infection in Immunocompromised Child. *Emerging Infectious Disease journal* 14:854.
436. Debiaggi M, Canducci F, Sampaolo M, Marinozzi MC, Parea M, Terulla C, Colombo AA, Alessandrino EP, Bragotti LZ, Arghittu M, Goglio A, Migliavacca R, Romero E, Clementi M. 2006. Persistent Symptomless Human Metapneumovirus Infection in Hematopoietic Stem Cell Transplant Recipients. *The Journal of Infectious Diseases* 194:474-478.
437. Oketch JW, Kamau E, Otieno GP, Otieno JR, Agoti CN, Nokes DJ. 2019. Human metapneumovirus prevalence and patterns of subgroup persistence identified through surveillance of pediatric pneumonia hospital admissions in coastal Kenya, 2007–2016. *BMC Infectious Diseases* 19:757.
438. Roberts SR, Compans RW, Wertz GW. 1995. Respiratory syncytial virus matures at the apical surfaces of polarized epithelial cells. *Journal of Virology* 69:2667-2673.
439. Hornsleth A, Loland L, Larsen LB. 2001. Cytokines and chemokines in respiratory secretion and severity of disease in infants with respiratory syncytial virus (RSV) infection. *J Clin Virol* 21:163-70.
440. Malmo J, Moe N, Krokstad S, Ryan L, Loevenich S, Johnsen IB, Espevik T, Nordbø SA, Døllner H, Anthonsen MW. 2016. Cytokine Profiles in Human Metapneumovirus Infected Children: Identification of Genes Involved in the Antiviral Response and Pathogenesis. *PLOS ONE* 11:e0155484.

441. Guerrero-Plata A, Casola A, Garofalo RP. 2005. Human metapneumovirus induces a profile of lung cytokines distinct from that of respiratory syncytial virus. *Journal of virology* 79:14992-14997.
442. Bakker SE, Duquerroy S, Galloux M, Loney C, Conner E, Eleouet JF, Rey FA, Bhella D. 2013. The respiratory syncytial virus nucleoprotein-RNA complex forms a left-handed helical nucleocapsid. *J Gen Virol* 94:1734-8.
443. Ruigrok RW, Crepin T, Kolakofsky D. 2011. Nucleoproteins and nucleocapsids of negative-strand RNA viruses. *Curr Opin Microbiol* 14:504-10.
444. Fields BN, Knipe DMDM-, Howley PM. 2013. Paramyxoviridae in *Fields virology / editors-in-chief, David M. Knipe, Peter M. Howley ; associate editors, Jeffrey I. Cohen ... [et al.]*. Fields virology, 6th ed. ed. Philadelphia : Wolters Kluwer Health/Lippincott Williams & Wilkins, c2013., United States.
445. Norrby E, Marusyk H, Orvell C. 1970. Morphogenesis of respiratory syncytial virus in a green monkey kidney cell line (Vero). *J Virol* 6:237-42.
446. Carromeu C, Simabuco FM, Tamura RE, Farinha Arcieri LE, Ventura AM. 2007. Intracellular localization of human respiratory syncytial virus L protein. *Arch Virol* 152:2259-63.
447. Becker S, Rinne C, Hofsass U, Klenk HD, Muhlberger E. 1998. Interactions of Marburg virus nucleocapsid proteins. *Virology* 249:406-17.
448. Nao N, Sato K, Yamagishi J, Tahara M, Nakatsu Y, Seki F, Katoh H, Ohnuma A, Shirogane Y, Hayashi M, Suzuki T, Kikuta H, Nishimura H, Takeda M. 2019. Consensus and variations in cell line specificity among human metapneumovirus strains. *PLoS One* 14:e0215822.
449. Henle W. 1950. Interference phenomena between animal viruses; a review. *J Immunol* 64:203-36.
450. Ziegler JE, Horsfall FL. 1944. INTERFERENCE BETWEEN THE INFLUENZA VIRUSES : I. THE EFFECT OF ACTIVE VIRUS UPON THE MULTIPLICATION OF INFLUENZA VIRUSES IN THE CHICK EMBRYO. *The Journal of experimental medicine* 79:361-377.

451. Andrewes CH. 1942. Interference by One Virus with the Growth of Another in Tissue-Culture. *British Journal of Experimental Pathology* 23:214-220.
452. Yan XL, Li YN, Tang YJ, Xie ZP, Gao HC, Yang XM, Li YM, Liu LJ, Duan ZJ. 2017. Clinical characteristics and viral load of respiratory syncytial virus and human metapneumovirus in children hospitalized for acute lower respiratory tract infection. *J Med Virol* 89:589-597.
453. Franz A, Adams O, Willems R, Bonzel L, Neuhausen N, Schweizer-Krantz S, Rüggeberg JU, Willers R, Henrich B, Schroten H, Tenenbaum T. 2010. Correlation of viral load of respiratory pathogens and co-infections with disease severity in children hospitalized for lower respiratory tract infection. *Journal of Clinical Virology* 48:239-245.
454. Martin ET, Kuypers J, Wald A, Englund JA. 2012. Multiple versus single virus respiratory infections: viral load and clinical disease severity in hospitalized children. *Influenza Other Respir Viruses* 6:71-7.
455. Derdowski A, Peters TR, Glover N, Qian R, Utley TJ, Burnett A, Williams JV, Spearman P, Crowe JE, Jr. 2008. Human metapneumovirus nucleoprotein and phosphoprotein interact and provide the minimal requirements for inclusion body formation. *J Gen Virol* 89:2698-708.
456. Leyrat C, Renner M, Harlos K, Grimes JM. 2013. Solution and crystallographic structures of the central region of the phosphoprotein from human metapneumovirus. *PLoS One* 8:e80371.
457. Llorente MT, Garcia-Barreno B, Calero M, Camafeita E, Lopez JA, Longhi S, Ferron F, Varela PF, Melero JA. 2006. Structural analysis of the human respiratory syncytial virus phosphoprotein: characterization of an alpha-helical domain involved in oligomerization. *J Gen Virol* 87:159-69.
458. Barik S. 1992. Transcription of human respiratory syncytial virus genome RNA in vitro: requirement of cellular factor(s). *J Virol* 66:6813-8.
459. Huang YT, Romito RR, De BP, Banerjee AK. 1993. Characterization of the in vitro system for the synthesis of mRNA from human respiratory syncytial virus. *Virology* 193:862-7.

460. Burke E, Dupuy L, Wall C, Barik S. 1998. Role of cellular actin in the gene expression and morphogenesis of human respiratory syncytial virus. *Virology* 252:137-48.
461. Julie G, Paul SM, Winifred D, Brian F, Rosalind LS, Hart CA. 2003. Human Metapneumovirus in Severe Respiratory Syncytial Virus Bronchiolitis. *Emerging Infectious Disease journal* 9:372.
462. Luis EC, Abubaker MBN, Winifred D, Ricardo QG, Julie G, Hart CA. 2003. Human Metapneumovirus and Respiratory Syncytial Virus, Brazil. *Emerging Infectious Disease journal* 9:1626.
463. Debiaggi M, Canducci F, Ceresola ER, Clementi M. 2012. The role of infections and coinfections with newly identified and emerging respiratory viruses in children. *Virol J* 9:247.
464. Xepapadaki P, Psarras S, Bossios A, Tsolia M, Gourgiotis D, Liapi-Adamidou G, Constantopoulos AG, Kafetzis D, Papadopoulos NG. 2004. Human Metapneumovirus as a causative agent of acute bronchiolitis in infants. *J Clin Virol* 30:267-70.
465. Canducci F, Debiaggi M, Sampaolo M, Marinozzi MC, Berrè S, Terulla C, Gargantini G, Cambieri P, Romero E, Clementi M. 2008. Two-year prospective study of single infections and co-infections by respiratory syncytial virus and viruses identified recently in infants with acute respiratory disease. *J Med Virol* 80:716-23.
466. Viazov S, Ratjen F, Scheidhauer R, Fiedler M, Roggendorf M. 2003. High prevalence of human metapneumovirus infection in young children and genetic heterogeneity of the viral isolates. *J Clin Microbiol* 41:3043-5.
467. Yoshida L-M, Suzuki M, Nguyen HA, Le MN, Dinh Vu T, Yoshino H, Schmidt W-P, Nguyen TTA, Le HT, Morimoto K, Moriuchi H, Dang DA, Ariyoshi K. 2013. Respiratory syncytial virus: co-infection and paediatric lower respiratory tract infections. *European Respiratory Journal* 42:461-469.
468. Moe N, Krokstad S, Stenseng IH, Christensen A, Skanke LH, Risnes KR, Nordbø SA, Døllner H. 2017. Comparing Human Metapneumovirus and

- Respiratory Syncytial Virus: Viral Co-Detections, Genotypes and Risk Factors for Severe Disease. *PLoS One* 12:e0170200.
469. Semple MG, Cowell A, Dove W, Greensill J, McNamara PS, Halfhide C, Shears P, Smyth RL, Hart CA. 2005. Dual Infection of Infants by Human Metapneumovirus and Human Respiratory Syncytial Virus Is Strongly Associated with Severe Bronchiolitis. *The Journal of Infectious Diseases* 191:382-386.
470. Foulongne V, Guyon G, Rodière M, Segondy M. 2006. Human Metapneumovirus Infection in Young Children Hospitalized With Respiratory Tract Disease. *The Pediatric Infectious Disease Journal* 25:354-359.
471. van Woensel JBM, Bos AP, Lutter R, Rossen JWA, Schuurman R. 2006. Absence of human metapneumovirus co-infection in cases of severe respiratory syncytial virus infection. *Pediatric Pulmonology* 41:872-874.
472. Isaac L, Carla W, James D, David F, Marie LL, Jeffrey SK. 2004. Human Metapneumovirus and Severity of Respiratory Syncytial Virus Disease. *Emerging Infectious Disease journal* 10:1318.
473. Griffiths C, Drews SJ, Marchant DJ. 2017. Respiratory Syncytial Virus: Infection, Detection, and New Options for Prevention and Treatment. *Clinical Microbiology Reviews* 30:277-319.
474. Tayyari F, Marchant D, Moraes TJ, Duan W, Mastrangelo P, Hegele RG. 2011. Identification of nucleolin as a cellular receptor for human respiratory syncytial virus. *Nature Medicine* 17:1132-1135.
475. Johnson TR, McLellan JS, Graham BS. 2012. Respiratory syncytial virus glycoprotein G interacts with DC-SIGN and L-SIGN to activate ERK1 and ERK2. *J Virol* 86:1339-47.
476. Hallak LK, Spillmann D, Collins PL, Peeples ME. 2000. Glycosaminoglycan sulfation requirements for respiratory syncytial virus infection. *J Virol* 74:10508-13.

477. Feldman SA, Audet S, Beeler JA. 2000. The fusion glycoprotein of human respiratory syncytial virus facilitates virus attachment and infectivity via an interaction with cellular heparan sulfate. *J Virol* 74:6442-7.
478. Feldman SA, Hendry RM, Beeler JA. 1999. Identification of a linear heparin binding domain for human respiratory syncytial virus attachment glycoprotein G. *J Virol* 73:6610-7.
479. Krzyzaniak MA, Zumstein MT, Gerez JA, Picotti P, Helenius A. 2013. Host cell entry of respiratory syncytial virus involves macropinocytosis followed by proteolytic activation of the F protein. *PLoS Pathog* 9:e1003309.
480. White J, Matlin K, Helenius A. 1981. Cell fusion by Semliki Forest, influenza, and vesicular stomatitis viruses. *J Cell Biol* 89:674-9.
481. Ohnishi S, Yoshimura A. 1984. [Infectious cell entry mechanism of enveloped viruses]. *Uirusu* 34:11-24.
482. Yoshimura A, Kuroda K, Kawasaki K, Yamashina S, Maeda T, Ohnishi S. 1982. Infectious cell entry mechanism of influenza virus. *J Virol* 43:284-93.
483. White JM, Delos SE, Brecher M, Schornberg K. 2008. Structures and mechanisms of viral membrane fusion proteins: multiple variations on a common theme. *Crit Rev Biochem Mol Biol* 43:189-219.
484. Klenk H-D, Rott R, Orlich M, Blodorn J. 1975. Activation of influenza A viruses by trypsin treatment. *Virology* 68:426-439.
485. Kaverin NV, Webster RG. 1995. Impairment of multicycle influenza virus growth in Vero (WHO) cells by loss of trypsin activity. *J Virol* 69:2700-2703.
486. Abe M, Tahara M, Sakai K, Yamaguchi H, Kanou K, Shirato K, Kawase M, Noda M, Kimura H, Matsuyama S, Fukuhara H, Mizuta K, Maenaka K, Ami Y, Esumi M, Kato A, Takeda M. 2013. TMPRSS2 is an activating protease for respiratory parainfluenza viruses. *J Virol* 87:11930-5.
487. Bertram S, Dijkman R, Habjan M, Heurich A, Gierer S, Glowacka I, Welsch K, Winkler M, Schneider H, Hofmann-Winkler H, Thiel V, Pöhlmann S. 2013. TMPRSS2 activates the human coronavirus 229E for

- cathepsin-independent host cell entry and is expressed in viral target cells in the respiratory epithelium. *J Virol* 87:6150-60.
488. Gierer S, Bertram S, Kaup F, Wrensch F, Heurich A, Krämer-Kühl A, Welsch K, Winkler M, Meyer B, Drosten C, Dittmer U, von Hahn T, Simmons G, Hofmann H, Pöhlmann S. 2013. The Spike Protein of the Emerging Betacoronavirus EMC Uses a Novel Coronavirus Receptor for Entry, Can Be Activated by TMPRSS2, and Is Targeted by Neutralizing Antibodies. *Journal of Virology* 87:5502-5511.
489. Glowacka I, Bertram S, Müller MA, Allen P, Soilleux E, Pfefferle S, Steffen I, Tsegaye TS, He Y, Gnirss K, Niemeyer D, Schneider H, Drosten C, Pöhlmann S. 2011. Evidence that TMPRSS2 activates the severe acute respiratory syndrome coronavirus spike protein for membrane fusion and reduces viral control by the humoral immune response. *J Virol* 85:4122-34.
490. Heurich A, Hofmann-Winkler H, Gierer S, Liepold T, Jahn O, Pöhlmann S. 2014. TMPRSS2 and ADAM17 cleave ACE2 differentially and only proteolysis by TMPRSS2 augments entry driven by the severe acute respiratory syndrome coronavirus spike protein. *J Virol* 88:1293-307.
491. Shirato K, Kawase M, Matsuyama S. 2013. Middle East respiratory syndrome coronavirus infection mediated by the transmembrane serine protease TMPRSS2. *J Virol* 87:12552-61.
492. Hoffmann M, Kleine-Weber H, Schroeder S, Krüger N, Herrler T, Erichsen S, Schiergens TS, Herrler G, Wu NH, Nitsche A, Müller MA, Drosten C, Pöhlmann S. 2020. SARS-CoV-2 Cell Entry Depends on ACE2 and TMPRSS2 and Is Blocked by a Clinically Proven Protease Inhibitor. *Cell* 181:271-280.e8.
493. Hoffmann M, Kleine-Weber H, Pöhlmann S. 2020. A Multibasic Cleavage Site in the Spike Protein of SARS-CoV-2 Is Essential for Infection of Human Lung Cells. *Molecular Cell* 78:779-784.e5.

494. Jaimes JA, Millet JK, Whittaker GR. 2020. Proteolytic cleavage of the SARS-CoV-2 spike protein and the role of the novel S1/S2 site. *iScience* doi:<https://doi.org/10.1016/j.isci.2020.101212:101212>.
495. Laporte M, Naesens L. 2017. Airway proteases: an emerging drug target for influenza and other respiratory virus infections. *Current Opinion in Virology* 24:16-24.
496. Zhirnov OP, Klenk HD, Wright PF. 2011. Aprotinin and similar protease inhibitors as drugs against influenza. *Antiviral Research* 92:27-36.
497. Yamaya M, Shimotai Y, Hatachi Y, Lusamba Kalonji N, Tando Y, Kitajima Y, Matsuo K, Kubo H, Nagatomi R, Hongo S, Homma M, Nishimura H. 2015. The serine protease inhibitor camostat inhibits influenza virus replication and cytokine production in primary cultures of human tracheal epithelial cells. *Pulmonary Pharmacology & Therapeutics* 33:66-74.
498. Gibo J, Ito T, Kawabe K, Hisano T, Inoue M, Fujimori N, Oono T, Arita Y, Nawata H. 2005. Camostat mesilate attenuates pancreatic fibrosis via inhibition of monocytes and pancreatic stellate cells activity. *Lab Invest* 85:75-89.
499. Mathieu C, Ferren M, Jurgens E, Dumont C, Rybkina K, Harder O, Stelitano D, Madeddu S, Sanna G, Schwartz D, Biswas S, Hardie D, Hashiguchi T, Moscona A, Horvat B, Niewiesk S, Porotto M. 2019. Measles Virus Bearing Measles Inclusion Body Encephalitis-Derived Fusion Protein Is Pathogenic after Infection via the Respiratory Route. *J Virol* 93.
500. Iketani S, Shean RC, Ferren M, Makhsous N, Aquino DB, des Georges A, Rima B, Mathieu C, Porotto M, Moscona A, Greninger AL. 2018. Viral Entry Properties Required for Fitness in Humans Are Lost through Rapid Genomic Change during Viral Isolation. *mBio* 9.
501. Palermo LM, Uppal M, Skrabanek L, Zumbo P, Germer S, Toussaint NC, Rima BK, Huey D, Niewiesk S, Porotto M, Moscona A. 2016. Features of Circulating Parainfluenza Virus Required for Growth in Human Airway. *mBio* 7:e00235.

502. Ulloa L, Serra R, Asenjo A, Villanueva N. 1998. Interactions between cellular actin and human respiratory syncytial virus (HRSV). *Virus Research* 53:13-25.
503. Radhakrishnan A, Yeo D, Brown G, Myaing MZ, Iyer LR, Fleck R, Tan BH, Aitken J, Sanmun D, Tang K, Yarwood A, Brink J, Sugrue RJ. 2010. Protein analysis of purified respiratory syncytial virus particles reveals an important role for heat shock protein 90 in virus particle assembly. *Mol Cell Proteomics* 9:1829-48.
504. Mitra R, Baviskar P, Duncan-Decocq RR, Patel D, Oomens AGP. 2012. The Human Respiratory Syncytial Virus Matrix Protein Is Required for Maturation of Viral Filaments. *Journal of Virology* 86:4432-4443.
505. Stefanska I, Romanowska M, Donevski S, Gawryluk D, Brydak LB. 2013. Co-infections with influenza and other respiratory viruses. *Adv Exp Med Biol* 756:291-301.
506. McArdle AJ, Turkova A, Cunnington AJ. 2018. When do co-infections matter? *Current Opinion in Infectious Diseases* 31:209-215.
507. Aguilera ER, Pfeiffer JK. 2019. Strength in numbers: Mechanisms of viral co-infection. *Virus Research* 265:43-46.
508. Reperant LA, Osterhaus ADME. 2017. AIDS, Avian flu, SARS, MERS, Ebola, Zika... what next? *Vaccine* 35:4470-4474.
509. Thèves C, Crubézy E, Biagini P. 2016. History of Smallpox and Its Spread in Human Populations. *Microbiol Spectr* 4.
510. Holzmann H, Hengel H, Tenbusch M, Doerr HW. 2016. Eradication of measles: remaining challenges. *Med Microbiol Immunol* 205:201-8.
511. Monath TP, Vasconcelos PF. 2015. Yellow fever. *J Clin Virol* 64:160-73.
512. Musso D, Gubler DJ. 2016. Zika Virus. *Clin Microbiol Rev* 29:487-524.
513. Olival KJ, Hayman DTS. 2014. Filoviruses in bats: current knowledge and future directions. *Viruses* 6:1759-1788.
514. de Wit E, van Doremalen N, Falzarano D, Munster VJ. 2016. SARS and MERS: recent insights into emerging coronaviruses. *Nat Rev Microbiol* 14:523-34.

515. Yang Y, Peng F, Wang R, Guan K, Jiang T, Xu G, Sun J, Chang C. 2020. The deadly coronaviruses: The 2003 SARS pandemic and the 2020 novel coronavirus epidemic in China. *J Autoimmun* 109:102434.
516. Sauter D, Kirchhoff F. 2019. Key Viral Adaptations Preceding the AIDS Pandemic. *Cell Host Microbe* 25:27-38.
517. Hemelaar J. 2012. The origin and diversity of the HIV-1 pandemic. *Trends Mol Med* 18:182-92.
518. Reperant LA, Kuiken T, Osterhaus AD. 2012. Adaptive pathways of zoonotic influenza viruses: from exposure to establishment in humans. *Vaccine* 30:4419-34.
519. Dawood FS, Iuliano AD, Reed C, Meltzer MI, Shay DK, Cheng PY, Bandaranayake D, Breiman RF, Brooks WA, Buchy P, Feikin DR, Fowler KB, Gordon A, Hien NT, Horby P, Huang QS, Katz MA, Krishnan A, Lal R, Montgomery JM, Mølbak K, Pebody R, Presanis AM, Razuri H, Steens A, Tinoco YO, Wallinga J, Yu H, Vong S, Bresee J, Widdowson MA. 2012. Estimated global mortality associated with the first 12 months of 2009 pandemic influenza A H1N1 virus circulation: a modelling study. *Lancet Infect Dis* 12:687-95.
520. Sutton TC. 2018. The Pandemic Threat of Emerging H5 and H7 Avian Influenza Viruses. *Viruses* 10.
521. Long JS, Mistry B, Haslam SM, Barclay WS. 2019. Host and viral determinants of influenza A virus species specificity. *Nat Rev Microbiol* 17:67-81.
522. Porter A, Goldfarb J. 2019. Measles: A dangerous vaccine-preventable disease returns. *Cleve Clin J Med* 86:393-398.
523. Falzarano D, Feldmann H. 2013. Vaccines for viral hemorrhagic fevers--progress and shortcomings. *Curr Opin Virol* 3:343-51.
524. Parkman PD, Hopps HE. 1988. Viral vaccines and antivirals: current use and future prospects. *Annu Rev Public Health* 9:203-21.
525. Melnick JL. 1989. Viral vaccines: achievements and challenges. *Acta Virol* 33:482-93.

526. Pierce BG, Keck ZY, Fong SK. 2016. Viral evasion and challenges of hepatitis C virus vaccine development. *Curr Opin Virol* 20:55-63.
527. Mumford JA. 2007. Vaccines and viral antigenic diversity. *Rev Sci Tech* 26:69-90.
528. Masmejan S, Baud D, Musso D, Panchaud A. 2018. Zika virus, vaccines, and antiviral strategies. *Expert Rev Anti Infect Ther* 16:471-483.
529. Burton DR. 2002. Antibodies, viruses and vaccines. *Nat Rev Immunol* 2:706-13.
530. Afrough B, Dowall S, Hewson R. 2019. Emerging viruses and current strategies for vaccine intervention. *Clinical and experimental immunology* 196:157-166.
531. Zappa A, Amendola A, Romanò L, Zanetti A. 2009. Emerging and re-emerging viruses in the era of globalisation. *Blood transfusion = Trasfusione del sangue* 7:167-171.
532. Pekosz A, Glass GE. 2008. Emerging viral diseases. *Maryland medicine : MM : a publication of MEDCHI, the Maryland State Medical Society* 9:11-16.
533. Lau SKP. 2018. Molecular Research on Emerging Viruses: Evolution, Diagnostics, Pathogenesis, and Therapeutics. *International journal of molecular sciences* 19:398.
534. Yamayoshi S, Kawaoka Y. 2019. Current and future influenza vaccines. *Nat Med* 25:212-220.
535. Nguyen AM, Noymer A. 2013. Influenza mortality in the United States, 2009 pandemic: burden, timing and age distribution. *PloS one* 8:e64198-e64198.
536. Viboud C, Simonsen L, Fuentes R, Flores J, Miller MA, Chowell G. 2016. Global Mortality Impact of the 1957-1959 Influenza Pandemic. *J Infect Dis* 213:738-45.
537. Calisher CH, Childs JE, Field HE, Holmes KV, Schountz T. 2006. Bats: important reservoir hosts of emerging viruses. *Clinical microbiology reviews* 19:531-545.

538. Luis AD, Hayman DTS, O'Shea TJ, Cryan PM, Gilbert AT, Pulliam JRC, Mills JN, Timonin ME, Willis CKR, Cunningham AA, Fooks AR, Rupprecht CE, Wood JLN, Webb CT. 2013. A comparison of bats and rodents as reservoirs of zoonotic viruses: are bats special? *Proceedings Biological sciences* 280:20122753-20122753.
539. Field H SK, Kung N, Simon C, Waltisbuhl D, Hobert H, et al. . 2008. Hendra virus outbreak with novel clinical features. *Emerging Infectious Diseases*. doi:10.3201/eid1602.090780doi:10.3201/eid1602.090780.
540. Wong KT, Robertson T, Ong BB, Chong JW, Yaiw KC, Wang LF, Ansford AJ, Tannenberg A. 2009. Human Hendra virus infection causes acute and relapsing encephalitis. *Neuropathology and Applied Neurobiology* 35:296-305.
541. Wang L-F, Harcourt BH, Yu M, Tamin A, Rota PA, Bellini WJ, Eaton BT. 2001. Molecular biology of Hendra and Nipah viruses. *Microbes and Infection* 3:279-287.
542. Corman VM, Muth D, Niemeyer D, Drosten C. 2018. Chapter Eight - Hosts and Sources of Endemic Human Coronaviruses, p 163-188. *In* Kielian M, Mettenleiter TC, Roossinck MJ (ed), *Advances in Virus Research*, vol 100. Academic Press.
543. Hamre D, Procknow JJ. 1966. A New Virus Isolated from the Human Respiratory Tract. *Proceedings of the Society for Experimental Biology and Medicine* 121:190-193.
544. McIntosh K, Dees JH, Becker WB, Kapikian AZ, Chanock RM. 1967. Recovery in tracheal organ cultures of novel viruses from patients with respiratory disease. *Proceedings of the National Academy of Sciences* 57:933-940.
545. van der Hoek L, Pyrc K, Jebbink MF, Vermeulen-Oost W, Berkhout RJM, Wolthers KC, Wertheim-van Dillen PME, Kaandorp J, Spaargaren J, Berkhout B. 2004. Identification of a new human coronavirus. *Nature Medicine* 10:368-373.

546. Woo PCY, Lau SKP, Chu C-m, Chan K-h, Tsoi H-w, Huang Y, Wong BHL, Poon RWS, Cai JJ, Luk W-k, Poon LLM, Wong SSY, Guan Y, Peiris JSM, Yuen K-y. 2005. Characterization and Complete Genome Sequence of a Novel Coronavirus, Coronavirus HKU1, from Patients with Pneumonia. *Journal of Virology* 79:884-895.
547. Drosten C, Günther S, Preiser W, van der Werf S, Brodt H-R, Becker S, Rabenau H, Panning M, Kolesnikova L, Fouchier RAM, Berger A, Burguière A-M, Cinatl J, Eickmann M, Escriou N, Grywna K, Kramme S, Manuguerra J-C, Müller S, Rickerts V, Stürmer M, Vieth S, Klenk H-D, Osterhaus ADME, Schmitz H, Doerr HW. 2003. Identification of a Novel Coronavirus in Patients with Severe Acute Respiratory Syndrome. *New England Journal of Medicine* 348:1967-1976.
548. Cheng VCC, Lau SKP, Woo PCY, Yuen KY. 2007. Severe Acute Respiratory Syndrome Coronavirus as an Agent of Emerging and Reemerging Infection. *Clinical Microbiology Reviews* 20:660-694.
549. Zaki AM, van Boheemen S, Bestebroer TM, Osterhaus ADME, Fouchier RAM. 2012. Isolation of a Novel Coronavirus from a Man with Pneumonia in Saudi Arabia. *New England Journal of Medicine* 367:1814-1820.
550. Arabi YM, Balkhy HH, Hayden FG, Bouchama A, Luke T, Baillie JK, Al-Omari A, Hajeer AH, Senga M, Denison MR, Nguyen-Van-Tam JS, Shindo N, Bermingham A, Chappell JD, Van Kerkhove MD, Fowler RA. 2017. Middle East Respiratory Syndrome. *New England Journal of Medicine* 376:584-594.
551. Bogoch II, Watts A, Thomas-Bachli A, Huber C, Kraemer MUG, Khan K. 2020. Pneumonia of unknown aetiology in Wuhan, China: potential for international spread via commercial air travel. *Journal of travel medicine* 27:taaa008.
552. Lu H, Stratton CW, Tang Y-W. 2020. Outbreak of pneumonia of unknown etiology in Wuhan, China: The mystery and the miracle. *Journal of medical virology* 92:401-402.

553. Rothan HA, Byrareddy SN. 2020. The epidemiology and pathogenesis of coronavirus disease (COVID-19) outbreak. *Journal of autoimmunity* 109:102433-102433.
554. Du Toit A. 2020. Outbreak of a novel coronavirus. *Nature reviews Microbiology* 18:123-123.
555. Lu R, Zhao X, Li J, Niu P, Yang B, Wu H, Wang W, Song H, Huang B, Zhu N, Bi Y, Ma X, Zhan F, Wang L, Hu T, Zhou H, Hu Z, Zhou W, Zhao L, Chen J, Meng Y, Wang J, Lin Y, Yuan J, Xie Z, Ma J, Liu WJ, Wang D, Xu W, Holmes EC, Gao GF, Wu G, Chen W, Shi W, Tan W. 2020. Genomic characterisation and epidemiology of 2019 novel coronavirus: implications for virus origins and receptor binding. *Lancet (London, England)* 395:565-574.
556. Wan Y, Shang J, Graham R, Baric RS, Li F. 2020. Receptor Recognition by the Novel Coronavirus from Wuhan: an Analysis Based on Decade-Long Structural Studies of SARS Coronavirus. *Journal of virology* 94:e00127-20.
557. Mahase E. 2020. Covid-19: death rate is 0.66% and increases with age, study estimates. *Bmj* 369:m1327.
558. Baud D, Qi X, Nielsen-Saines K, Musso D, Pomar L, Favre G. 2020. Real estimates of mortality following COVID-19 infection. *Lancet Infect Dis* doi:10.1016/s1473-3099(20)30195-x.
559. Udugama B, Kadhiresan P, Kozlowski HN, Malekjahani A, Osborne M, Li VYC, Chen H, Mubareka S, Gubbay JB, Chan WCW. 2020. Diagnosing COVID-19: The Disease and Tools for Detection. *ACS nano* 14:3822-3835.

Vita

Employment	Summit Biosciences Product Development Scientist Lexington, Kentucky	(Current)
Education	Doctor of Philosophy Molecular and Cellular Biochemistry University of Kentucky, Lexington KY	(2020)
	Bachelor of Applied Science, Biological Sciences Bluefield State College, Bluefield WV	(2015)
Research	Graduate Research Assistant Principal Investigator: <u>Rebecca Dutch, Ph.D.</u>	(2016-Present)
	Summer Research Assistant, Marshall University WV-INBRE summer research internship. Principal Investigator: <u>Piyali Dasgupta Ph.D.</u>	(2014)
	Undergraduate Research Assistant, Bluefield State College Principal Investigator: <u>Tesfaye Belay Ph.D.</u>	(2013-2015)
Publications	First Authorship: “Respiratory Syncytial Virus (RSV) and human metapneumovirus (HMPV) infections in 3-D human airway tissues expose an interesting dichotomy in viral replication, spread, and inhibition by neutralizing antibodies”. Journal of Virology. 2020 August; JVI.01068-20.	(2020)
	Co-First Authorship: “SPINT2 inhibits proteases involved in activation of both influenza viruses and metapneumoviruses”. Virology.2020 April;543:43-45. 10.1016/j.virol.2020.01.004.	(2020)

- First Authorship:** “Human metapneumovirus fusion protein triggering: Increasing complexities by analysis of new HMPV fusion proteins” *Virology*. 2019 May; 531:248-254. 10.1016/j.virol.2019.03.003 (2019)
- Presentations**
- Novel Concepts in Virology** (2020)
Oral presentation at the Novel Concepts in Virology international meeting in Barcelona, Spain
- American Society for Virology** (2019)
Oral presentation at the annual American Society for Virology meeting
- ISIRV 11th RSV Symposium** (2018)
Poster presentation at the 11th International Respiratory Syncytial Virus Symposium
- Infectious Diseases Research Day** (2018)
Poster presentation at the annual University of Kentucky Infectious Diseases Research Day
- FASEB-Virus Structure and Assembly** (2018)
Poster presentation at the Federation of American Societies for Experimental Biology: Virus structure and assembly meeting.
- SERVC** (2018)
Oral presentation at the annual Southeastern Regional Virology Conference.
- Infectious Diseases Research Day** (2017)
Poster presentation at the annual University of Kentucky Infectious Diseases Research Day
- American Society for Virology** (2017)
Poster presentation at the annual American Society for Virology meeting

	ASBMB	(2017)
	<u>Poster presentation</u> at the Annual Society of Biochemistry and Molecular Biology meeting	
	ABRCMS	(2014)
	<u>Poster presentation</u> of summer research project at the Annual Biomedical Research Conference for Minority Students	
	WV-INBRE Oral Presentation	(2014)
	<u>Oral presentation</u> at Marshall University studying "The role of capsaicin as a natural therapeutic for small cell lung cancer". Research was conducted in the lab of Dr. Piylali Dasgupta.	
	WV-INBRE Poster Presentation	(2014)
	<u>Poster presentation</u> of the summer research project at the WV-INBRE research conference at West Virginia University	
Honors/ Awards	University of Kentucky Office of Biomedical Education travel award	(2020)
	University of Kentucky Max Steckler Research Fellowship	(2018)
	American Society of Virology travel award	(2017)
	Annual Society of Biochemistry and Molecular Biology travel award	(2017)
	University of Kentucky Graduate Student Travel Award	(Ind. 2012)
	Phi Eta Sigma Freshman Honor Society	(2012-2015)
	Bluefield State College President's list	(2011)
	Bluefield State College Dean's list	

Leadership	<p>Elected Director of IT- Biomedical Graduate Student Organization (2017-2019) Director of Information Technology. Duties include creating and maintaining the organization website, integration and application of new technologies, aiding the compilation of contact information databases and serving on the executive board to vote on decisions for the organization</p> <p>Lab manager, Bluefield State College (2013-2015) Principal Investigator: Dr. Tesfaye Belay Ph.D. Manage the research laboratory. Duties include ordering material, managing inventory, organizing work schedules, setting up labs for the professor, and assistance of two other senior level students with experiments as well as training of undergraduate students in the lab.</p> <p>Elected Secretary of the Bluefield State Biomedical Club (2014-2015) Secretary of Biomedical Club at Bluefield State College Duties are to maintain club minutes and research opportunity library as well as communicate with students in the college of science. Was also part of the initial group that helped found this club.</p>
Service	<p>Ronald McDonald House (2018) Prepared dinner for families at the Ronald McDonald House along with the Biomedical Graduate Student Organization volunteers</p> <p>Poster Session Judge (2018) Volunteer judge for the University of Kentucky College of Medicine post-doctoral science poster competition.</p>

	<p>Science Fair Judge (2018) Volunteer judge for the Kentucky American Water 2018 Science Fair in Lexington, Kentucky.</p>
	<p>Science Fair Judge (2014) Science fair judge for Pike View Middle School's science fair with the involvement of our Biomedical Club at Bluefield State College.</p>
	<p>Breast Cancer Awareness (2014) Aided Bluefield State Biomedical Club in organizing a powder-puff football game charity event in conjunction with Bluefield College for breast cancer awareness month.</p>
	<p>Bluefield State College Scientific Community Outreach Program (2014) Completed 10 hours of scientific community outreach. This included informing individuals in the community on scientific information and opportunities for children and parents.</p>
Teaching/ Mentoring	<p>Mentor within the Dutch Laboratory at University of Kentucky (2016-2020) Aid fellow graduate, undergraduates and high school students with experimental design and techniques as well as providing relevant background and understanding of the projects.</p>